Investigating Phototropin-dependent responses in Chlamydomonas reinhardtii

Georgios Kepesidis

Université Grenoble Alpes

THÈSE

Pour obtenir le grade de

DOCTEUR DE L'UNIVERSITÉ GRENOBLE ALPES

Spécialité : Chimie Biologie

Arrêté ministériel : 25 mai 2016

Présentée par

Georgios KEPESIDIS

Thèse dirigée par **Dimitris PETROUTSOS**

préparée au sein du **Laboratoire LPCV - Laboratoire de Physiologie Cellulaire Végétale**
dans **l'École Doctorale Chimie et Sciences du Vivant**

Etude des réponses dépendantes de la phototropine chez *Chlamydomonas reinhardtii*

Investigating Phototropin-dependent responses in *Chlamydomonas reinhardtii*

Thèse soutenue publiquement le **1 juin 2022**,
devant le jury composé de :

Madame Christel CARLES
Professeur à l'Université Grenoble Alpes (President)

Madame Elena MONTE
Chercheur CSIC, Centre de Recerca en Agrigenòmica (Rapporteur)

Monsieur Matteo BALLOTTARI
Professeur associe, University of Verona, (Rapporteur)

Monsieur Pierre CROZET
Maitre de conference, Université Sorbonne (Examinateur)

Monsieur Norbert ROLLAND
Directeur de recherche CNRS, Grenoble (Examinateur)

Summary

Light is crucial for life on earth, especially for photosynthetic organisms; it is a source of spatiotemporal information perceived by photoreceptor proteins, as well as the energy source that fuels photosynthesis. However, when absorbed in excess, it can be toxic for the photosynthetic cells leading to reactive oxygen species formation; this is avoided by the photoprotective mechanism qE (quenching of energy). *Chlamydomonas reinhardtii* is a model unicellular green alga, which is widely used for genetic and cellular studies, including those concerning light perception and utilization. *C. reinhardtii* accurately senses the information provided by light and regulates important cellular functions, including gene expression, sexual life cycle, phototaxis, photosynthesis, and photoprotection, using a network of specialized photoreceptors. It is equipped with a single-copy phototropin, four cryptochromes, eight rhodopsin-like proteins, as well as the UV-B photoreceptor UVR8.

Among these photoreceptors, phototropin (PHOT) appears to have a multifaceted role in *C. reinhardtii* physiology; it has been shown to control gametogenesis at low nitrogen availability, expression of genes encoding chlorophyll and carotenoid biosynthesis, the size of the eyespot and photoprotection. Specifically on the later, under high light PHOT regulates positively the induction of LHCSR3, a nucleus-encoded and chloroplast-localized protein, which is the main actor of qE.

PHOT is a blue-light activated, plasma membrane associated Serine/ Threonine kinase, that undergoes phosphorylation upon irradiation with UVA and blue light. Only a handful of substrates of PHOT have been identified in higher plants, but not in *C. reinhardtii*. My goal was to elucidate the PHOT-dependent responses in *C. reinhardtii* and to identify possible interactors of the protein. For this, I employed a strategy involving comparative phosphoproteomic analyses, as well as targeted mutant strain screening.

On this Thesis, I am presenting data from two comparative phosphoproteomic analyses. On the first I compared the phosphoproteome of low- and high-light

acclimated WT and *PHOT*-deficient cells (Δ*phot*). This attempt aimed to explore the role of phototropin in the transition from low light to high light and to identify putative PHOT-dependent regulators of photoprotection. The second phosphoproteomic analysis allowed the comparison of the phosphoproteome of dark-acclimated and shortly blue-light-exposed wild-type (WT) and Δphot cells in order to elucidate the early PHOT-dependent phosphorylating events. Both datasets revealed a diverse set of proteins whose phosphorylation is regulated by PHOT, as well as the involvement of PHOT in a number of different cellular responses.

I am also presenting the involvement of a PHOT-regulated serine/threonine protein kinase, hereafter FLKIN, in the control of LHCSR3 accumulation and the Carbon Concentrating Mechanism (CCM). Phosphorylation levels of FLKIN increase fivefold when shifting wild type cells from low to high intensity light; in the Δ*phot* mutant FLKIN remains highly phosphorylated independently of the light intensity. The mutant lacking *FLKIN* was found to over-accumulate LHSCR3 and has higher qE, in comparison with the WT, even under non-saturating light intensities. It also induces the transcripts of proteins involved in the CCM in higher levels than the WT. We propose that FLKIN acts as a repressor of LHCSR3 and the CCM genes at low light conditions. Additionally, the Δ*flkin* strain shows a growth defect in autotrophic medium, as well as bigger cell size and higher chlorophyl content. Δ*flkin* has also higher photosynthetic capacity than the WT in all growth conditions.

I, finally, revealed the involvement of PHOT in the Chloroplast Unfolded Protein Response (cpUPR) in response to proteotoxic stress. MARS1, a protein kinase involved in the cpUPR was found to be highly phosphorylated upon exposure to blue light in a PHOT-dependent manner. Furthermore, my data show that the induction of VIPP2 and HSP22E/F proteins, upregulated in response to oxidative stress by the cpUPR, is impaired in the Δ*phot* mutant.

Résumé

La lumière est cruciale pour la vie sur terre, en particulier pour les organismes photosynthétiques ; elle est une source d'informations spatio-temporelles perçues par les protéines photoréceptrices, ainsi que la source d'énergie qui alimente la photosynthèse. Cependant, lorsqu'elle est absorbée en excès, elle peut être toxique pour les cellules photosynthétiques, entraînant la formation d'espèces réactives de l'oxygène ; ce phénomène est évité par le mécanisme de la photoprotection qE (quenching of energy). Chlamydomonas reinhardtii est une algue verte unicellulaire modèle, largement utilisée pour les études génétiques et cellulaires, notamment celles concernant la perception et l'utilisation de la lumière. *C. reinhardtii* détecte avec précision les informations fournies par la lumière et régule d'importantes fonctions cellulaires, notamment l'expression génétique, le cycle de vie sexuel, la phototaxie, la photosynthèse et la photoprotection, à l'aide d'un réseau de photorécepteurs spécialisés. Il est équipé d'une phototropine à copie unique, de quatre cryptochromes, de huit protéines de type rhodopsine, ainsi que du photorécepteur UV-B UVR8.

Parmi ces photorécepteurs, la phototropine (PHOT) semble avoir un rôle multiple dans la physiologie de *C. reinhardtii* ; il a été démontré qu'elle contrôle la gamétogenèse à faible disponibilité en azote, l'expression des gènes codant pour la biosynthèse de la chlorophylle et des caroténoïdes, la taille du point oculaire et la photoprotection. Plus précisément sur ce dernier point, sous une lumière élevée, PHOT régule positivement l'induction de LHCSR3, une protéine codée dans le noyau et localisée dans le chloroplaste, qui est le principal acteur de qE.

PHOT est une sérine/thréonine kinase activée par la lumière bleue, associée à la membrane plasmique, qui subit une phosphorylation lors de l'irradiation par les UVA et la lumière bleue. Seule quelques substrats de PHOT ont été identifiés chez les plantes supérieures, mais pas chez *C. reinhardtii*. Mon objectif était d'élucider les réponses dépendantes de PHOT chez *C. reinhardtii* et d'identifier des protéines éventuellement interagissant avec la PHOT. Pour cela, j'ai employé une stratégie impliquant des analyses phosphoprotéomiques comparatives, ainsi que le criblage ciblé de souches mutantes.

Dans cette thèse, je présente les données de deux analyses phosphoprotéomiques comparatives. Dans la première, j'ai comparé le phosphoprotéome de cellules WT et de cellules déficientes en PHOT (Δ*phot*) acclimatées à une lumière faible ou forte. Cette tentative visait à explorer le rôle de la phototropine dans la transition de la lumière faible à la lumière forte et à identifier les régulateurs putatifs de la photoprotection dépendants de PHOT. La deuxième analyse phosphoprotéomique a permis de comparer le phosphoprotéome des cellules de type sauvage (WT) et Δphot acclimatées à l'obscurité et exposées brièvement à la lumière bleue, afin d'élucider les événements de phosphorylation PHOT-dépendants précoces. Les deux ensembles de données ont révélé un ensemble diversifié de protéines dont la phosphorylation est régulée par PHOT, ainsi que l'implication de PHOT dans un certain nombre de réponses cellulaires différentes.

Je présente également l'implication d'une protéine kinase sérine/thréonine régulée par PHOT, ci-après FLKIN, dans le contrôle de l'accumulation de LHCSR3 et du mécanisme de concentration du carbone (CCM). Les niveaux de phosphorylation de FLKIN sont multipliés par cinq lorsque l'on fait passer les cellules de type sauvage d'une lumière de faible intensité à une lumière de forte intensité ; chez le mutant Δphot, FLKIN reste fortement phosphorylée indépendamment de l'intensité lumineuse. On a constaté que le mutant dépourvu de FLKIN suraccumule LHSCR3 et présente un qE plus élevé que le WT, même sous des intensités lumineuses non saturantes. Il induit également les transcrits des protéines impliquées dans le CCM à des niveaux plus élevés que le WT. Nous proposons que FLKIN agit comme un répresseur de LHCSR3 et des gènes CCM dans des conditions de faible lumière. De plus, la souche Δflkin présente un défaut de croissance en milieu autotrophe, ainsi qu'une taille de cellule plus importante et une teneur en chlorophylle plus élevée. Δ*flkin* a également une capacité photosynthétique supérieure à celle de la souche WT dans toutes les conditions de croissance.

Enfin, j'ai révélé l'implication de PHOT dans la réponse aux protéines non repliées du chloroplaste (cpUPR) en réponse à un stress protéotoxique. MARS1, une protéine kinase impliquée dans la cpUPR, est fortement phosphorylée lors de l'exposition à la lumière bleue de manière PHOT-dépendante. De plus, mes données montrent que

l'induction des protéines VIPP2 et HSP22E/F, régulées en réponse au stress oxydatif par la cpUPR, est altérée chez le mutant Δ*ph**o**t*.

Index

1.INTRODUCTION

1.1 Role of light for living organisms 12

1.1.1 Photosynthesis 12

1.1.2 Light as an environmental cue (photoreceptors) 16

1.2 Chlamydomonas as a model organism 23

1.3 Phototropin in Chlamydomonas 30

1.3.1 Evolution 30

1.3.2 Structure 33

1.3.3 Activation mechanism 36

1.3.4 Localisation 39

1.3.5 Cellular role/ responses 40

1.3.6 PHOT interactors in *Arabidopsis* 42

1.4 Protection from photooxidative stress in the chloroplast of Chlamydomonas: Photoprotection (quenching of energy) and the chloroplast Unfolded Protein Response (cpUPR) 45

1.4.1 Photoprotection in *Chlamydomonas* 45

1.4.2 The chloroplast Unfolded Protein Response (cpUPR) is a major quality control retrograde signal 54

1.5 Aim of this thesis 57

2.MATERIALS AND METHODS

Strains and conditions 61

Verification of the CLiP library mutants 62

Chlorophyl measurements 63

Cell measurements 63

Different light conditions 64

CO_2 experiments 64

Sampling for mass spectrometry (low light acclimated cells exposed to high light) 65

Sampling for mass spectrometry (dark acclimated cells exposed to blue light) 65

Experiments with H_2O_2 66

Experiments with Metronidazole (MZ) 66

Experiments with DCMU 67

Fluorescence-based measurements 67

In-silico DNA designs 68

Genomic DNA extraction 68
Plasmid construction and Gibson assembly 69
Bacteria transformation and plasmid purification 73
Plasmid purification 75
Algae transformation 76
Screening of transformants 78
Cut with the restriction enzymes 79
Colony pcr 79
Protein extraction and quantification for Immunoblotting 80
Immunoblotting 82
RNA extraction 83
cDNA synthesis 84
qPCR 85
Graphs design 86

3.RESULTS/DISCUSSION

3.1 Exploring the role of Phototropin in the transition from low light to high light. 88
3.1.1. Analysis of the phosphoproteome dataset 88
3.1.2 Study of the Cre16.g694950 mutant (Δ*flkin*) 94
3.2 Elucidating early, PHOT-dependent phosphorylating events in Chlamydomonas. 120
3.2.1. Setup and conditions 120
3.2.2. Analysis of the phosphoproteome dataset 122
3.2.3 Study of the Δ*Cop6* mutant 129
3.2.4 PHOT is involved in the cpUPR response 131

4.CONCLUSION 138

5.REFERENCES 142

Scientific communication 159

Acknowledgments 161

1. INTRODUCTION

1.1 Role of light for living organisms

Sunlight is crucial for the biome and its survival, and it represents one of the most important abiotic cues for the living organisms. The totality of the organisms on earth, from unicellular bacteria and microalgae to more complex ones such as humans, has developed multiple adaptations in order to adapt to light's intensity, quality and diurnal presence. Additionally, living organisms have developed responses to light's harmful properties. Light can also be utilised as an energy source to produce organic compounds from autotrophic organisms.

1.1.1 Photosynthesis

Sunlight reaches the surface of earth in a daily basis and fuels photosynthesis, providing most of the metabolic energy on our planet. Photosynthesis represents the light-driven fixation of atmospheric CO_2 and its reduction into sugars and is being performed by photosynthetic organisms, such as cyanobacteria, algae and land plants. This reaction produces the majority of the atmospheric oxygen.

Despite some adaptive variations between the different photosynthetic organisms, the basic process of photosynthesis is common. Photosynthesis is being performed in two set of reactions: the electron transport chain (ETR) reactions in the thylakoid membranes of the chloroplast and the Calvin-Benson cycle which occurs in the stroma.

The absorption of light is done by pigment molecules in the thylakoid membranes, such as chlorophylls a and b, carotenoids, lutein, zeaxanthin, violaxanthin, antheraxanthin and neoxanthin. The most common photosynthetic pigments are the chlorophylls, which absorb in blue and red and emit in green, which explains the green colour of the leaves of land plants, as well as the colour of green algae. The light energy is being collected by the photosynthetic pigments at the antennas and transferred to a pair of chlorophyll molecules that reside in the reaction centres of photosystem II (PSII) and photosystem I (PSI). The antennas are being formed by pigment-binding protein complexes, called Light Harvesting Complexes (LHCs), at the photosystems.

After light absorption, the excited chlorophyl molecule (^{1}Chl*) can return to its ground state via three possible ways. First, it can transfer its excitation energy to the reaction centres and thus, initiating the ETR and fuelling photosynthesis. It can also re-emit the excitation energy as Chl fluorescence or the excitation energy can be thermally dissipated by non- photochemical quenching (NPQ) (Muller, Li, and Niyogi 2001) (Erickson, Wakao, and Niyogi 2015). NPQ is a photoprotective mechanism which dissipates the excess absorbed light energy as heat. Those three processes (Chlorophyl fluorescence emission, photosynthesis, NPQ) are occurring antagonistically, which means that changes on the yield of the one, will dynamically affect the yield of the other two in contrast. Thus, the measurement of chlorophyl florescence can be informative of the changes on the yield of photosynthesis and NPQ at any given time (Maxwell and Johnson 2000).

PSII uses the energy from light to oxidize water to oxygen (Fig. 1.1). PSII is a chlorophyl-protein complex which carries out this reaction, as the only enzyme in nature which can catalyse the splitting of water into protons, electrons and oxygen. The electron derived from water is being, then, transferred to the electron acceptor plastoquinone, which is being reduced to plastoquinol. The electrons carried by plastoquinol are being received by the enzyme complex Cytochrome b_6f, which is located in the thylakoid membrane. Cytochrome b_6f subsequently reduces with the received electrons the small water-soluble electron carrier plastocyanin, which resides in the lumen. A second light-driven reaction is carried out by Photosystem I. PSI oxidizes plastocyanin and reduces the stroma-localised ferredoxin. Ferredoxin can then be used by the ferredoxin–$NADP^+$ reductase (FNR) enzyme to reduce $NADP^+$ to NADPH.

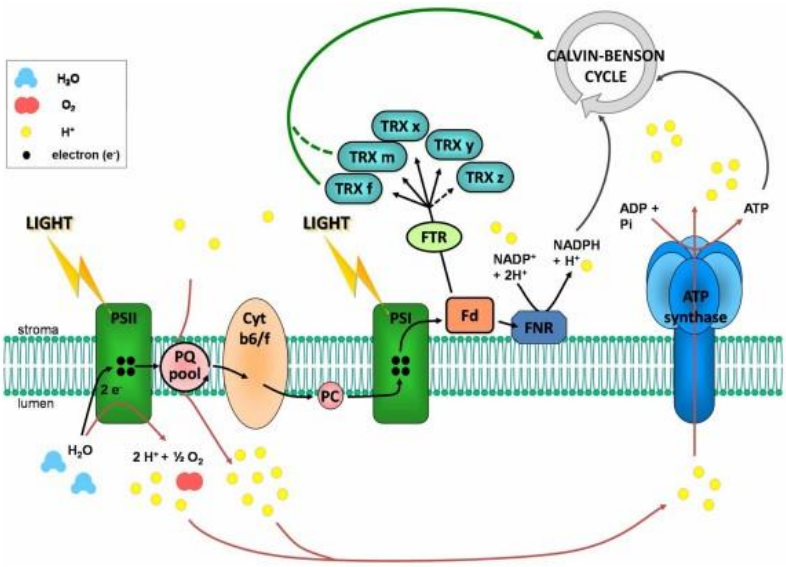

Figure 1.1: The Electron Transport Chain (ETR) and the light regulation of the Calvin-Benson cycle. PSII uses the energy from light to oxidize water to oxygen and to produce 2 protons. The electron derived from water is being, then, transferred to plastoquinone (PQ), which is being reduced to plastoquinol. These electrons are being then received by Cytochrome b_6f, which subsequently reduces plastocyanin. A second light-driven reaction is carried out by Photosystem I. PSI oxidizes plastocyanin and reduces ferredoxin (Fd). Ferredoxin can then be used by the ferredoxin–NADP⁺ reductase (FNR) to reduce NADP+ to NADPH. At the same time, protons are pumped into the thylakoid lumen, by the Cytochrome b_6f, while it transfers electrons from the PSII to PSI. The proton gradient (ΔpH) which is being generated across the thylakoid membrane is used by the ATP synthase for ATP production from ADP and inorganic phosphate (Pi). The chemical energy from ATP and NADPH is used for the formation of sugars by the Calvin-Benson cycle. Ferredoxin can also reduce thioredoxins (TRX) via the ferredoxin NADP reductase (FTR). The reduced TRXs regulate the light-driven activation of four enzymes of the Calvin-Benson cycle. Taken from (Michelet et al. 2013).

At the same time, protons are pumped into the thylakoid lumen, as a result of the water-splitting reaction at PSII and the plastoquinol oxidation at Cytochrome b_6f (Fig. 1.1). Thus, a proton gradient (ΔpH) is being generated across the thylakoid membrane, which is used by the ATP synthase for ATP production. The ATP synthase resides in the thylakoid membrane and catalyses the synthesis of ATP from ADP and inorganic phosphate (Pi). ΔpH, other than the synthesis of ATP, is also responsible for the down-regulation of the light harvesting, since high ΔpH (low luminal pH) can trigger NPQ (Briantais et al. 1979) (Niyogi, Grossman, and Bjorkman 1998) . Both ATP and NADPH generated by the ETR will be used as energy molecules in the Calvin Benson cycle.

The Calvin-Benson cycle occurs in the stroma of the chloroplast converting CO_2 into carbohydrates, after a series of reactions. The reactions of the Calvin-Benson cycle utilise the ATP and NADPH, which have been produced during the ETR as energy

donors and, eventually, they produce ADP, P_i and $NADP^+$. Light regulates the Calvin-Benson cycle, not only by leading to the production of NADPH and ATP, but also by regulating the activity of several of its enzymes. The light-regulated activation of these enzymes is being mediated by the ferredoxin/ thioredoxin system, consisting of the stroma-localised proteins ferredoxin (Fd), ferredoxin/thioredoxin reductase (FTR) and thioredoxin (TRX) (Fig. 1.1) (Buchanan 1991) (Buchanan et al. 2002) (Michelet et al. 2013). More specifically, ferredoxin can transfer an electron to TRX via FTR and the reduced TRX regulates the activation of four enzymes of the Calvin-Benson cycle (phosphoribulokinase (PRK), glyceraldehyde-3-phosphate dehydrogenase (GAPDH), fructose-1,6-bisphosphatase (FBPase), and sedoheptulose-1,7-bisphosphatase (SBPase)) via reduction of regulatory disulphide bonds at these enzymes. This reduction leads to their light-driven activation.

The primary step of the Calvin-Benson cycle is the CO_2 assimilation by the Ribulose bisphosphate carboxylase/oxygenase, or Rubisco, which carboxylates ribulose-1,5-biophosphate into 3-phosphoglycerate. Rubisco is the dominant carbon-fixing enzyme in photosynthetic organisms. Despite the significant role of this enzyme to the global primary biomass production, Rubisco's catalyst activity is extremely slow, it is not selective for CO_2, and its ability to bind O_2 is compromising its carboxylase activity. More specifically, the oxygenase activity of Rubisco results in the synthesis of phosphoglycerate and the initiation of the energy-consuming process of photorespiration (Abadie et al. 2016). Especially for aquatic photosynthetic organisms, CO_2 availability becomes even more challenging by the slow diffusion rate of CO_2 in the water in comparison with the air (around 10.000 times slower). Another issue that challenges the cellular availability of CO_2 is the fact that in high pH, inorganic carbon takes the form of HCO_3^- , instead of CO_2 (Gehl and Colman 1985). Algae have developed a series of adaptations to overcome those obstacles, called CO_2-concentrating mechanisms (CCMs) (Moroney and Ynalvez 2007). In general, those mechanisms aim to import HCO_3^- within the cells and the chloroplast via a series of ion transporters, to dehydrate HCO_3^- into CO_2 with the action of carbonic anhydrases, and to increase the local concertation of CO_2 around Rubisco in order to promote its carboxylase activity over the oxygenase one.

1.1.2 Light as an environmental cue (photoreceptors)

Additionally, to the fundamental role of light on photosynthesis, light is also a source of spatiotemporal information for cells and organisms. The sunlight can reach a vast variety of ecosystems, some of them in excess and some of them in deficit, such as in great depths of aquatic environments. Organisms have developed adaptations in regards to different light intensities, light quality and the diurnal presence of light, in order to optimize their survival in different ecosystems. They have also developed light-sensing systems, linked to cellular signalling pathways in order to modulate their cellular responses in accordance to a continuously variable environment.

Those light-sensing systems have been mostly based on photoreceptors, proteins which turn light of a specific quality into a cellular signal. Photoreceptors are gaining their light-sensing abilities from some non-protein photopigments which are attached to their molecule. Those pigments, when sensing the light, they react via photoisomerization or photoreduction which results in conformational changes to the photoreceptor and its final activation in order to initiate the transmission of the cellular signal. These photopigments or chromophores vary between the photoreceptors and characterise the type of the photoreceptor they are attached to. For example, retinylidene proteins contain retinal as a chromophore, biliproteins contain bilin and flavoproteins flavin. An exception to this is the UV-sensing plant photoreceptor UVR8, which does not possess an external photopigment, but instead, it senses light via tryptophan residues within its protein sequence (Rizzini et al. 2011) (Christie et al. 2012).

In animals, we often refer as ‘’photoreceptors’’ to photoreceptor-containing neuroepithelial cells in the retina, such as the mammalian rods, cones and intrinsically photosensitive retinal ganglion cells (ipRGCs). Those cells contain photoreceptor proteins, such as rhodopsins, photopsins and melanopsins, which when triggered by light of a specific quality and intensity, they cause the change of the cell’s membrane potential, a fundamental step for colour-vision.

While animals have adapted their photosensory systems in accordance to their ability to move and to their survival needs (search for food, sense predators, need for orientation sensing, etc), plants photoreceptors have been developed to serve different adaptation needs. More specifically, plant photoreceptors are mainly used for the maximal optimisation of their photosynthetic apparatus, as well as for their developmental programming. The sessility of higher plants highlights even more their need of acclimation towards the available light source. On the other hand, in microalgae, photoreceptors cover the need for the orientation of these motile organisms within their aquatic environments, as well as for the programming of their development and reproduction.

Higher plants and microalgae express a variety of photoreceptors which can absorb light of wavelengths from almost all the spectrum of visible and UV light (Fig. 1.2). First, there are the phytochromes, bilin-containing photoreceptors which absorb in the red/far-red spectrum, allowing the competition with neighbouring plants for photosynthetically active red light. The covalently attached bilin molecules enable phytochromes to photoconvert between the red and far-red absorbing forms (Rockwell, Su, and Lagarias 2006). Phytochromes are widespread in higher plants. In angiosperms there are 3 conserved genes encoding the apoproteins of phytochromes (*PHYA*, *PHYB* and *PHYC*), while additional phytochromes have been identified in dicotyledons as result of gene duplication events during the evolution (Inoue, Nishihama, and Kohchi 2017) (Franklin and Quail 2010). Phytochromes in plants participate in responses such as germination (Shinomura et al. 1996) (Botto et al. 1996), de-etiolation (Nagatani, Reed, and Chory 1993) (Somers et al. 1991), gravitropism (Liscum and Hangarter 1993), shade avoidance responses (Robson, Whitelam, and Smith 1993) (Devlin et al. 1999), cell elongation and root hair growth (Reed et al. 1993), the development of stomata (Boccalandro et al. 2009) (Casson et al. 2009) and photoperiodic flowering (Johnson et al. 1994) (Mockler et al. 2003).

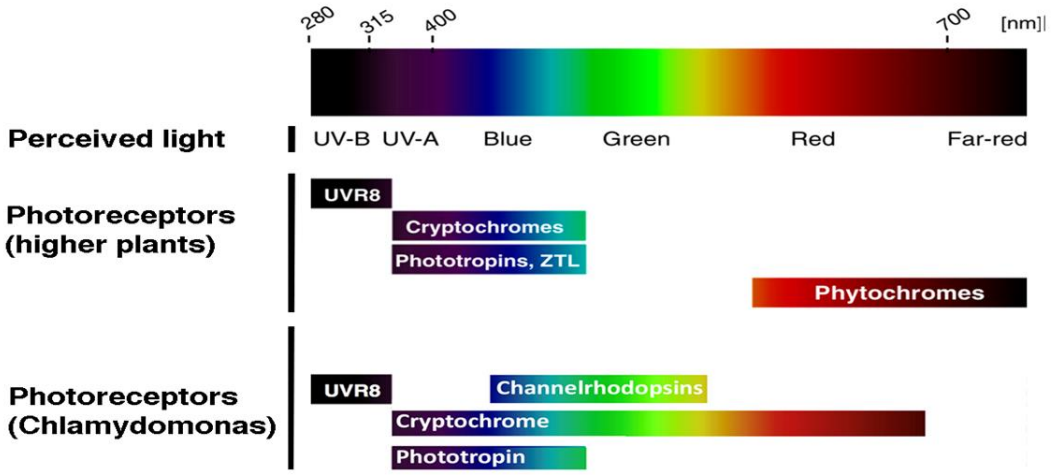

Figure 1.2: The families of photoreceptors in higher plants and in the model green alga Chlamydomonas reinhardtii, alongside their corresponding absorption spectrums. Both in higher plants and in C. reinhardtii we find the UV-B photoreceptor UVR8 and the blue light photoreceptors Cryptochromes and Phototropins. Land plants do not contain rhodopsins. While the phytochrome family of photoreceptors is not encoded by the genome of C. reinhardtii, it's the animal-type CRY that can perceive red light, alongside yellow and blue when it is fully reduced. Figure modified from (Heijde and Ulm 2012).

The rapid attenuation of red and far-red light with depth in aquatic environments (Morel 1988) (Depauw et al. 2012) is forcing algal species to utilise light of shorter wavelengths. However, phytochromes are present in some streptophyte algae and cyanobacteria (Falciatore and Bowler 2005) (Rockwell and Lagarias 2010). While the phytochrome family of photoreceptors is not encoded by the genome of *Chlamydomonas reinhardtii*, a model chlorophytic algae, this organism can synthesize phycocyanobilin, a bilin chromophore (Duanmu et al. 2013). More specifically, the genome of *C. reinhardtii* contains the cyanobacterial-derived genes of a heme oxygenase (HMOX1) that catalyses the conversion of heme to biliverdin and a ferredoxin-dependent bilin reductase (PCYA) that converts biliverdin to phycocyanobilin. Both enzymes are active and produce the final product *in vivo*.

UV-B radiation has the highest energy from the light spectrum and it can damage DNA and lead to mutations, as well as impair the photosynthetic apparatus. The acclimation to UV-B light is being controlled by the UV-B-sensing photoreceptor UV RESISTANCE LOCUS 8 (UVR8). UVR8, while in a homodimer form, perceives the UV-B radiation via an intrinsic tryptophan, monomerizes and increases its nuclear accumulation. The monomer of UVR8 interacts with the E3 ubiquitin ligase CONSTITUTIVELY PHOTOMORPHOGENIC1 (COP1) and the heterodimer initiate the

signalling pathway for UV-B acclimation (Rizzini et al. 2011). COP1 interacts with the SUPPRESSOR OF PHYA 1 (SPA1) and other components of E3 ubiquitin ligase complexes to ubiquitinate the bZIP transcription factor ELONGATED HYPOCOTYL 5 (HY5). HY5 induces UV-B acclimation genes and photomorphogenesis responses. The interaction between UVR8 and COP1 promotes HY5 expression, possibly by functional disassociation of COP1 from the COP1-SPA1-containing E3 ubiquitin ligase complexes (Oravecz et al. 2006) (Huang et al. 2013).

UVR8 was first described in *Arabidopsis thaliana*. However, it has been functionally conserved throughout the green lineage, from the *Chlorophytes*, where it first appears, to bryophytes, lycophytes, and angiosperms (Fernandez et al. 2016). *C. reinhardtii* contains a UVR8 protein, as well as an orthologue of *Arabidopsis* COP1 (Tilbrook et al. 2016). *Chlamydomonas* UVR8 has structural similarity to the *Arabidopsis* UVR8 and, as the latter one, it monomerizes in response to UVB light, interacts with the orthologue of COP1 and initiates a UV-B- triggered cellular signal. The level of functional conservation of UVR8 between those two evolutionarily distant organisms is showcased by the fact that *Chlamydomonas* UVR8 can interact with the *Arabidopsis* COP1 in a yeast-two-hybrid assay. Also, *Chlamydomonas* UVR8 can restore the UV-B signalling in a *uvr8* null mutant in *Arabidopsis (Tilbrook et al. 2016)*. UVR8 in *C. reinhardtii* mediates the UV-acclimation response and also, induces photoprotection by upregulation of the genes of the photoprotection proteins LHCSR1, PSBS and LHCSR3 (Allorent et al. 2016) (Tokutsu, Fujimura-Kamada, Yamasaki, et al. 2019). This signalling pathway and the roles of those proteins in photoprotection will be analysed in detail in the following chapters.

Rhodopsins are photoreceptors, containing opsin apoproteins and a covalently linked retinal, which absorbs the light and mediates the light-induced signal (Hubbard and Kropf 1958). Rhodopsins are widely spread throughout all the three kingdoms: bacteria, archaea and eukaryotes. However, no rhodopsins have been found in land plants. Rhodopsins are mainly divided into two groups: animal and microbial rhodopsins, or type I and type II, respectively (Ernst et al. 2014). Animal rhodopsins are G-protein-coupled receptors found in the rod cells of the retina, where they function as the primary photoreceptor molecules of vision (Palczewski 2006).

Microbial rhodopsins, such as bacteriorhodopsin in bacteria or channelrhodopsin in green algae, are membrane proteins which can function as light-sensing pumps or channels (Govorunova et al. 2017) (Gushchin and Gordeliy 2018).

In *C. reinhardtii*, two animal type rhodopsins were identified in the eyespot, a light-sensitive organelle important for phototactic orientation, Chlamyrhodopsin 1 (COP1) and Chlamyrhodopsin 2 (COP2) (Deininger et al. 1995). Two microbial rhodopsins have been also found in *C. reinhardtii*, channelrhodopsin 1 and 2 (ChR1 and ChR2), which are being encoded by the genes COP3 and COP4, respectively (Fig. 1.3). Both of them are light-gated ion channels; ChR1 is selective for H^+ and ChR2 conducts Na^+, K^+, and Ca^{2+} (Nagel et al. 2002) (Nagel et al. 2003). ChRs mediate photophobic responses and phototaxis by depolarizing the eyespot membrane and, eventually, the flagellar membrane upon light absorption. This results in a change of the algal orientation toward a light source (Sineshchekov, Jung, and Spudich 2002) (Govorunova et al. 2004) (Berthold et al. 2008). The eyespot-located ChR1 is shown to be downregulated by another photoreceptor, phototropin (PHOT) (Trippens et al. 2012). The functional analyses and expression of those channelrhodopsins into different organisms has created the field of optogenetics (Boyden et al. 2005) (Li et al. 2005) (Ishizuka et al. 2006) where light- responsive channels are expressed in different organisms to control the activity of neurons or other cell types in a light-dependent manner. This technique has enabled us to advance our understanding or the human neuron system and the function of the brain. Eight microbial- type rhodopsins, containing a histidine kinase domain and a response regulator at their C'-terminus, have been also identified in the genome of *C. reinhardtii* (COP5-COP12), constituting the subfamily of histidine kinase rhodopsins (HKRs) (Fig. 1.3) (Kateriya et al. 2004). Those HKRs share strong sequence homology and, possibly, functions, while those are in large not identified.

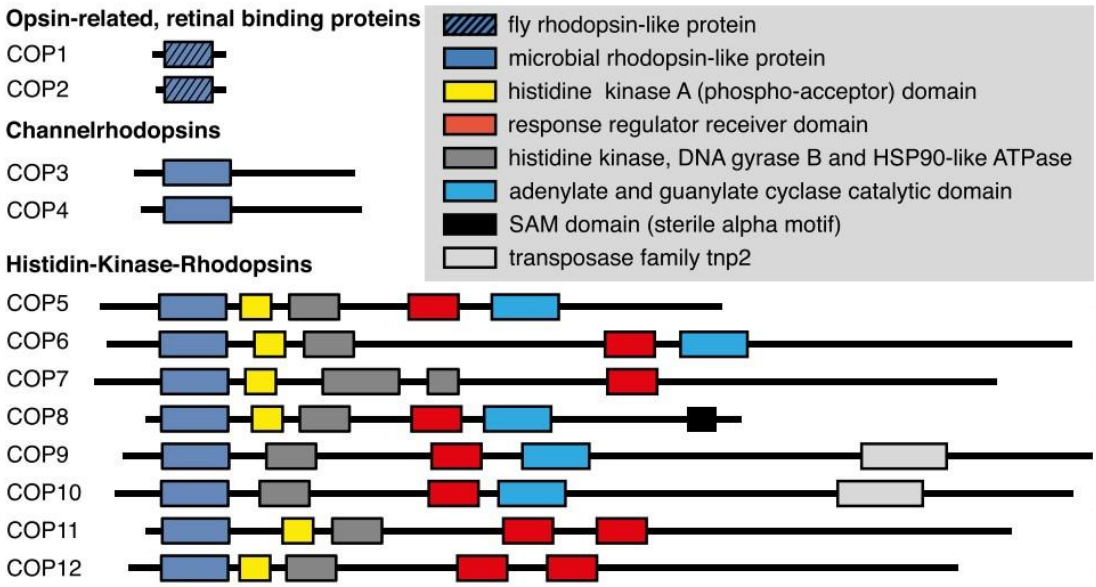

Figure 1.3: The 12 rhodopsins found in the genome of C. reinhardtii and their domain structures. Figure modified from (Greiner et al. 2017).

Blue-light signalling is essential for organisms and its perception is being mediated by flavoprotein receptors, such as the photolyase/cryptochrome superfamily, phototropins and members of the Zeitlupe family. Each class of these photoreceptors oxidises flavin as a light-absorbing chromophore.

Cryptochromes and photolyases form a superfamily of photoreceptors, which absorb blue and UV-A light. Despite their great amino acid similarities, cryptochromes have lost or reduced the DNA repair abilities of photolyases and, instead, have developed novel signalling abilities. Cryptochromes are distributed among eubacteria, archaea and eukaryote and can be roughly divided into three subfamilies: plant cryptochromes, animal cryptochromes, and cryptochrome DASH proteins (DASH: Drosophila, Arabidopsis, Synechocystis, Homo) (Chaves et al. 2011). Animal-type cryptochromes can be further divined into types I and II and they are closely related to photolyases. Plant cryptochromes mediate seedling growth, photoperiodic flowering and entrainment of the circadian clock in plants (Chaves et al. 2011), while animal cryptochromes are responsible for circadian clock responses (Ceriani et al. 1999) (Kume et al. 1999) and magnetoreception (Gegear et al. 2010) (Ritz, Adem, and Schulten 2000).

Cryptochromes are being activated when blue-light illumination activates them, by photoreducing the flavin from its oxidized form (FADox) at its dark inactive state to FADHo. FADHo can be further reduced by subsequent illumination with a photon of either blue or green light to FADH. The reoxidation of FADHo to its inactive fully oxidized form occurs instantly in the presence of molecular oxygen.

The first cryptochrome has been discovered in the model plant *Arabidopsis thaliana* and got the name CRY1 (Ahmad and Cashmore 1993). In total, two more cryptochromes have been identified in *Arabidopsis thaliana*, CRY2 and CRY3. In the nuclear genome of *C. reinhardtii,* cryptochromes of all three major groups have been identified. More specifically, *C. reinhardtii* expresses one plant-type cryptochrome (CPH1 or pCRY) (Reisdorph and Small 2004), one animal-type cryptochrome (aCRY) (Beel et al. 2012) and two DASH-type cryptochromes (CRY-DASH1 and CRY-DASH2) (Beel et al. 2012) (Beel et al. 2013). While *C. reinhardtii* genome, up to our knowledge, does not encode a red-light photoreceptor, such as phytochrome, it's the aCRY that can perceive red light, alongside yellow and blue when it is at its fully reduced state. Furthermore, in contrast with higher plants CRYs, the oxidation of aCRY is independent of oxygen concentration (Spexard et al. 2014).

Phototropin (PHOT) is also a flavin-containing photoreceptor, with a serine/threonine kinase domain which undergoes autophosphorylation upon blue-light illumination. Phototropin was first discovered in *Arabidopsis thaliana* and was named after its role in mediating phototropism (Christie et al. 1999). The sensory region of PHOT is consisted of two conserved domains, LOV1 and LOV2 (LOV stands for Light Oxygen and Voltage), which bind one flavin mononucleotide (FMN) as a chromophore each, stoichiometrically (Christie et al. 1999). PHOT-controlled cellular responses in *C. reinhardtii* are in the centre of the studies of this thesis and therefore, PHOT'S evolution, structure, activation mechanism and cellular role in higher plants and in *Chlamydomonas* will be analysed in detail in chapter 1.3.

Finally, higher plants contain several others LOV-containing photoreceptors other than phototropin, which constitute the Zeitlupe family proteins. The Zeitlupe family comprises of three photoreceptors: Zeitlupe (ztl), Flavin-binding kelch repeat F-box 1 (fkf1) and LOV kelch protein 2 (lkp2). Those proteins regulate responses associated

with the regulation or the circadian clock and the photoperiodic control of flowering in *Arabidopsis* (Somers et al. 2000) (Nelson et al. 2000) (Schultz et al. 2001). Proteins of the Zeitlupe family have not been identified in the genome of *C. reinhardtii* (Merchant et al. 2007) or other model green algae, such as *V. carteri* and *O. tauri* (Corellou et al. 2009) (Prochnik et al. 2010).

1.2 Chlamydomonas as a model organism

C. reinhardtii is a well-established model organism for studying photosynthesis, chloroplast biology, cell cycle control, and cilia structure and function, based on a number of unique characteristics (Salome and Merchant 2019).

C. reinhardtii is a ciliated unicellular green alga, which has diverged from the ancestor of plants more than one billion years ago (Yoon et al. 2004). Green algae are the closest relatives to land plants; they are part of the green lineage and they have emerged from the algae division of Chlorophyta and Charophyta, the same division from which land plants came from. *C. reinhardtii* belongs to the Chlorophyta phylum.

The *C. reinhardtii* cell has two cilia or flagella of equal length that are located at one pole of the cell and are used for phototaxis, in order to optimise the light exposure during photosynthesis, as well as for cell-cell recognition during mating (Fig. 1.4).

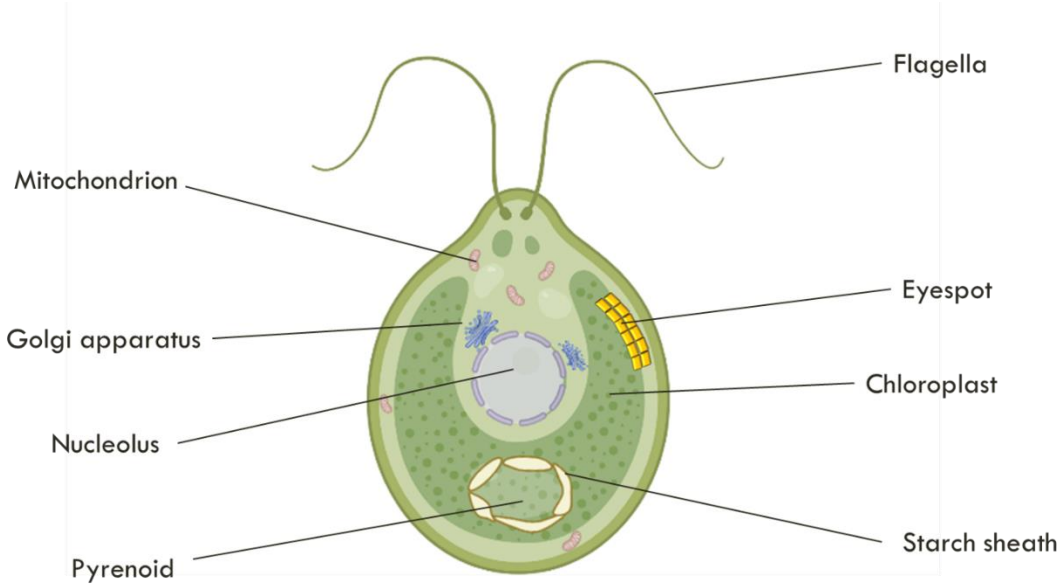

Figure 1.4: The C. reinhardtii cell.

More than half of the cell is being occupied by a cup-shaped chloroplast (Sager and Palade 1957) (Engel et al. 2015). In the chloroplast, there is also a spherical structure, called the pyrenoid. It is located at the pole opposing the flagella, which contains high local concentrations of Rubisco. Rubisco plays an essential role for the fixation of CO_2 and its localisation in the pyrenoid serves the optimisation of the CO_2-Concentrating mechanisms (CCM).

Within the chloroplast, there is an orange- to red- coloured spot, as observed by bright-field microscopy, called the eyespot. The eyespot is localised at the chloroplast membranes and it is composed of two layers of carotenoid-rich globules (Fig. 1.5). This structure mediates phototaxis, via light-regulated flagellar movement, which happens under the regulation of ChR1 and ChR2 (Harz et al. 1992) (Hegemann 1997) (Eitzinger et al. 2015) (Engel et al. 2015).

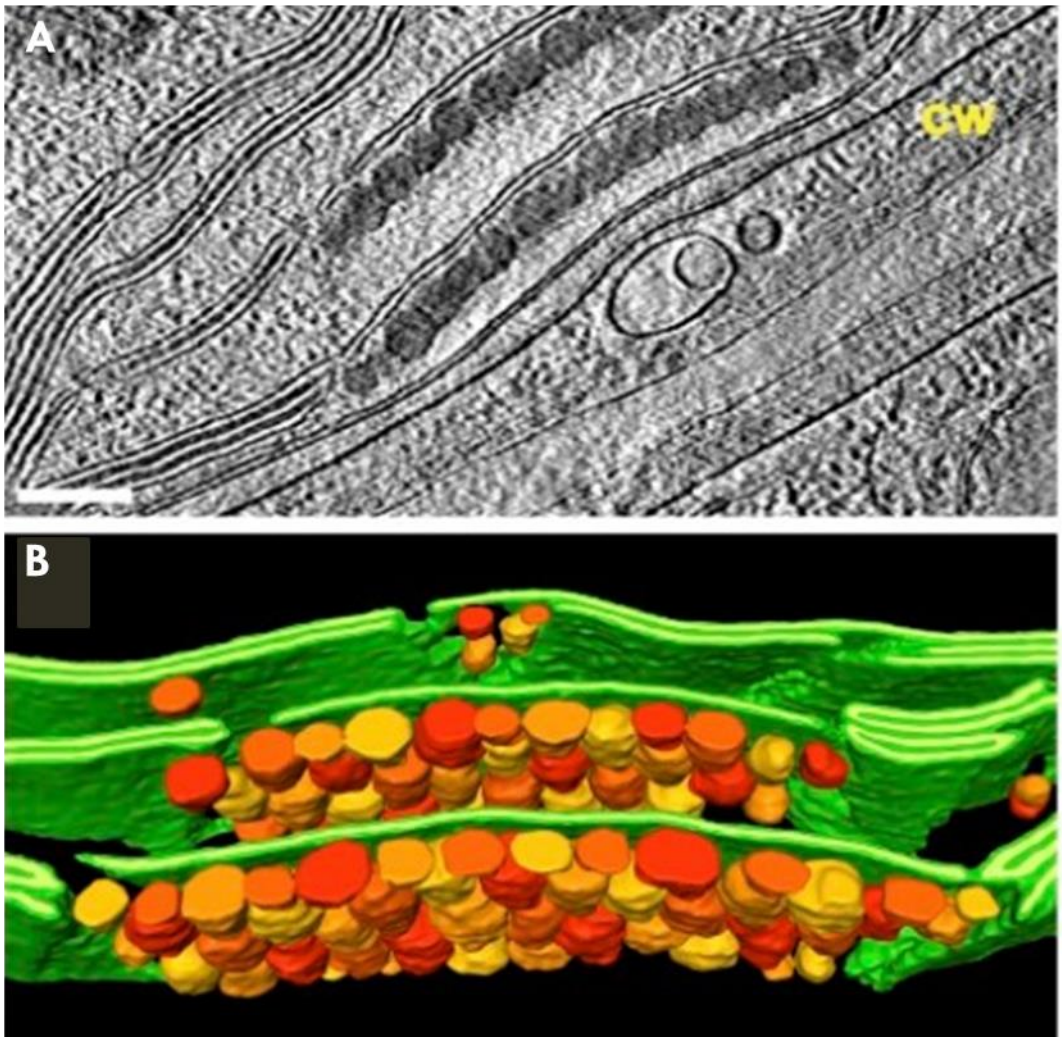

Figure 1.5: The 3D architecture of the eyespot. A) Image of the eyespot as viewed via cryo-electron tomography and B) the corresponding 3D segmentation from A) showing just the thylakoid membranes (green) and the eyespot globules (red, orange and yellow). As it can be observed, the eyespot apparatus consists of two arrays of globules, separated by and packed within neighbouring thylakoids. Images taken from (Engel et al. 2015).

C. reinhardtii has a haploid nuclear genome, which is particularly useful for genetic studies, since loss-of-function mutations lead to immediately observable phenotypes, as opposed to the diploid organisms. The whole nuclear genome from 39 independent *C. reinhardtii* strains and 12 field isolates has been sequenced (Flowers et al. 2015) (Gallaher et al. 2015). Other than the nuclear genome, *C. reinhardtii* also contains chloroplast and mitochondrial genomes, both of which have been sequenced (Gallaher et al. 2018). The chloroplast genome is being organised in large protein-DNA complexes, called nucleoids. Each *C. reinhardtii* cell contains approximately 80 copies of the chloroplast genome (Gelvin, Heizmann, and Howell 1977) (Gallaher et al. 2018)

and each genome contains 99 genes, including genes involved in the chloroplast gene translation, photosynthesis and CO_2 fixation (such as the large subunit of Rubisco), as well as the genes for the subunits of a plastid-encoded RNA polymerase (PEP). The mitochondrial genome consists of a linear molecule of 15.8 Kbp of length, significantly smaller from the mitochondrial genomes of land plants (Gallaher et al. 2018). This genome encodes 8 proteins (7 of which being subunits of the respiratory chain or the ATP synthase) and fragments of 3 tRNAs and 15 rRNAs. It is estimated that approximately 130 copies of the mitochondrial genome are present in each cell.

A big number of molecular tools and technologies are available for experimental design with *C. reinhardtii*. Forward genetics can be easily achieved by inducing mutations in each of the three genomes of the cell (nuclear, chloroplast and mitochondrial) by either exposure to mutagens (such us UV, X-ray and gamma irradiation, ethylmethanesulfonate (EMS), N-methyl-N-nitro-N-nitrosoguanidine (MNNG) and methylmethanesulfonate (MMS)) or by insertional mutation. The latter is done usually with the use of a linearized plasmid or a PCR product that includes a selection marker (Jinkerson and Jonikas 2015). If mutants are available in both mating types, combination of mutants can be achieved by crossing.

Nuclear transformation in *C. reinhardtii* is straightforward and intensively studied. Despite though, the recent advances in the field, successful heterologous transgene expression is still being observed in poor rates (Schroda 2019). This can be attributed to the elevated GC content (64%) in the nuclear genome, as well as at the intron density (6.4 introns/gene on average) (Merchant et al. 2007). Transgene expression in *C. reinhardtii* is also found to be specifically silenced by an epigenetic pathway (Neupert et al. 2020).

The efficiency of the transgene expression has been facilitated by the use of strong constitutive promoters, such as PSAD, RBCS2, and a chimeric RBCS2 promoter combined with regulatory elements from the HSP70A promoter. The introduction and spreading of introns, such as the one of the first intron of RBCS2 (rbcS2i1), into codon optimised transgenes can increase their expression, despite their size or the repetition of their sequences (Wichmann et al. 2018) (Baier et al. 2018). Indeed, the insertion of rbcS2i1 in optimized positions within a transgene recruits the transcriptional

machinery and minimises the exons' length, leading to improved expression of that gene. This finding led to the development of the web tool "Intronserter'' (https://bibiserv.cebitec.uni-bielefeld.de/intronserter) (Jaeger, Baier, and Lauersen 2019). Intronserter aims to be a flexible and reliable tool for codon optimisation and optimal intron spreading, in order to provide ready-to-be-synthetised DNA sequences with minimal exon lengths to be used for transformation. Additionally, the CRISPR/Cas9 technology has been adapted for *C. reinhardtii* , widening the variety of ways of genetic manipulations on this organism's genome and facilitating the modification and inactivation of genes by directed gene targeting (Baek et al. 2016) (Baek et al. 2018) (Shin et al. 2016) (Greiner et al. 2017) (Guzman-Zapata et al. 2019) (Shin et al. 2019) (Cazzaniga et al. 2020) (Song et al. 2020) (Kim et al. 2020) (Kang et al. 2020) (Picariello et al. 2020) (Dhokane, Bhadra, and Dasgupta 2020) (Park, Asbury, and Miller 2020) (Cecchin et al. 2021) (Sizova et al. 2021) (Akella et al. 2021) (Asadian et al. 2022).

An insertional mutant library of *C. reinhardtii*, generated by the *Chlamydomonas* Library Project (CLiP) is available for ordering, providing a multifunctional platform for mutant phenotype screening (Li et al. 2016) (Li et al. 2019). This project, funded by the National Science Foundation, has generated 62,389 mutant strains (up to 2019 (Li et al. 2019)) by random mutagenic insertion of a paromomycin resistance cassette in the CC-4533 strain. Since in about the 25% of the strains the indicated gene has not been disrupted, the presence of the insertion should be confirmed. The *Chlamydomonas* Recourse Centre (https://www.chlamycollection.org) is another online respiratory centre, which can provide wild type and mutant cultures of *C. reinhardtii*, as well as molecular reagents, kits and online cultivation and transformation protocols. The Joint Genome Institute's platform Phytozome (https://phytozome-next.jgi.doe.gov/) contains all the information collected on the nuclear genome, including sequences, annotations, and gene identifiers.

Thanks to its unique characteristics, *C. reinhardtii* has been widely used on a diverse set of research topics. Firstly, this green alga has been the subject of photosynthesis studies. *C. reinhardtii* is a facultative autotroph, which can grow in the presence of the reduced carbon acetate in the dark, while retaining a functional photosynthetic

apparatus. This ability has allowed the isolation and study of light-sensitive photosynthesis mutants of *C. reinhardtii* (Levine 1960) (Chua and Bennoun 1975) (Chua, Matlin, and Bennoun 1975) (Piccioni, Bennoun, and Chua 1981) (Spreitzer and Mets 1981) (Wakao et al. 2021). Additionally, the photosynthetic apparatus of *C. reinhardtii*, as well as the CBC enzyme Rubisco share big level of similarity with the corresponding ones from the land plants, such as the model plant *Arabidopsis thaliana* (Fig. 1.6). Consequently, studying the photosynthetic apparatus in *C. reinhardtii* leads to results that can be adapted for higher plants as well, while maintaining the manipulation advantages of a unicellular organism, such as less needed space for growth and shorter generation times.

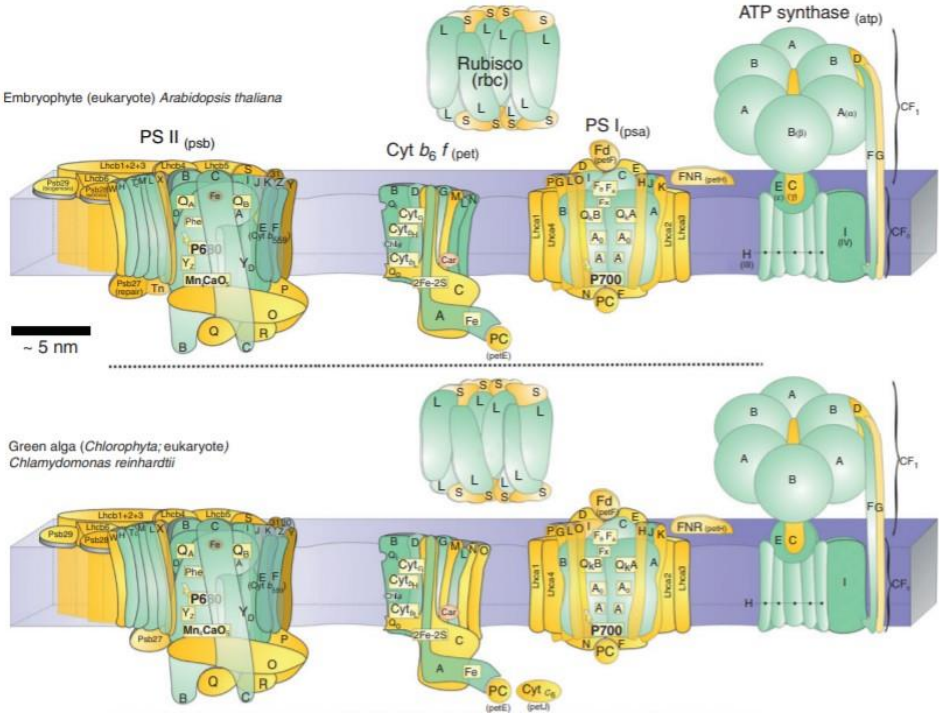

Figure 1.6: The structure of the ETR proteins and complexes (Photosystem II (PSII), Cytochrome b_6f (Cyt b_6f), Photosystem I (PSI), Plastocyanin (PC), Ferredoxin (Fd), ferredoxin–NADP+ reductase (FNR) and ATP synthase), as well as the structure of Rubisco (rbc) from Arabidopsis thaliana (upper part) and from C. reinhardtii (lower part). As it is shown, the structure of the photosynthetic apparatus and of Rubisco is almost identical between the two organisms. The only difference is the presence of Cytochrome c_6 (Cyt c_6) in C. reinhardtii, which acts as an alternative electron carrier to plastocyanin under conditions of copper limitation. Image taken from (Allen et al. 2011).

C. reinhardtii is, additionally, widely used as a subject for cilia structure, function and sensing studies (Dutcher 2014) (Wingfield and Lechtreck 2018) (Salome and Merchant 2019). The scientific interest in the eukaryotic cilia is intense, since defects on the

human cilia proteins can lead to serious health disorders, called ciliopathies. The cilia of *C. reinhardtii* are well conserved though the ciliated eukaryotic organisms and they are easily dispensable in the lab (while retaining the viability of the cell). Those advantages have let *C. reinhardtii* to prevail as a study organism in this field.

Another research topic on *C. reinhardtii* is the study of the circadian system, which regulates almost the entirety of the fundamental cellular responses. Diurnal transcriptomic analyses and gene expression datasets reveal that over 80% of the transcribed genes show strong periodicity between day and night in *C. reinhardtii* (Zones et al. 2015) (Strenkert et al. 2019).

As it was discussed in the first chapter, light represents a very important environmental cue for cellular programming. The above-mentioned unique characteristics of *C. reinhardtii* can justify its ongoing rendering to a model organism for sensory photoreceptor studies and their corresponding signalling pathways. *C. reinhardtii* contains a surprisingly big number of photoreceptors for a unicellular organism. Up to date, 18 photoreceptors are found in the genome of *C. reinhardtii,* including 12 rhodopsins that bind retinal, 4 cryptochromes, PHOT and UVR8 (Greiner et al. 2017). The most well-studied of those photoreceptors of *C. reinhardtii* are shown in Fig. 1.7. What makes photoreception studies even more fascinating in *C. reinhardtii* is the fact that, despite sharing a number of common photoreceptors with higher plants, there are some significant regulatory differences which highlight the evolutionary adaptation throughout the green lineage. For instance, there are two copies of Phototropin in *Arabidopsis,* in contrast with the single PHOT copy in *C. reinhardtii ,* with some distinct and some overlapping functions and with distinct light sensitivities (Christie 2007). The roles of *C. reinhardtii* PHOT and *Arabidopsis* PHOTs also vary significantly, since CrPHOT can regulate gene expression (Im et al. 2006) (Petroutsos et al. 2016) (CrPHOT regulation is going to be elaborated extensively in the next chapter), while AtPHOTs regulate rapid cellular adaptations such as chloroplast relocation, stomatal opening and phototropism (Kagawa and Wada 2002) (Christie 2007) (Inoue, Takemiya, and Shimazaki 2010). Additionally, despite the fact that the genome of *C. reinhardtii* does not encode Phytochrome, the red-light photoreceptor of land-plants, bilin (the chromophore of phytochromes) can be

synthetised in *C. reinhardtii*. More specifically, the enzymes HMOX1, a heme oxygenase and PCYA, a ferredoxin-dependent bilin reductase can synthetise phycocyanobilin, a procedure which is essential for the PSI accumulation in daylight (Wittkopp et al. 2017).

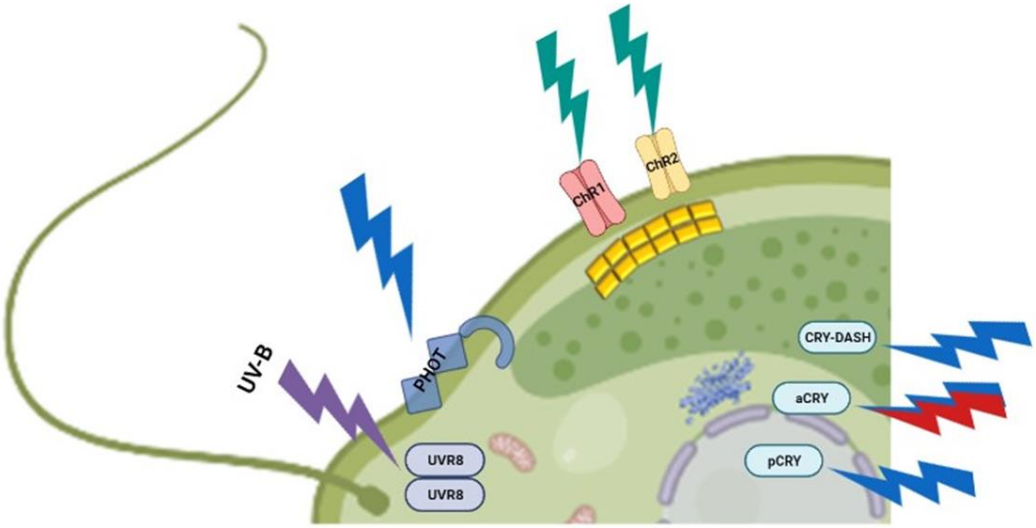

Figure 1.7: The most well studied photoreceptors in C. reinhardtii. UVR8 can be found both in the cytoplasm and in the nucleus. At its inactive form it exists as a homodimer and UV-B irradiation leads to the monomerization and nuclear accumulation of this molecule (Kaiserli and Jenkins 2007) (Favory et al. 2009) (Tilbrook et al. 2016). Phototropin (PHOT) is a blue-light photoreceptor which is being located in the plasma membrane (Huang, Merkle, and Beck 2002) (Huang, Merkle, and Beck 2002) and the flagella (Huang, Kunkel, and Beck 2004) and its localisation in the eyespot has been proven by proteomic data (Schmidt et al. 2006). Channelrhodopsin 1 and 2 (ChR1 and ChR2) are light-gated ion channels, localised in the plasma membrane and are part of the eyespot apparatus (Kateriya et al. 2004). One plant-type Cryptochome (pCRY), one animal-type Cryptochrome (aCRY) and two DASH-type Cryptochromes (CRY-DASH1 and CRY-DASH2) are also found in C. reinhardtii. aCRY is found in the nucleus of vegetative cells and mostly in the cytosol during the night cycle (Franz-Badur et al. 2019). pCRY is predicted to be localised in the nucleus, but there is still lack of experimental data (Kroth, Wilhelm, and Kottke 2017). CRY-DASH1 contains a chloroplast transit peptide and it is exclusively found in the chloroplast (Rredhi et al. 2021). All Cryptochromes are blue-light regulated, but aCRY can perceive red light, alongside yellow and blue when it is at its fully reduced state.

1.3 Phototropin in Chlamydomonas

1.3.1 Evolution

Phototropin (PHOT) is a blue-light activated Ser/Thr kinase that undergoes autophosphorylation upon irradiation and is located at the plasma membrane of

several algae and higher plants' cells. PHOT senses the blue light via two photoreceptive domains, LOV1 and LOV2 (Christie et al. 1999). Despite the existence of the LOV domains as blue-light sensors in structurally diverse proteins in organisms from all the three kingdoms of life (Crosson, Rajagopal, and Moffat 2003) (Krauss et al. 2009), phototropins are found uniquely to the green lineage. A phylogenetic study, based on genomic and transcriptomic data from land plants and algae revealed that the phototropins originated in an ancestor of Viridiplantae (the clade that includes land plants and green algae), since no phototropin homologues have been found in glaucophytes or in red algae (Fig. 1.8) (Li et al. 2015). In algae, phototropins exist in single copies with the exception of Zygnematales, where they exist in two (PHOTA and PHOTB). The multi-copy existence of phototropins in land plants, such as in *Arabidopsis thaliana*, which expresses two copies of PHOT (PHOT1 and PHOT2), is due to independent duplications in mosses, ferns, and seed plants (Fig. 1.8). Those duplications events were coupled with functional evolution of phototropins, since every duplicated PHOT also diverged so to specialize in responding in either low– or high-light, while keeping some overlapping functions with the ''ancestral'' one (Christie 2007). The independence of PHOT duplication led to the suggestion that a single PHOT ancestral sequence was the one which gave rise to the multiple gene copies throughout the green lineage and that seed plant PHOT1 and PHOT2 do not have orthologs outside of seed plants. This comes in contrast with a previous suggestion, which was based on limited taxonomic data, that the seed plant PHOT2 ortholog is the ancestral phototropin and that PHOT1 evolved in a later time (Galvan-Ampudia and Offringa 2007).

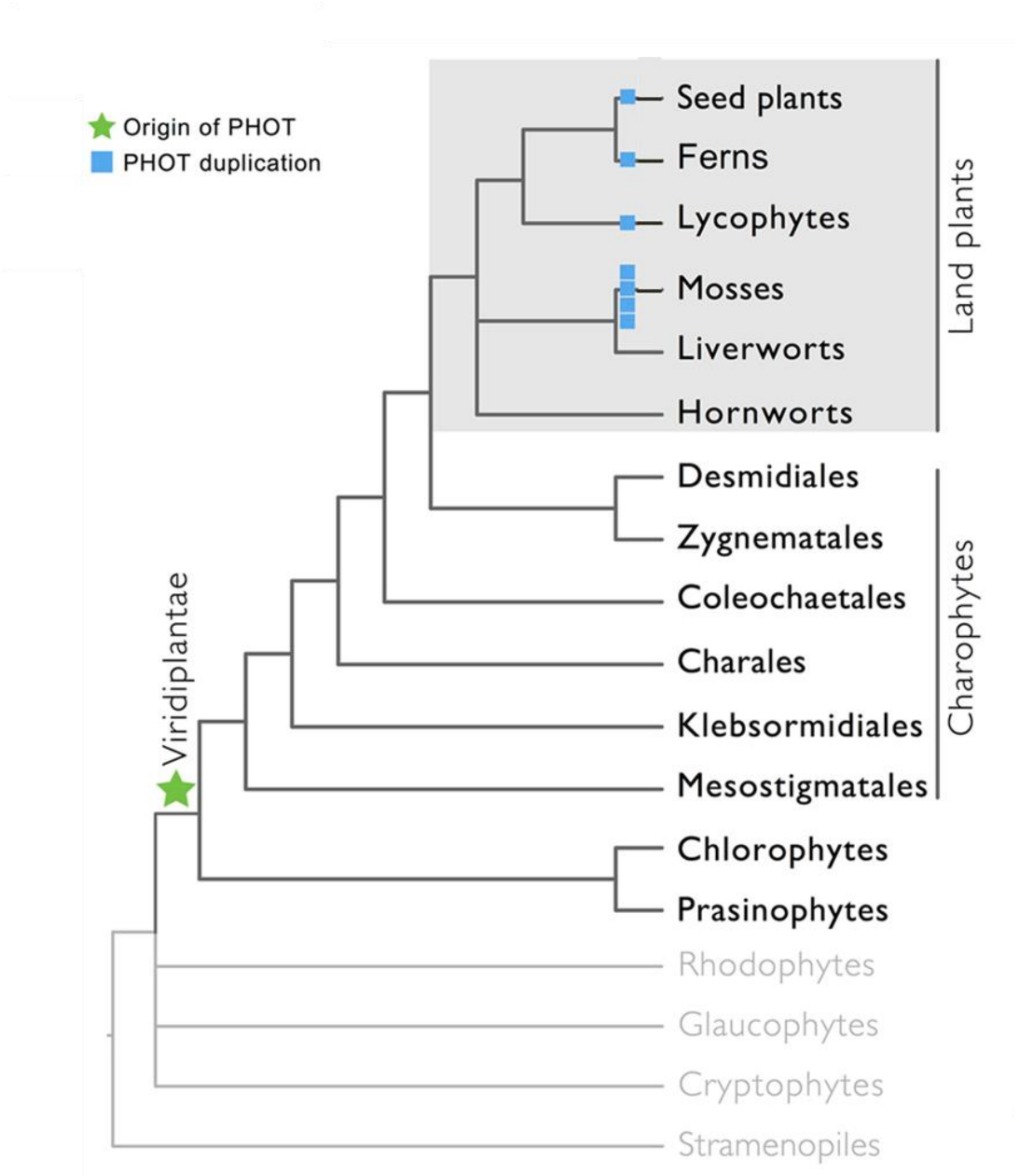

Figure 1.8: Presence and evolution of PHOT throughout the green lineage. PHOT is present in Land Plants and in green algae (Charophytes, Chlorophytes and Prasinophytes), but it has not been screened in Rhodophytes, Glaucophytes, Cryptophytes and Stramenopiles, leading to the indication that PHOT originated in a common ancestor of Viridiplantae (green star). Independent PHOT duplications (blue squares) happened in Seed Plants, Ferns, Lycophytes and Mosses. Image adapted from (Li et al. 2015)

At variance with higher plants, *C. reinhardtii* genome encodes for only one PHOT which is different at its structure and functions. *Chlamydomonas* phototropin is smaller than AtPHOTs (759aa compared to 996aa of AtPHOT1 and 915aa of AtPHOT2) (Fig. 1.9). It also lacks the N' terminal extension and around 70 amino acids of the linker region between LOV1 and LOV2, as is found in higher plants' phototropins (Huang, Merkle,

and Beck 2002). Those regions contain autophosphorylation sites in other PHOTs (Kinoshita et al. 2003) (Salomon et al. 2003) which are not conserved in CrPHOT. CrPHOT is more similar to AtPHOT2 (39% protein sequence identity) than with AtPHOT1 (35% identity) (Huang, Merkle, and Beck 2002). Also, CrPHOT exist in monomeric form (Okajima et al. 2014), while *Arabidopsis* PHOTs are proposed to form dimers via their LOV1 domains (Nakasako et al. 2008) and to internalize from the plasma membrane upon blue-light activation (Kaiserli et al. 2009). Despite those differences and the relatively low homology, CrPHOT can complement several physiological responses mediated by PHOT1 and PHOT2 in *Arabidopsis*, indicating a possible similarity in the activation mechanism and signal transduction between CrPHOT and the AtPHOTs (Onodera et al. 2005).

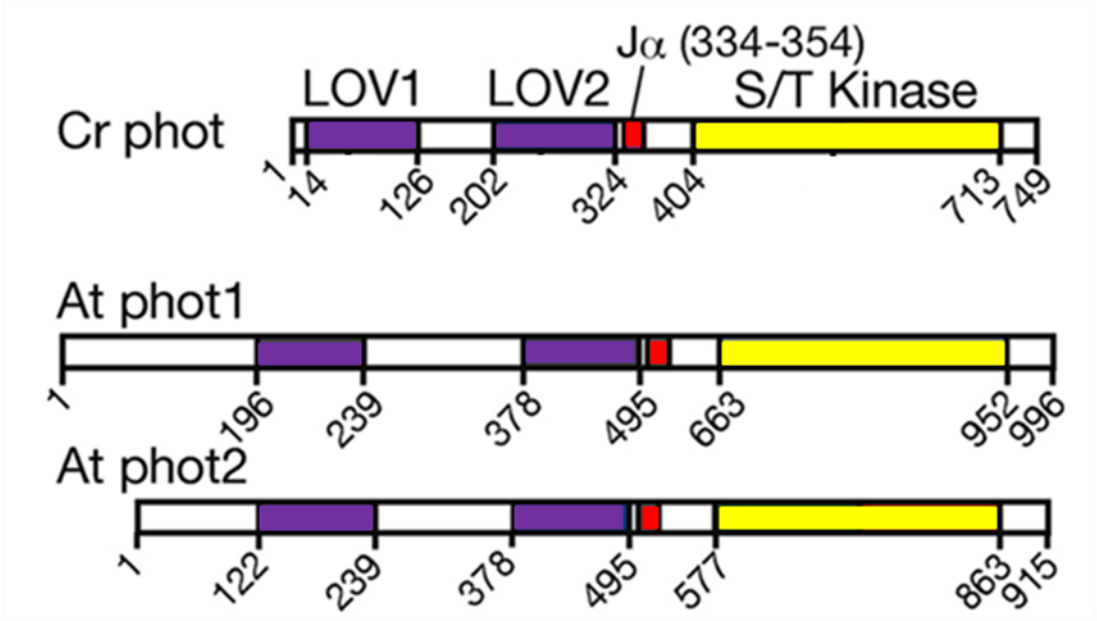

Figure 1.9: Secondary structure and length of the CrPHOT, in comparison with AtPHOT1 and AtPHOT2. The LOV domains (LOV1 and LOV2) are indicated with purple colour, the Ja helix with red and the Ser/Thr kinase domain with yellow. Image adapted from (Okajima et al. 2014).

1.3.2 Structure

PHOT consists of a sensory region at its N' terminal half of the molecule and a regulatory one at its C' terminal. The sensory region is being constituted by two conserved domains, LOV1 and LOV2 (LOV stands for Light Oxygen and Voltage), which

appear in tandem (Fig. 1.9). Both LOV domains bind one flavin mononucleotide (FMN) as a chromophore each, stoichiometrically (Christie et al. 1999). The LOV domains have the aminoacid length of around 110aa (LOV2 is slightly longer than LOV1) and are highly conserved between the PHOTs from different organisms. Despite the fact that LOV1 and LOV2 share the same basic structure and have the same photocycles, they appear to have distinct roles on the photoreceptor's activation (Christie et al. 2002). Blue-light sensing requires both LOV domains *in planta* (Sullivan et al. 2008), but the one cannot replace the function of the other (Kaiserli et al. 2009). LOV2 is being flanked by two helices, the A'α helix at its N-terminus and the Jα helix at its C-terminus, which are critical for the activation of the photoreceptor (Harper, Neil, and Gardner 2003) (Sullivan et al. 2008) (Cho et al. 2007). Up to date there is not experimental validation of such helices flanking LOV1.

The signalling/ regulatory part of the phototropin, which is located at the C' terminal of the molecule, consists of a Ser/Thr kinase domain (Fig. 1.9), which places phototropin in the AGC family of protein kinases (cAMP-dependent protein kinase, cGMP-dependent protein kinase G, and phospholipid-dependent protein kinase C) (Bogre et al. 2003). In the kinase domain, the ATP -binding catalytic cleft is being enclosed in between two subdomains: the N-lobe and the C-lobe. Within the catalytic clef there is an ATP-binding residue, called ''gatekeeper'' (Schnabel et al. 2018). There is also the activation loop (A-loop), which originates from the C-lobe and is often located between the two lobes (Fig. 1.10). Fourier Transform Infrared (FT-IR) spectroscopy on the full-length CrPHOT, obtained from E. coli, revealed that the activation loop is unstructured and it adopts an alpha helical structure in the dark, while undergoing major conformational changes after blue-light illumination (Pfeifer et al. 2010). Autophosphorylation of the activation loop at containing sites initiates the kinase activity.

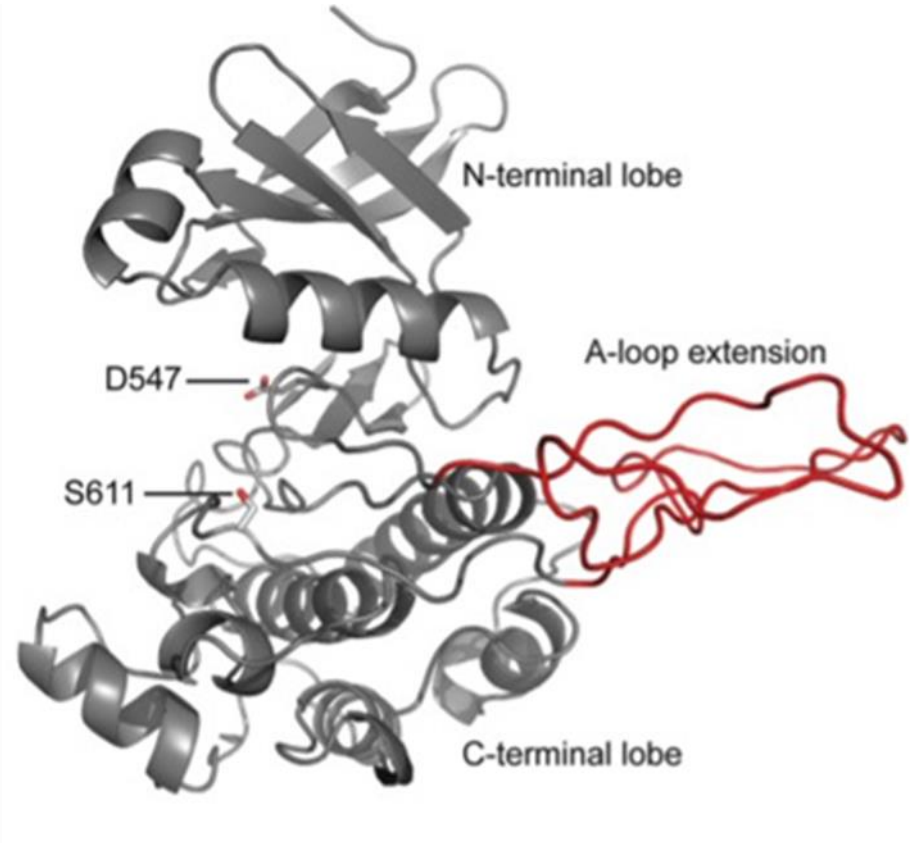

Figure 1.10: 3D model structure of the kinase domain at CrPHOT, created by MODELER (Sali and Blundell 1993) with the use of 30 crystal structures of homologous kinases as templates. The N- and C- terminal lobe enclose the catalytic cleft. The Activation loop (A-loop), coloured red, originates from the C-lobe (D547-S611, indicated here) and it is located between the two lobes. Image adapted from (Pfeifer et al. 2010).

Small angle x-ray scattering (SAXS) data on the full-length CrPHOT revealed for the first time a tandem arrangement of LOV1, LOV2 and the kinase domain, both in dark and under blue light exposure (Okajima et al. 2014). The same study also suggests that CrPHOT has an overall shape of a chair, with the kinase domain being the chair's base and the LOV domains being the backrest, slightly offset from the legs (Fig.1.11). After blue light irradiation, LOV2 extends substantially away from the kinase domain, while the LOV1-LOV2-kinase angle rotates without altering the initial distance between LOV1 and LOV2.

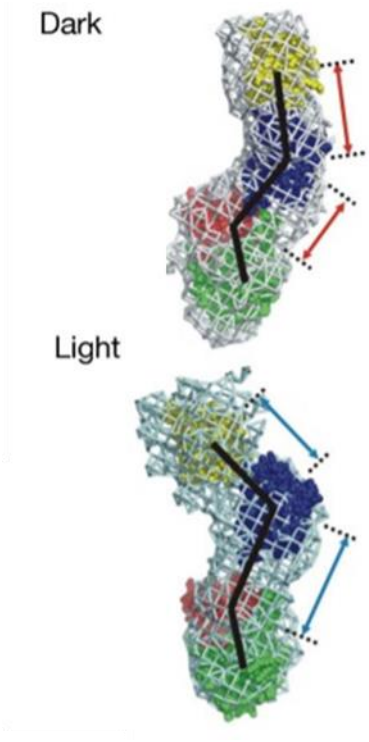

Figure 1.11: Low resolution molecular models of full CrPHOT in dark and after blue-light illumination. LOV1 is shown with yellow, LOV2 with dark blue, the N-lobe of the kinase domain with red and the C-lobe with green. The positions of each domain are references with black bars. The position and orientation between each domain are indicated with red arrows in the dark and with blue arrows in the light. The models were restored with the use of the SAXS profiles of S> 0.006 $Å^{-1}$. Image adapted from (Okajima et al. 2014).

Despite the data obtained from SAXS, the crystal structure of the full length CrPHOT is not available yet. However, the crystal structure of the LOV1 in the dark and after the light illumination has been revealed, providing interesting insights on the photocycle of the domain. (Fedorov et al. 2003).

1.3.3 Activation mechanism

The structure of PHOT and the arrangement of LOV1, LOV2 and the kinase domain, facilitate the activation of the protein upon blue light irradiation and the transmission of the cellular signal.

The perception of blue light is mediated by the chromophore FMN (flavin mononucleotide) which is bound to each of the LOV domains non-covalently in the

dark (Crosson and Moffat 2001). In the dark, the FMN is its ground state and it absorbs maximally near 447 nm (D450) (Fig. 1.12) (Christie et al. 1999) (Salomon et al. 2000) (Swartz et al. 2001). After blue-light illumination, the FMN forms a covalent bond with a conserved cysteine residue of the LOV domain via its C4(a) atom, forming a cysteinyl photoadduct which absorbs at around 390nm (S390) (Crosson and Moffat 2001) (Fedorov et al. 2003). This adduct is reversible in darkness and thermally decays from S390 to D450 within seconds to minutes, depending on the LOV domain (Kasahara et al. 2002) (Christie et al. 2012). This photocycle and its duration is characteristic for each LOV domain and its positively corelated with the photosensitivity of the kinase activation (Okajima, Kashojiya, and Tokutomi 2012) (Hart et al. 2019).

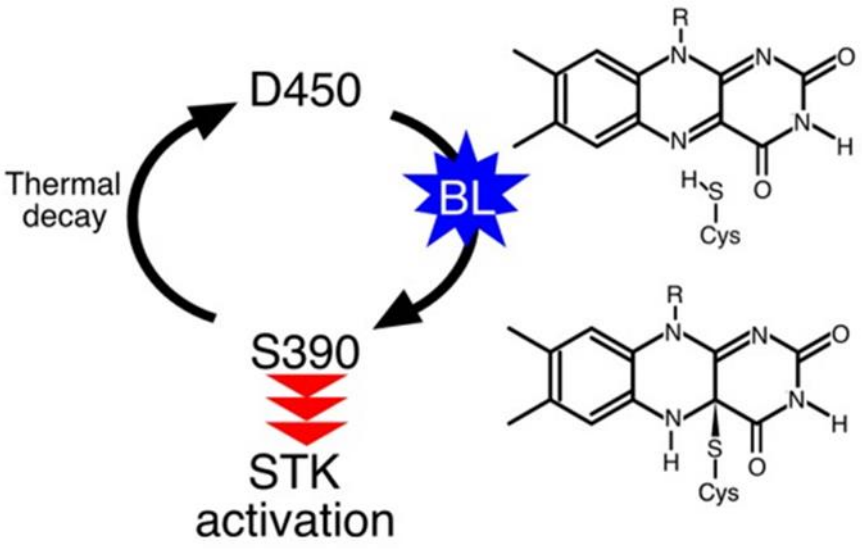

Figure 1.12: Schematic representation of the photocycle of LOV2. In the dark, the FMN, at its ground state, absorbs near 447 nm (D450). After blue-light illumination, the FMN forms a covalent bond with a conserved cysteine residue of the LOV domain via its C4(a) atom. The formed cysteinyl photoadduct absorbs at around 390nm (S390). The FMN returns back to its ground state (D450) in the dark via thermal decay. Image adapted from (Okajima 2016).

While LOV2, alongside the A'α and the Jα helix on each side of it, is necessary and sufficient by itself to activate the kinase domain (Christie et al. 2002) (Harper, Neil, and Gardner 2003) (Sullivan et al. 2008) (Cho et al. 2007), the role of LOV1 is, to a big part, elusive. However, there is evidence that the presence of LOV1 enhances the light sensitivity of PHOT, since at CrPHOT the photosensitivity of the kinase is dropping to less than half when LOV1 is truncated (Okajima et al. 2014).

Upon blue light illumination of LOV2, the Jα helix dissociates and the subsequent conformational changes lead to the disruption of the inhibition of kinase by LOV2 which occurs in darkness (Fig. 1.13) (Harper, Neil, and Gardner 2003) (Pfeifer et al. 2010). The structure of LOV2-Jα helix-kinase ''opens up'', enabling the kinase domain to increase its phosphorylation activity and possibly to interact with a signalling partner. The activation loop, which can serve as a second interaction site for protein-protein interaction, also goes through conformational changes at CrPHOT, an observation which has been disputed for AtPHOTs (Takakado et al. 2017). The kinase of CrPHOT is also able of auto-phosphorylation, thought in significantly lower rate than AtPHOTs (Onodera et al. 2005).

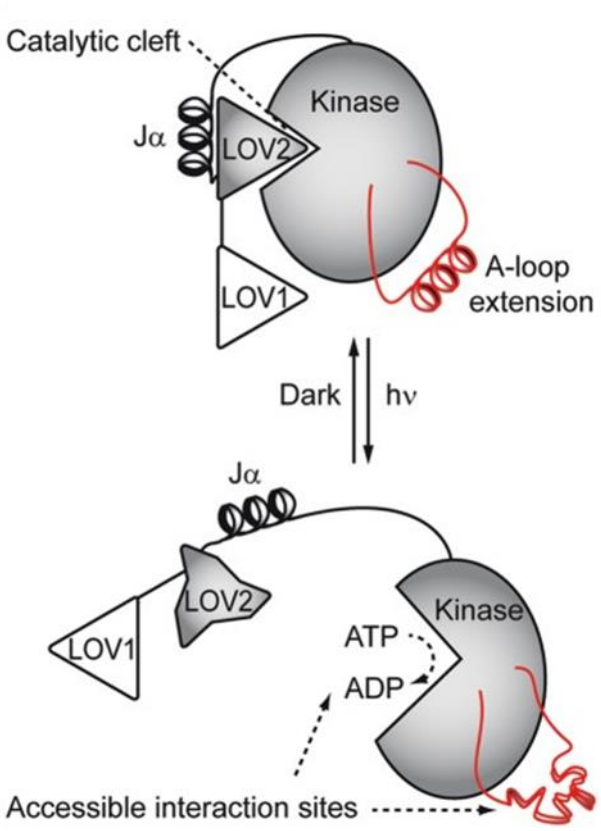

Figure 1.13: Activation mechanism of CrPHOT. In the dark, the kinase is being inhibited by LOV2. When blue light illuminates LOV2, the Jα helix dissociates, which leads to conformational changes. These conformational changes enable the activation of the kinase. The activation loop (A-loop) acts as a second interaction site and also goes through conformational changes upon light illumination. Image adapted from (Pfeifer et al. 2010).

Surprisingly and in contrast with higher plants' PHOTs, CrPHOT is able to transduce the light-induced signal in an alternative way to the kinase-mediated phosphorylation.

More specifically, overexpression of a LOV1-LOV2 fragment in a PHOT-knocked out strain was able to affect the eyespot size and phototaxis, a PHOT-regulated phenotype, in a light-dependent manner (Trippens et al. 2012). The fact that the signal was transduced without the presence of the kinase, lead to the hypothesis that CrPHOT is able to mediate the blue-light signal also by protein-protein interaction.

1.3.4 Localisation

Despite the fact the PHOT is highly hydrophilic and does not have membrane-spanning domain, in higher plants it is mainly localized in the inner membrane of the cells (Sakamoto and Briggs 2002). In accordance to this, *Chlamydomonas* PHOT is also mainly located to the plasma membrane, as evidenced by immunoblotting on the proteins at the membrane fraction (Huang, Merkle, and Beck 2002) (Huang, Merkle, and Beck 2002).

Furthermore, the presence of PHOT in the flagella of both vegetative cells and gametes has been verified by fractionation experiments, as well as immunofluorescent localization techniques (Fig. 1.14) (Huang, Kunkel, and Beck 2004). Around 4% of the total protein was found in the flagella, as shown by densitometry analysis of Western blot results on fractionated protein samples. This result shows an enrichment of PHOT in that organelle relative to the cell body, since the volume of flagella comprises approximately the 0.5% of the whole cell. Surprisingly enough, PHOT was also detected in the axonemes of the flagella, instead of its membrane, which is a continuum with the cell body membrane. All these findings lead to the conclusion that PHOT has a unique role at this organelle and reveal a possible sensing role for the flagella. The presence of PHOT in the axonemes fraction of the flagella was further confirmed by proteomic analysis, based on mass spectrometry (Pazour et al. 2005).

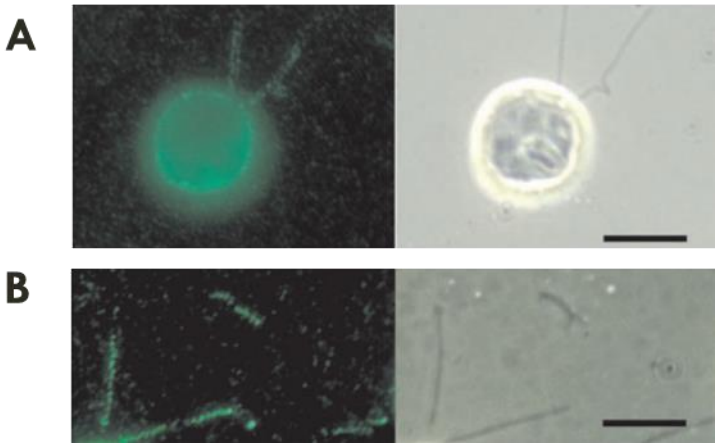

Figure 1.14: Observation of the localisation of PHOT in C. reinhardtii via immunofluorescence. A) Immunolocalization of PHOT in a C. reinhardtii cell. B) Immunolocalization of PHOT in the flagella. As evidenced, PHOT is present in the cellular membrane of the cell, as well as in the flagella.

Additionally, the presence of the photoreceptor in the eyespot has been verified by proteomic analysis of the purified eyespot apparatus (Schmidt et al. 2006).

1.3.5 Cellular role/ responses

A number of different physiological responses mediated by PHOT has been revealed in *C. reinhardtii*. At first, CrPHOT is suggested to play a principal role on sexual life cycle and gametogenesis- related responses (Huang and Beck 2003). More specifically, it was shown that in an RNAi mutant with reduced phototropin levels, the steps of conversion of pregametes to gametes, reactivation of gametes inactivated in dark and germination of zygotes were impaired. A study of the same RNAi mutant from (Huang and Beck 2003) led to the suggestion that PHOT is also the photoreceptor responsible for the blue-light mediated inactivation of chemiotaxis towards ammonium in the pre-gametes and their subsequent gaining of mating competence (Ermilova et al. 2004). This result, however, has been contested since a PHOT mutant strain, which had its *PHOT* gene knocked out via the CRISPR/Cas9 technique, was able to mate with a wild type strain (Greiner et al. 2017).

Additionally, CrPHOT is shown to control the expression of proteins involved in the synthesis of chlorophylls, carotenoids, Chl-binding proteins and LHC apoproteins. In

particular, it controls the expression of glutamate-1-semialdehyde aminotransferase (GSAT), phytoene desaturase (PDS) and the major LHCII polypeptide LHCBM6 when transitioning from darkness to very low fluence blue light (Im et al. 2006). Those proteins were shown to be induced when the cell was transitioned from darkness to very low intensity of blue light (1 μmol photons m^{-2} sec^{-1} or lower) in the WT, while this induction was largely suppressed in the PHOT knocked-down strain (the RNAi line studied in (Huang and Beck 2003) and (Ermilova et al. 2004)). While the expression of those proteins was being promoted under very low blue light fluence rates (0.2 μmol photons m^{-2} sec^{-1}), relatively higher ones (5 and 25 μmol photons m^{-2} sec^{-1}) did not lead to proportionately higher transcript or protein levels. This indicates probably a blue-light-dependent but light-intensity-independent phenotype. Another interesting point of this study was that low-fluence red light was also causing the induction of the expression of GSAT and LHCBM6, while this induction was also suppressed in the PHOT knockout strain. This suggests a possible interaction between PHOT and a red-light photoreceptor. Since the *C. reinhardtii* genome does not have a phytochrome gene, it could be the fully reduced form of aCRY which could play the role of that red-light photoreceptor and form this signalling synergy with PHOT or a yet to be identified protein acting as red-light receptor.

CrPHOT, also acts on the regulation of phototaxis by desensitizing the size of the eyespot (Trippens et al. 2012). Indeed, in a PHOT knocked-out strain, created by homologous recombination (Zorin et al. 2009), the ability of the eyespot to dynamically change its size in a light-dependent manner was supressed. Complementation with just the kinase domain of PHOT, led to a light-independent reduction of the eyespot size. Surprisingly, overexpression of just the LOV1+LOV2 domain was also able to rescue the phototactic phenotype, suggesting a possible signalling role for the LOV domains, independent of the kinase. Additionally, CrPHOT is also mediating the downregulation of channelrhodopsin-1 (ChR1), an eyespot-located photoreceptor with a major role in phototaxis, but does not affect ChR2. This phenotype was also rescued by complementation with the kinase domain, but in this case complementation with the LOV1+LOV2 fragments had no effect on ChR1 levels.

Finally, CrPHOT was found to be the mediator of a blue-light signal that induces photoprotection in *C. reinhardtii*. More specifically, it was shown that PHOT controls the transcription of *LHCSR3.1* and *LHCSR3.2*, both encoding LHCSR3 (Petroutsos et al. 2016). LHCSR3 is the key protein effector of qE, the major photoprotective mechanism in *C. reinhardtii*. Deletion of PHOT (at the homologous recombination mutant strain from (Zorin et al. 2009)) leads to a photosensitive phenotype, where the cultures are bleached under high light conditions as an indication of cell death (Fig. 1.15). The details of this signalling pathway, as well as the role of LHCSR3 will be analysed extensively in the next chapter.

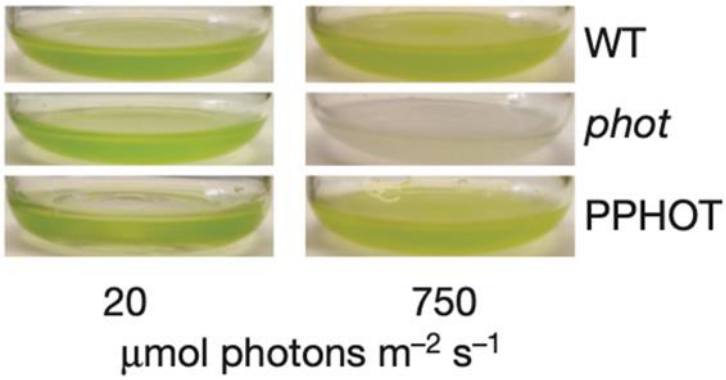

Figure 1.15: Effect of high light on the physiology of the phot mutant. Cultures of the WT (cw15-302), phot (a phot-knockout mutant strain, created via homologous recombination (Zorin et al. 2009)) and the phot complemented line (PPHOT) were grown under low (20 µmol photons m^{-2} sec^{-1}) and high (750 µmol photons m^{-2} sec^{-1}) light conditions for 20h. Under high light, the phot strain got bleached out, while the WT and the PPHOT remained green. Image adapted from (Petroutsos et al. 2016)

1.3.6 PHOT interactors in *Arabidopsis*

Despite the fundamental role that CrPHOT plays in cellular signalling in *C. reinhardtii*, no direct substrate of its kinase or interactor has been found up to date. However, proteins which directly interact with PHOT have been found in *Arabidopsis thaliana*, and the nature of those interactions could be particularly useful for such studies in CrPHOT.

AtPHOTs mediate phototropism, which is the reorientation of shoot growth towards a directional light source. A key signalling component of phototropism is NON-PHOTOTROPIC HYPOCOTYL 3 (NPH3). Based on yeast-two-hybrid and coimmunoprecipitation approaches, NPH3 was found to directly interact with AtPHOT1 and AtPHOT2 via its C-terminal region (Motchoulski and Liscum 1999) (Lariguet et al. 2006) (de Carbonnel et al. 2010). Recently, a chemical-genetic approach has been applied to verify this interaction and to identify the specific residue of NPH3 which gets phosphorylated by PHOT. With the use of a gatekeeper engineered AtPHOT1, which can accommodate the bulky ATP analogue N6-benzyl-ATPγS as a thiophospho-donor (Schnabel et al. 2018), it was revealed that the S744 of NPH3 gets phosphorylated in a PHOT-dependent manner (Sullivan et al. 2021). In darkness, NPH3 is phosphorylated and forms a membrane-associated complex with PHOT (Pedmale and Liscum 2007). Within minutes after the activation of PHOT by blue light, NPH3 gets rapidly dephosphorylated and becomes internalised into aggregates, which diminishes its interaction with PHOT (Haga et al. 2015) (Sullivan et al. 2019). However, under continuous light, the reconstitution of the AtPHOT1-NPH3 complex is essential for the phototropic signalling. The reconstruction of this complex is assisted by the protein ROOT PHOTOTROPISM 2 (RPT2). RPT2, which is additionally involved in stomatal opening, is also directly interacting with AtPHOT1 independently of NPH3, as evidenced by yeast-two-hybrid and immunoprecipitation assays (Inada et al. 2004) (Sullivan et al. 2009). This interaction occurs between the N-terminal region of PRT2 and the LOV domains. A protein belonging to the NPH3/RPT2-like (NRL) family, designated as NPH3-like (NPH3-L), has been also identified as a PHOT interactor via yeast-two-hybrid screening of an Arabidopsis cDNA library with full-length AtPHOT1 (Sullivan et al. 2009).

Hypocotyl phototropism is also mediated by proteins of the PKS (PHYTOCHROME KINASE SUBSTRATE) family. This family of phytochrome signalling components contains four members in *Arabidopsis* (PKS1-PKS4). PKS1 and PKS2 interact with AtPHOT1, AtPHOT2 and NPH3, as shown by GST pull-down assay and coimmunoprecipitation (Lariguet et al. 2006) (de Carbonnel et al. 2010). PKS4 is

additionally found to interact with AtPHOT1 both *in vivo* and *in vitro* and it gets phosphorylated in a PHOT-dependent manner (Demarsy et al. 2012).

AtPHOT1 interaction with the protein ABCB19 (ATP- Binding Cassette B19) has also been verified. ABCB19 is an auxin efflux transporter and it is implicated in phototropism. The interaction between ABCB19 and AtPHOT1 has been verified by yeast-two-hybrid, co-immunoprecipitation, mass spectrometry and bimolecular fluorescence complementation (BiFC) (Christie et al. 2011). ABCB19 binds to the C'-terminus of AtPHOT1, which includes the kinase domain and this interaction inhibits the activity of the former.

AtPHOT1 is also shown to interact with different members of the 14-3-3 protein family. The 14-3-3 proteins are key regulators of signalling in all eucaryotic cells by binding to a number of different signal-transporting proteins, including kinases. 14-3-3ϕ protein binds to immunoprecipitated AtPHOT1 upon its autophosphorylation (Inoue, Takemiya, and Shimazaki 2010). The binding sites for 14-3-3ϕ are two serine residues (S350A and S376A), which are located in the region between the two LOV domains. Yeast-two-hybrid and far-western blot assays have revealed the interaction of PHOT with other isoforms of 14-3-3 proteins, such as 14-3-3λ and 14-3-3κ (Sullivan et al. 2009).

The same yeast-two-hybrid screen from (Sullivan et al. 2009) revealed the interaction between AtPHOT1 and the ADP-ribosylation factors ARF2 and ARF7. These proteins play instrumental role at the budding and fusion of the vesicles. The binding of the ARF proteins with AtPHOT1 occurs during dark and it is being disrupted by blue light.

In plants, stomata regulate the gas exchange between the plant and the atmosphere and open in response to low CO_2 concentrations to maximize the photosynthetic efficiency. Two proteins involved in the opening of the stomata are directly interacting with AtPHOT1, BLUS1 (Blue Light Signalling 1) and CBC1 (CONVERGENCE OF BLUE LIGHT AND CO_2 1). BLUS1 is a Ser/Thr kinase, which mediates the blue-light signal from the phototropins to the H+- ATPase during the stomatal opening in guard cells. BLUS1 is a direct substrate of AtPHOT1, as evidenced by coimmunoprecipitation, and its phosphorylation is dependent on both AtPHOT1 and AtPHOT2 (Takemiya et al. 2013).

The N-terminus of BLUS1, which includes its kinase domain, interacts with both the LOV domains and the kinase domain of AtPHOT1. While the kinase domain of AtPHOT1 is responsible for the phosphorylation of BLUS1, the LOV domains are considered to act as inhibitors of the kinase. CBC1 also mediates the stomatal opening by linking signals coming from both blue-light radiation and low CO_2 concentrations in the guard cells. Pull-down and BiFC assays revealed the direct phosphorylation of CBC1 by AtPHOT1 both *in vivo* and *in vitro*. The phosphorylation of CBC1 occurs independently from the presence of BLUS1 (Hiyama et al. 2017).

1.4 Protection from photooxidative stress in the chloroplast of Chlamydomonas: Photoprotection (quenching of energy) and the chloroplast Unfolded Protein Response (cpUPR)

1.4.1 Photoprotection in *Chlamydomonas*

Besides being the energy fuel of photosynthesis and a source of information, light can also be toxic for the photosynthetic cells when absorbed in excess. Indeed, when light is absorbed beyond the photosynthetic capacity of CO_2 fixation, it can cause photooxidative damage to the cell, most commonly via the formation of reactive oxygen species (ROS). ROS, such as superoxide (O_2^-), the hydroxyl radical ($OH^\cdot$) and hydrogen peroxide (H_2O_2), are by-products of an over-reduced electron transport chain and can cause multiple physiological defects, including protein and lipid damage as well as DNA mutations. To avoid the damage created by excess light, *C. reinhardtii* has evolved a number of photoprotection mechanisms.

A dominant photoprotective mechanism, designated qE (energy-dependent quenching) represents the harmless dissipation of excess absorbed light energy as heat (Li et al. 2009). This rapidly induced (within seconds) and rapidly relaxed (from seconds to minutes) process requires the formation of a proton gradient across the thylakoid membrane (ΔpH) for its formation (Briantais et al. 1979). When

photosynthesis is saturated by high light, the thylakoid lumen becomes more acidic due to the generated ΔpH by the electron transport chain. In parallel, the efflux of H+ through ATP synthase is limited due to the low consumption of ATP by the Calvin-Benson cycle, keeping the ΔpH high. Therefore, high ΔpH acts as a cellular signal for excess light to trigger qE.

Triggering qE requires both specific proteins and pigments that are controlled by transcriptional and post-transcriptional processes. In *C. reinhardtii*, qE depends on the nucleus-encoded, chloroplast-localized proteins LHCSR3, LHCSR1 and PSBS, which are present in many algae and lower plants such as moss (Alboresi et al. 2010). These proteins belong to the Light Harvesting Complex-Stress Related subfamily (Niyogi and Truong 2013).

LHCSR3 is being encoded by the nearly identical genes *LHCSR3.1* and *LHCSR3.2*. The promoter regions of both those gens have also high similarity (Peers et al. 2009) (Maruyama, Tokutsu, and Minagawa 2014). In cells where those genes are being disrupt, qE is being impaired and the cultures show reduced fitness in high light conditions (Fig. 1.16) (Peers et al. 2009).

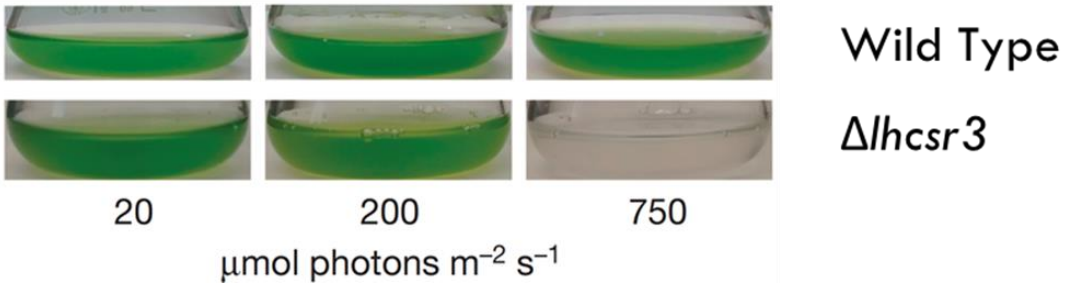

Figure 1.16: Effect of the LHCSR3 depletion on the physiology of the cells in high-light conditions. Cultures of the WT and of a LHCSR3 knockout strain (Δlhcsr3), described in (Peers et al. 2009) were grown under 20, 200 and 750 µmol photons m^{-2} sec^{-1} for 16h. As evidenced, the Δlhcsr3 strain under high light (750 µmol photons m^{-2} sec^{-1}) bleaches out due to his enhanced photosensitivity. Important to notice here the phenotypical similarities of the Δlhcsr3 strain with the Δphot strain (Fig. 1.15). Image modified from (Petroutsos et al. 2016).

LHCSR1 is being encoded by *LHCSR1* which is located upstream of *LHCSR3.1* and *LHCSR3.2* on the same chromosome. LHCSR1 is 82% identical to LHCSR3 and it differs with the latter at the C-terminus and the N-terminal chloroplast transit peptide. While LHCSR1 is being expressed, as LHCSR3, under high light conditions, it is evident that

this protein alone is not sufficient for full qE induction (Peers et al. 2009). However, it can significantly contribute to qE under certain conditions; in cells which were completely depleted of PSII and PSI and were grown in LHCSR3-supressing mixotrophic medium, a small amount of LHCSR1 was able to induce qE, even in the absence of LHCSR3 (Dinc et al. 2016). In addition to this, a mutant strain which had totally suppressed levels of LHCSR3 but overaccumulated LHCSR1 was able to partially induce qE in high light (Ruiz-Sola et al. 2021).

While LHCSR1 and LHCSR3 are present in algae but not in vascular plants, PSBS is in both and it appears to sense and communicate excess excitation through protonation of glutamate residues that are exposed in the thylakoid membrane lumen (Niyogi and Truong 2013). PSBS in *C. reinhardtii* is transiently expressed in cells exposed to high light (HL) (Tibiletti et al. 2016) (Correa-Galvis et al. 2016) and accumulates when cells are exposed to UV-B irradiation (Allorent et al. 2016). The precise contribution of PSBS in *C. reinhardtii* photoprotective responses is still unresolved (Redekop et al. 2020).

1.4.1.1 LHCSR3: Localisation and activation mechanism

LHCSR3 belongs to the family of the light-harvesting complex (LHC) proteins, which are located at the thylakoid membranes of the chloroplast. LHCSR3 is docked in the thylakoid membranes via 3 trans-membrane α-helices (helix A, B, and C) and also contains two amphipathic helices (helix D and E), which are exposed to the thylakoid lumen (Fig. 1.17). Helices D and E contain protonable residues which act synergistically for sensing the luminal pH (Ballottari et al. 2016). Mostly dimeric LHCSR3 complexes are specifically associated with PSII, via binding with the antenna supercomplex C_2S_2 (Semchonok et al. 2017) and the chlorophyl-binding protein CP26, while the binding of LHCSR3 to PSI via the antenna subunit LHCII has been strongly implied (Girolomoni et al. 2019). Additionally, as highly evidenced, LHCSR3 interacts with other LHC proteins, such as LHCBM1 (Ferrante et al. 2012). During the state transitions, LHCSR3, among other LHC proteins can relocate to PSI (Allorent et al. 2013). Based on a sequence alignment of LHCSR3 with LHC, it has been proposed that LHCSR3 is able to

bind 8 chlorophyl molecules and 2 carotenoids (Liguori et al. 2016). An earlier approach on that matter had predicted the attachment of 6.7 ± 1.9 chlorophylls and of 2 carotenoids per molecule of LHCSR3 (Bonente et al. 2011).

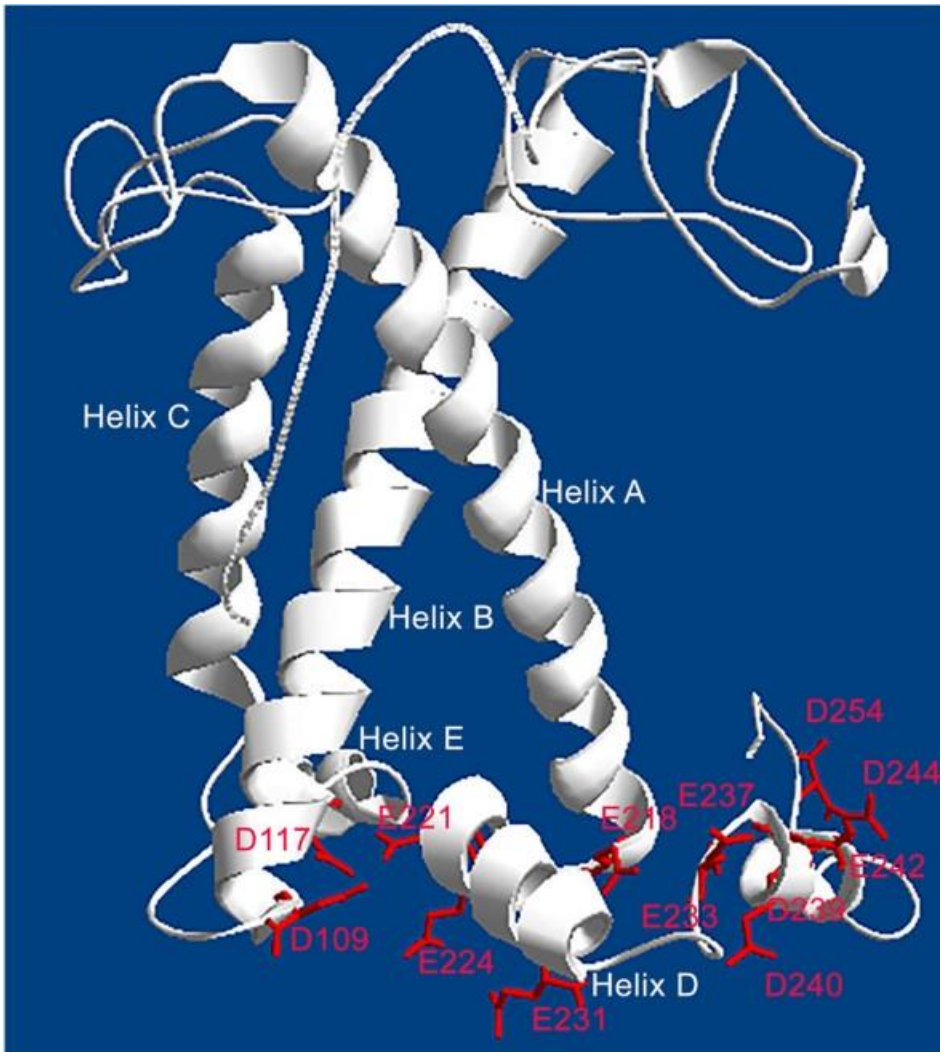

Figure 1.17: The 3D structure model of LHCSR3. The Helices A, B and C are trans-membrane and the helices E and D are amphipathic. Highlighted with red there are several aminoacid residues which are predicted to be exposed to the thylakoid lumen. The 3D structure was created using as template the 3D structures of other LHC proteins. Image taken from (Ballottari et al. 2016).

At neutral pH, LHCSR3 exists at its light-harvesting mode, assisting the energy transfer to the PSII. Under high-light stress conditions, LHCSR3 senses the drop of the luminal pH via its C-terminus and switches to the energy-dissipative conformation. The C-terminus of LHCSR3 is exposed to the thylakoid lumen and it is rich in acidic residues, which are able to sense the variation of the pH (Liguori et al. 2013) (Ballottari et al. 2016) (Camargo et al. 2021). LHCSR3 is proposed to act both as the sensor of the

chloroplast luminal pH and as the holder of multiple quenching sites which act in cooperation for the energy dissipation (Perozeni, Cazzaniga, and Ballottari 2019). The exact mechanism of quenching the excess energy to heat is still largely elusive, though a number of experimental-based hypotheses have been recently emerged. According to (Kim et al. 2017), at a first level, the expression of LHCSR3 and its association with the PSII complex lead to inhibition of the energy transfer to the chlorophyl- binding protein CP47, which is close to its binding site. When protonated by the acidification of the lumen, LHCSR3 quenches the excitation energy of the LHCs. Another one from (Perozeni, Cazzaniga, and Ballottari 2019) suggests the possibility of LHCSR3 not being the direct quencher, but rather act as a pH-controlled trigger for other LHC proteins to dissipate the excitation energy.

1.4.1.2 Regulation of LHCSR3 expression

LHCSR3 is considered to be generally a stress response factor and its induction is highly regulated in *C. reinhardtii*. A number of specific environmental signals, as well as key-proteins which regulate LHCSR3 have been described in the literature.

LHCSR3 is a key component of photoprotection and, therefore, it would have been expected to be induced under light. Indeed, both the transcript is being induced and the protein is being expressed during light illumination and especially under high light intensities (Richard, Ouellet, and Guertin 2000) (Ledford et al. 2004) (Naumann et al. 2007) (Yamano, Miura, and Fukuzawa 2008) (Maruyama, Tokutsu, and Minagawa 2014). This constitutes light as the primary condition for LHCSR3 expression.

For the light-dependent expression of LHCSR3, active photosynthesis is required. In PSI and PSII deficient mutant strains, no LHCSR3 is expressed, even after 2h exposure to high light. The same inhibition was observed after the addition of DCMU and DBMIB (Petroutsos et al. 2011), chemicals that disrupt the electron transport chain at the PSII and the cytochrome b6f, respectively (Trebst 2007).

Nitrogen, sulfur, iron and phosphorus are essential nutrients for *C. reinhardtii* and their limitation from the growth medium causes developmental defects and induces corresponding stress responses. The *LHCSR3* transcript gets upregulated in both nitrogen and sulfur starvation conditions, as evidenced by transcriptomic and microarray analyses (Miller et al. 2010) (Toepel et al. 2011) (Zhang et al. 2004) (Gonzalez-Ballester et al. 2010).. Furthermore, a comparative proteomic analysis revealed that LHCSR3 is among the proteins with the biggest induction under iron-deficient conditions (Naumann et al. 2007). This result was further supported by quantitative RT-PCR for *LHCSR3* mRNA and Western blot. The levels of the *LHCSR3* transcript are also increased after phosphate deprivation (Moseley, Chang, and Grossman 2006).

The concentration of Ca^{2+} has a key role for *C. reinhardtii* in various cellular responses, such as in phototaxis, photosynthesis and stress-related signalling. CAS (calcium sensor) is a calcium-specific binding protein, localised in the thylakoid membranes in higher plants and in *C. reinhardtii*, which acts as a mediator of the Ca^{2+} signal. CAS plays a role on the LHCSR3 expression, since in strains where *CAS* is being knocked-down, LHCSR3 expression is lower and the strains are highly photosensitive (Petroutsos et al. 2011). The phenotype of the *cas* mutants was rescued by a 10-fold increase in Ca^{2+} concentration in the growth medium. Calmodulin, another widely spread calcium-binding messenger protein, also controls the expression of LHCSR3. In the presence of W7, a calmodulin inhibitor, LHCSR3 is being supressed, both at the protein and at the transcript level (Petroutsos et al. 2011) (Maruyama, Tokutsu, and Minagawa 2014). Interestingly, CAS is also responsible for the regulation of the CCM (CO_2 concentrating mechanism), highlighting a relation between Ca^{2+}- and low CO_2-dependent signalling; CAS is required for the expression of a number of CCM-related genes and, also, is relocating from all over the chloroplast to the pyrenoid in low CO_2/ light conditions (Wang et al. 2016).

The expression of LHCSR3 is also controlled by photoreception. First, the UVB photoreceptor UVR8 is inducing LHCSR3, alongside LHCSR1 and PSBS. Upon UV-B exposure, the homodimer UVR8 monomerizes to allow its interaction with the E3 ubiquitin ligase COP1. A signalling pathway is thus initiated that induces the

expression of LHCSR1, PSBS, and to a lesser extent, LHCSR3 (Allorent et al. 2016). Indeed, the UVR8-knocked-out mutant showed significantly lower expression of UV-B induced LHCSR3. However, LHCSR3, in contrast with LHCSR1 and PSBS, has stronger expression in high visible light than under UV-B in the wild type.

LHCSR3 is being mainly, though, regulated by blue light. Indeed, LHCSR3 gets preferentially overaccumulated under blue light, over any other wavelength in the visible spectrum (Petroutsos et al. 2016). Additionally, qE induction is more effective under blue light illumination than under red, despite the fact that both light qualities can be absorbed equally by the cells. The blue light signal is being transmitted exclusively by PHOT and not the other family of blue-light photoreceptors, the Cryptochromes. As it was mentioned in the previous chapter, the Δ*phot* strain was photosensitive and that was a result of lower expression of LHCSR3, both in transcript and in protein levels. PHOT also regulates the expression of the other photoprotection genes, *LHCSR1* and *PSBS*, thought probably under a different signalling cascade, as it has been hypothesised by (Aihara et al. 2019).

The molecular pathways interconnecting PHOT and LHCSR3 still remain largely unknown. However, some key components of this signalling pathway have been already described. At first, the PHOT-mediated signal for LHCSR3 induction requires as second messengers the cyclic nucleotides cAMP or cGMP downstream of PHOT, as evidenced after treatment of the Δ*phot* cells with IBMX, a cAMP and cGMP phosphodiesterases inhibitor (Petroutsos et al. 2016). Furthermore, two PHOT suppressor loci were found to be involved in the LHCSR3 induction: DE-ETIOLATED 1 (det1) and DAMAGED DNA-BINDING 1 (ddb1), both of which being a part of the E3 ubiquitin ligase complex CUL4–DDB1^{DET1} (Fig. 1.18) (Aihara et al. 2019). In dark, this complex supresses LHCSR3 induction. PHOT is being hypothesised to supress the E3 ubiquitin ligase complex, either directly or indirectly, in a blue-light dependent manner.

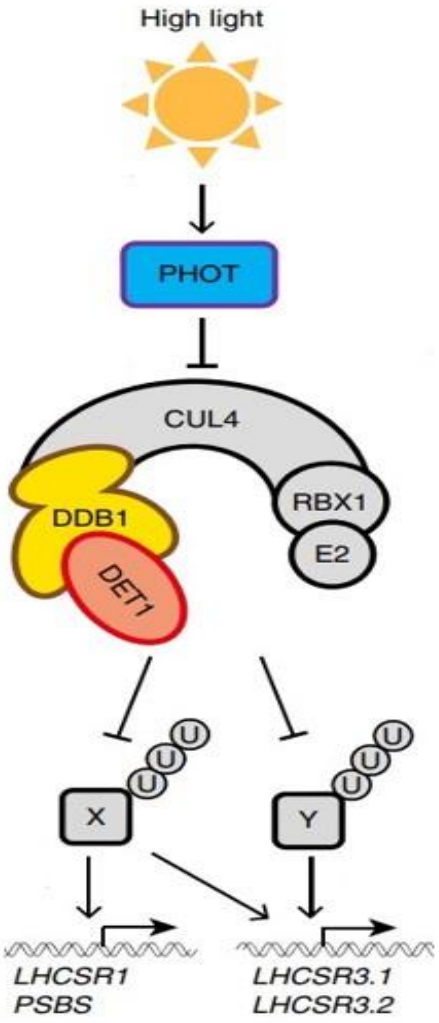

Figure 1.18: Proposed schematic model of the PHOT-mediated pathway that controls photoprotection. After high light irradiation PHOT gets activated and supresses, either directly or indirectly, the E3 ubiquitin ligase complex CUL4–DDB1^{DET1} . This ubiquitin complex in dark ubiquitinates their targets, which are responsible for LHCSR3, LHCSR1 and PSBS transcription. Image modified from (Aihara et al. 2019).

The regulation of LHCSR3 expression gets even more complicated by the recent findings that the transcription factor CrCO (CONSTANS), which in higher plants mediates the circadian-clock-regulated flowering process, is responsible for the gene activation of LHCSR3 (Tokutsu, Fujimura-Kamada, Matsuo, et al. 2019) (Gabilly et al. 2019). CrCO in low light or in darkness is being degraded by a CUL4-SPA1/COP1 E3 ubiquitin ligase complex. In high light, it promotes the transcription of *LHCSR3.1* and *LHCSR3.2* through direct promoter binding, in complex with the Nuclear transcription Factor Ys (NF-Ys). Under UV-B light, UVR8 makes a complex with SPA1 and COP1,

which leads to the inhibition of the E3 ubiquitin ligase and the accumulation of CrCO (Tokutsu, Fujimura-Kamada, Matsuo, et al. 2019).

The extra- and intra- cellular levels of CO_2 represent an essential environmental cue for cellular signalling and are responsible for LHCSR3 regulation. Evidentially, the transcript for LHCSR3 is being highly induced under low (0.033 to 0.041%) and very low (0.011 to 0.015%) CO_2 (Miura et al. 2004) (Fang et al. 2012). Opposingly, high CO_2 supresses both the expression of the transcript and the accumulation of the protein (Fang et al. 2012) (Polukhina et al. 2016).

The environmental levels of CO_2, when they are restricted, induce also the CO_2 concentrating mechanism (CCM), which represents an effective adaptation of *C. reinhardtii* and other aquatic organisms in limiting CO_2 conditions. The proteins of the CCM are including bicarbonate (HCO_3^-) transporters in the plasma membrane and in the chloroplast envelope which assist the import of inorganic carbon in the chloroplast against the concertation or pH gradient, as well as carbonic anhydrases which interconvert HCO_3^- and CO_2 in order to increase the concertation of the second around the site of its fixation, at Rubisco (Moroney and Ynalvez 2007) (Wang, Stessman, and Spalding 2015). Many of those proteins are under the control of the CCM transcription regulator CIA5. A fascinating link between the CCM and photoprotection has been revealed from the fact that the *LHCSR3* expression is also under the control of CIA5, alongside the CCM genes (Fang et al. 2012) (Ruiz-Sola et al. 2021) (Redekop et al. 2021).

The significance of the intracellular CO_2 at the regulation of photoprotection has been highlighted recently by our team (Ruiz-Sola et al. 2021). The intercellular concertation of CO_2 is being dynamically regulated by the production of CO_2 from the mitochondrial metabolism and its fixation in the chloroplast during the Calvin-Benson cycle (Fig. 1.19). In high-light conditions, when the fixation rates are high, CO_2 become depleted and both LHCSR3 and the CCM genes are being induced via the CIA5 regulation. These responses can be also induced in total CO_2- depletion conditions in the dark, a fact that proves the partial light-independence of this pathway. Individually though from the CO_2/CIA5 pathway, light has a clear impact on the expression of *LHCSR3*, alongside *LHCSR1* and *PSBS* and this can be a result of the PHOT-induced pathway (Petroutsos

et al. 2016) (Aihara et al. 2019). In conclusion, low CO_2 levels changes the landscape of regulation and can obviate the need for light in the activation of qE and CCM genes (Ruiz-Sola et al. 2021).

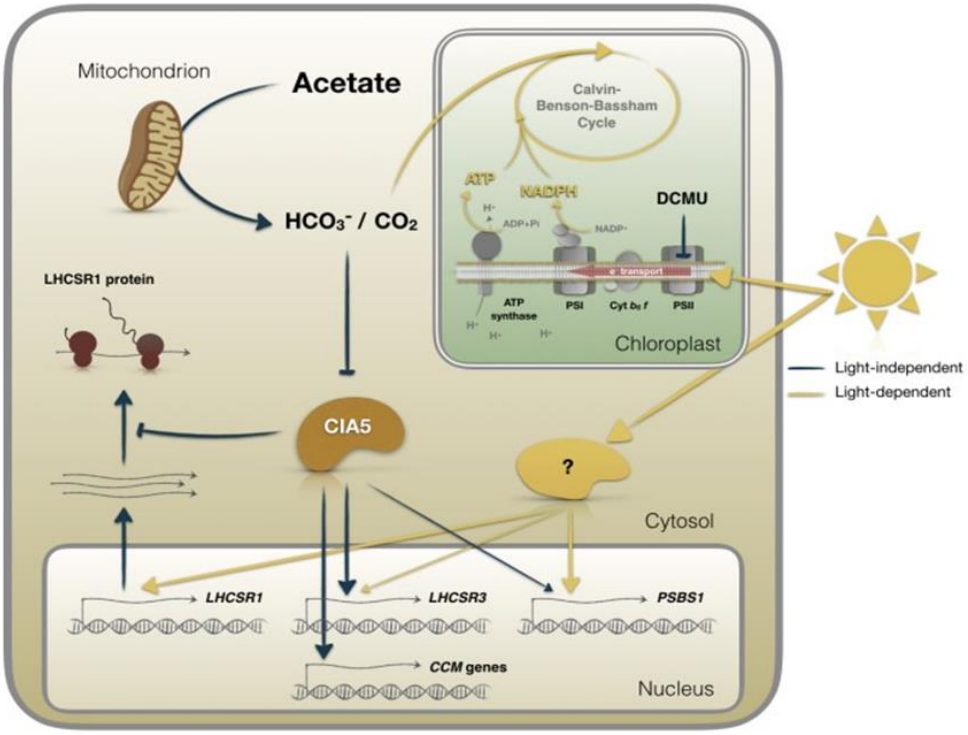

Figure 1.19: LHCSR3 and CCM regulation from the intracellular CO_2 levels. The intercellular levels of CO_2 are being dynamically regulated by its production from the acetate metabolism in the mitochondria and its fixation in the chloroplast during the Calvin-Benson cycle. In high-light, CO2 is being fixated in high rates and it becomes depleted. LHCSR3 and the CCM genes are being, then, induced via the CIA5 regulation. Opposingly, when the CO_2 levels are high, this pathway is being supressed. CIA5 also suppresses the translation of LHCSR1. Also, light has a strong impact of the expression of LHCSR3, LHCSR1 and PSBS. This exclusively light-dependent regulation can be a result of the PHOT-induced pathway.

1.4.2 The chloroplast Unfolded Protein Response (cpUPR) is a major quality control retrograde signal

The chloroplast Unfolded protein response (cpUPR) is a recently proposed chloroplastic retrograde signal, which gets triggered under proteotoxic stress and acts as an organelle quality control pathway. Here we will take a closer look on this signalling pathway, the conditions which trigger it, its components and the genes which it regulates.

Nucleus-encoded proteins which are about to be localised in the chloroplast are, at first, not completely folded so they can enter though the organelle's membranes from the cytoplasm. Once they enter the chloroplast, they get rapidly processed and folded by proteins which mediate protein folding. However, under stress conditions, such as nutrient starvation, elevated temperature or high light, which leads to an increased production of reactive oxygen species (ROS), this procedure gets compromised. The damaged or not properly folded proteins are led to proteolysis by a group of chloroplastic proteolytic proteins such as the protease Clp1.The action of Clp1 is of such importance for the whole cell, that its depletion leads to overaccumulation of unfolded proteins and eventually cellular death (Huang et al. 1994) (Ramundo et al. 2014). This overload of unfolded proteins, caused by Clp1 depletion or naturally from extensive stress conditions triggers the chloroplast unfolded protein response (cpUPR) (Fig. 1.20). The cpUPR, thus, represents a retrograde signal from the chloroplast to the nucleus and it upregulates the production of a number of proteins, such as proteases, chaperons, ubiquitins, heat shock proteins and proteins involved in thylakoid membrane assembly, all of which can contribute on the restoration of the protein homeostasis at the chloroplast (Ramundo et al. 2014).

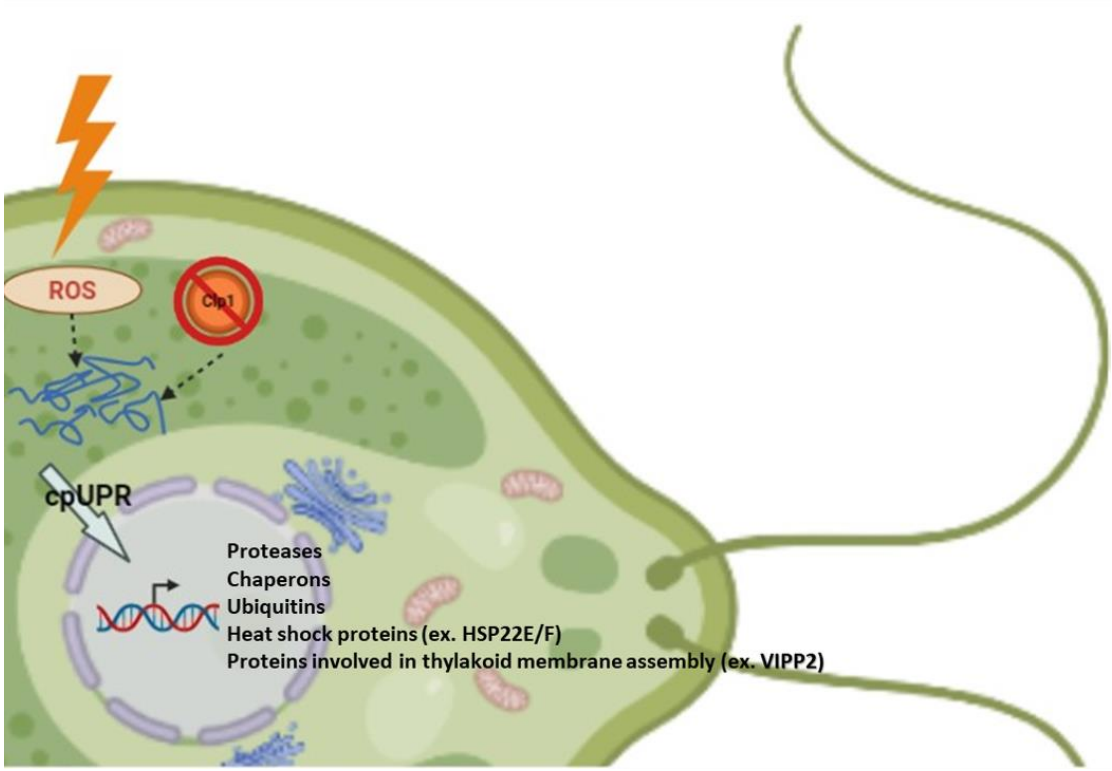

Figure 2.20: The chloroplast Unfolded Protein Response (cpUPR). The creation of ROS as a result of high light stress or the depletion of the chloroplast protease Clp1, lead to the compromise of the protein folding machinery of the chloroplast. The overaccumulation of non-properly folded proteins trigger a retrograde signal from the chloroplast to the nucleus for the induction of a number of genes such as proteases, chaperons, ubiquitins, heat shock proteins and proteins involved in thylakoid membrane assembly. This pathway represents the cpUPR. HSP22 E/F and VIPP2 are the one of the earliest and most sensitive responsive genes of the cpUPR.

Among the earliest and most sensitive responsive genes to cpUPR is *VIPP2* (Ramundo et al. 2014), the protein of which (VIPP2) is considered to be involved in the thylakoid's membrane assembly. VIPP2 gets also induced, both at transcript and protein levels, under high light (Nordhues et al. 2012) and after the addition of H_2O_2 in the medium (Blaby et al. 2015) (Theis et al. 2020) but not under heat shock stress (Nordhues et al. 2012). The strong induction of VIPP2 after Clp1 depletion led to its use as a reporter gene for the cpUPR activation (Perlaza et al. 2019).

Another strongly upregulated gene upon the cpUPR activation is the one that expresses the heat shock protein HSP22 E/F (Ramundo et al. 2014). The expression of HSP22E/F is being promoted by a variety of stress-related conditions, such as high light (Theis et al. 2020), heat shock (Muhlhaus et al. 2011), oxidative stress by H_2O_2 (Blaby

et al. 2015), and phosphorus and sulfur deprivation (Moseley, Chang, and Grossman 2006) (Zhang et al. 2004) (Nguyen et al. 2011).

VIPP2 can interact with HSP22E/F at the chloroplast membranes after exposure to H_2O_2, an interaction that is proposed to aim in the repair of the membrane after oxidative stress (Theis et al. 2020). VIPP2 is also hypothesised to regulate HSP22 E/F induction via a retrograde signal, while supressing the expression of *LHCSR3* (Theis et al. 2020).

Recently, the first component of the cpUPR signalling pathway has been identified in the cytoplasmic kinase MARS1 (Mutant Affected in chloroplast-to-nucleus Retrograde Signalling) (Perlaza et al. 2019). This discovery came after a cpUPR-mutants screening with the use of a reporter strain, with was able to produce a fused protein of VIPP2 and yellow fluorescent protein (YFP). MARS1 transmits the retrograde signal from the chloroplast via its kinase domain. Indeed, mutants lacking MARS1 or complemented with an inactive-kinase-form of the protein are unable to express VIPP2 and HSP22 E/F under oxidative stress, induced by high light or metronidazole, a H_2O_2 generating drug.

A cooperative transcriptomic analysis between the wild type and the *mars1* mutant under oxidative stress, revealed a set of transcripts which are heavily dependent on MARS1. Those, include, other than VIPP2 and HSP22 E/F, genes involved in chloroplast protein homeostasis, ROS detoxification, RNA metabolism, autophagy, and sulfur uptake. Interestingly, *LHCSR3.1* and *LHCSR3.2* were not affected by the depletion of MARS1.

1.5 Aim of this thesis

Blue light serves as a fundamental environmental cue for photosynthetic organisms and especially for algae. It is the dominant wavelength during the early morning and late evening hours, when the sun is way below the horizon, giving the signal for the start and the finish of the daily light cycle. Additionally, since red-light gets rapidly

attenuated by depth in aquatic environments, blue-light is the one which can be mainly perceived in greater depths. This explains the great importance and complexity of the activity of the blue light photoreceptors, and especially Phototropin. *C. reinhardtii*, a unicellular green alga and a model organism for molecular and cellular studies, serves as the ideal platform for the exploration of the blue-light responses.

While phototropins in plants regulate relatively rapid cellular responses, such as stomata opening, chloroplast relocation and phototropism, all of which contribute to the optimal photosynthetic efficiency, in *C. reinhardtii* the unique copy of PHOT seems to initiate signalling pathways that end up to the transcriptional regulation of specific genes in the nucleus. The most significant role of PHOT, as described so far, is the regulation of photoprotection and more specifically, the induction of LHCSR3 (Petroutsos et al. 2016). The molecular pathways interconnecting PHOT and LHCSR3, however, still remain largely unknown. Judging by the fact that LHCSR3 is being regulated also by a variety of different environmental conditions, most of them stress-related, one could wonder if there is a connection between those responses and the PHOT pathway, and what is the exact nature of it. Another key question that hasn't been addressed so far is the following: which are the early events of the PHOT-dependent signalling pathways in *C. reinhardtii*? Finding out phototropin-interacting or phototropin-regulated proteins and characterizing their role on the PHOT signalling pathways is at the centre of interest of my PhD project.

To achieve this goal, we employed phosphoproteomics to identify putative PHOT interactors in *C. reinhardtii* by comparing low and high light-exposed, as well as dark-acclimated and blue-light-exposed wild-type (WT) and phototropin-deficient cells (Δ*phot*). We screened for several proteins that are phosphorylated in a (blue) light-dependent manner in the WT and are not phosphorylated in the Δ*phot* mutant. This led us, at first, to the extensive study of a mutant strain (Δ*flkin*) which was able to overaccumulate LHCSR3, even in non-saturating light intensities. We also discovered that MARS1 gets phosphorylated in a PHOT-dependent manner, introducing a possibility of the PHOT involvement at the cpUPR response. Generally, based on my 3-year-long study, we are able to shed light on the interconnections between the blue-

light signalling and other important responses, such as photoprotection, CO_2 acclimation and oxidative stress response.

2. MATERIALS AND METHODS

Strains and conditions

All the *C. reinhardtii* strains were maintained in solid Tris-acetate-phosphate (TAP) medium (Gorman and Levine 1965) containing 1.5% Agar (A1296-500G, Sigma-Aldrich), in the presence of 100ng/µl Carbenicillin to prevent growth of bacterial contaminants, at 19 ^{o}C. The collection was replated on a weekly basis. For the precultures, the inoculum was taken from the solid cultures and got diluted in 25 ml of TAP in 100 ml Erlenmeyer flasks.

The precultures were grown under 20 µmol photons m^{-2} s^{-1} at 23 ^{o}C, shaken at 125 rpm. Every two days, they were transferred to fresh TAP medium in 250ml Erlenmeyer flasks and diluted to 1 million cells/ml (50ml total volume in 250ml Erlenmeyer flasks). The precultures were used for experiments after two dilutions.

For the experiments, cells were collected by centrifugation and transferred to either new TAP or to Sueoka's high salt medium (HSM) (Sueoka 1960), depending on the experimental setup, at a chlorophyl concentration of 4µg chlorophyl/ ml and 25ml final volume (in 100 ml Erlenmeyer flasks). They were acclimated overnight either in dark or in low light (20 µmol photons m^{-2} s^{-1}), as detailed in the results section). The following day they were transferred under the predetermined light intensities.

The *C. reinhardtii* strain CC125 was used as WT for the experiments with the Δ*phot* and the Δ*Cop6* strains. The CC4533 strain was used as WT for the experiments with Δ*flkin*. The Δ*phot* mutant (defective in PHOT; gene ID: Cre03.g199000) and the Δ*Cop6* (defective in Cop6; gene ID: Cre11.g467678) mutants were generated by CRISPR-CAS9 (Greiner et al. 2017). The ΔCop6 strain had been kindly offered to us by Peter Hegemann's lab. The pphotA9 strain is a PHOT complemented line described in (Redekop et al. 2021). The Δ*flkin* strain has been purchased by the Chlamydomonas Resource centre (Cheng et al. 2017) described as CDS mutant of the gene Cre16.g694950 (Insertion junction: LMJ.RY0402.047835_1; mutant strain: LMJ.RY0402.047835).

Verification of the CLiP library mutants

The CLiP mutant strains contain a paromomycin resistance gene on their disruption cassette (Cheng et al. 2017). For the first level of screening, when purchased, the strains were spread in a TAP+ 1.5% Agar plate containing 10ng/μl paromomycin. After approximately one week, their growth was observed in comparison with a negative control (in this case the CC4533 strain which had no resistance to paromomycin).

The website of the CLiP library (https://www.chlamylibrary.org/) is suggesting a pair of primers for each strain in order to verify the disruption of the gene by the mutation cassette. These primers bind upstream and downstream of the disruption locus. Thus, in a colony pcr, the amplified region will be approximately 2kb (the size of the mutation cassette) bigger than the one in a negative control (in this case, the CC4533 strain). The protocol for colony pcr is being described in a following section.

The proposed by the CLiP library primers, in almost all the cases, were not successfully amplifying the desired regions. Therefore, a different strategy had been followed. A primer had been designed to bind at the 3' terminus of the mutation cassette (5'-fp-GCACAGACGTTACAGCACAC) and was used as a forward primer. As the revers primer, the proposed revers primer from the CLiP library was used, which was binding downstream of the disruption locus. For the Δ*flkin* genotyping, the reverse primer was the rp-3'-ACCGTAAAGGTACGCACCAG. If the region between the 3' of the cassette and the binding locus of the revers primer was amplified in the strain but not in the negative control (CC4533), that would verify the presence of the mutation cassette at the indicated gene.

Specifically for the genotyping of Δflkin, multiple pairs of primers were tested, as it is described at the Results. Those primers (binding upstream or downstream of the cassette and on the cassette) are shown in Table 2.1.

Table 2.1: The primers used for the genotyping of the Δflkin strain

Primer name	Sequence
scr-flkin cds-fw	5'-ACCGTAAAGGTACGCACCAG

scr-flkin cds-rev	5’-TCGAAACTTGAGGACAGGCT
scr-flkin intron-fw	5’-TGGCCACCGTACTGATGTAA
scr-flkin intron-rev	5’- GACAGCGCAAGAAAAGTTCC
cib1-1	5’-GCTGCCTGATGGATGGTTCT
cib1-3	5’-TTTATACCGGATGGGTGCCG
cib1-5	5’-CCATGTGAGAGTTTGCCGTG
oMJ913	5’-GCACCAATCATGTCAAGCCT
oMJ944	5’-GACGTTACAGCACACCCTTG

Finally, just for the case of Δ*flkin*, a qPCR was done to verify if the mRNA of the disrupted gene was transcribed. qPCR is described in a next section and the qPCR primers are shown in table 2.2.

Chlorophyl measurements

For the chlorophyl estimation, 1ml of culture was taken in an Eppendorf tube. The sample had been spun down in 15.000 rpm for 5 min in room temperature. The pellet was resuspended with 1 ml of 100% methanol and the mixture was spun down in 15.000 rpm for 5 min in room temperature. The supernatant was transferred to a transparent cuvette and the it was set for absorbance measurement at the photospectrometer at 652, 655, 750 nm. The calculation of chlorophyl content per ml, based on the absorbance values was done based on (Porra, Thompson, and Kriedemann 1989).

Cell measurements

From each culture 475μl were taken and transferred into an Eppendorf tube. 25μl of acetic acid were added in the tube and mixed by pipetting up-and-down. If the cultures were highly concentrated (over 7 million cells/ml), dilutions were performed

accordingly, so the sample would not contain cell concertation over 7 million cells/ml. 17µl of the mixture were deposited on both sides of a Malassez slide and covered with a coverslip. The slide was put on Countess™ II FL Automated Cell Counter for the cell counting. The indicated result was divided by two, as indicated by the machine's instructions. The average cell diameter was also automatically indicated and noted.

For the Δ*flkin* growth curves, three samples were taken from each flask, and two independent measurements were carried out from each sample.

Different light conditions

Unless otherwise stated, low light conditions corresponded to 20 µmol photons m^{-2} s^{-1}. For higher light intensities, blue and red-light treatments, the cultures were placed under a led panel (Neptune LED, France). The light was adjusted accordingly with a ULM-500 Universal Light Meter & Data Logger (Walz, Germany).

Samples for mRNA were taken at t_0 after 1h of exposure at each light quality/intensity. Samples for protein were taken at the time points indicated at the Results.

CO_2 experiments

For the CO_2 experiments, after the appropriate number of cells were transferred to HSM, the cultures were purred in 80 mL capacity cylindrical glass columns. The cultures were supplemented with air enriched with 5% CO_2 through a plastic tube interconnecting the CO_2 supplier with a glass cylinder tube within the column. This glass tube was realising the air in the form of intense bubbling at the bottom of the column. The CO_2 concentration was measured in the air stream coming out of the headspace of the column using the CO_2 Probe GMP251 connected to the MI70 data logger from Vaisala (Vantaa, Finland). The columns were placed in front of a led panel, the light intensity of which was measured with a ULM-500 Universal Light Meter & Data Logger (Walz, Germany) and adjusted accordingly.

The cultures were incubated in low light for 16h and then they were exposed to high light (600 µmol photons m^{-2} s^{-1}) for 1h.

Samples for mRNA were taken after the right before the exposure to high light and after 1h of exposure to high light.

Sampling for mass spectrometry (low light acclimated cells exposed to high light)

The experiments and sampling were performed by Aguila Ruiz Sola, a former post-doc student of our team, prior to my arrival. The analysis and the biological evaluation of the phosphoproteomic data was performed by me. CC-125 and Δphot cultures were acclimated in HSM in low light (LL; 15 µE $m^{-2}s^{-1}$) for 16h and were subsequently exposed to HL (300 µE $m^{-2}s^{-1}$) for 3h. LL and HL samples were collected from both strains (5 replicates per strain/ condition of approximate wet weight of 0.5g) and the cell pellets were sent to the lab of Leslie Hicks (University of North Carolina at Chapel Hill) for mass spectrometry. The method for the phosphoproteome quantification is described in (Ford et al. 2020).

Sampling for mass spectrometry (dark acclimated cells exposed to blue light)

For the phosphoproteomic analysis, an inoculum from the precultures of CC125 and Δ*phot* was taken and transferred into HSM. The new cultures had the cell concentration of 4 million cells/ml in a final volume of 200ml (in 1L Erlenmeyer flasks). For each strain there were 5 biological replicates. The cultures were acclimated into darkness overnight (complete darkness in the room has been reassured).

The next day, 25ml samples were taken in 50ml flacon tubes, containing 25ml of -70°C cold 70% methanol for t_0. Cold methanol was used for the quenching of metabolism, as described in (Lee and Fiehn 2008). The samples were centrifuged in max speed in

4°C for 10min. The supernatant was rapidly removed and the pellets were frozen in liquid N_2. After that, the Falcon tubes were stored in -80°C.

The remaining cultures (200ml) were transferred into low profile 75 cm^2 Falcon® cell culture flasks. Each time, a single pair of flasks (CC125 and Δ*phot*) was being placed under blue light (100 μmol photons m^{-2} s^{-1}) for 5min in rotation with the other pairs. Samples were taken after 5min of blue light illumination (25ml of samples in 50ml Falcon tubes, containing 25ml of -70°C cold 70% methanol). No other light source was present at the room during sampling. After every sampling round, the samples were centrifuged in max speed in 4 °C for 10min, the supernatant was rapidly removed, the pellets were frozen in liquid N_2 and the Falcon tubes were stored in -80°C.

After the preparation of all the samples at the same day, all the tubes stored at -80°C were put in a box with dry ice and shipped for mass spectrometry at the lab of Leslie Hicks (University of North Carolina at Chapel Hill). The method for the phosphoproteome quantification is described in (Ford et al. 2020).

Experiments with H_2O_2

A stock solution of 200mM of H_2O_2 has been prepared in a 15ml Falcon tube, at final volume 4ml, by adding 54.4μl of 50% w/v H_2O_2 (Hydrogen peroxide solution, Sigma-Aldrich, Ref.: 516813-500ML) to 4ml water. This solution will be 100x. The solution was always kept on ice.

At the t_0 of each experiment, to the cultures intended to grow with H_2O_2, 250μl from the 200mM H_2O_2 stock solution were added to each of those flasks, to final concertation of 2mM.

Samples for mRNA were taken at t_0 after 1h of incubation. Samples for protein were taken at t_0 after 4h of incubation at 50 μmol photons m^{-2} s^{-1}.

Experiments with Metronidazole (MZ)

Before every experiment involving Metronidazole treatment, 300ml of TAP medium was prepared and autoclaved. Directly after the autoclavation and while the medium was still hot, 58mg of Metronidazole analytical standard (MZ) (M3761, Sigma- Aldrich) were directly added to final concertation of 1.1mM in the bottle and the medium was shaken vigorously as it was described at (Perlaza et al. 2019). This medium was inoculated by the cells which were purposed to be treated with MZ.

Samples for mRNA were taken at t_0 after 1h of incubation. Samples for protein were taken at t_0 after 15h of incubation at 50 µmol photons m^{-2} s^{-1}.

Experiments with DCMU

Stock solutions of 40µM DCMU (3-(3,4-dichlorophenyl)-1,1-dimethylurea) (D2425, Sigma- Aldrich) were prepared in H_2O. Those were serving as 1000x dilutions. The appropriate amount of DCMU was added from the stock solutions to the cultures.

Samples for protein were taken after 4h of incubation.

Fluorescence-based measurements

The fluorescence-based photosynthetic parameters (Y(II) and NPQ) were measured with a pulse modulated amplitude fluorimeter (MAXI-IMAGING-PAM, HeinzWaltz GmbH, Germany). Before the measurements, cells were acclimated to darkness for 15 min in 25ml Erlenmeyer flasks (2ml of culture in total), at 250rpm. From each initial culture, 200µl were transferred into a black 96-well plate in triplicates. Chlorophyll fluorescence was recorded under different intensities of actinic light; starting with measurements in the dark, followed by measurements at 21 µmol photons m^{-2} s^{-1} and 336 µmol photons m^{-2} s^{-1} and finishing with measurements of fluorescence relaxation in the dark.

The calculations of the Fv/Fm, the rETR and the NPQ were based on (Genty, Briantais, and Baker 1989). The relative photosynthetic electron transfer rate (rETR) was

calculated as (Fm' − F)/Fm' × I; F and Fm' are the fluorescence yield in steady state light and after a saturating pulse in the actinic light, respectively and I is the light irradiance in μmol photons m^{-2} s^{-1}. The NPQ was calculated as (Fm − Fm')/Fm'; Fm is the maximal fluorescence yield in dark-adapted cells. The effective photochemical quantum yield of photosystem II was calculated as Y(II) = (Fm'-F)/Fm'. The qE value was calculated as the difference between the last point of the NPQ curve at 336 μmol photons m^{-2} s^{-1} and the point after 3min of the dark relaxation. This estimation was based on the fact that qE represents the fraction of NPQ that is rapidly reversible in the dark.

In-silico DNA designs

All the *in-silico* designs and predictions were done with the use of SnapGene.

Genomic DNA extraction

Total genomic DNA (gDNA) has been extracted by *C. reinhardtii* in order to amplify the endogenous *flkin* gene and to use it for the complementation of the Δ*flkin* strain.

For the gDNA extraction, the Gentra® Puregene® Tissue Kit (QIAGEN) was used. 1 ml of liquid preculture being in exponential phase of growth was added into an Eppendorf tube. 300 μl of cell lysis solution were added and the sample was vortexed vigorously for 5–10 s at high speed. Then, 1.5μl of Puregene Proteinase K (20 mg/ml) was added and the dilution was mixed by inverting the tube 25 times. The tube was left incubating at 55°C at a thermomixer for 90 min for the completion of the cell lysis. The tube had been inverted 10 times every 30 min. After that, the sample was cooled in room temperature for 5 min. 100μl of protein precipitation solution were added, the tube was vortexed vigorously for 20 s at high speed and was let to incubate on ice for 15 min. The sample was then centrifuged at max speed for 5 min. The supernatant was pureed into an Eppendorf tube containing 300μl of isopropanol and the tube was inverted gently 50 times to mix the sample. Another centrifuge took place at max

speed for 1 min. The supernatant was carefully discarded, leaving the DNA pellet, and the tube was left upside-down on a clean piece of absorbent paper. For the wash, 300µl of 70% ethanol were added, and the tube was inverted several times. The tube was centrifuged at max speed for 1 min and the DNA was let to air dry at room temperature for 15 min. 50µl of DNA hydration solution were added to the pellet and the mixture was incubated at 65°C at a thermomixer for 1 h to dissolve the DNA. Finally, the samples were incubated at room temperature overnight with gentle shaking at a thermomixer and the next day they were transferred to a new Eppendorf tube after a quick centrifugation.

Plasmid construction and Gibson assembly

The *flkin* gene (Cre16.g694950), including the 5'UTR and without the stop codon and the 3'UTR had been amplified via pcr from the genomic DNA, with the use of the primers (fp-5'-TAAGGGATTCGGAGGGGGTT, rp-3'- TACGGAAGGCCTCAGTCGTA), which recognised genomic regions upstream of the 5'UTR and downstream of the 3'UTR respectively. The genomic area of interest was taken from Phytozome v.13 (https://phytozome-next.jgi.doe.gov/) and the primers have been designed with the help of the online tool Primer-BLAST from NCBI (https://www.ncbi.nlm.nih.gov/tools/primer-blast/).

The amplification was done with pcr. After multiple rounds of protocol optimisation, and the use of three different enzymes (KOD Hot Start DNA Polymerase (Sigma-Aldrich), Phusion® High-Fidelity DNA Polymerase (NEB) and Platinum™ SuperFi II DNA Polymerase (Invitrogen™), the genomic part had been amplified under the following protocol with the use of Platinum™ SuperFi II DNA Polymerase (Invitrogen™): 4µl 5x buffer, 1µl DMSO, 1µl 10µM forward primer, 1µl 10µM revers primer, 2µl 2mM DNTPs, 1µl of 100ng of genomic DNA, 0.4µl of the enzyme and 9.6 µl of ddH_2O. The pcr was done in a Mastercycler X50 PCR Cycler (Eppendorf, Germany) and the following program was set:

Cycle step	Temperature (°C)	Time	Cycles
Initial denaturation	98	5 min	1
Denaturation Annealing Extension	98 69 72	10s 5s 64s	30
Final extension	72 4	5min hold	1

The pcr product was mixed with 6x orange DNA dye, produced by the team and was deposited on an 0.8 % agarose gel (0.8% agarose, 50ml 1x Tris-acetate-EDTA (TAE) buffer, 5µl SYBR Safe DNA Gel Stain (Thermo Fisher Scientific)). The TAE buffer was consisting of 40 mM TRIS base, 20 mM acetic acid and 1 mM of EDTA disodium salt dihydrate. A 50X stock solution of TAE was routinely prepared. At the first well of the gel, 5µl of the SmartLadder (200 to 10,000 bp Molecular Weight Marker) had been deposited. The gel had been electrophoresed at 120V for approximately 40min and the gel has been projected at a Molecular Imager® Gel Doc™ (BioRad). Observation and analysis of the DNA gels were done with the software Image Lab.

The desired band was cut over a transilluminator panel and put in a clean Eppendorf tube. The clean-up of the pcr product was done with the Monarch® DNA Gel Extraction Kit. The suggested protocol from the kit was followed and the quantity and quality of the final product was observed at a Thermo Scientific™ NanoDrop™ 2000/2000c Spectrophotometer.

That product was later used for a second round of pcr, this time with the Gibson primers, which were compatible with the plasmid vector (pRAM118). The Gibson primers (fp-5'- cacaacaagcccagttGTAAGCTAAGTGCACAAGGTGGG, rp-3'- cacccagatctccgttCGACACCTTGGGGCGG) were designed on SnapGene. For the pcr, the following protocol has been followed with the use of Platinum™ SuperFi II DNA Polymerase (Invitrogen™): 4µl 5x buffer, 1µl DMSO, 1µl 10 µM forward primer, 1µl 10 µM revers primer, 2µl 2mM DNTPs, 1µl of 10ng of the DNA template, 0.4µl of the enzyme and 9.6 µl of ddH_2O. The pcr was done in a Mastercycler X50 PCR Cycler (Eppendorf, Germany) and the following program was set:

Cycle step	Temperature (°C)	Time	Cycles
Initial denaturation	98	5 min	1
Denaturation Annealing Extension	98 72 72	10s 5s 46s	30
Final extension	72 4	5min hold	1

The pcr product had been extracted and quantified as described earlier.

The vector, pRAM118, had been kindly offered to us by Silvia Ramundo's lab. This plasmid was constructed by replacing the aphVIII paromomycin resistance gene with the aphVII hygromycin resistance gene from plasmid pLM005 (Mackinder et al. 2016). The vector contained a PsaD promoter and a CrVenus-3xFLAG as a tag gene. It also contained an AmpR gene under an AmpR promoter, which confers resistance to carbenicillin (for the transformed bacteria selection). It also contained an AphVII gene, interrupted by the RBCS2 intron and regulated under the *Chlamydomonas* beta-2-tubullin promoter and the RBCS2 3'UTR. This gene confers resistance to hygromycin, which would be the selection marker for the algae transformation. Finally, between the PsaD promoter and the CrVenus-3xFLAG, there were under the regulation of the LacZ promoter elements promoter an anti-sense gene for the lac operator and, downstream of that, the LacZ-alpha fragment of beta-galactosidase. The lac repressor binds to the lac operator to inhibit transcription in *E. coli*. This inhibition can be revealed by adding lactose or isopropyl-beta-D-thiogalactopyranoside (IPTG). A map of the plasmid, taken from SnapGene is shown in Fig.2.1.

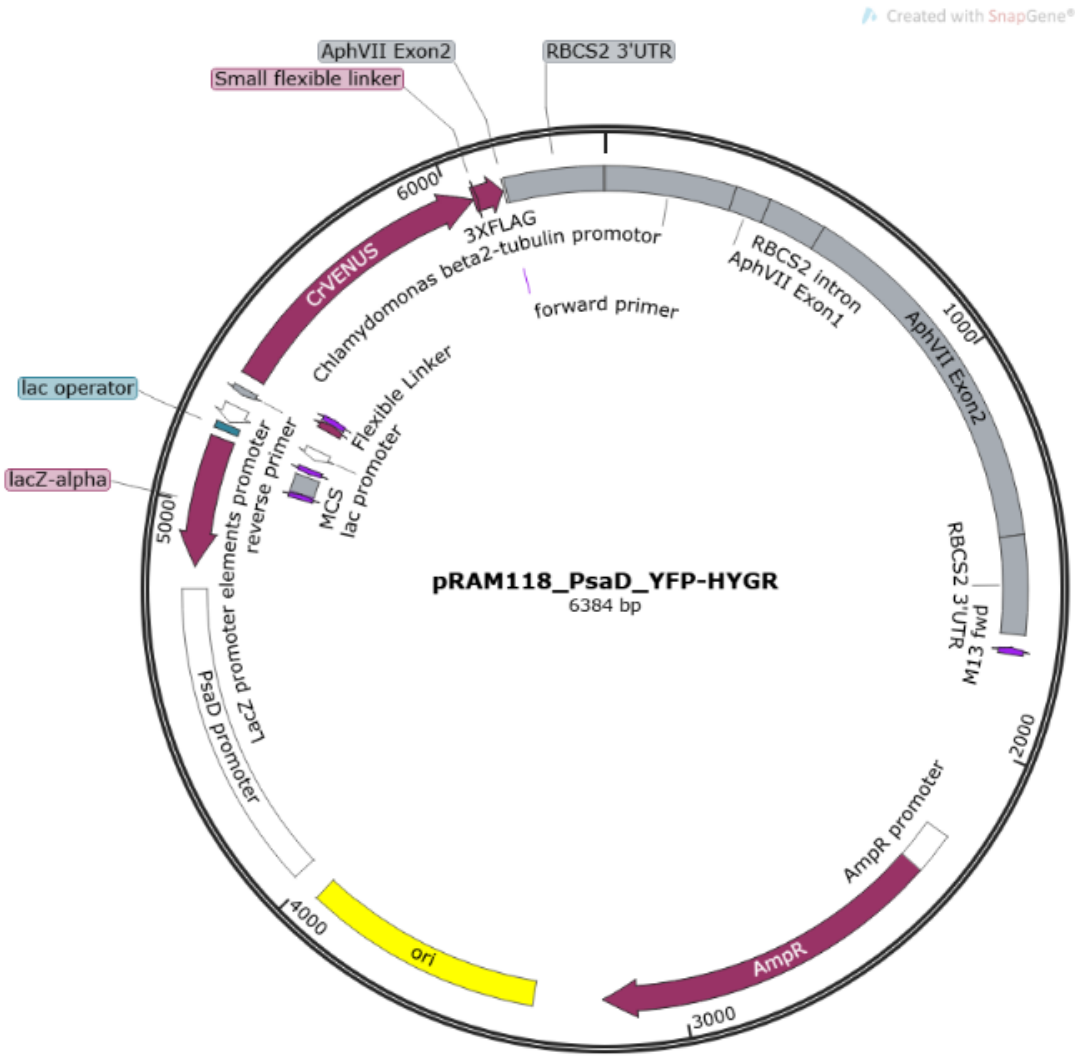

Figure 2.1: Map of the vector pRAM118. Taken from SnapGene

The plasmid was cut with the restriction enzyme HpaI. This restriction enzyme cuts in two regions within the plasmid, one directly after the PsaD promoter, and one directly before the CrVenus-3xFLAG, creating two linearized parts: one containing the lac operator and the lacA-alpha genes with their promoter and one with the rest of the plasmid. After the restriction enzyme cut (see corresponding section), the final product was deposited on an 0.8 % agarose gel with the DNA marker and the bigger band was cut and purified as it was described above.

The big band of the linearized plasmid and the 5'UTR-*flkin* construct were used for Gibson assembly (Gibson et al. 2009). The Gibson Assembly (GA) 5X min contained 50% Tris HCl 1M pH 7.5, 5% $MgCl_2$ 1M, 1% dATP 100mM, 1% dCTP 100mM, 1% dGTP

100mM, 1% dTTP 100mM, 0,5% DTT 1M, 24.7% PEG-8000, 0.5% NAD 100mM. For the Gibbson assembly, 5µl containing 100ng of the vector and 50ng of the gene of interest were added in 15µl of the reaction mix (26.7% GA 5X, 0.03% T5 exonuclease NEB (M0363S) 10u/µl, 1.7% Phusion High fidelity DNA polymerase NEB (M0530S) 2u/µl, 13.3% Taq DNA ligase NEB (M0208) 40u/µl). The reaction mix was stored at -20°C in an Eppendorf tube. The reaction solution was put at 50°C at a thermomixer for 60min.

After the end of the reaction, the quantity and quality of the product had been estimated by a Thermo Scientific™ NanoDrop™ 2000/2000c Spectrophotometer and it was used for bacteria transformation, as it is described below. The expected product after the Gibson assembly is shown in Fig.2.2.

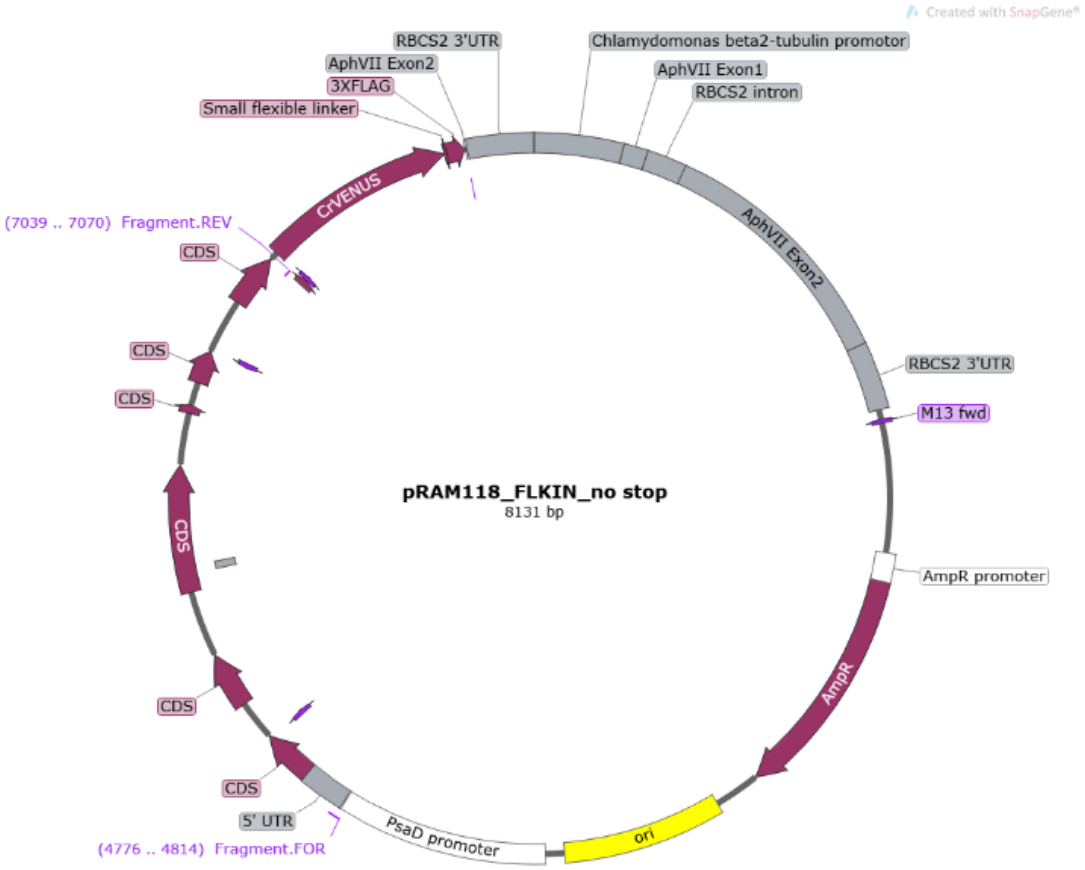

Figure 2.2: Map of the final construct for flkin complementation. Taken from SnapGene

Bacteria transformation and plasmid purification

For the bacteria transformation, a stock of competent E. *coli* cells had been produced, based on (Inoue, Nojima, and Okayama 1990). For this, E. *coli* cells were grown in a plate containing 3.5% LB Agar (LB Broth with agar (Lennox), Sigma-Aldrich). A few cells were taken by a microbiological loop and used as an inoculum to 250ml of SOB media, pH 7 (2% bactotryptone, 0.5% bacto-yeast extract, 0.05% NaCl, 1% 250 mM KCl, 0.5% 2M $MgCl_2$). The cultures were grown at 20^oC, 180rpm until they reach the OD of approximately 0.6 (around two days of culture). The OD was measured by the absorbance at 600nm at a photospectrometer. The cultures were collected and transferred into 50ml Falcon tubes on ice for 10 min. The tubes were spun down at max speed for 10 min at 4°C. The pellet was resuspended in 80 ml ice-cold transformation buffer; pH 6.7 (0.3% 10 mM PIPES Na salt, 0.2% 15 mM $CaCl_2$, 1.9% 250 mM KCl, 1.1% 55 mM $MnCl_2$). The samples were placed on ice for 10 min and spun again at max speed for 10 min at 4°C. The pellets were resuspended in 20 ml of ice-cold transformation buffer. DMSO was added, while the samples were being swirled, to final concentration of 7 %. After incubation on ice for 10 min, the samples were dispensed into freezing Eppendorf tubes (50µl per tube). This step was done in the cold room (4^oC). The tubes were finally frozen in liquid N_2 and transferred to -80°C, where they were stored.

For the transformation, a tube of competent bacteria cells was taken from the -80^oC and thawed on ice for 10min. Another tube was used as a negative control (the plasmid was not added in that). 0.5 ng of the plasmid were added directly to the tube and the mixture was incubating on ice for 30min. Then, the cultures were moved at 42^oC at a thermomixer for one minute and returned to ice for 2min (heat shock). 450ml of 2% liquid LB medium was added to the tube and the cultures were let to incubate at 37^oC for 1h, under minimal shacking at a thermomixer. The sample was spun down at max speed for 2min in room temperature and the supernatant was removed by quickly inverting the tube. The pellet was resuspended into the residual medium and deposited by a pipette (around 50µl) on a plate containing LB medium+ Agar+ the selective antibiotic, which in this case was 100ng/ml carbenicillin. The inoculum was spread with a microbiological stroller until the liquid was completely evaporated. Both plates (+ and – the plasmid) were put on a furnace (37^oC) and were

let to incubate there overnight. The next morning, the plates were checked for colonies. The expected outcome will be the negative control to have significantly less colonies (or ideally no colonies) than the plate with the bacterial transformants.

To further verify the success of the transformation, a few random colonies had been used for colony pcr with the following primers: 5'-fp- GTAAGCTAAGTGCACAAGGTGGG, 3'-rp- CGACACCTTGGGGCGG. These primers bind at the 3' end of the PsaD promoter and at the 5' of the CrVenus and the expected size of the amplification would be around 2.3 kbp. Colonies with the verified possession of the plasmid were used for the plasmid purification.

Plasmid purification

For the plasmid purification the NucleoSpin Plasmid, Mini kit for plasmid DNA (Macherey Nagel) wad used. Colonies selected from the plate were used as inoculum in 5ml of 2% LB medium with the addition of the selection antibiotic (in this case 100ng/ml carbenicillin) in a Caplugs™ (Evergreen Scientific) Sterile Polystyrene Culture Tube. The cultures were put in a rotating incubator at 180rpm at 37^{o}C and were let for 6h.

After the incubation, the cultures were transferred to 15ml Falcon tubes and were centrifuged at max speed for 10min in room temperature. For the plasmid purification, the protocol proposed by the kit was followed exactly.

After the end of the elution, the quantity and the quality of the plasmid were checked on a Thermo Scientific™ NanoDrop™ 2000/2000c Spectrophotometer. To furtherly check the integrity of the plasmid, the product was cut by the restriction enzymes EcoRV and AseI. Those enzymes cut uniquely at the AphVII promoter and the AmpR gene respectively, creating two linearized products: one of 5182 bps and one of 2949bps. The expected size of the produced bands was checked on an agarose gel (the restriction enzyme cut protocol is described in detail in another section).

The plasmid was also sent for sequencing at © Eurofins Scientific 2021, following the instructions of the website (https://www.eurofinsgenomics.eu/en/custom-dna-sequencing/eurofins-services/tubeseq-service/). 5 samples containing 5μl of 100ng of the plasmid/μl were sent with the following primers: 5'- GCCTTGTTTTGCACCGCTAA, 5'-TGTGTTCTGTGCCACCTGTT, 5'-TCCTGATCAACCTCACGCAC, 5'-ACTGGTGCGTACCTTTACGG, 5'- TTCTGGCGACTCTCGAACAC. Each primer was sent in an Eppendorf tube containing 20μl of the primer (10mM). Each DNA sample sent was sequenced by one of the primers.

Algae transformation

The algae transformation occurred via electroporation. The plasmid was cut with the restriction enzyme AseI, which cuts uniquely at the AmpR gene, creating a linearized product. This product was cleaned-up by the Monarch® PCR & DNA Cleanup Kit. The suggested protocol of the kit had been followed. The quantity and quality of the product had been estimated by the Thermo Scientific™ NanoDrop™ 2000/2000c Spectrophotometer.

For the algae transformation, three alterations of the same protocol had been followed. Both CC4533 (as an overexpression strain) and Δ*flkin* cells had been transformed. For both strains, cells were grown in TAP medium at 20 μmol photons m^{-2} s^{-1} to cell density around 2 million cells/ml. An appropriate volume of culture was taken in order to get 40 million cells in a 50ml Falcon tube. The tube was spun down by centrifugation at 3000 rpm for 10min in room temperature. The supernatant was discarded and the pellet was resuspended in 5 mL of GeneArt® MAX Efficiency® Transformation Reagent (electroporation reagent, ER). The mixture was spun down by centrifugation at 3000 rpm for 10min in room temperature. The supernatant was discarded and the pellet was resuspended in 400 μL of ER and transferred to a sterile microtube. Following the protocol described in (Mackinder et al. 2016), 81 ng of DNA were added to the in 400 μL of ER. The resulting mixture was used for 3 transformations.

2 different types of incubation to that mixture had been followed, as a procedure of optimising the transformation success. At first, heat shock had been applied. The mixture was being incubated for 30 min at 40℃ in a thermomixer with gentle mixing at 350 rpm and the cells were let to recover for 30 min at room temperature. With this treatment, the final transformants were limited in number, so this step had been replaced by a cold-treatment. During this step, for each transformation, 120 µL of the cells + DNA mixture were transferred to an ice-cold electroporation cuvette (EC-002S NEPA Electroporation Cuvettes, 2mm gap) just before electroporation. The cuvette was left on ice for 5 minutes before electroporation. This adjustment also failed to increase the success of the transformation and therefore, after following the optimisation approaches of other members of the team, this step had been completely ignored from the protocol.

After the mix was transferred to the electroporation cuvettes, the cells were immediately electroporated with the DNA. The electroporation happened at the NEPA21 Super Electroporator (NEPAGENE). The settings of the machine were as follows:

Poring Pulse						Transfer Pulse					
V	Length (ms)	Interval (ms)	No.	D. Rate (%)	Polarity	V	Length (ms)	Interval (ms)	No.	D. Rate (%)	Polarity
300	**8**	**50**	**2**	**10**	**+**	**20**	**50**	**50**	**1**	**40**	**+/-**

The cells were mixed and the cuvette was placed into the CU500 cuvette chamber. The impedance value was checked. The range of the impedance value should have been between 1.8-2.1 kΩ. If not, the volume of the cells at the cuvette had been adjusted accordingly. After the electroporation pulses, each cuvette was taken out of the chamber and the cells were allowed to recover on the bench for 15 minutes. 500 µL of TAP-40 mM sucrose solution was used to retrieve the electroporated cells using a Pasteur pipette. The mixture was transferred to a 15-mL Falcon tube and the tube

was filled up to 10 mL with TAP-40 mM sucrose solution. The Falcon tubes were placed horizontally in the incubator and were let to incubate for 16 hours to allow the cells to recover and express the antibiotic-resistance genes. The cultures were centrifuged at 3000 rpm for 5 minutes in room temperature and the supernatant was pureed-off, leaving approximately 200-400 µL of residual supernatant. This volume was used to resuspend the pellet. The cells were transferred on TAP + 1.5% agar plates and spread evenly. 5ng/µl of hygromycin was added in the TAP+ Agar plates for the selection and 100 µg/mL of carbenicillin to avoid other microbial contaminations. Empty plates, as well as plates containing CC4533 and Δ*flkin* cells which had been electroporated without the DNA had been used as negative control. The plates were placed under continuous light and when the colonies appeared, they were screened.

Screening of transformants

First, the colonies of the transformants that grew at the selective medium plates were transferred at new TAP+ 1.5% Agar plates (+5ng/µl Hygromycin, 100ng/µl Carbenicillin) in a determined order. The new plates were Greiner Bio-One Square Petri Dishes with Vents (Thermo Fisher scientific). The colonies were let to grown in the new plates with the selective medium for approximately a week under continuous light.

Then, with the help of a sterile pipette tip, part of each colony was transferred in a 96-well plate, each well of which containing 200µl of TAP medium. The initial order of the colonies has been followed in the 96-well plates. The liquid cultures were let to be incubated in an incubator at low light for approximately 5-7 days.

The liquid cultures had been directly transferred to a black 96-well plate and they were screened for the YFP fluorescence. A YFP-overexpression strain was used as a positive control and the background strain (CC4533 or Δ*flkin*) was used as a negative control. The fluorescence measurements were done at a Tecan Infinite® M1000. At first, the intensity of fluorescence emitted from the YFP was measured (excitation 515nm, emission 550nm), and then the one emitted from the chlorophyl (excitation 440nm,

emission 680nm). The fluorescence of the chlorophyl was measured as an indication of the cell concentration at each well. The fluorescence of YFP was normalized to the fluorescence of the chlorophyl. The transformants that showed significantly higher YFP fluorescence than the negative control had been selected and grown in 25ml of TAP (100ml Erlenmeyer flasks).

Those selected colonies had been further screened for FLAG via immunoblotting. As a positive control a FLAG overexpressor strain has been used and as a negative the background strain (CC4533 or Δ*flkin*).

Cut with the restriction enzymes

The restriction enzymes HpaI, EcoRV and AseI had been used as described previously. For the digestion using HpaI, in an Eppendorf tube there were added 1 μg of DNA, 5μl (1X) of 10X rCutSmart Buffer and 1.0 μl (5 units) of HpaI (NEB, #R0105S). The reaction incubated at 37°C for 1 hour.

For the digestion using EcoRV, in an Eppendorf tube there were added 1 μg of DNA, 5μl (1X) of 10X rCutSmart Buffer and 1.0 μl (20 units) of EcoRV-HF® (NEB, #R3195). The reaction incubated at 37°C for 15 min.

For the digestion using EcoRV and AseI, in an Eppendorf tube there were added 1 μg of DNA, 5μl (1X) of 10X rCutSmart Buffer, 1.0 μl (20 units) of EcoRV-HF® (NEB, #R3195) and 1.0 μl (10 units) of AseI (NEB, #R0526). The reaction incubated at 37°C for 15 min.

For the digestion using AseI, in an Eppendorf tube there were added 1 μg of DNA, 5μl (1X) of 10X rCutSmart Buffer and 1.0 μl (10 units) of AseI (NEB, #R0526). The reaction incubated at 37°C for 15 min.

Colony pcr

Colony pcr was done for the verification of the CLiP mutant strains and during the screening of the bacteria transformants for the *flkin* complementation.

For the algae samples, a few cells of the colony of interest were taken with a microbiology loop and put in an Eppendorf tube containing 50 µL of 10mM EDTA, pH 8.0. The cells were spread at the wall of the tube and then well-fixed in the liquid. The tube was vortexed for 10 sec, put in a thermomixer at 100°C for 10 min, cooled at 4°C at an ice box and vortexed again for 10 sec. The sample was then centrifuged for 1min in max speed in room temperature and the supernatant was transferred in a new Eppendorf. This was used as the DNA template for the next step.

For the bacteria transformants, this step was ignored and cells from each colony of interest were added directly into the pcr mix via a microbiological loop.

For the colony pcr, the Phire Plant Direct PCR Master Mix (Thermo Scientific) was used. For each reaction, 25 µl of 2X Phire Plant Direct PCR Master Mix, 1µl of each primer (10 µM), and 22µl of H_2O were added in a pcr tube. Then, either 1µl of the algae DNA sample or some bacterial cells were added in the tube. The tube was put on a Mastercycler X50 PCR Cycler (Eppendorf, Germany) and the following program was set:

Cycle step	**Temperature (°C)**	**Time**	**Cycles**
Initial denaturation	98	5 min	1
Denaturation Annealing Extension	98 *Depending on the Tm values of each primer pair 72	5s 5s 20s/kb	40
Final extension	72 4	1min hold	1

The annealing temperature was calculated by the online tool NEB Tm calculator (https://tmcalculator.neb.com).

Protein extraction and quantification for Immunoblotting

For the immunoblotting analysis, 5ml of samples were taken each time from the cultures, in 15ml Falcon tubes (always kept in ice from the moment of the sampling). The samples were centrifuged at max speed for 10min in 4^{o}C. The supernatant was removed by quick invert of the tubes over a waste dispenser. The pellets were resuspended with the residual medium and transferred into an Eppendorf tube (final volume approximately 200μL). The tubes were centrifuged at max speed for 10min in 4^{o}C. The supernatant was removed. For the quantification based on equal protein, the pellets were resuspended in 50μl of HEPES buffer (5 mM HEPES-NaOH pH 7.5; 10 mM EDTA; 10 mM NaF; 1μl of 1x protease inhibitor solution (Roche, complete, EDTA-free, 11873580001)). For the quantification based on equal protein, the pellets were not resuspended. The tubes were put directly into a tank containing liquid N_2. After that, the samples were stored at -80^{o}C.

For the sample preparation for Western Blot and the protein quantification, two different protocols were followed. At first, the samples were quantified based on equal chlorophyl. Based on that protocol, 50 μl of the loading buffer (5% SDS; 30% Sucrose) was added directly to the samples, while they were remaining frozen. The samples were boiled for 1min at 100 ^{o}C at a thermomixer and then centrifuged at max speed for 15 min at 4 ^{o}C. 5 μL of the supernatant were added to 995 μL of 100% methanol. Chlorophyl was measured and calculated as it was described in the according section. 5μg of Chlorophyl were deposited at each well of the gel. This protocol led to consistent misloading and it was abandoned.

Later, the samples were quantified based on equal protein. According to this protocol, 1 mL of 80% acetone was added on the cell pellets. The resuspension was done by gently pipetting the acetone up and down while dissolving the pellet. The samples were let on ice for 30 min and then centrifuged at max speed at 4°C for 20 min. The supernatant was discarded and the microtubes were put upside-down on a paper for the acetone left to be removed. 50 μL of 1x protease inhibitor solution (Roche, complete, EDTA-free, 11873580001) were added in each sample and mixed by pipetting up-and-down. Then, 50 μL of 2x lysis buffer (1 mL of 1M Tris HCl pH 6.8 (final 100 mM), 2 mL of SDS 20% (final 4%), 0.4 mL of 0.5 M EDTA (final 20 mM), 6.6 mL of water) were added. The samples were let on the bench for 15 min and then

centrifuged at room temperature for 5 min in max speed. The supernatant was transferred to a new microtube and stored at -80^{o}C.

The protein quantification was done via the BCA method, with the use of the Pierce™ BCA Protein Assay Kit, Thermo Scientific™. In new Eppendorf tubes, the samples were diluted 1:25 (final volume 200µl). 25µl of each diluted sample were added in a transparent 96-well plate in triplicates. For standards, bovine serum albumin samples of known concentrations, provided by the kit, were used (500 µg/ml, 250 µg/ml, 125 µg/ml, 25 µg/ml and blank). 100µl of the working buffer (provided by the kit) were added at each well and the plate was put at an incubator at 37^{o}C for 30min. After that, the absorbance of each well was measured at 569nm at a Tecan Infinite® M1000. A standard curve had been designed based on the standards and the protein quantity had been estimated in accordance. 5µg of protein (total volume of 9µl) from each sample were deposited at a new Eppendorf with 3µl of SDS loading buffer and boiled at 100^{o}C at a thermomixer for 5min.

Immunoblotting

For the immunoblotting, home-made 5-13 % SDS-PAGE gels were prepared (Separation gel: 0.8ml H_2O, 2.1ml acrylamide, 1.3ml lower tris (1.5M Tris pH 8.8, 0.4% SDS), 20.2 µl EDTA, 0.7ml sucrose 2M, 1.3µl TEMED, 61.5µl APS 10%. Stacking gel: 1.4ml H2O, 0.4ml acrylamide, 0.6 ml upper tris (0.5M Tris pH 6.8, 0.4% SDS), 10.3 µl EDTA, 2.6µl TEMED, 25.5µl APS 10%). SDS-Protein samples of 5 µg protein were loaded on the gels (12µl/ well), with the protein ladder (Precision Plus Protein™ Dual Color Standards, BIO RAD). Laemmli (0.3% Tris base, 1.4% glycine, 0.1% SDS, pH 8.3) was used as an electrophoresis running buffer. The migration occurred at 85V.

The proteins were then transferred onto nitrocellulose membranes (Amsterdam Protran Premium 0.45µm NC). The wet transfer buffer consisted of 80% Laemmli and

20% Ethanol (96%). The wet transfer was happening with the presence of an ice cooler container and under continuous stirring at 105V for 1h.

After the transfer, the membranes were incubated with 5% commercial milk, diluted into TBS-T (0.2% Tris base, 0.8% NaCl, 0.05% v/v triton x100) for 1h. For each primary antibody there were 2h of incubation at slow rotation, separated by 3 10-minute-long washes with TBS-T. When time restrictions required it, the membrane was left incubating with a primary antibody overnight in the cold-room (4^{o}C). The membranes were incubated with the secondary antibody for 1h and after 3 10-min washes they were projected.

Antisera against LHCSR1 (AS14 2819), LHCSR3 (AS14 2766), ATPb (AS05 085) and CoxIIb (AS06 151) were from Agrisera (Vännäs, Sweden). The antiserum for FLAG (F3165-1MG) was from Sigma. Antisera against VIPP2 and HSP22E/F were kindly offered to us from the lab of Michael Schroda. For the detection of PHOT, an anti-LOV1 antiserum was used, as it has been described in (Zorin et al. 2009).

ATPb was primarily used as a loading control, but also CoxIIb has been used as well, when the signal from the ATPb was counteracting with other unspecific signals.

The primary antisera were kept in dilutions with TBS-T (1/25000 for LHCSR1, LHCSR3, VIPP2, HSP22E/F, ATPb, CoxIIb and FLAG and 1/ 2000 for LOV) with 0.02% (w/v) of NaN_3 (to prevent microbial contamination) in the fridge (4^{o}C) and they were used at maximum for 5 incubations. An anti-rabbit horseradish peroxidase–conjugated antiserum was used for the detection of LHCSR1, LHCSR3, LOV, VIPP2, HSP22 E/F, ATPb and CoxIIb and an anti-mouse antiserum for the detection of FLAG.

The blots were developed with ECL detection reagent, and images of the blots were obtained using a CCD imager (ChemiDoc MP System, Bio-Rad) or Amersham™ImageQuant 800. For the densitometric quantification, data were normalized to the loading control.

RNA extraction

Samples (10ml in 15ml Falcon tubes on ice) were collected after 1h of every light or chemical treatment. The samples were spun down by centrifugation at max speed in 4^{o}C for 10min. 1 ml of TRI Reagent® (Sigma, USA) was added per 10 million cells and the mixture was transferred into an Eppendorf safe-lock tube. The tubes were frozen in a container with liquid N_2 and stored at -80^{o}C.

On the day of the extraction, 0.2 ml of chloroform per 1 ml TRI Reagent used for homogenization were added to the tubes. The tubes were vortexed for 15s and then let to incubate for 3 min at room temperature. The samples were centrifuged at 12,000 rpm for 15 min at 4°C and the upper aqueous phase was pipetted out into a new RNase-free tube. 0.5ml of 100% isopropanol /per ml of TRI Reagent was then added to the aqueous phase. The samples were mixed thoroughly and were let to incubate at room temperature for 10 minutes. The tubes were centrifuged at 12,000 rpm for 10 min at 4°C and the supernatant was removed from the tube, leaving only the RNA pellet. The pellet was washed with 1 ml of 75% ethanol (in DEPC- treated water) per 1 ml of TRI Reagent used in the initial homogenization and the samples were centrifuged at 5,000 rpm for 3 min at 4°C. After discarding the wash, there was another brief centrifuge to collect the residual liquid and pipette them out. The RNA pellet was air-dried for 3 min. 50µl of RNase-free water were added and the RNA pellet was completely resuspended by pipetting up and down.

The RNA quantity and quality of each sample was estimated by Thermo Scientific™ NanoDrop™ 2000/2000c Spectrophotometer.

cDNA synthesis

For the cDNA synthesis, the SensiFAST™ cDNA Synthesis Kit was used. 1µg of RNA was added in a pcr tube, with 5µl of 5x TransAmp Buffer and 1µl of the reverse transcriptase (H_2O was added up to 20µl).

The tube was put on a Mastercycler X50 PCR Cycler (Eppendorf, Germany) and the following program was set: 25 °C for 10 min, 42 °C for 15 min, 85 °C for 5 min and 4 °C hold.

qPCR

The cDNA samples were first diluted 1:5 with H_2O to a final volume of 50µl.

For the reactions, 96-well plates were used. In each plate the cDNA(s) of interest was measured, always alongside the housekeeping gene, which was *gblp*. *gblp* is a gene encoding G protein subunit-like protein (Schloss 1990). For each sample there were 3 technical replicates. The primers used were ordered from ThermoFisher Scientific and are shown at table 2.2.

Table 2.2: The qPCR primers used. The transcript and gene ID and the gene name are indicated at the corresponding columns

Transcript name	**Gene ID (V12.5)**	**Gene name**	**Forward primer**	**Revers primer**
Cre06.g278222.t1.1	Cre06.g278222	*gblp*	TGGCTTTCTCGGTGGACAAC	CTCGCCAATGGTGTACTTGC
Cre08.g367500.t1.1	Cre08.g367500	*Lhcsr3.1*	CACAACACCTTGATGCGAGATG	CCGTGTCTTGTCAGTCCCTG
Cre08.g365900.t1.2	Cre08.g365900	*Lhcsr1*	GAGTCTGAGATCACCCACGG	CCGATCTGCTGGAAGTGGTA
Cre01.g016600.t1.2	Cre01.g016600	*Psbs1*	TAAACCGTGTATTGGAACTCCG	CTCTGCACGCGGCGTGTT
Cre09.g399552.t1.1	Cre09.g399552	*Lcr1*	GCACCAGCATACACCAAAATC	CAGAAAACAGAACGACCAAAGC
Cre10.g452800.t1.2	Cre10.g452800	*lcib*	TGCATAAGAGCGGATGTAGC	CGGTAGTCAGCATCAGTCATC
Cre05.g248400.t1.2	Cre05.g248400	*Cah4*	CGAAAAGCTGCATGAACTCACC	GCCCGTAGGCTACAGTTTTC
Cre06.g309000.t1.2	Cre06.g309000	*lcia*	AGATTTGATAACGGCAGGACC	CCTATCCCATGTCATTCCCAC
Cre09.g415700.t1.2	Cre09.g415700	*Cah3*	AACCTGGAAGGGTGTGTGTG	CACTTCTCGAAGCTGCCGTA
Cre16.g694950.t1.1	Cre16.g694950	*flkin*	GGATCTTTACGAGGACGCGA	GTGCCCATTGCAACCAGAAG
Cre11.g468050.t1.2	Cre11.g468050	*Vipp2*	CATCATGCATTTGGCAGGTCTC	AATGAGAGGTGCGACGACCAAC
Cre14.g617400.t1.2	Cre14.g617400	*Hsp22f*	TGCGCACGCGACATTATCAAAG	GTACAAACCAGCCATGCGCTCAG

For each reaction, 10µL of SsoAdvanced Universal SYBR Green Supermix (BioRad), 0.6 µL of 10 µM forward primer, 0.6 µL of 10 µM reverse primer, 3.8 µL of H_2O and 5 µL of diluted cDNA were added in a well. The plate was covered with a PCR Plate Heat Seal #1814035 (BioRad) and the reactions were performed and quantitated in a Bio-Rad CFX96 system.

The relative expression values were calculated in relativity to *gblp* from the Cq values.

Graphs design

All the graphs designs and the statistical analyses were done on Prism 7 (Graphpad Software, LLC).

3. RESULTS AND DISCUSSION

3.1 Exploring the role of Phototropin in the transition from low light to high light.

3.1.1. Analysis of the phosphoproteome dataset

In order to characterize the PHOT-dependent phosphoproteome and to identify putative PHOT interactors, a comparative phosphoproteomic approach has been applied. The phosphoproteome of the WT and Δ*phot* after low light (16h at 15 µmol photons m^{-2} s^{-1}) acclimation and after exposure to HL (20 min at 300 µmol photons m^{-2} s^{-1}) was quantified and analysed. The phosphoproteomic analysis was coupled with a whole-cell proteomic analysis.

From the phosphoproteomic analysis, 2,680 unique phosphopeptides from 1524 proteins were identified. After multiple-sample test ANOVA testing, 1486 sites were found to change significantly their abundance between the two genotypes and two conditions. Hierarchical clustering was performed to determine unique trends in the dataset (Fig.3.1). From this clustering, the phosphosites were clustered into 4 groups, based on their abundance trends in the four conditions.

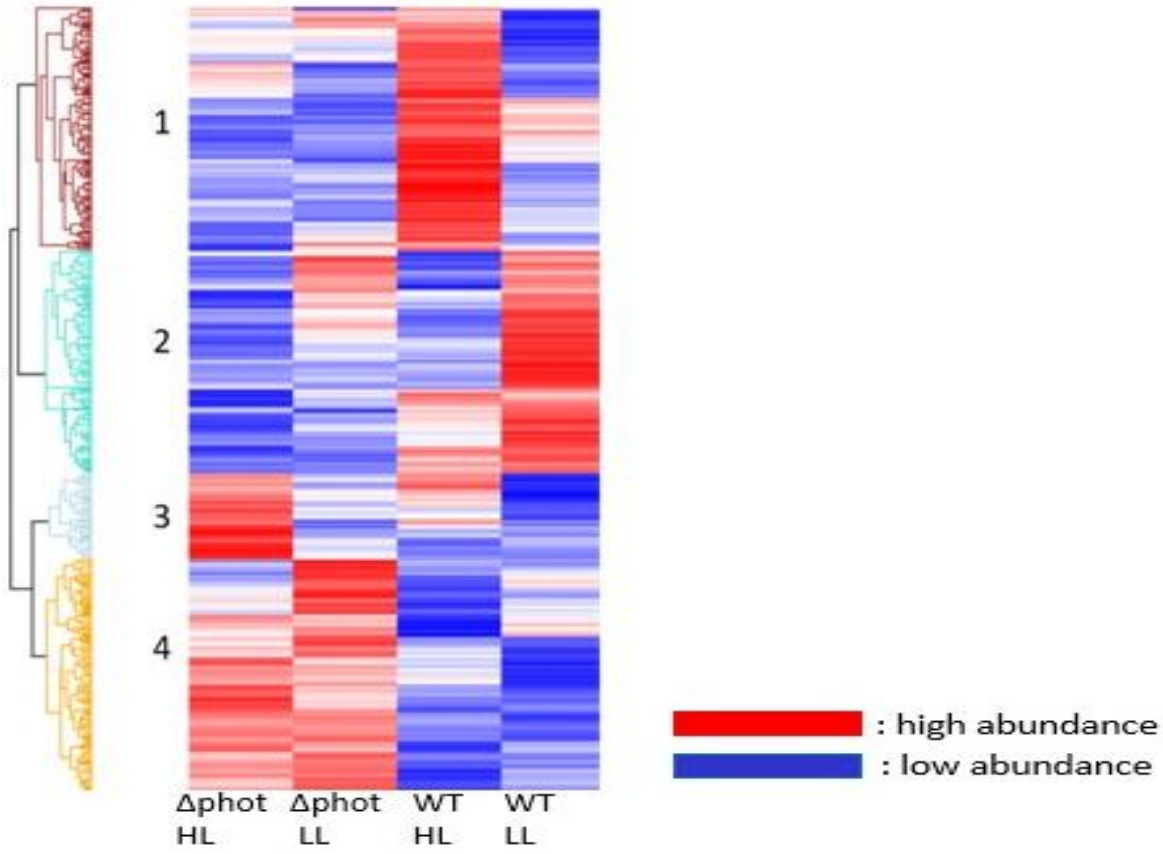

Figure 3.1: Hierarchical clustering of the phosphosites with significant changes in their abundance, based on 4 unique phosphorylation trends. Each horizontal line represents a phosphosite and each column corresponds to one of the four conditions. Blue stands for low abundance and red for high abundance. The strain and the light condition are indicated at the bottom of each column.

A motif analysis was also performed (Fig. 3.2), which depicts over-represented aminoacidic patterns from the peptide sequence data in each cluster. The observed sequences were extended from the phosphorylated residue to 7 residues in either primary sequence direction. The motif analysis was done with the use of the online tool MotifX (https://motif-x.med.harvard.edu/motif-x) (Schwartz and Gygi 2005) (Chou and Schwartz 2011). We observe that there is not a specific pattern that emerges significantly in clusters 1-3. However, in cluster 4 there is a large number of acidic residues (aspartic and glutamic acid, D and E respectively) downstream of the phosphorylated residue, which is predominantly Serine (S). Cluster 4 contains the phosphosites which are in high abundance in Δ*phot* and low abundance in the WT, independently of the light condition.

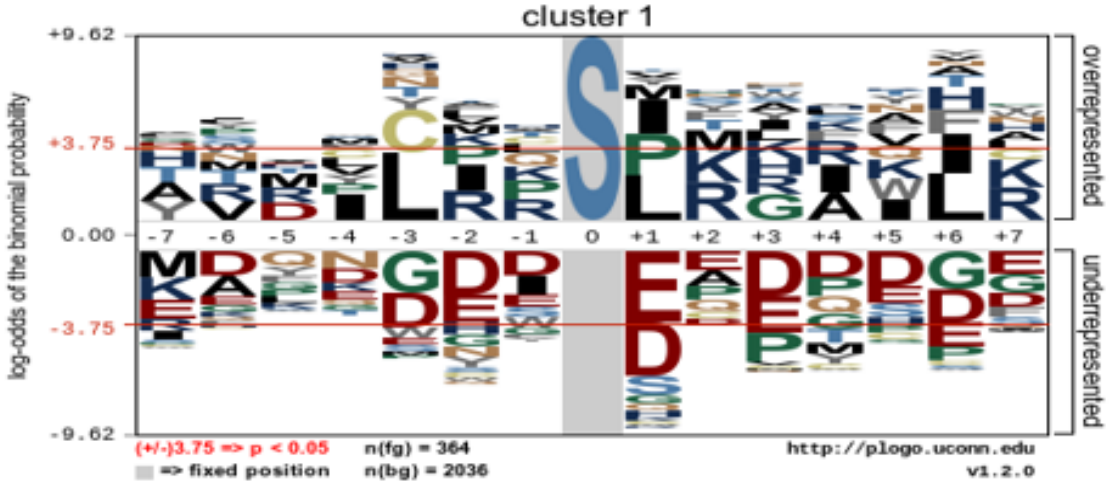
cluster 1
+9.62
+3.75
0.00
-3.75
-9.62
log-odds of the binomial probability
overrepresented
underrepresented
-7 -6 -5 -4 -3 -2 -1 0 +1 +2 +3 +4 +5 +6 +7
(+/-)3.75 => p < 0.05
=> fixed position
n(fg) = 364
n(bg) = 2036
http://plogo.uconn.edu
v1.2.0

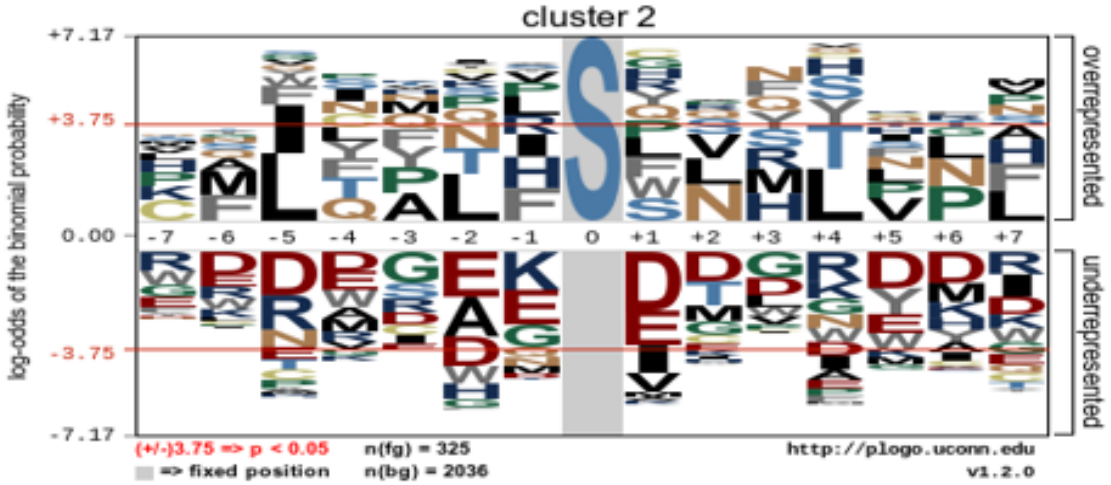
cluster 2
+7.17
+3.75
0.00
-3.75
-7.17
log-odds of the binomial probability
overrepresented
underrepresented
-7 -6 -5 -4 -3 -2 -1 0 +1 +2 +3 +4 +5 +6 +7
(+/-)3.75 => p < 0.05
=> fixed position
n(fg) = 325
n(bg) = 2036
http://plogo.uconn.edu
v1.2.0

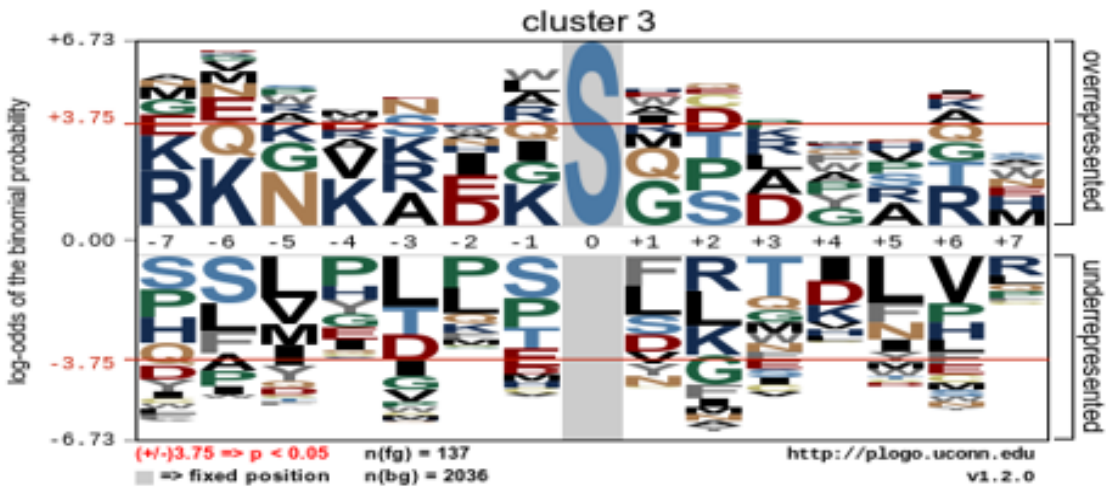
cluster 3
+6.73
+3.75
0.00
-3.75
-6.73
log-odds of the binomial probability
overrepresented
underrepresented
-7 -6 -5 -4 -3 -2 -1 0 +1 +2 +3 +4 +5 +6 +7
(+/-)3.75 => p < 0.05
=> fixed position
n(fg) = 137
n(bg) = 2036
http://plogo.uconn.edu
v1.2.0

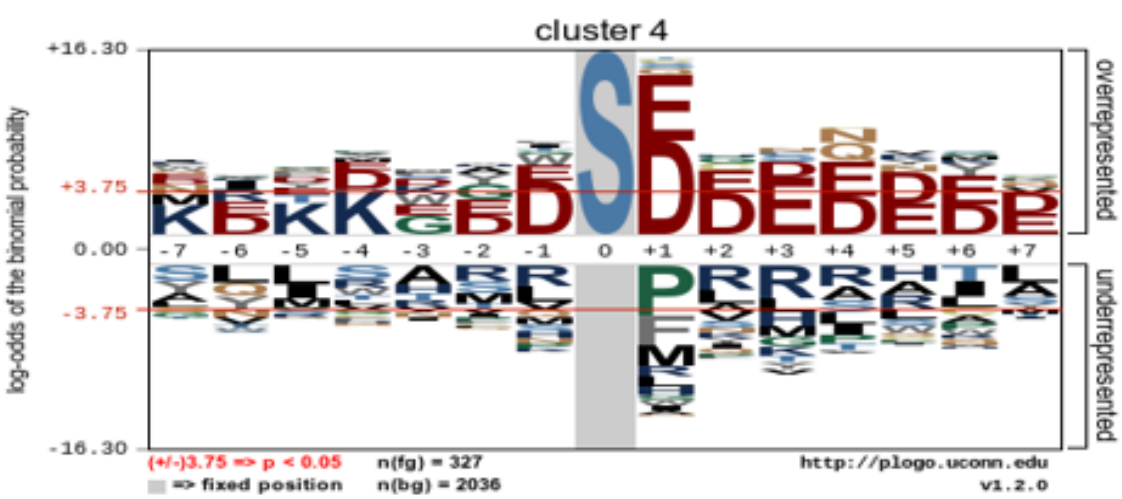
cluster 4
+16.30
+3.75
0.00
-3.75
-16.30
log-odds of the binomial probability
overrepresented
underrepresented
-7 -6 -5 -4 -3 -2 -1 0 +1 +2 +3 +4 +5 +6 +7
(+/-)3.75 => p < 0.05
=> fixed position
n(fg) = 327
n(bg) = 2036
http://plogo.uconn.edu
v1.2.0

Figure 3.2: Motif analysis depicting over-represented aminoacidic patterns from the peptide sequence data in each cluster. Each residue is represented by their unique one-letter abbreviations. The colour of each residue represents the group of amino acids in which it belongs (ex. the acidic residues are shown with red). Serine (S) is the phosphorylated residue and is placed in the middle of each pattern. Residues which are above the x axis are overrepresented and those which are below are underrepresented.

For the whole cell proteome, 2,352 proteins were identified (1,560 with more than one unique peptide). From multiple-sample test ANOVA testing, 1,300 proteins were found to change significantly and hierarchical clustering was performed to determine unique trends in the dataset (Fig. 3.3). From this clustering, 4 unique abundance trends have emerged.

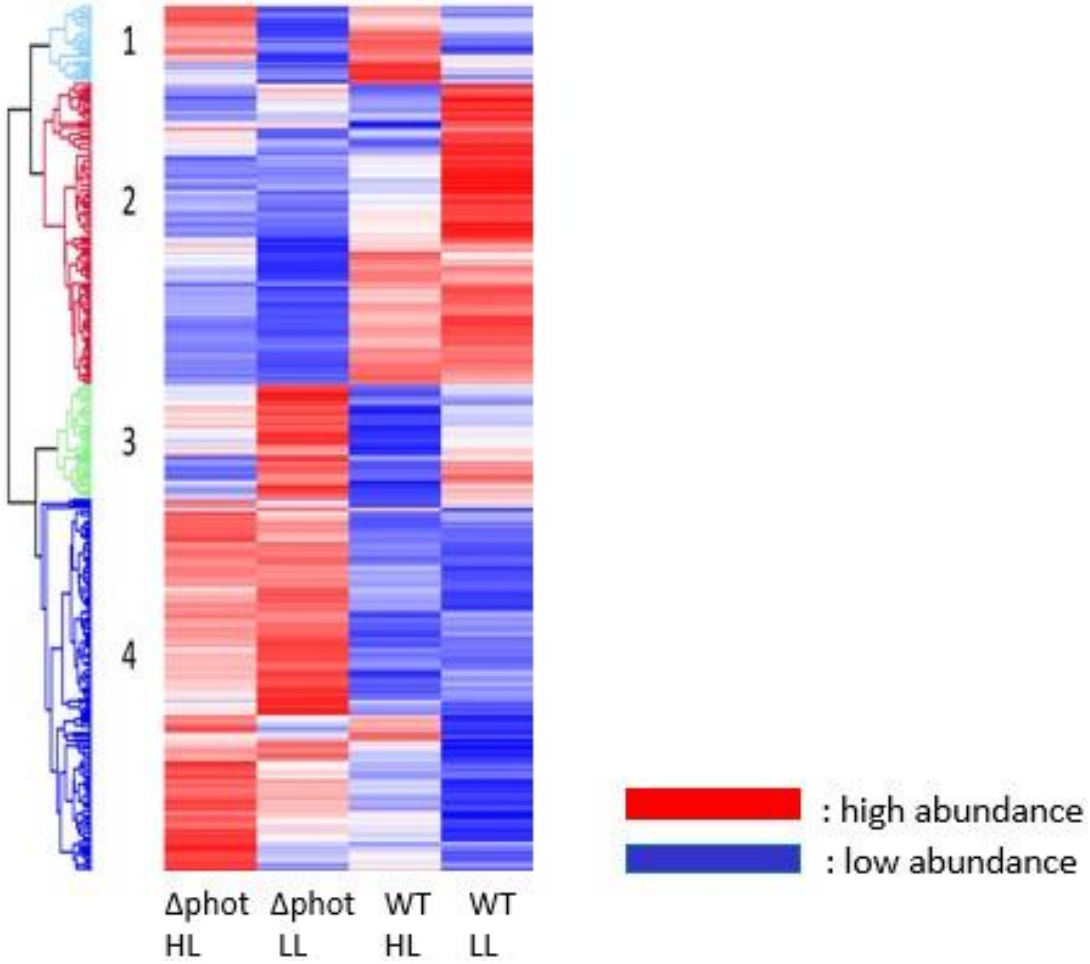

Figure 3.3: Hierarchical clustering of the proteins with significant changes in their abundance, based on 4 unique trends. Each horizontal line represents a protein and each column corresponds to one of the four conditions. Blue stands for low abundance and red for high abundance. The strain and the light condition are indicated at the bottom of each column.

From the dataset of the phosphoproteome, we decided to sort out the phosphosites which increase their abundance at least 2-fold in the WT when transferred from low

light to high light, while their abundance was not increased in Δ*phot* more than 2-fold. The changes of the abundance of the phosphosites needed also to be statistically significant. Those phosphosites were considered to be phosphorylated on a PHOT-dependent manner directly or indirectly. Because their phosphorylation was also responsive to high-light, those phosphosites could also be involved in the induction of LHCSR3. This shorting resulted to 131 phosphosites from 113 proteins.

As it was expected, a great number of those shorted-out phosphoproteins were kinases and phosphatases. The phosphatases included a halo acid dehalogenase (HAD)-like hydrolase and a member of the Protein phosphatase 2C (PP2C) family. Concerning the kinases, multiple non-specific Ser/Thr- kinases have also emerged from this list, alongside two calcium dependent kinases (calcium binding protein kinase 34 and a CDPK-related kinase), numerous signalling kinases (such as a PB1 domain-containing protein tyrosine kinase and a protein kinase with octicosapeptide Phox/ Bem1p domain), a mitogen- activated leucine- rich repeat kinase and cNMP-dependent kinases. The last group shows particular interest, given the fact that cNMP (cAMP and cGMP) are shown to be involved in the signalling that leads to LHCSR3 induction (Petroutsos et al. 2016). A cNMP-dependent kinase, product of the gene Cre12.g499500, shows a 3-fold difference in abundance in the WT, from low to high light, while in the Δ*phot* its abundance shows no statistically significant change. Among the unspecific ser/thr kinases, the product of the Cre16.g694950 gene has shown a 5-fold difference in abundance in the WT between the two light conditions and the study of its role in the LHCSR3 induction has been the focus if the following chapter.

This list of proteins also reveals a possible connection between PHOT and the carbon concentrating mechanism (CCM). More specifically, phosphorylation of the carbonic anhydrase 7 (CAH7), and of two other CCM-related proteins, Low CO_2-inducible 23 (LCI23) and Low-CO_2 inducible protein C (LCIC) is shown to be PHOT-regulated. Both LCI23 and LCIC are being controlled by the CCM-regulating factor CIA5/CCM1, as a response to low CO_2 conditions (Miura et al. 2004). The role of LCIC in particular for CCM, has been partially elucidated. LCIC is being diffused in the chloroplast stroma under high (5%) and low (0.033 to 0.04%) CO_2 conditions, but it is being aggregated

around the pyrenoid under very low CO_2 (0.011 to 0.015%), where it forms a complex with the other CCM protein LCIB (Yamano et al. 2010). The LCIB/LCIC complex is suggested to prevent the leakage of CO_2 from the pyrenoid by converting CO_2 into the stromal HCO_3^-. A possible regulation of CCM by PHOT would be a fascinating case for future studies and it is only recently that it was shown that PHOT participates in the regulation of CCM by suppressing QER7, a squamosa binding transcription factor which supresses qE and CCM-related genes (Arend et al. 2022).

The LHCSR3 induction is shown to be regulated by the action of ubiquitin complexes (Aihara et al. 2019) (Gabilly et al. 2019) (Tokutsu, Fujimura-Kamada, Matsuo, et al. 2019). Interestingly, in our list, there is a ubiquitin-specific protease, product of the Cre02.g117850 gene, which shows a 3-fold increase in abundance between low and high light in the WT.

This list of phosphoproteins contains 7 membrane transporters, including the sodium proton exchanger SOS1 and the sulphate transporter pleiotropic drug resistance 6. The presence of a Ca^{2+} transporter (Autoinhibited Ca^{2+} -ATPase, isoform 8) in the list is of particular importance, given the fact that the cellular Ca^{2+} flux is a regulator of the LHCSR3 induction signal (Petroutsos et al. 2011).

The initiation of protein synthesis seems also to be under partial control of PHOT. More specifically, two components of the eukaryotic translation initiation factor 3 (eIF-3) complex (products of the genes Cre03.g144847 and Cre04.g217550) are shown in the list of the PHOT-regulated phosphoproteins. The second one, in particular, shows 5 different phosphosites with increased abundances from low to high light in the WT. PHOT additionally regulates the phosphorylation of proteins involved in the ribosomal structure (Ribosomal protein L24e family protein, Ribosomal protein L30/ L7 family protein and Ribosomal L29 family protein).

A surprising presence in this list is the one of three homotherm- related proteins (products of the genes Cre09.g408676, Cre03.g168100 and Cre24.g755747). Based on the gene ontologies (GOs) of these proteins, they are ice-binding proteins which respond to freezing. Thus, it is particularly intriguing to investigate the reason of the

increase of the abundance of their respected phosphoproteins after exposure to high light, where there is an expected elevation of the temperature.

3.1.2 Study of the Cre16.g694950 mutant (Δ*flkin*)

3.1.2.1 Selection of FLKIN out of the phosphoproteomic dataset

Out of the phosphoproteome list, at first, I choose a number of proteins and ordered the corresponding mutant strains. The choice of those proteins was done based on their biological proximity to a possible candidate as an intermediator of the PHOT signalling pathway, their abundance trends in the dataset and the availability of CDS mutants of their genes on the CliP library.

A specific protein that attracted my attention was the product of the gene Cre16.g694950. The Cre16.g694950 gene encodes for a non-specific Ser/Thr kinase, which is being co-expressed with flagella-localised proteins. Hereafter, this protein will be referred as FLKIN. FLKIN is a non-specific Ser/Thr kinase with an estimated size of 44.3 kDa. The kinase domain is located close to the C' terminus of the protein. It is worth mentioning that the phosphorylated form of FLKIN, which has been detected in our phosphoproteomics dataset, has a phospho-group at Ser127, which is outside of the kinase domain (Fig. 3.4).

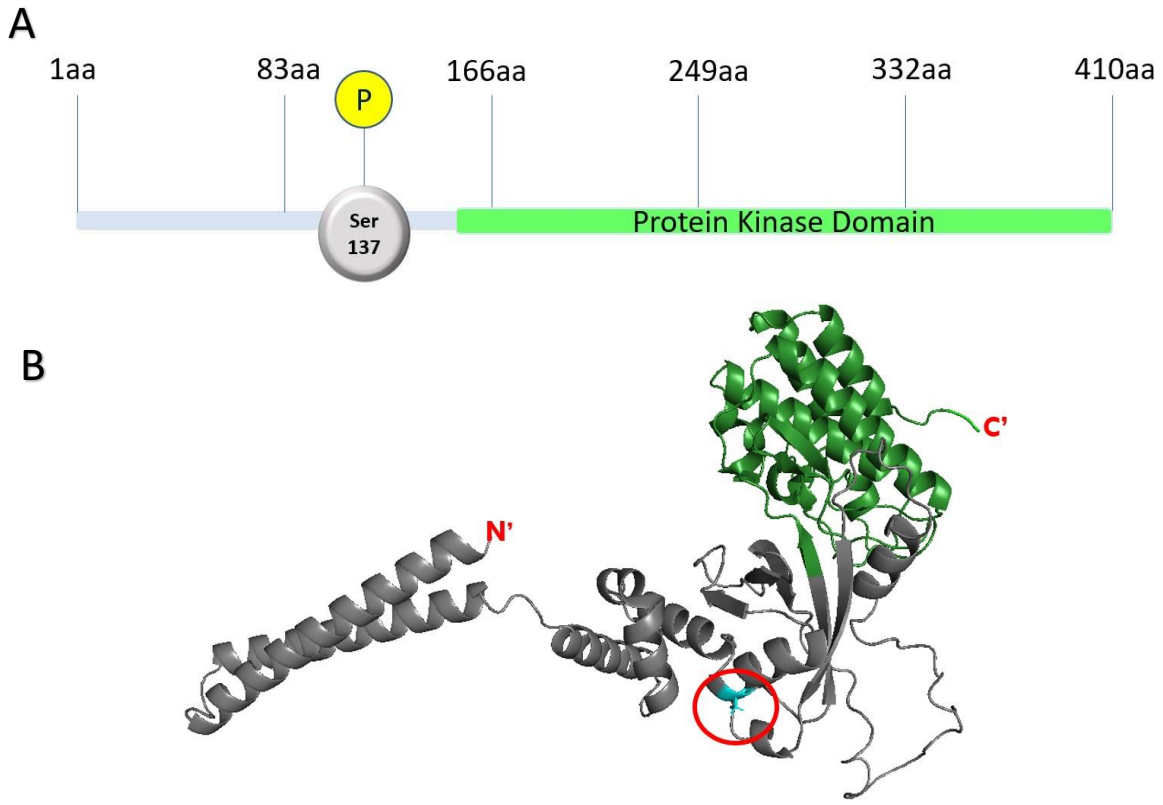

Figure 3.4: A) Map of functional annotations and site of the phosphorylation at the FLKIN (by Prosite). The Protein Kinase Domain, which is being highlighted by light green colour, corresponds at the entry PS50011 at Prosite. Indicated here, the Ser residue that gets phosphorylated, according to our phosphoproteomic data (Ser127). B) Predicted 3D structure of FLKIN by AlphaFold (Jumper et al. 2021). The molecule was visualised in the PyMOL Molecular Graphics System, Version 1.2r3pre, Schrödinger, LLC. The N' and C' terminus of the protein are being indicated. Ser127, the phosphorylated residue, is also being indicated with blue in a red circle.

The abundance of the phosphoprotein was increased fivefold in the WT (when shifting from LL to HL) but was practically unchanged in the *Δphot* mutant and remained at high phosphorylation levels in both LL and HL (Fig. 3.5).

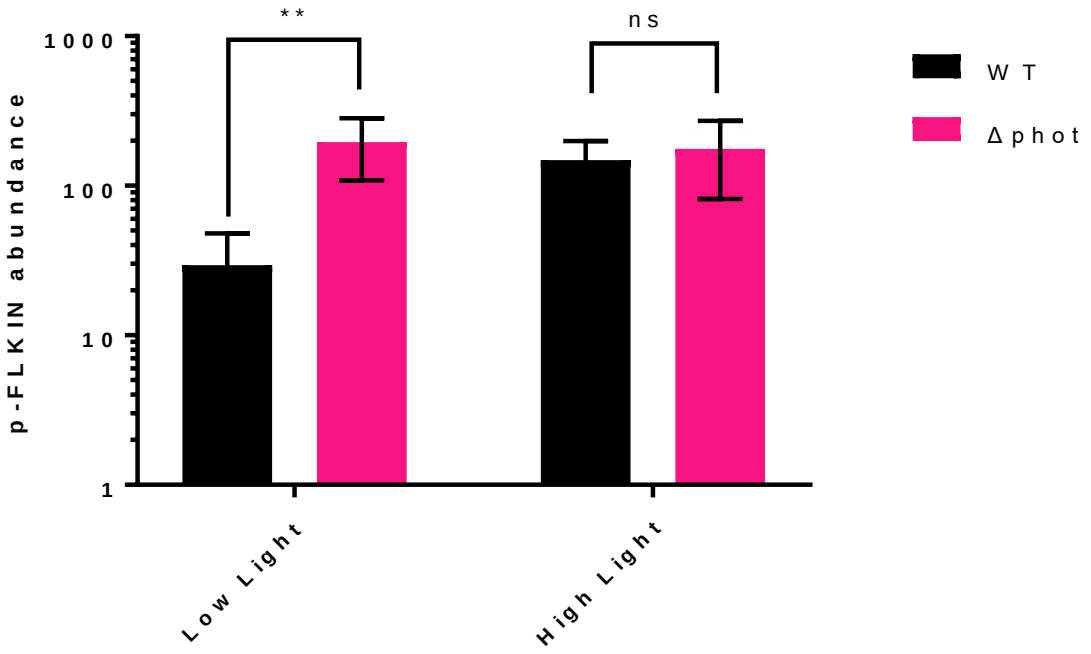

Figure 3.5: The abundance of p-FLKIN in the WT and Δphot after 16h of exposure to low light (15 µmol photons m^{-2} s^{-1}) and after 20min exposure under high light (300 µmol photons m^{-2} s^{-1}).

3.1.2.2. Ordering and genotyping of the Δflkin mutant strain

In order to study the possible role of FLKIN in the PHOT-controlled LHCSR3 induction, I ordered an *FLKIN* knockout strain from the Chlamydomonas Library Project (CLiP) (Li et al. 2016) (Li et al. 2019). This strain, named Δ*flkin*, was described to contain a disruption cassette at the 2nd exon of the *FLKIN* gene. This gene is located at the 16th chromosome and has a size of 2939 bp. The parental strain of Δ*flkin* was the CC4533 WT.

To investigate the exact position of the cassette insertion, I amplified via pcr a genomic region from the mutant, from the first intron to the 3' of the cassette. This genomic region was purified and sent for sequencing. The sequencing results showcased that the exact position of the insertion was actually upstream of the indicated locus, within the 2nd intron (Fig. 3.6). Therefore, Δ*flkin* is not a CDS mutant as initially believed to be, but an intronic one.

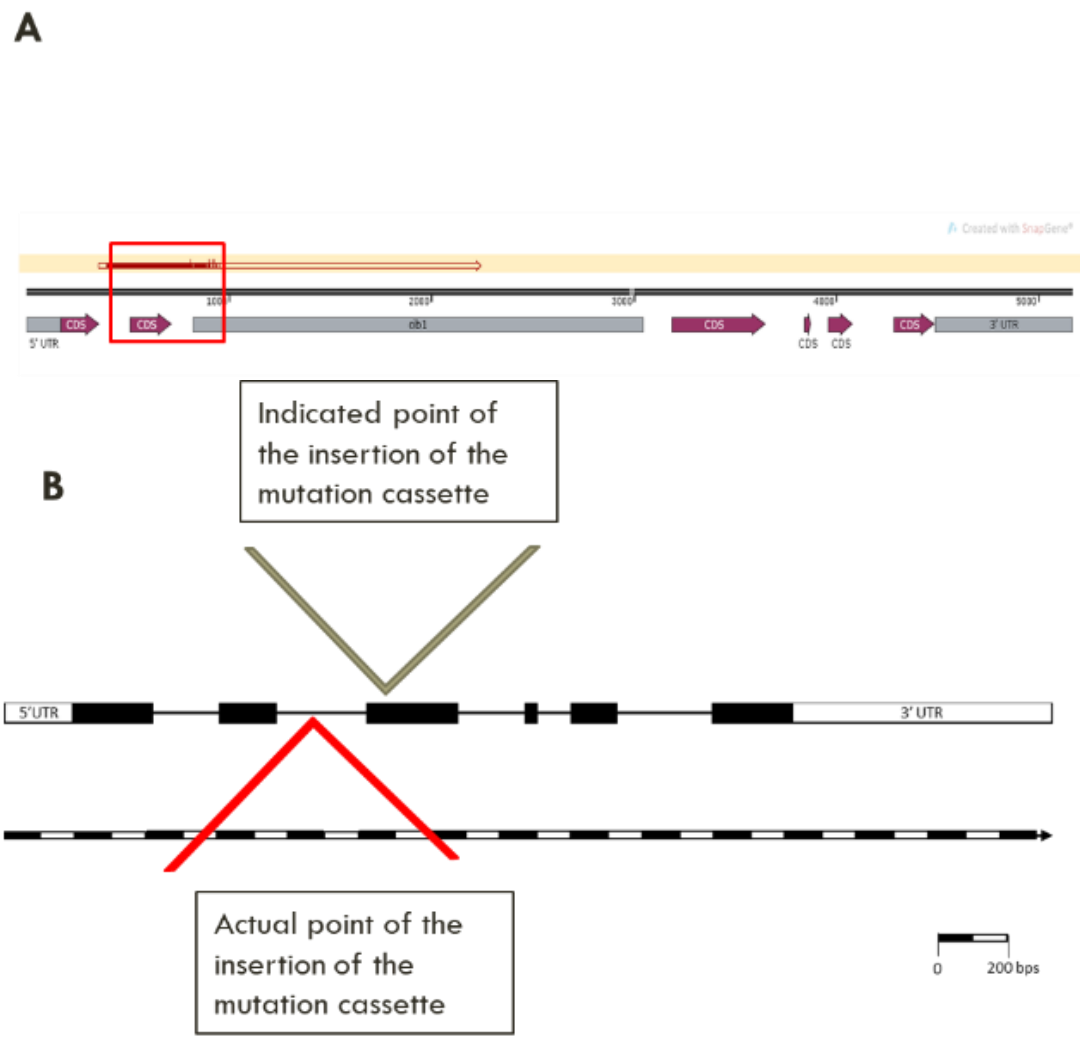

Figure 3.6: Investigating the exact disruption locus of the Cre16.g694950 gene by the mutation cassette at the Δflkin strain. A) The sequencing results. The red box indicates the genomic part which was amplified via pcr, purified and sent for sequencing. The sequencing was done by Macrogen Europe, Amsterdam, The Netherlands. The image was taken from SanpGene. B) Schematic representation of the Cre16.g694950 gene, the indicated point of the insertion of the mutation cassette (by the CliP library) and the actual point of the insertion, as it was revealed by the sequencing results. The scale indicates the size of the genomic part in base pairs (bps)

This result had been further verified by pcr results. More specifically, multiple set of primers were tested on the genomic DNA of the WT and the mutant, as shown in detail in Fig. 3.7. These primers were designed to bind either genomic regions within *FLKIN*, or loci within the disruption cassette. In the first case a difference of size between the WT and Δ*flkin* was expected, while in the second case I was expecting to amplify

genomic regions only in the mutant. From the results of this pcr it was verified that the cassette was indeed inserted in the second intron of *FLKIN*.

A

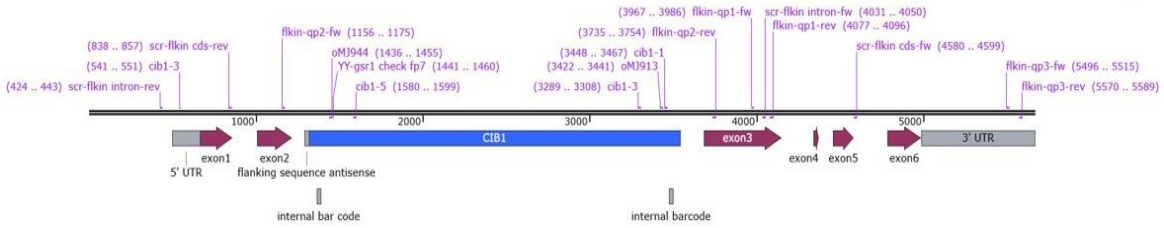

B

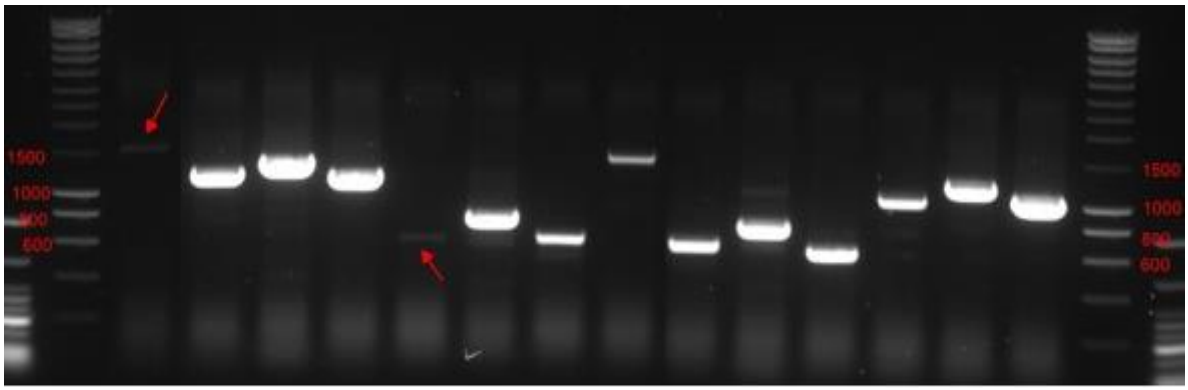

C

lane	gDNA	Forward primer	Revers primer	Expected band size
1	low molecular weight marker			
2	smart ladder marker			
3	wt	scr-flkin cds-fw	scr-flkin cds-rev	1539
4	flkin	scr-flkin cds-fw	omj913	1178
5	flkin	scr-flkin cds-fw	cib1-3	1311
6	flkin	scr-flkin cds-fw	cib1-1	1152
7	flkin	omj944	scr-flkin cds-rev	618
8	flkin	cib1-5	scr-flkin cds-rev	762
9	flkin	fp7	scr-flkin cds-rev	623
10	wt	scr-flkin intron-fw	scr-flkin intron-rev	1404
11	flkin	scr-flkin intron-fw	omj913	629
12	flkin	scr-flkin intron-fw	cib1-3	762
13	flkin	scr-flkin intron-fw	cib1-1	603
14	flkin	omj944	scr-flkin intron-rev	1032
15	flkin	cib1-5	scr-flkin intron-rev	1176
16	flkin	fp7	scr-flkin intron-rev	1037

Figure 3.7: Genotyping of the Δflkin strain. A) Map of the FLKIN gene and the insertion locus of the mutation cassette (CIB1, in blue). Indicated, all the primers used and their corresponding recognising loci. Taken from snap gene. B) The PCR results, explained by the table in C). Some indicative sizes of the ladder are indicated. C) Explanation of each line observed in the pcr result of B), alongside the corresponding sets of primers tested on the genomic DNA of the WT and Δflkin. On the table, the predicted band size for each set of primers is also indicated.

The subsequent question that arose was if this intronic mutant was able to produce the transcript of *FLKIN* or not. I investigated this via qPCR. I used the primers flkin-qp2-fw and flkin-qp2-rv (as shown in 3.8A), which amplify a region between the 5' of the second exon and the 3' of the third exon (on either side of the disruption locus). Anti-

GBLP primers were also used as a control. From this result, I saw that this region can be amplified at the cDNA of the WT (Average C_q =34.44, average C_q for GBLP= 23.18), but not at the Δ*flkin* (Average C_q =0, average C_q for GBLP= 19.85). Therefore, I considered that this genomic region of *FLKIN* cannot be transcribed and the strain is a *FLKIN*-knockout mutant.

3.1.2.3 Δflkin over-expresses LHCSR3, especially in non-saturating light intensities

In early phenotypical experiments, cultures from the WT and Δ*flkin* were grown in HSM in low light overnight and then were exposed to 300 µmol photons m^{-2} s^{-1} for 4h. The results showed that this strain has a strong phenotype of LHCSR3 overaccumulation under high light (Fig. 3.8). Because those early results were highly interesting, further follow-up experiments were planned with Δ*flkin*.

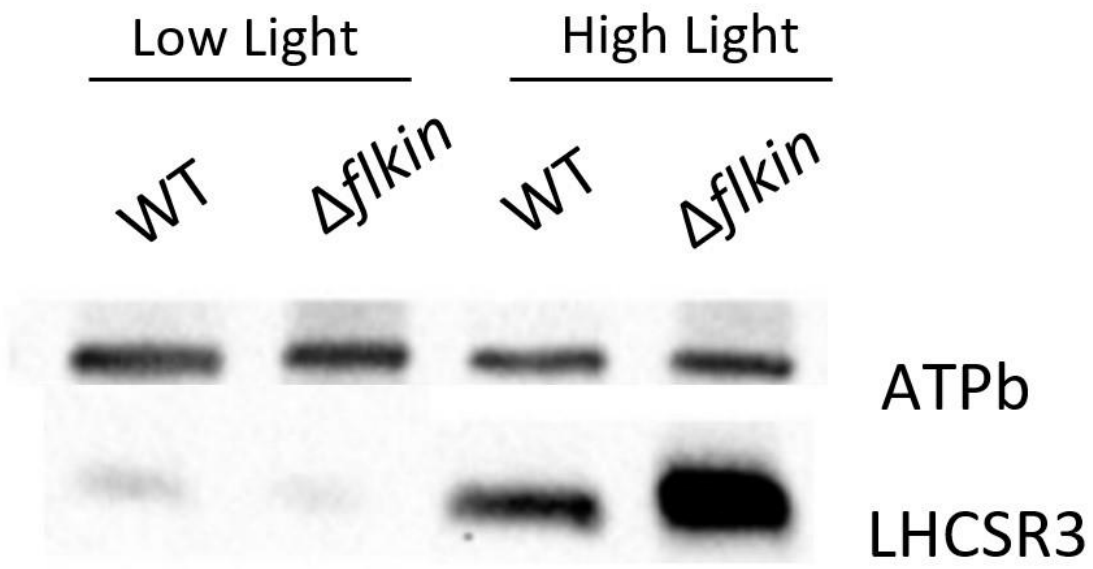

Figure 3.8: Western Blot on the LHCSR3 levels at the Wild Type (WT) and Δflkin after 4h exposure at Low Light (15 µmol photons m^{-2} s^{-1}) and High Light (300 µmol photons m^{-2} s^{-1}). The cultures had been incubated in phototrophic medium (HSM) and under complete darkness overnight, before the High Light and Low Light exposure. The anti-ATPb antibody was used as a loading control

In order to determine the sensitivity of Δ*flkin* to light for the induction of LHCSR3, I shifted dark acclimated cultures of WT and *Δflkin* to five different light intensities: 15, 50, 100, 300 and 600 µmol photons m^{-2} s^{-1} (hereafter also indicated as "µE"). I took

samples after the overnight dark acclimation and after 1h (RNA) and 4h (protein and photosynthesis) of exposure to the different light intensities.

Δflkin seems to be able to induce LHCSR3 in lower light intensities than the WT, as observed specifically at 100 µmol photons m^{-2} s^{-1} (Fig. 3.9), where the difference in LHCSR3 accumulation between the mutant and the WT is large. The difference in LHCSR3 levels under higher light intensities (300 and 600 µmol photons m^{-2} s^{-1}), though, is statistically insignificant.

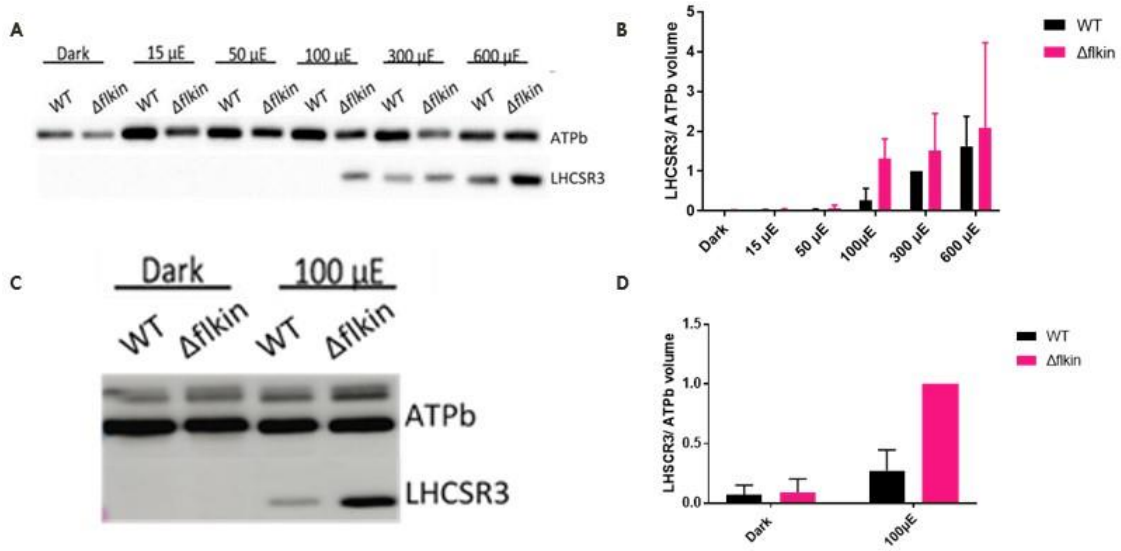

Figure 3.9: A) LHCSR3 levels at the WT and Δflkin after the overnight dark acclimation and after 4h exposure to 15, 50, 100, 300 and 600 µmol photons m^{-2} s^{-1} of light intensity. Anti-ATPb was used as a loading control. B) Densitometry analysis of three independent repeats of the experiment shown in A). Normalized to WT at 300 µmol photons m^{-2} s^{-1}. C) LHCSR3 levels at the WT and Δflkin after the overnight dark acclimation and after 4h of exposure to 100 µmol photons m^{-2} s^{-1} of light intensity. Anti-ATPb was used as a loading control. D) Densitometry analysis of three independent repeats of the experiment shown in C). Normalized to Δflkin at 100 µmol photons m^{-2} s^{-1}.

The NPQ induction is also notably higher in the mutant after 4h under 100, 300 and 600 µmol photons m^{-2} s^{-1}. Especially at 100 µmol photons m^{-2} s^{-1}, the difference between the two strains is very high (Fig. 3.10). The same trend was observed for the qE, as represented by the sharp drop of the NPQ curve during the transition from high light to dark. The difference in qE is significant at the cultures exposed to 100 µmol photons m^{-2} s^{-1}, while in higher light intensities no statistically significant difference was observed between the two strains.

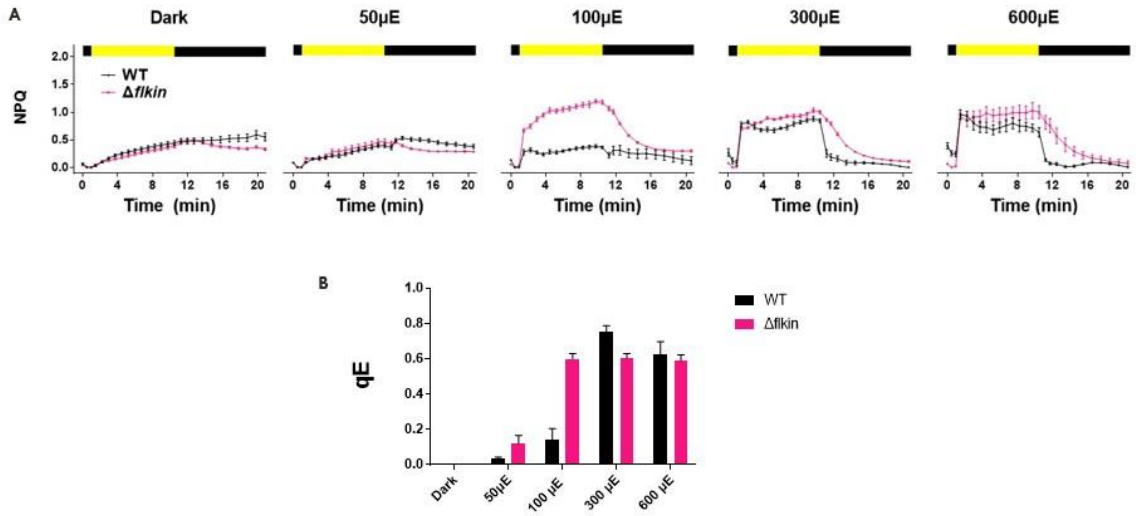

Figure 3.10: A) The NPQ curves from the WT and Δflkin, after the cultures were exposed to dark (overnight) and under 50, 100, 300 and 600 µmol photons m^{-2} s^{-1} for 4h. B) The calculated qE from the NPQ curves in A)

From the photosynthetic measurements (Fig. 3.11), we observe that the values of Fv/Fm (corresponding to the Y(II) measured in the dark at the beginning of the measurement), which represents the photosynthetic capacity of the strains, are higher in the mutant than the WT under all the studied light intensities, indicating that the mutant maintains more oxidized state of the plastoquinol pool in the dark as compared to the WT. The drop of the Fv/Fm of both strains at the higher light intensities (notably at 300 and 600 µmol photons m^{-2} s^{-1}) is probably due to photoinhibition, caused by the prolonged exposure to stressful light intensities. At variance with the Fv/Fm values, the quantum efficiency of PSII Y(II) (measured in the presence of light) was found to be similar in WT and mutant (Fig. 3.11B).

A

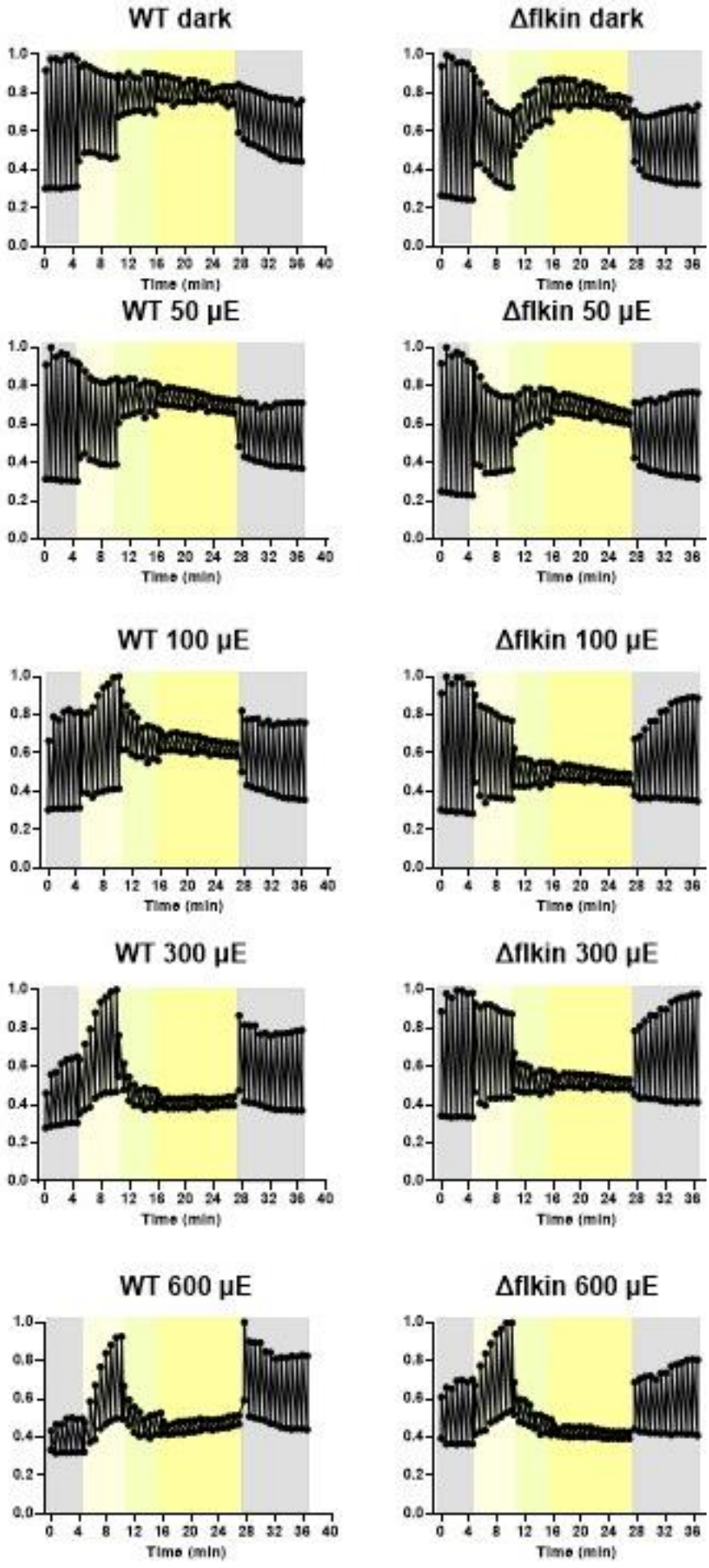
WT dark
Δflkin dark
WT 50 µE
Δflkin 50 µE
WT 100 µE
Δflkin 100 µE
WT 300 µE
Δflkin 300 µE
WT 600 µE
Δflkin 600 µE
Time (min)

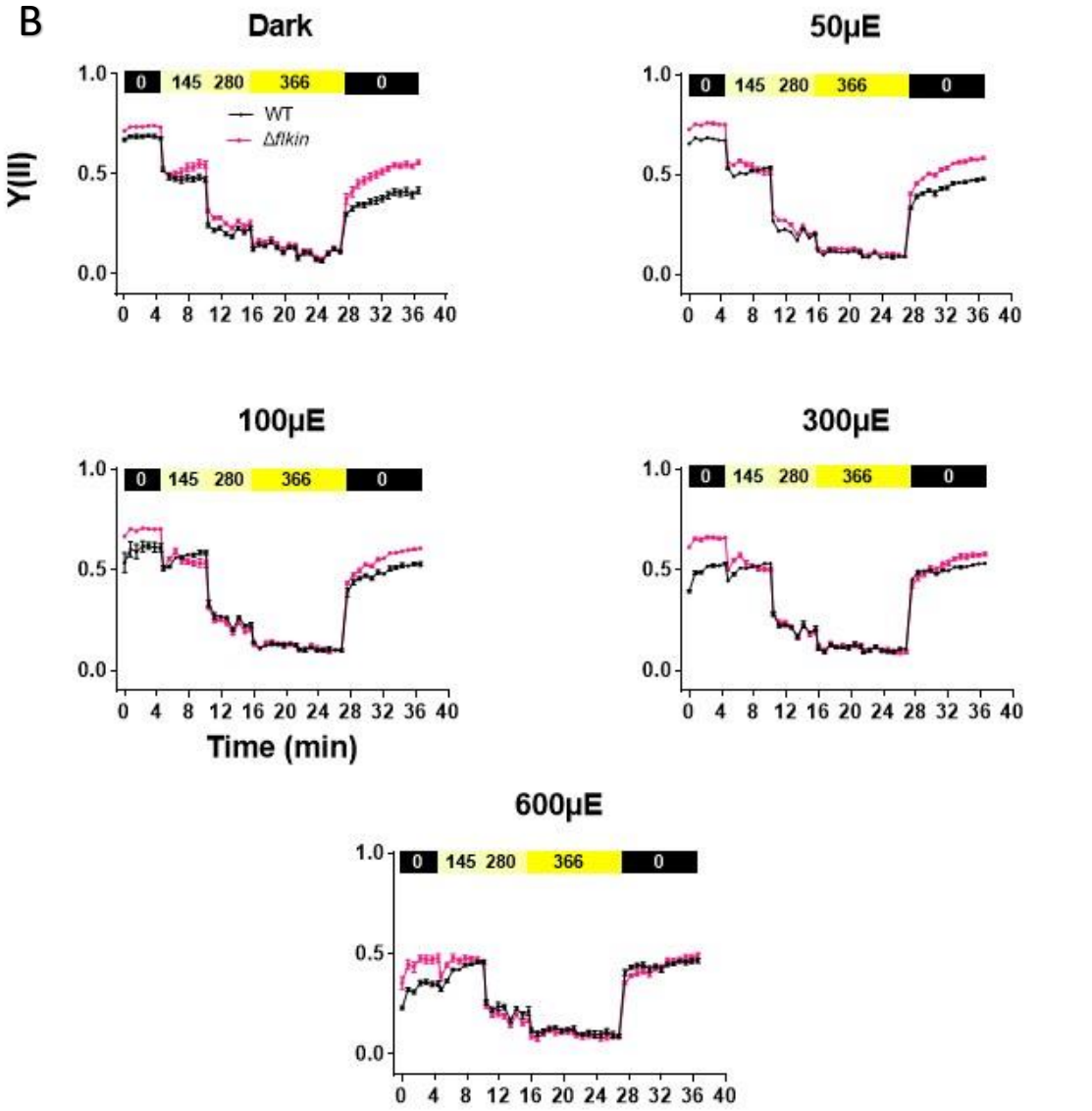
B
Dark
50µE
100µE
300µE
600µE
Y(II)
Time (min)
0
145
280
366
WT
Δflkin

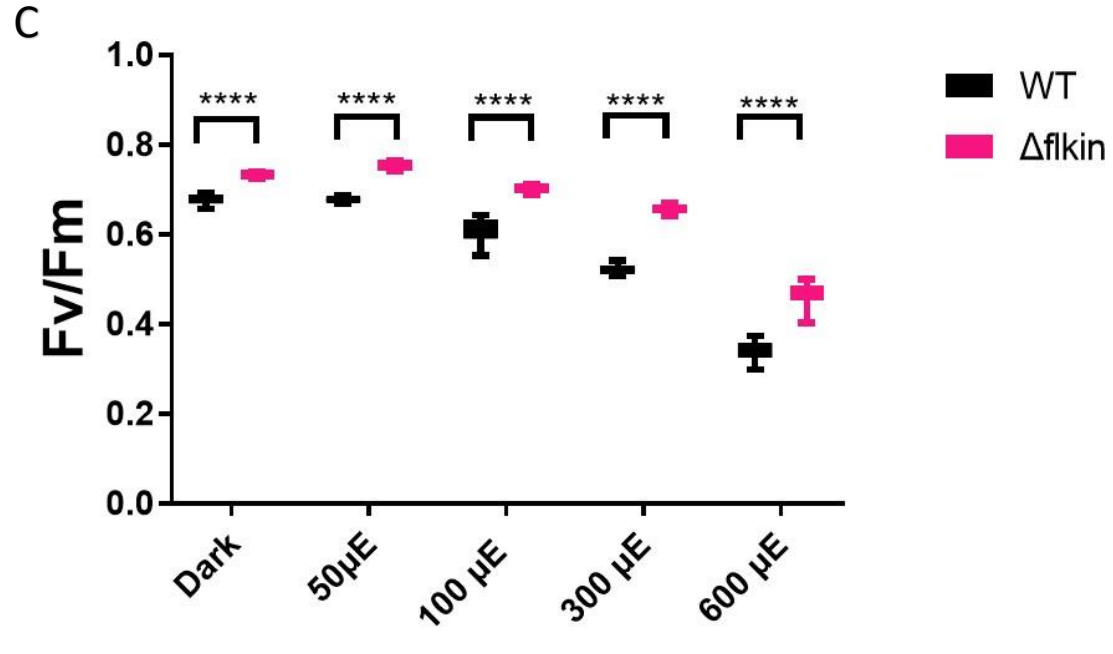
C
Fv/Fm
****
WT
Δflkin
Dark
50µE
100 µE
300 µE
600 µE

Figure 3.11: A) Raw data of in vivo chlorophyll fluorescence (normalized to Fm) for the WT and Δflkin cultures, exposed to dark (overnight) and under 50, 100, 300 and 600 µmol photons m^{-2} s^{-1}. The chlorophyl fluorescence was measured in dark (gray) and under 145 µmol photons m^{-2} s^{-1} (light yellow), 280 µmol photons m^{-2} s^{-1} (yellow) and 366 µmol photons m^{-2} s^{-1} (dark yellow). B) The Y(II) curves, corresponding to the measurements shown in A). C)The Fv/Fm values of Δflkin and the WT after the overnight dark incubation and after 4h of exposure to 50, 100, 300 and 600 µmol photons m^{-2} s^{-1} of light intensity. For the significance of the differences at each condition a 2-way ANOVA test was performed with 95% confidence interval (P value: 0.1234 (ns), 0.032 (*), 0.0021 (**), 0.0002 (***), < 0.0001 (****))

I next addressed whether the overexpression of LHCSR3 protein in the *Δflkin* is also reflected at the transcriptional level. Real-time reverse transcription PCR (RT-qPCR) was performed on samples taken from both strains after the overnight dark acclimation and after 1h of exposure to 100 µmol photons m^{-2} s^{-1}. The results show that *Δflkin* overexpresses *LHCSR3* at the mRNA level (probed as *LHCSR3.1*). I also checked the expression levels of the two other qE-related genes, *LHCSR1* and *PSBS*. My data (Fig. 3.12) indicate that expression levels *LHCSR1* are unaffected by the *FLKIN* mutation, while *PSBS* levels (probed as *PSBS1*) are slightly higher in the mutant. Given the tight interconnection of LHCSR3 and CCM gene expression (Ruiz-Sola et al. 2021) I also investigated the expression levels of selected CCM-related genes in WT and *Δflkin* namely: *LCIA* (encodes an inorganic carbon transporter), *LCIB* (encodes a protein involved in the CO_2 uptake), *CAH3* and *CAH4* (encode carbonic anhydrases) and *LCR1* (encodes a transcriptional factor). The results, shown in Fig. 3.12, show that all the studied transcripts are at the same levels in both strains in the dark and increase their abundance after the exposure to 100 µmol photons m^{-2} s^{-1}. This is in accordance to (Ruiz-Sola et al. 2021) and can be explained by the fact that by shifting from darkness to 100 µmol photons m^{-2} s^{-1} the CO_2 concentration decreases due the to the photosynthetic activity and therefore the CCM is activated. With the exception of *LHCSR1*, all those transcripts are in higher levels in Δ*flkin* than in the WT after the light exposure. Especially for *LHCSR3.1*, those results are in accordance with the protein accumulation. These data showcase that, other than photoprotection, also the CCM response is stronger in the mutant strain, adding a new line of evidence that LHCSR3 and CCM gene expression are tightly co-regulated as recently shown (Ruiz-Sola et al. 2021) (Arend et al. 2022).

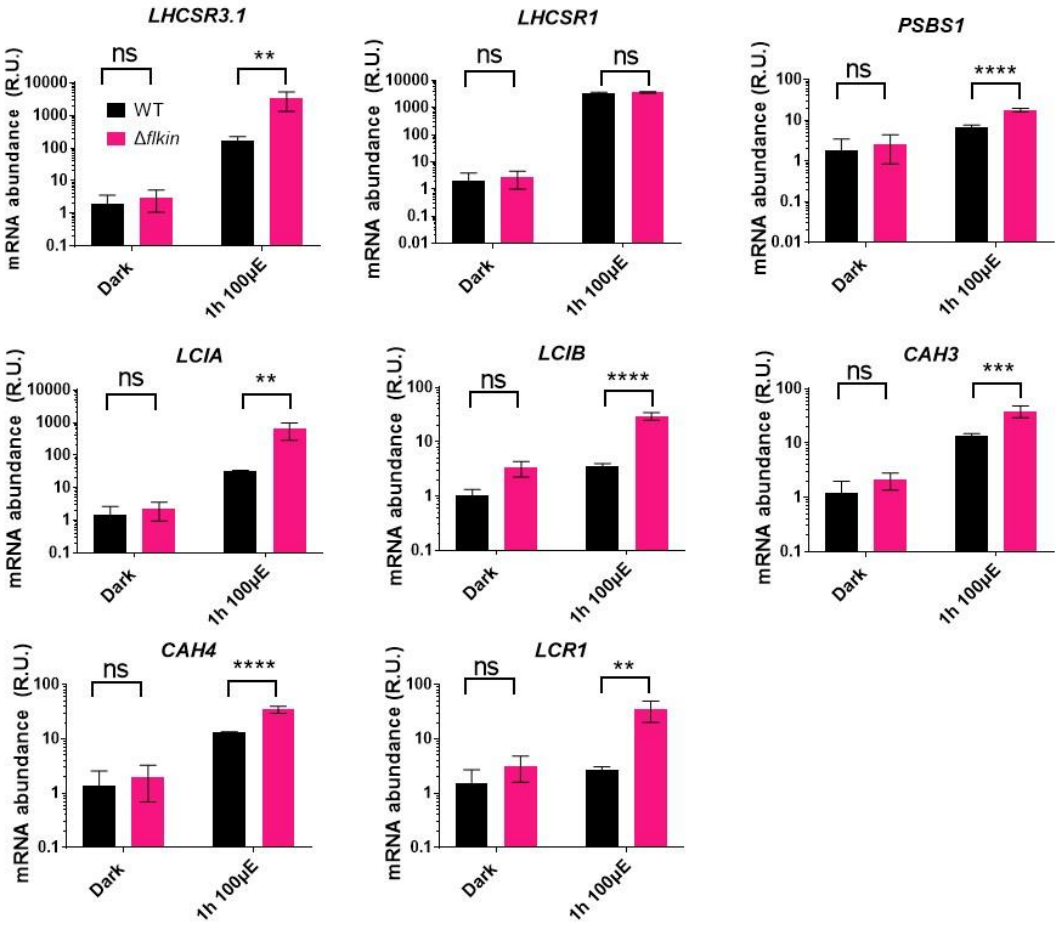

Figure 3.12: The abundances of 7 transcripts in the WT and Δflkin after overnight dark acclimation and 1h of exposure to 100 µmol photons m^{-2} s^{-1}. Those transcripts are LHCSR3.1, LHCSR1, PSBS, LCIA, LCIB, CAH3, CAH4 and LCR1. The results were obtained after cDNA synthesis and qPCR (see Materials and Methods). For the significance of the differences at each condition a 2-way ANOVA test was performed with 95% confidence interval (P value: 0.1234 (ns), 0.032 (*), 0.0021 (**), 0.0002 (***), < 0.0001 (****))

3.1.2.4 Characterisation of the LHCSR3 induction in Δflkin

To investigate the effect of the pre-acclimation conditions on LHCSR3 accumulation in WT and *Δflkin,* cultures of the WT and the mutant strain were acclimated overnight in the dark either in phototrophic medium (HSM), as was the case for all the experiments so far, or in mixotrophic medium, containing acetate (TAP medium; described in Materials and Methods). Both sets of cultures were then transferred to HSM and exposed to 100 µmol photons m^{-2} s^{-1} for 4h. In agreement with my results presented in Fig. 3.9A, the *Δflkin* accumulated LHCSR3 protein while the protein was not even detectable in the WT. The data also indicate that in the *Δflkin* more LHCSR3

accumulated in the cultures that were pre-acclimated in TAP as compared with the ones acclimated to HSM (Fig. 3.13).

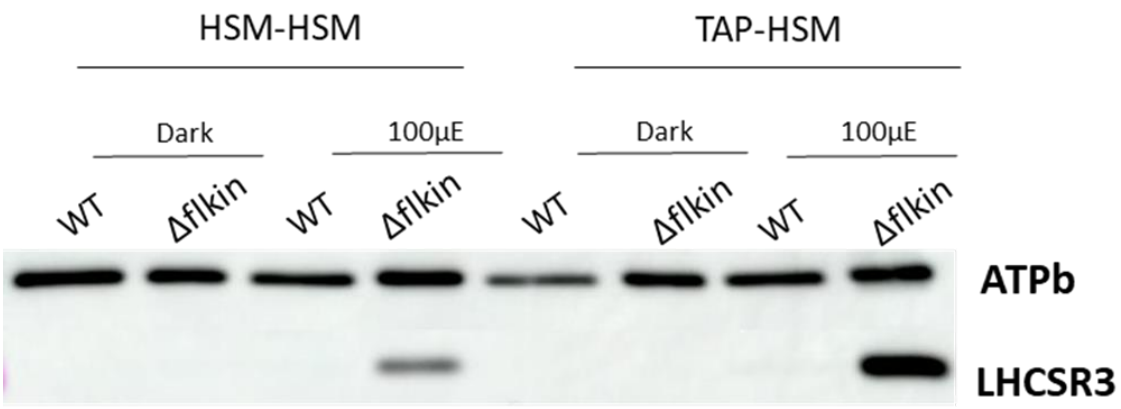

Figure 3.13: LHCSR3 levels at the WT and Δflkin after the overnight dark acclimation in HSM (indicated as HSM-HSM) and in TAP (indicated as TAP-HSM) and after 4h of exposure to 100 µmol photons m^{-2} s^{-1} of light intensity. Anti-ATPb was used as a loading control.

Accordingly, qE was higher at the cultures that had been pre-acclimated in TAP than at those which had been pre-acclimated in HSM (Fig. 3.14). In both cases, Δ*flkin* had higher qE than the WT, which is in line with the protein expression levels of LHCSR3 (Fig. 3.13).

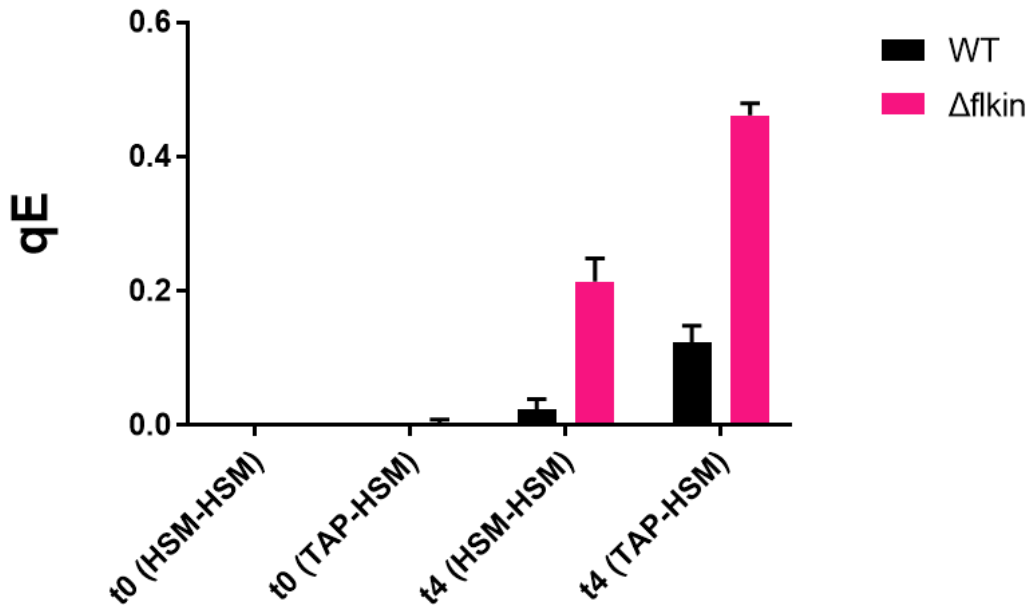

Figure 3.14: The calculated qE of Δflkin and the WT after the overnight dark acclimation in HSM (indicated as HSM-HSM) and in TAP (indicated as TAP-HSM) and after 4h of exposure to 100 µmol photons m^{-2} s^{-1} of light intensity

When the cells are grown in TAP, the intracellular concentration of CO_2 increases due to the acetate metabolism and simply the transfer to HSM medium (and removal of acetate) leads to an induction of LHCSR3 at the mRNA (Redekop et al 2021) and even at the protein level (Barth et al. 2014) during the exposure to high light, CO_2 levels are further reduced via fixation from the Calvin-Benson cycle, evidenced by the activation of the CCM genes (Fig. 3.12). In this line of thought it is perfectly normal that cells pre-acclimated in TAP accumulated more LHCSR3 as compared to the ones pre-acclimated to HSM, because they were submitted to more drastic changes in the concentration of CO_2.

Exposure of the cells to blue light preferentially leads to LHCSR3 accumulation in WT cells (Petroutsos et al. 2016). My next objective was to determine if such chromatic regulation is also an acting factor to the LHCSR3 over-expression in Δ*flkin*. To address this, cultures of both strains were shifted from dark to 15 µmol m^{-2} s^{-1} of white light and 300 µmol m^{-2} s^{-1} of white, blue and red light for 4h. As shown in Fig. 3.15, LHCSR3 in Δ*flkin* is more abundant in blue than in red light, in accordance with the known WT phenotype. Consistently, Δ*flkin* has higher LHCSR3 levels than the WT in all the tested light qualities and intensities.

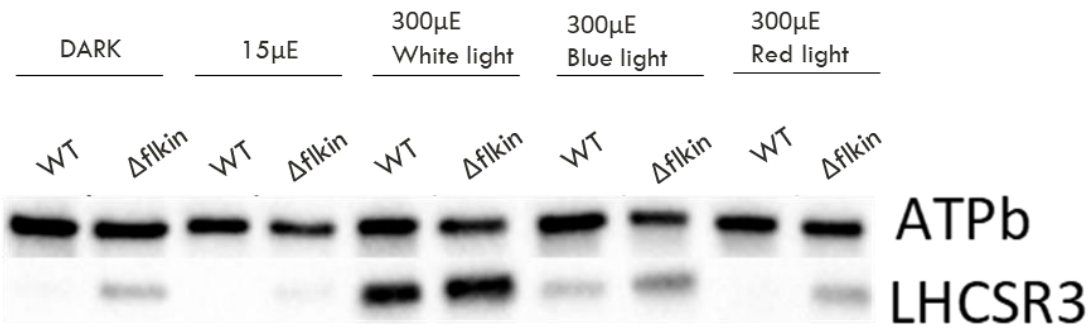

Figure 3.15: LHCSR3 levels at the WT and Δflkin after the overnight dark acclimation and after 4h exposure to 15 µmol m^{-2} s^{-1} of white light and 300 µmol m^{-2} s^{-1} of white, blue and red light. Anti-ATPb was used as a loading control.

In line with the LHCSR3 protein data, qE is preferentially induced by blue light in both WT and mutant, since it is almost half under red light that it is under blue light (Fig. 3.16). qE is higher under both red and blue light in the mutant, compared to the WT.

From these set of results, it is evidenced that LHCSR3 expression and qE induction remain chromatically regulated in Δ*flkin* and are induced by blue light.

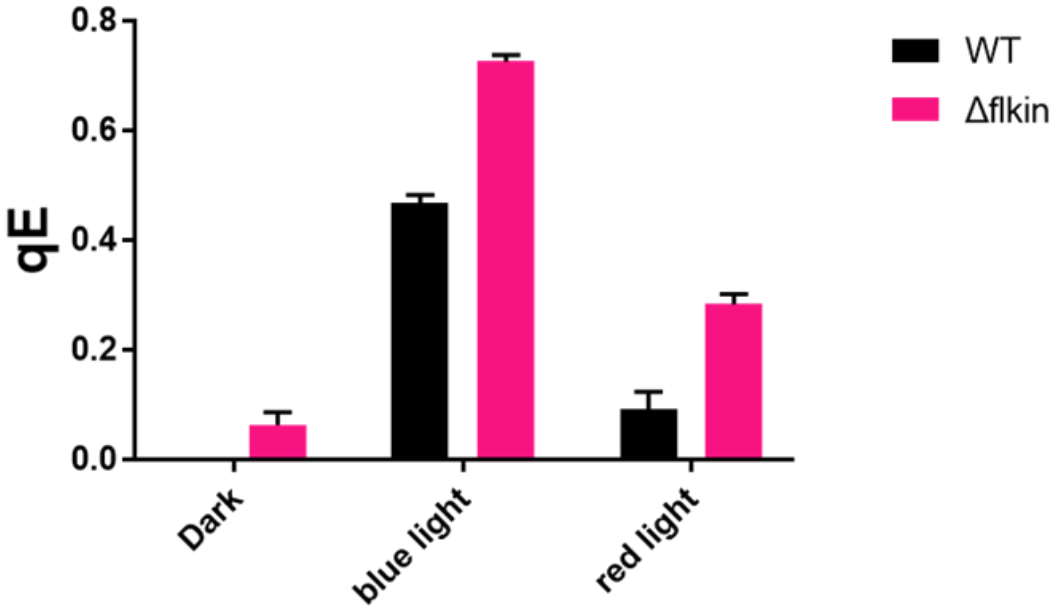

Figure 3.16: The calculated qE of Δflkin and the WT after the overnight dark acclimation after 4h of exposure to 300 µmol photons m^{-2} s^{-1} of blue and red light.

It has been reported that LHCSR3 expression requires active photosynthesis and that when the electron transfer chain is blocked at the PSII level by the chemical 3-(3,4-dichlorophenyl)-1,1-dimethylurea (DCMU), LHCSR3 induction is blocked as well (Petroutsos et al. 2011). I wanted to observe if this kind of regulation is also taking place in Δ*flkin*. For that reason, I exposed low light (15 µmol m^{-2} s^{-1}) acclimated WT and Δ*flkin* cultures to 100 µmol m^{-2} s^{-1} of blue and red light. I added DCMU in half of the cultures before the light exposure. From the results, the induction of LHCSR3 in Δ*flkin* seems to be affected not only by light quality (in red light we have less LHCSR3 that in the blue), but also by the addition of DCMU. Importantly, the overaccumulation of LHCSR3 in the mutant in comparison with the WT is consistently observable in every condition (Fig. 3.17). Finally, it is important to note that the LHCSR3 levels observed in the DCMU-treated samples reflect the existing LHCSR3 already present at low light conditions. Therefore, no LHCSR3 accumulation occurred in the presence of DCMU neither in WT or the mutant.

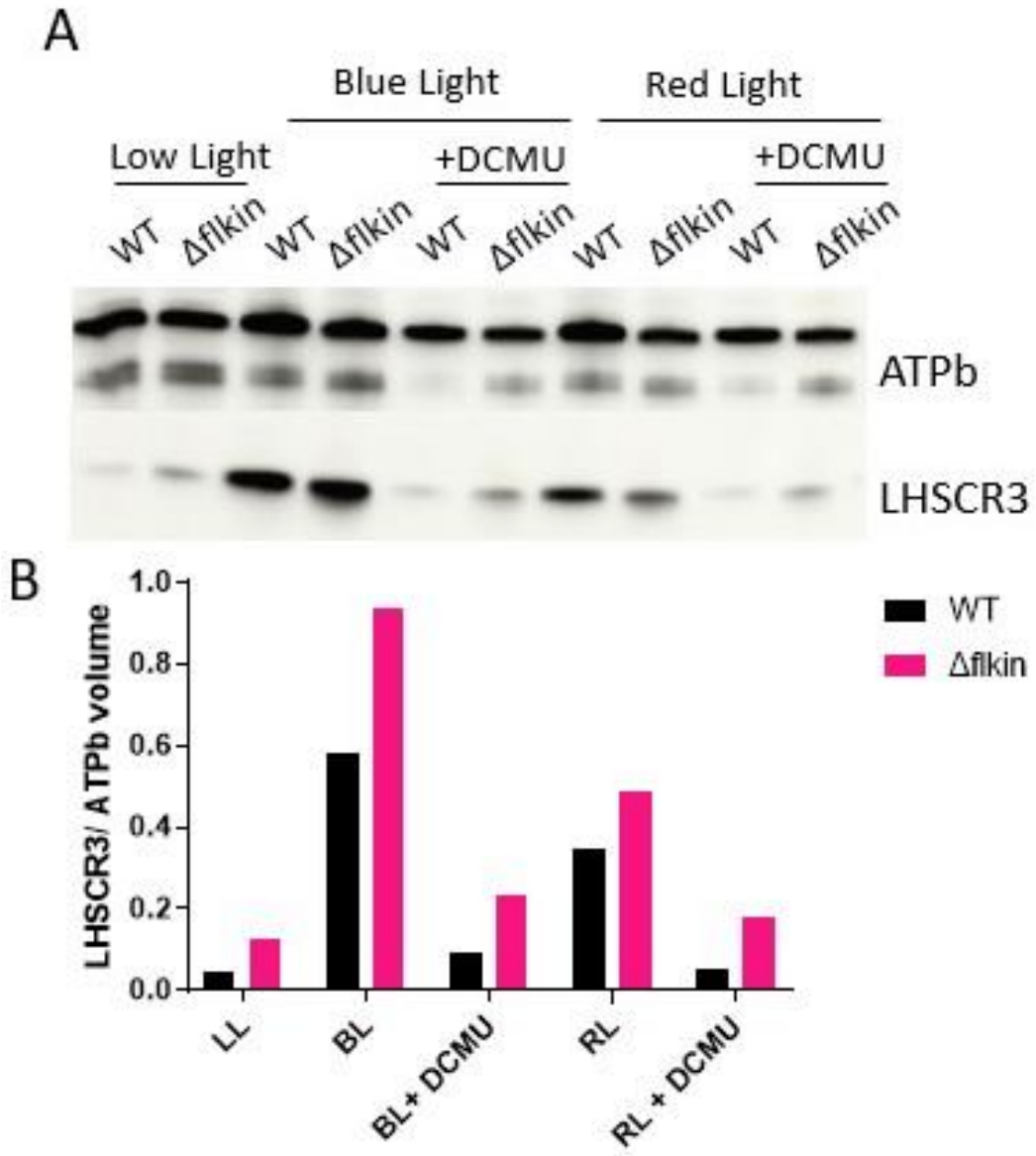

Figure 3.17: LHCSR3 levels at the WT and Δflkin after the overnight acclimation in low light (15 µmol m^{-2} s^{-1}) and after 4h incubation at 100 µmol m^{-2} s^{-1} of blue and red light, with and without the addition of DCMU. Anti-ATPb was used as a loading control. B) Densitometric analysis of the bands at the Blot in A).

The western blot results on LHCSR3 are coming in accordance with the NPQ measurements, where NPQ and qE is higher in the mutant than the WT, but it gets lower after the addition of DCMU. Furthermore, as shown previously, NPQ is higher is both cases under blue than under red light exposure (Fig. 3.18). To no surprise no NPQ was recorded in the DCMU-treated cells because no photosynthetic electron flow takes place under these conditions.

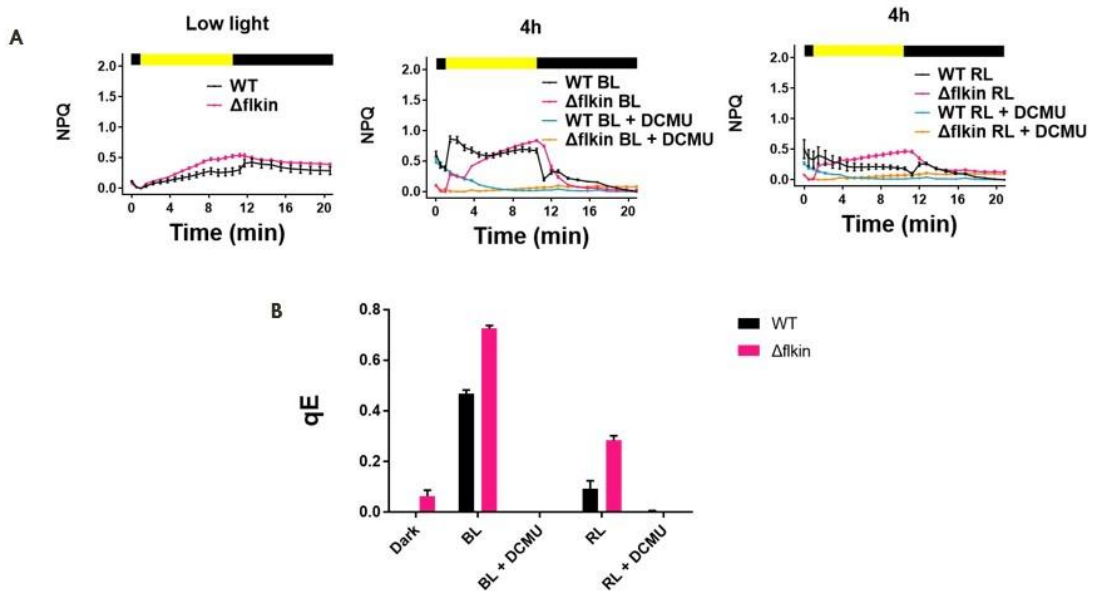

Figure 3.18: A) The NPQ curves from the WT and Δflkin, after the cultures were exposed to low light (15 µmol photons m^{-2} s^{-1}) overnight and under 100 µmol photons m^{-2} $s^{-1}$of blue and red light, with and without the addition of DCMU for 4h. B) The calculated qE from the NPQ curves in A).

3.1.2.5 Growth and physiology observation of the Δflkin strain

During the experiments with the Δ*flkin* strain, I observed a unique phenotype, concerning its growth and its cell size. More specifically, under certain conditions it seemed like this mutant strain had a defect on its growth in comparison with the growth of the WT. Also, its cells appeared to be bigger and containing more chlorophyll (''greener'' cultures). To study further those observations, I monitored the cell density, chlorophyl concertation and cell size of the WT and *Δflkin* cultures grown in TAP and in HSM, under three light intensities: 15, 100 and 300 µmol photons m^{-2} s^{-1}.

At low light intensity (15 µmol photons m^{-2} s^{-1}), the WT has a faster growth rate than Δ*flkin* and it reaches its stationary phase at higher cell density in both media (Fig. 3.19). At 100 and 300 µmol photons m^{-2} s^{-1} a clear growth defect was observed in HSM, where the WT has almost two times higher cell density than the *Δflkin* at their stationary phase. The growth defect of *Δflkin* was not observed in TAP medium, where both cultures reached in approximation the same cell density levels. These results indicate that Δ*flkin* has impaired phototrophic growth, a phenotype that can be

rescued by the addition of acetate (TAP medium), with the exception of the growth at 15 µmol photons m^{-2} s^{-1}, that remained somehow slower even in the presence of acetate.

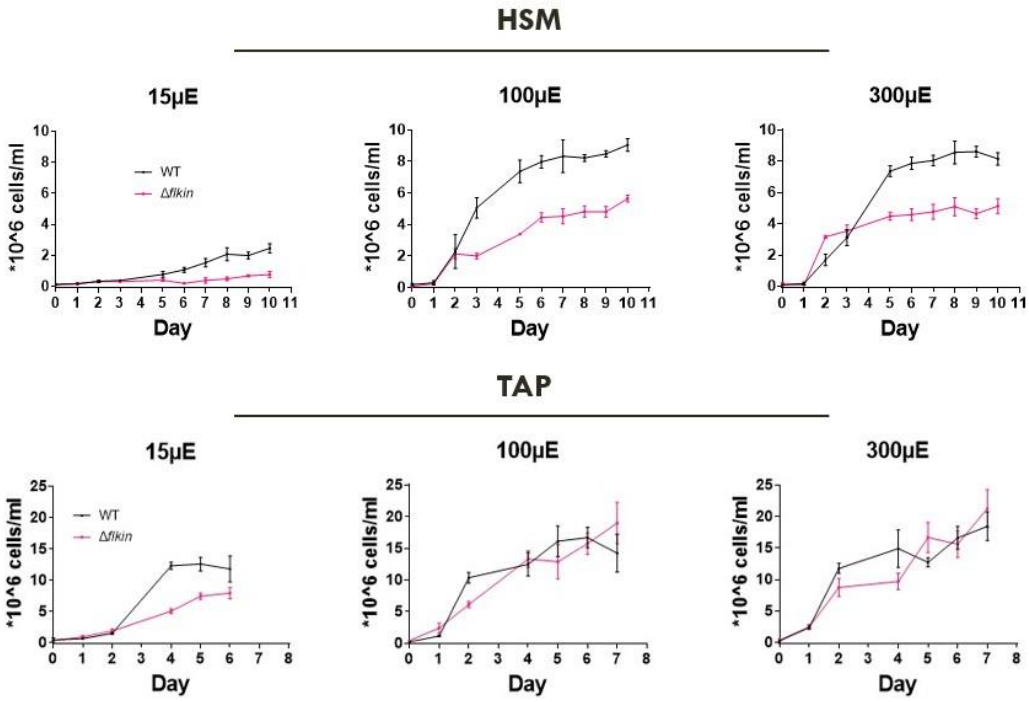

Figure 3.19: Observation of the growth of the WT and Δflkin. The strains were grown in TAP and in HSM under 15, 100 and 300 µmol photons m^{-2} s^{-1} and their cell density was measured in a daily basis. The cell density is indicated as millions of cells per ml of culture. The cell counting is being described in the Materials and Methods section.

Throughout this experiment, I also quantified the chlorophyll content of the cells and I could see that in HSM Δ*flkin* contains more chlorophyl per cell than the WT (Fig. 3.20, Table 3.1). The same observation can be made in TAP, when the cultures are growing in low light. However, in higher light intensities in TAP, the differences between the two cultures are not significant. Thus, we can conclude that low light and the absence of acetate from the medium, conditions where growth is impaired in the Δ*flkin* mutant, lead to accumulation of chlorophyll in the cells of Δ*flkin*.

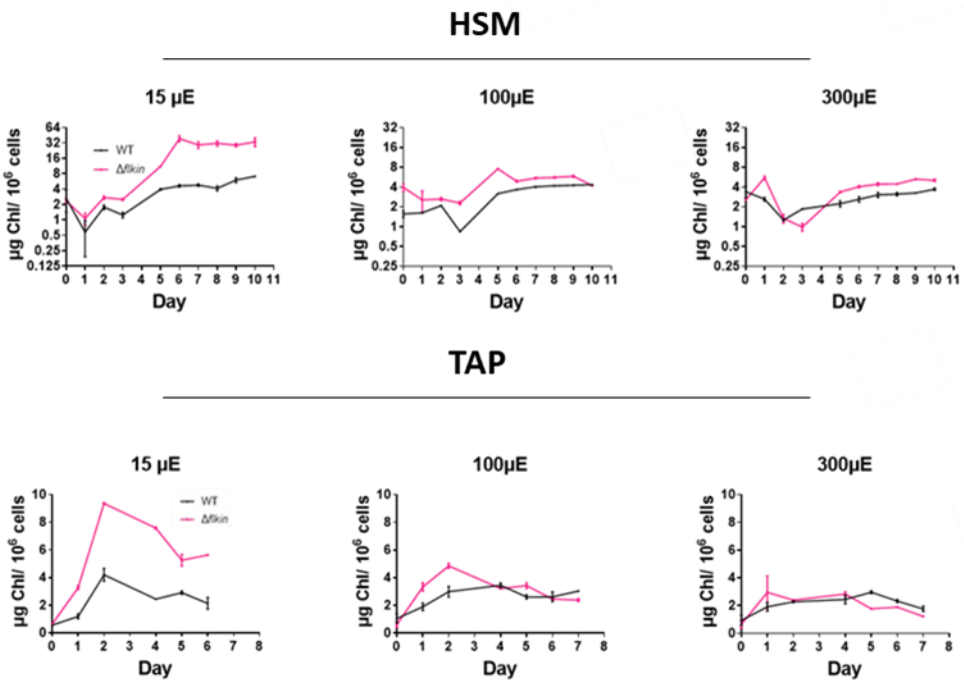

Figure 3.20: Observation of the chlorophyl content per million of cells at each day of the cultures of the WT and Δflkin. The strains were grown in TAP and in HSM under 15, 100 and 300 µmol photons m^{-2} s^{-1} and their chlorophyl content and cell density were measured in a daily basis. The chlorophyl content is indicated as µg of chlorophyl per million of cells. The chlorophyl measurements and the cell counting are being described in the Materials and Methods section.

The observed cell size from the Δ*flkin* cultures was also bigger than the one of the WT cells in both media and under all three light conditions (Fig. 3.21, Table 3.1). In TAP, under the high light conditions, the difference is consistent with the other conditions but is not statistically significant.

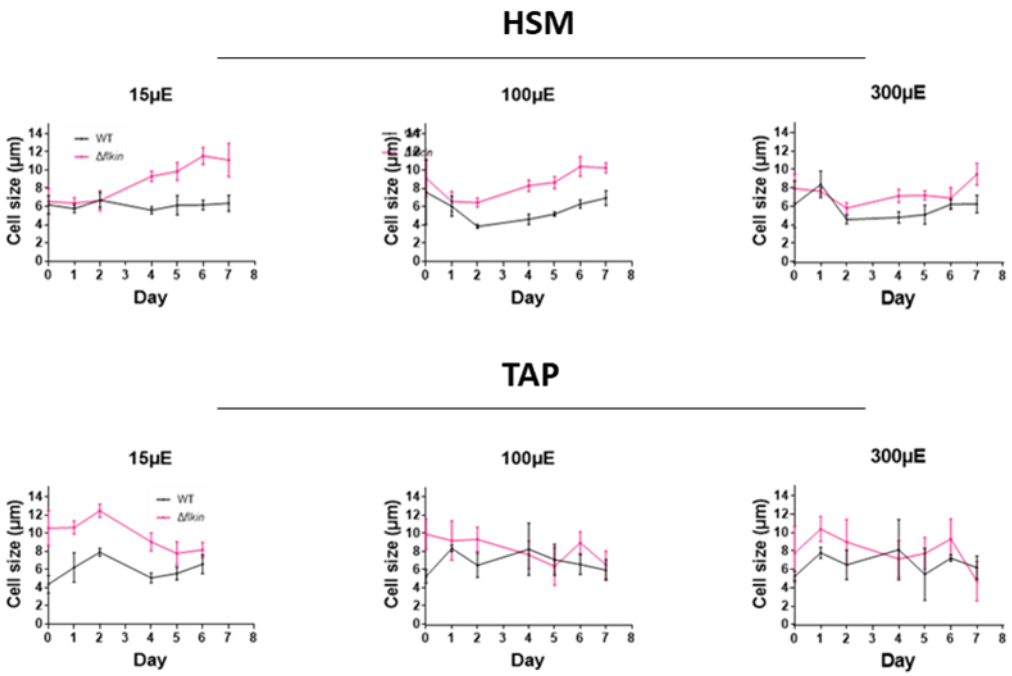

Figure 3.21: Observation of the size of the cells of the WT and Δflkin. The strains were grown in TAP and in HSM under 15, 100 and 300 µmol photons m^{-2} s^{-1} and the size of the cells was measured in a daily basis. The cell size is indicated as µm of the diameter of the cells. The cell diameter was calculated automatically from the Countess™ II FL Automated Cell Counter

Table 3.1: The average cell dimeter and average chlorophyl content of the WT and Δflkin. The strains were grown in TAP and in HSM under 15, 100 and 300 µmol photons m^{-2} s^{-1}. The average cell diameter is indicated in µm and was calculated automatically from the Countess™ II FL Automated Cell Counter. The cell size was measured in a daily basis. The average chlorophyl content is being indicated as µg of chlorophyl per million of cells. The chlorophyl measurements and the cell counting are being described in the Materials and Methods section. The chlorophyl concertation of each culture was measured in a daily basis.

	HSM					
	15µE		100µE		300µE	
	WT	Δflkin	WT	Δflkin	WT	Δflkin
Average cell diameter (µm)	6.12 ± 0.14	8.76 ± 0.84	5.77 ± 0.5	8.53 ± 0.6	5.92 ± 0.49	7.43 ± 0.42
Average chlrorophyl content (µg Chlorophyl/ million of cells)	4.17 ± 1.16	9.19 ± 2.03	2.83 ± 0.5	5.03 ± 0.62	2.5 ± 0.58	5.97 ± 1.57
	TAP					
	15µE		100µE		300µE	
	WT	Δflkin	WT	Δflkin	WT	Δflkin
Average cell diameter (µm)	5.95 ± 0.51	9.77 ± 0.72	6.84 ± 0.43	8.27 ± 0.54	6.64 ± 0.42	8 ± 0.69
Average chlrorophyl content (µg Chlorophyl/ million of cells)	2.24 ± 0.53	5.29 ± 1.26	2.53 ± 0.31	2.9 ± 0.49	2.09 ± 0.24	1.96 ± 0.32

3.1.2.6 Complementation of Δflkin

For the complementation of Δ*flkin*, the full *FLKIN* gene, including the introns, had been amplified via pcr from the genomic DNA of the WT. The fragment had been inserted

into the pRAM118 vector (Itakura et al. 2019) , under the control of the PsaD promoter (Fig. 3.22). The plasmid also contains the *APHVIII* gene, under the control of the *Chlamydomonas* beta2-tumbulin promoter, which provides resistance to hygromycin. This construct would be able to generate the fluorescent fusion protein of FLKIN-Venus. The construct had been assembled via the Gibson Assembly (Gibson et al. 2009) and the plasmid had been sequenced before transformation.

Figure 3.22: The pRAM118- flkin/CrVenus construct

Δ*flkin* and WT cells had been transformed in order to generate a complemented and an over-expressor stain, respectively. Unfortunately, despite the several attempts I did not succeed to get in hands a complemented line of Δ*flkin*. This task is now ongoing in the host team.

3.1.2.7 Discussion and future perspectives

Based on the results shown in this chapter, we can recognise the significance of FLKIN for a number of cellular responses, especially photoprotection and carbon utilisation. The lack of *FLKIN* expression in the Δ*flkin* mutant resulted in a unique phenotype for the strain, summarized in Fig. 3.23.

This strain is inducing photoprotection at lower light intensities than the WT, by accumulating more LHCSR3, the main photoprotection actor in *C. reinhardtii*, both at the transcript and protein levels. In line with the LHCSR3 protein levels, Δ*flkin* has higher qE as compared to the WT. It is tempting to propose that Δ*flkin* grows poorly in phototrophic conditions because of its higher qE and would therefore dissipate more absorbed energy into heat instead of directing it into the formation of biomass.

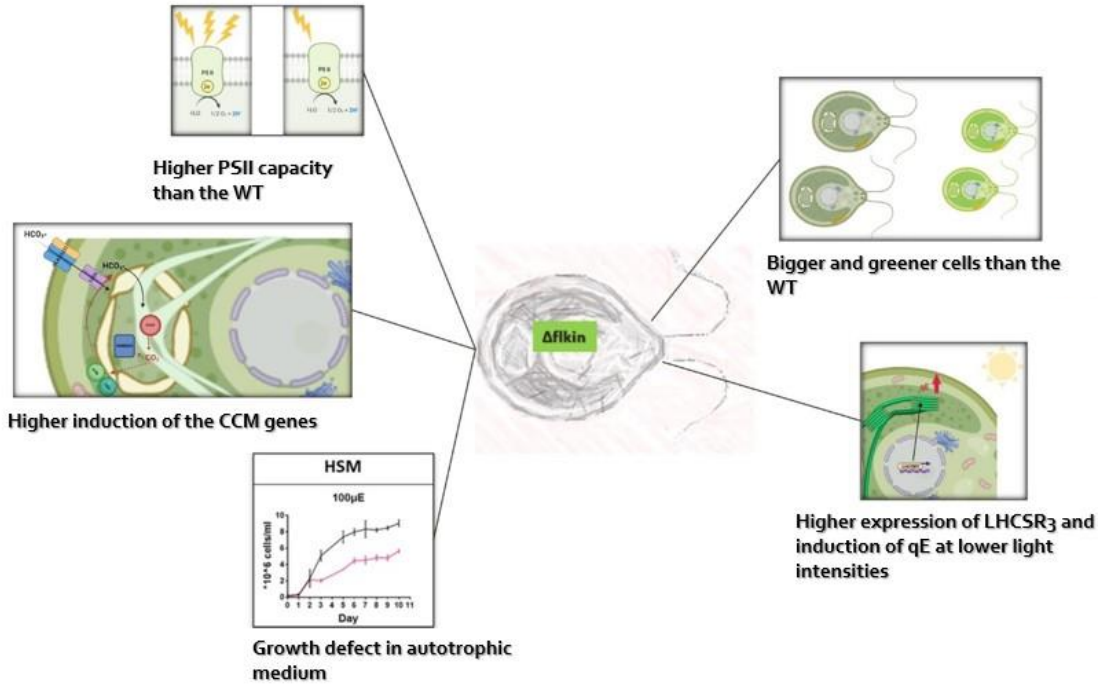

Figure 3.23: Graphic summary of the phenotype of Δflkin

Another important result concerning Δ*flkin* is its ability to induce in higher rates transcripts of proteins involved in the Carbon Concentrating Mechanism (CCM). This come in accordance with previous observations that the CCM proteins and LHCSR3 are tightly co-regulated (Fang et al. 2012) (Ruiz-Sola et al. 2021) (Redekop et al. 2021), which seems to be also the case in Δ*flkin*; both photoprotection and CCM transcripts are in higher abundance than the WT and are induced in non-saturating light intensities.

Finally, another important phenotype of the Δ*flkin* cells is their generally bigger size in diameter and their higher chlorophyl content. Given the differences of Δ*flkin* with the WT both in photosynthetic growth and the import of inorganic carbon, it is still unclear if this difference in cell size is due to metabolic differences or due to a defect on the cell cycle, where probably the cells are remaining in the vegetative stage for a prolonged time. The last hypothesis could have explained the slower growth of the strain, though there is no further evidence for this case. These questions, as many more, can be answered after the generation and study of the *Δflkin:FLKIN* complemented strain.

Now, based on these observations made in the Δ*flkin* knockout strain, what can we hypothesize about the cellular role and mode of action of FLKIN? At first, let's examine the regulatory relationship between PHOT and the phosphorylation of FLKIN. From the phosphoproteomic data it is shown that the abundance of p-FLKIN in the WT is low during low light and increases almost five-fold during the transition to high light (schematically shown in Fig. 3.24). This showcases that p-FLKIN is being regulated by the light intensity. In Δ*phot*, p-FLKIN abundance does not change between low and high light and is almost at the same levels as at the WT under high light. This shows that p-FLKIN is also being regulated by the presence of PHOT; in low light and with the presence of PHOT, p-FLKIN is in lower levels. This can mean that in the WT in low light either the total FLKIN protein levels are lower, or that FLKIN is not getting as highly phosphorylated as in high light.

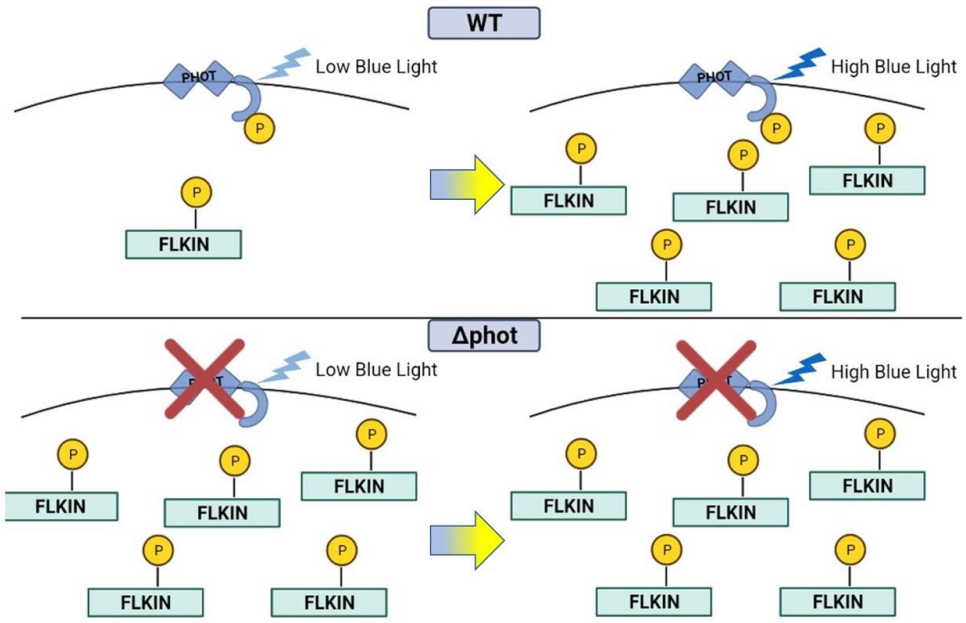

Figure 3.24: Schematic representation of the differences in the abundance of p-FLKIN between low and high light in the WT and Δphot, based on our phosphoproteomic dataset (graph shown in Fig. 3.5). Note here that there are no available data for the total protein abundance of FLKIN.

The answer to this wonder could have been given by the abundance of the total protein levels at the four conditions. Unfortunately, these data are not available, since FLKIN was not found in our whole-cell proteomic dataset. However, RNAseq data (Arend et al. 2022) comparing the WT and *Δphot* at LL and HL show that the *FLKIN*

transcript accumulation is impacted by the *phot* mutation (Fig. 3.25). More specifically, the transcript levels of *FLKIN* in Δ*phot* is almost the one third of the abundance in the WT in low light and almost half in high light. This, of course, cannot lead to safe conclusions about the protein levels, but it gives us a strong indication that lower abundance of p-FLKIN observed under low light in WT, in contrast with Δ*phot*, is possibly due to the de-phosphorylation of FLKIN.

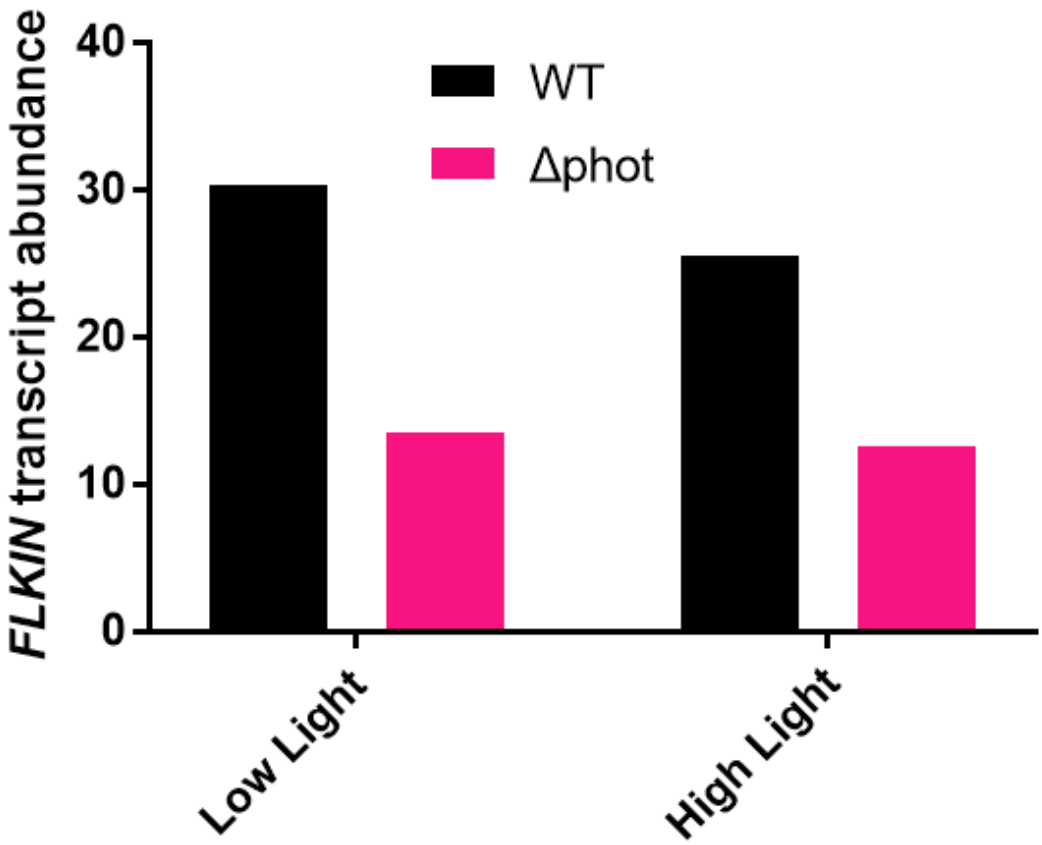

Figure 3.25: The transcript abundance of FLKIN in the WT and Δphot, under low light (15 µmol photons m^{-2} s^{-1}) and after 1h exposure under high light (300 µmol photons m^{-2} s^{-1}) (Arend et al. 2022)

Based on this assumption and on the fact that in the absence of *FLKIN* LHCSR3 and the CCM genes are being induced even in low light intensities, I built the following hypothesis model on the FLKIN function (shown in Fig. 3.26): In low light conditions, PHOT mediates the dephosphorylation of FLKIN. Since PHOT is a kinase and does not have phosphatase activity, this is maybe done via an intermediator protein

phosphatase. The dephosphorylated FLKIN, then, becomes activated and supresses the expression of LHCSR3 and the CCM genes. This kind of regulation is done for energy preservation of the cell; induction of photoprotection at low light intensities would mean loss of photosynthetically utile energy.

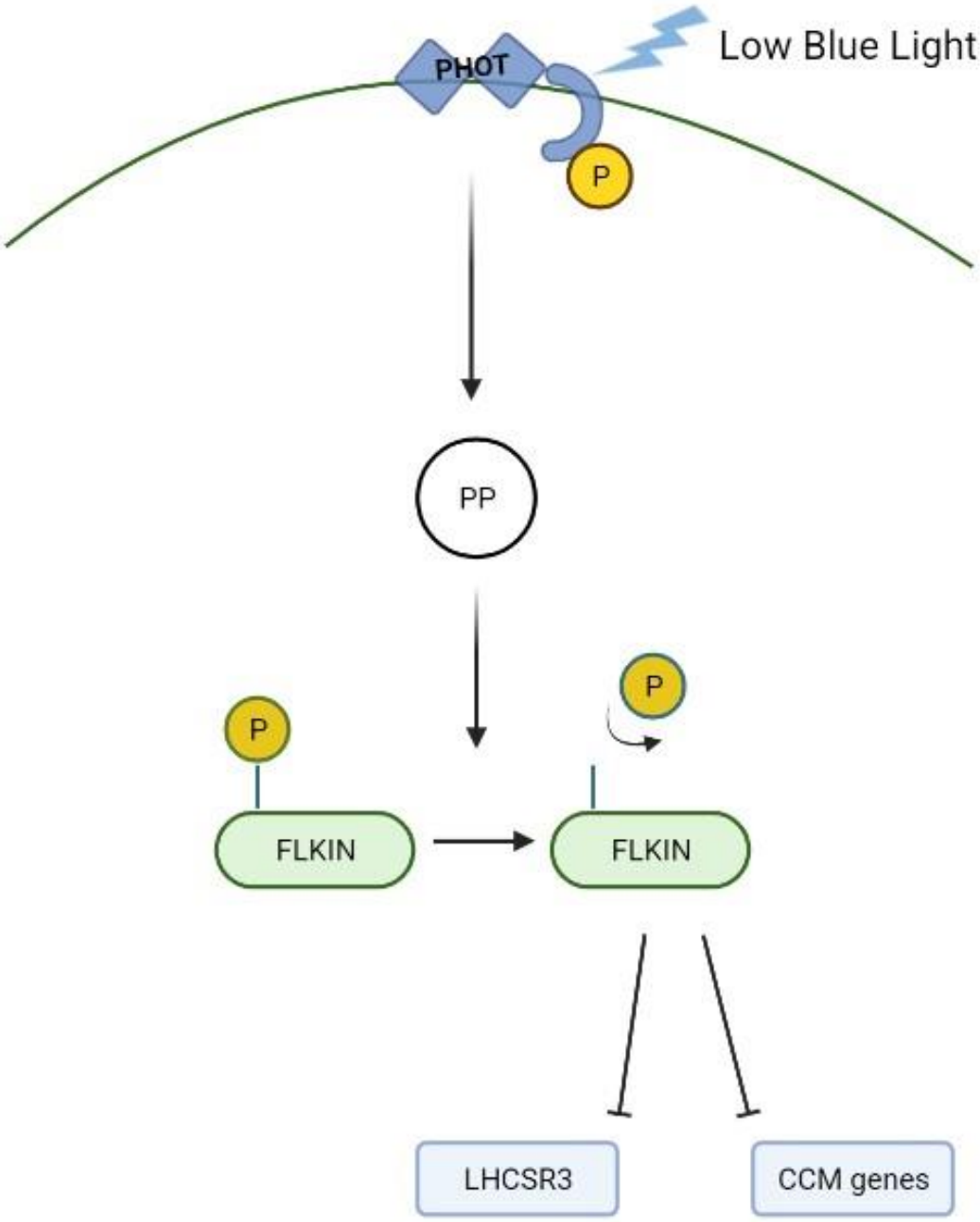

Figure 3.26: Proposed model for FLKIN activation and action. In low light intensities, PHOT mediates the dephosphorylation of FLKIN, possibly via a protein phosphatase (PP). The dephosphorylated form of FLKIN is then activated to supress the induction of LHCSR3 and of the CCM genes.

The characterisation of FLKIN as a suppressor of LHCSR3 can be furtherly backed up by the fact that its transcript abundance during the diurnal cycle follows an almost mirroring opposite trend than the corresponding one of LHCSR3, based on two publicly available RNAseq analyses (Zones et al. 2015) (Strenkert et al. 2019) (Fig. 3.27). Despite objective differences between the two analyses, due to different methodological approaches, we can conclude that generally *FLKIN* is mainly induced during the dark cycle, when photoprotection does not need to be activated, and *LHCSR3* during the light cycle, when the cell should be prepared to dissipate possibly harmful energy.

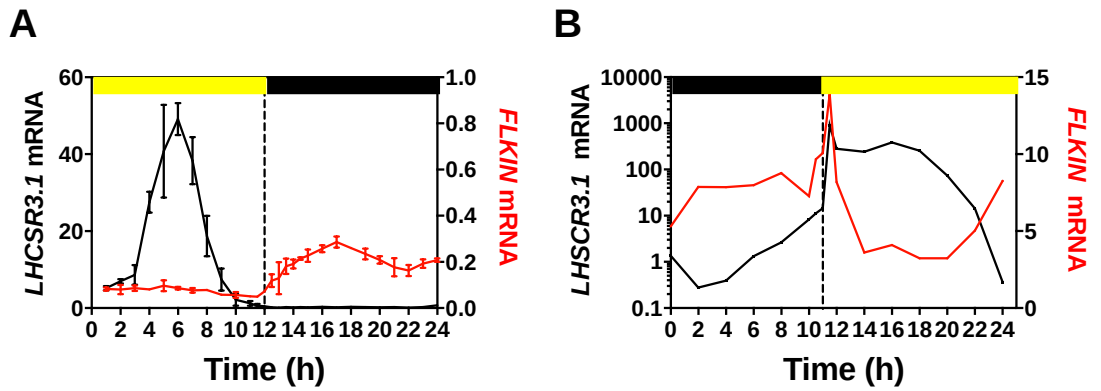

Figure 3.27: mRNA abundance for FLKIN during the day-night cycle in comparison with the abundance of the transcripts of LHCSR3 from (Zones et al. 2015) (A) and (Strenkert et al. 2019) (B). In (B), for better visualization of the data, the y axis is at log10 scale for the mRNA abundance of LHCSR3 and in linear scale for FLKIN.

From this hypothesis, some questions may arise. At first, one can wonder if PHOT is able to differentiate its signal between low and high light by itself or via another ''light-intensity- indicator'' player. It is shown that higher plant PHOTs have different sensitivities towards the light intensities and can alternate their responses accordingly to them (Zhao et al. 2013) (Harada et al. 2013) (Zhao et al. 2018) (Hart et al. 2019). It has also been shown that CrPHOT can initiate responses under a wide range of light intensities, from low fluence to high and stressful light (Im et al. 2006) (Petroutsos et al. 2016). However, not enough evidence for a light-intensity sensing ability for CrPHOT has been described yet and, thus, we cannot hypothesize on it further.

Another wonder concerns the cellular distance between PHOT and FLKIN. Are they interacting directly or via intermediate interactors? While it is known that PHOT is associated with the plasma membrane (Huang, Merkle, and Beck 2002) (Huang, Merkle, and Beck 2002), little is known about the localisation of FLKIN, and this knowledge would be useful for us to speculate on the previous question. However, according to the Predalgo subcellular localization prediction tool (as mentioned in Phytozome v.13) (Tardif et al. 2012), FLKIN is not predicted to be located in the nucleus, the mitochondria, the chloroplast or the secretory pathway. The same conclusion can be reached when using the online tools ChloroP (predicts the presence or absence of chloroplast transit peptides) (Emanuelsson, Nielsen, and von Heijne 1999); MitoProt II (predicts the presence or absence of a mitochondrial targeting sequence and the cleavage site) (Claros 1995) and cNLS Mapper (Predicts importin α-dependent nuclear localization signals) (Lin and Hu 2013). Additionally, FLKIN does not have any transmembrane helices, according to the online tool TMHMM Server v. 2.0 (Krogh et al. 2001). Therefore, it is highly possible that FLKIN is a cytoplasmic protein. The successful complementation of Δ*flkin* with FLKIN fused with a chromophore protein can also attribute to the localisation studies of FLKIN. Furthermore, *in vivo* and *in vitro* assays, such as Bimolecular fluorescence complementation, yeast-two-hybrid, co-immunoprecipitation and others can also showcase the possibility of an interaction between PHOT and FLKIN.

3.2 Elucidating early, PHOT-dependent phosphorylating events in Chlamydomonas.

3.2.1. Setup and conditions

In order to elucidate further the PHOT-regulated phosphorylations in *C. reinhardtii*, a new phosphoproteomic analysis has been performed. This time, the phosphoproteome of the two strains (WT and Δ*phot*) was compared during the

transition from darkness to blue light illumination for 5 min. This setup was aiming at focusing to the early phototropin-dependent phosphorylation events.

To verify if this exposure time and that light intensity were enough for the transcription of *LHCSR3* in the cell, I took samples from both strains right after the dark acclimation (t=0) and 5- and 60-min after exposure to blue Light (100 µE m^{-2} s^{-1}). Three flasks have been used from each strain and two samples were taken from each flask. qPCR has been performed to those samples to detect the *LHCSR3* transcript levels. The results are shown at Fig. 3.28. As it is shown, five-minute long exposure to blue Light (100 µE m^{-2} s^{-1}) leads to significant mRNA accumulation of *LHCSR3.1* (around 30-fold change in the case of the WT, 3-fold change in *Δphot)*. Therefore, 5min of exposure to blue light at this light intensity are enough to trigger the PHOT-controlled pathway that led to *LHCSR3* induction. The sampling at t=0 and t=5 min for the phosphoproteomics analyses was, thus, expected to allow meaningful insights on the early phosphorylation events upon illumination.

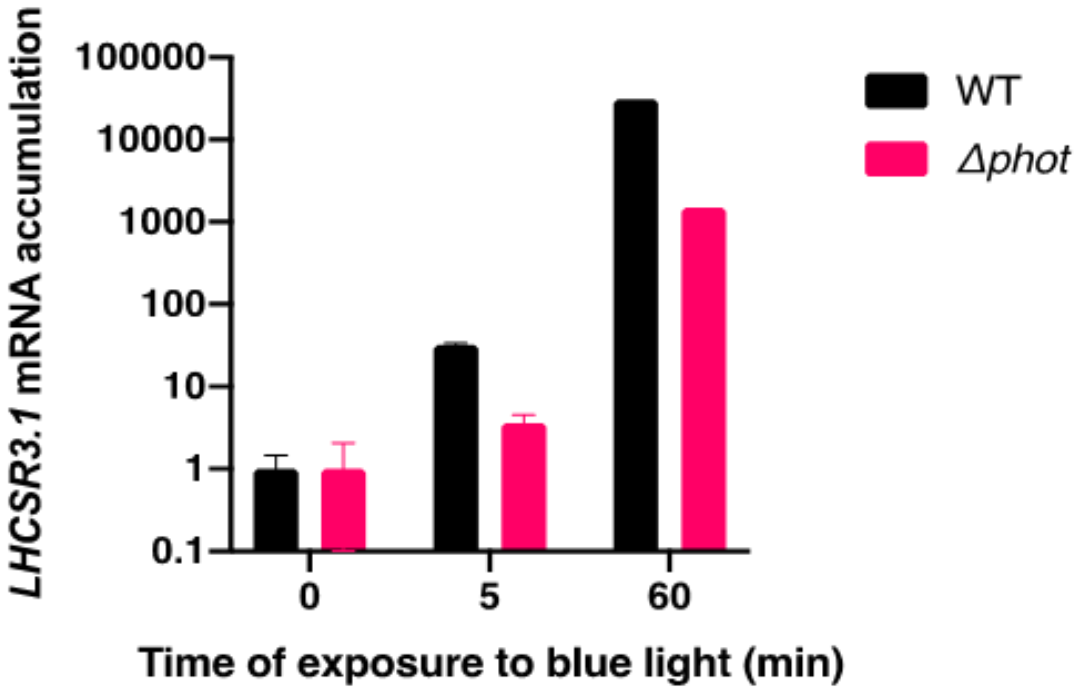

Figure 3.28: The transcript abundance of LHCSR3.1 in the darkness and after 5 and 60 min of exposure to Blue Light (100 µE m^{-2} s^{-1}), in the WT and in Δphot. The results were obtained after cDNA synthesis and qPCR (see Materials and Methods).

The growth and sampling conditions are described in details in the Materials and Methods. The protein samples from each strain and condition were sent to the lab of Leslie Hicks (University of North Carolina at Chapel Hill) for LC-MS/MS analyses. Prior to this step, the proteins had been digested and the phosphopeptides had been recovered with the use of TiO_2 beads, as described in (Wang et al. 2014).

3.2.2. Analysis of the phosphoproteome dataset

In total, 6273 unique phosphopeptides from 2618 phosphoproteins were identified. From the trend analysis that has been performed across the conditions, 12 clusters containing phosphopeptides with unique abundance trends have been emerged (Fig. 3.29). Cluster H contains the phosphopeptides of interest, which increase in abundance only in blue -light exposed WT samples. Cluster I has also particular interest, since it contains phosphopeptides which decrease in abundance after blue-light exposure in the WT but not in the Δ*phot* mutant.

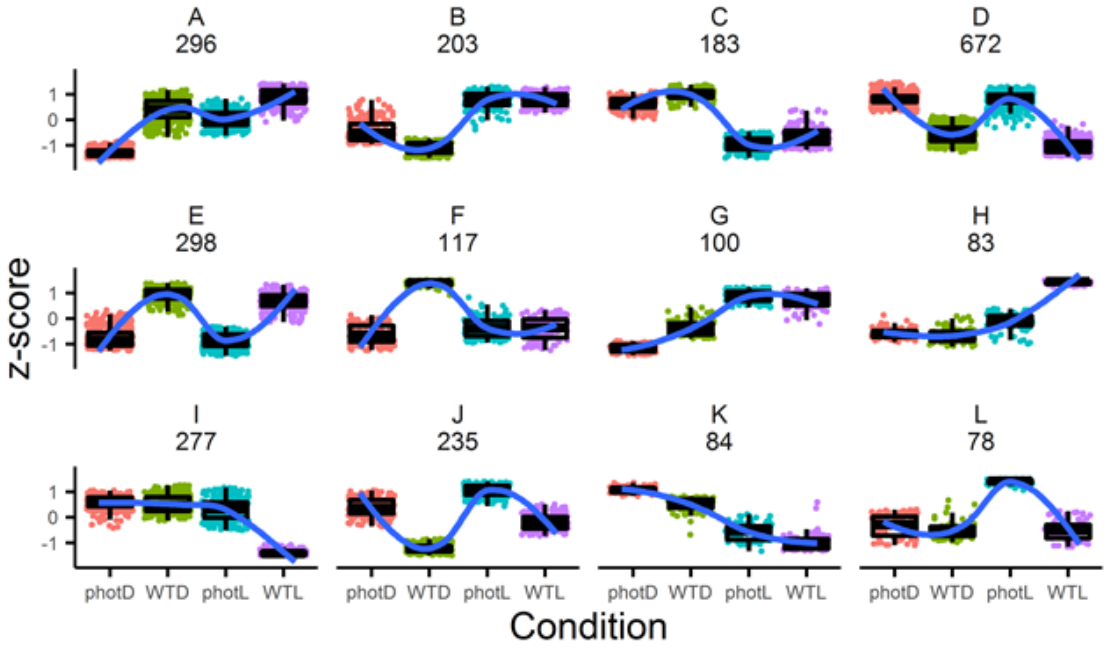

Figure 3.29: The 12 clusters (A-L) of the phosphopeptides showing unique abundance trends across the conditions. From the 6273 unique phosphopeptides, the 2626 ones which had FDR-adjusted p-value < 0.05 after one-way ANOVA were included in the clustering

A close look at the phosphopeptides at the clusters H and I reveals that PHOT regulates the phosphorylation of a diverse set of proteins in terms of localisation and cellular role. A first look on the localisation of these phosphoproteins (Fig. 3.30 and Fig. 3.31) reveals that the majority of proteins in cluster H and I are membrane-bound proteins, such as PHOT itself. Among those membrane proteins, we can find proteins involved in transmembrane transport, signal transduction and photoreception. The second biggest group of phosphoproteins in clusters H and I are proteins found in the cytoplasm. The cytoplasm is of course the loci of a variety of cellular activities, such as metabolism, signal transduction, cytokinesis and others. Additionally, 12 phosphoproteins from cluster H and 25 from cluster I are predicted to be localised in the nucleus. In between those phosphoproteins we observe some that are involved in signal transduction, microtubule organisation, transcription and epigenetic regulation, as well as the major chromatin-binding nucleolar protein Nucleolin. The presence in clusters H and I of signalling phosphoproteins located in the membranes, the cytoplasm and in the nucleus reveals that after 5min of blue light irradiation the PHOT-regulated signal can be transmitted rapidly through the whole cell body, and even up to the regulation of gene transcription in the nucleus. That is why also numerous transcription and epigenetic factors alternated their phosphorylation status from dark to blue light in a PHOT-dependent manner. Interestingly, 8 flagella localised phosphoproteins, involved in the cilia movement and biogenesis, are also found in cluster I.

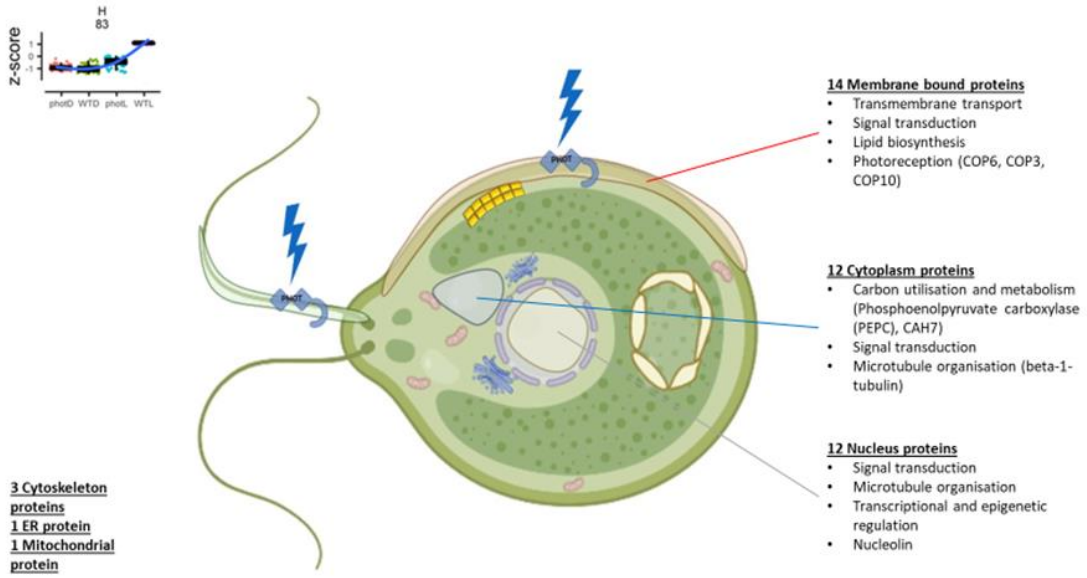

Figure 3.30: Localisation of the phosphopeptides which comprise cluster H, based on their localisation GOs.

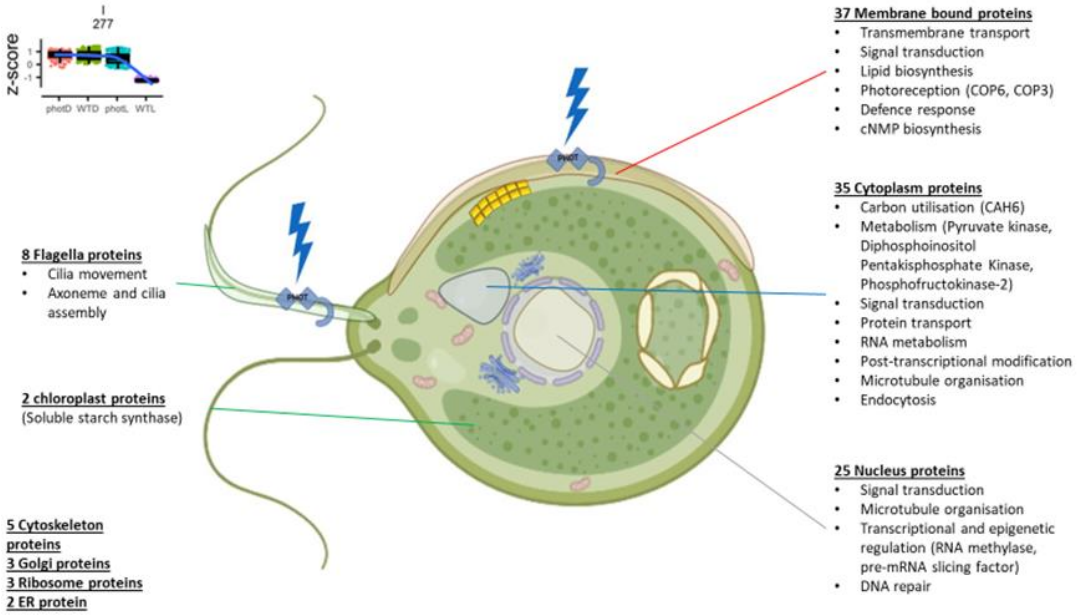

Figure 3.31: Localisation of the phosphopeptides which comprise cluster I, based on their localisation GOs.

It is also evident that a great number of biological processes are being controlled in a blue-light/PHOT-dependent manner. As we can see at Fig. 3.32, the majority of the phosphoproteins at the clusters H and I are being involved in signalling, such as phosphatases, CDPK-related kinases, mitogen-activated kinases (including NPK1), the cytokinesis-regulating proteins ataurora1 and ataurora3, the Golgi trafficking

regulator Phosphatidylinositol 4-kinase (PI4K) and others. As it was mentioned in the Introduction, the PHOT signal for the LHCSR3 induction requires as second messengers the cyclic nucleotides cAMP or cGMP downstream of PHOT (Petroutsos et al. 2016). A great number of phosphoproteins found in clusters H and I are involved in either the synthesis of cNMPs (6 Adenylate/guanylate cyclases), in binding with a cNMP (Flagellar Associated Protein 323) or in the hydrolysis of a cNMP (a 3',5'-cyclic-nucleotide phosphodiesterase). These phosphoproteins can, thus, be involved in the transmission of the PHOT signal to induce LHCSR3. Furthermore, it has been showcased that calcium and the calcium-binding protein Calmodulin are important signalling actors for the induction of LHCSR3 (Petroutsos et al. 2011) (Maruyama, Tokutsu, and Minagawa 2014). On that note, 4 kinases from cluster H and 12 kinases from cluster I are calcium-binding and/or calmodulin-regulated ones. A link between the sulfur limitation signalling and PHOT is revealed by the presence of the SNF1-related protein kinase, homologue of *Arabidopsis* SNRK1, in cluster I. This kinase is shown to be an essential messenger protein during sulfur limitation (Davies, Yildiz, and Grossman 1999).

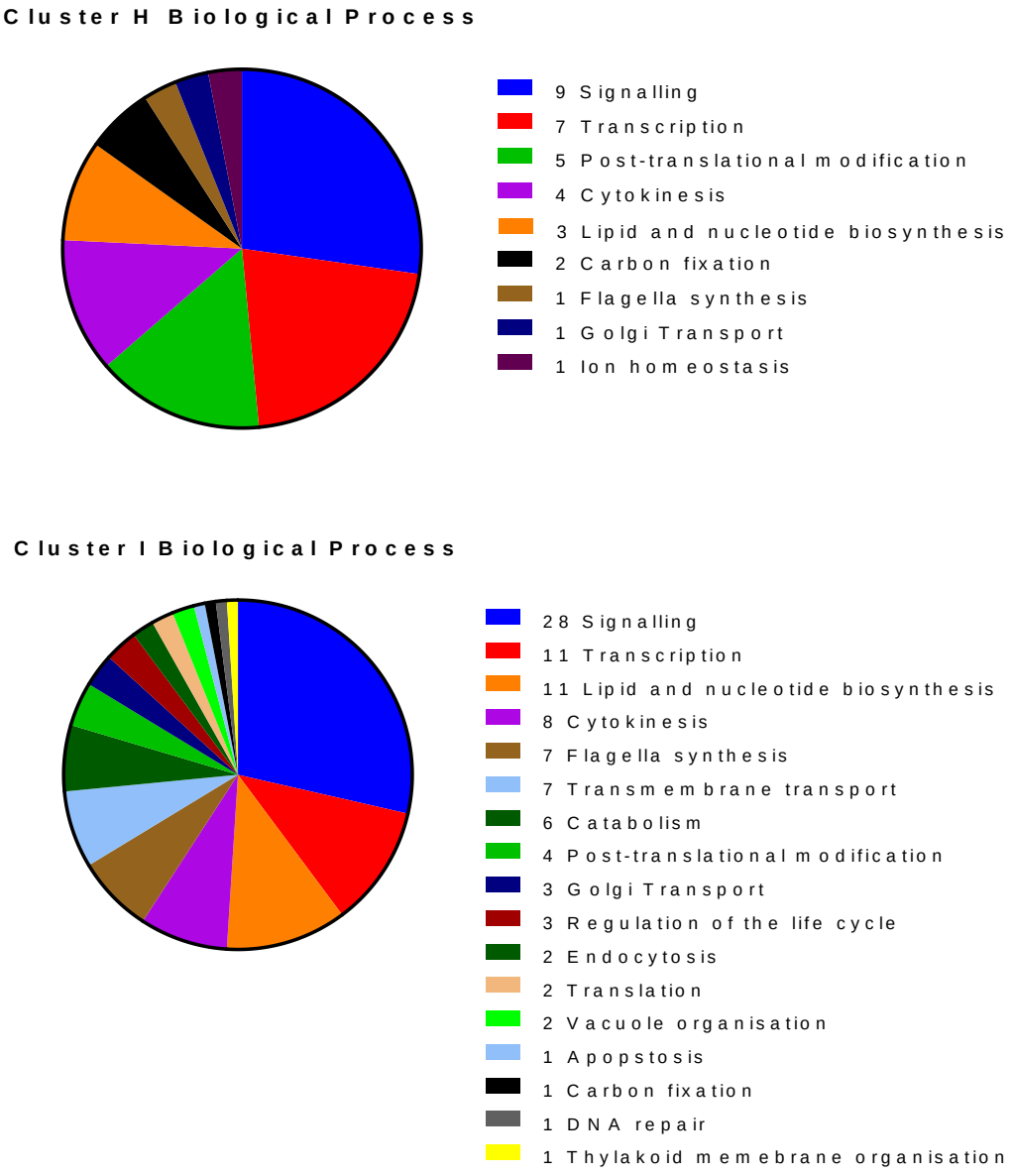

Figure 3.32: The biological processes at which the phosphoproteins at Cluster H and Cluster I are involved. This classification was done based on their Biological Process GOs.

The second most regulated biological process by *Chlamydomonas* PHOT is transcription, which comes in accordance with previous findings that PHOT in *C. reinhardtii* regulates gene expression (Im et al. 2006) (Petroutsos et al. 2016). The most interesting case of transcriptional factor found in our phosphoproteomic dataset, was the one of the protein Rhythm of Chloroplast 104 (ROC104). ROC104 mediates the circadian clock regulation of gene expression, and its deletion from the genome leads to arrhythmic mutants (Matsuo et al. 2020). A possible involvement of

PHOT and blue light in general on the circadian clock regulation would be a very interesting case for future studies. Clusters I and H also include proteins which are part of epigenetic regulation, such as the demethylation of histone H3-K9 and the organisation of chromatin.

A surprisingly big number of proteins involved in cytokinesis and the microtubule organisation (4 in cluster H and 8 in cluster I) are also regulated by PHOT, showing the importance of PHOT on mitosis. Other than ataurora1 and ataurora3, there are also the microtubule-binding kinesin motor protein and the microtubule monomer beta-1 tubulin, among others.

PHOT regulation of carbon availability and utilisation can be hypothesized, based on the presence of three carbonic anhydrases (CAH3, CAH6 and CAH7) in the clusters of interest. CAH3 is a well-characterised CCM protein, located at the thylakoid membranes which pass through the pyrenoid, and converts HCO_3^- to CO_2 close to its fixation loci by Rubisco (Sinetova et al. 2012). Indeed, it has been recently shown that PHOT supresses QER7, a transcriptional factor, acting as suppressor of CCM genes (Arend at al. 2022). The enzyme Phosphoenolpyruvate carboxylase, which is involved in the CO_2 fixation reactions, is also found in cluster H.

A very interesting outcome from our phosphoproteomic dataset is the PHOT-regulated phosphorylation of other photoreceptors. Three histidine kinase rhodopsins from the same photoreceptors' family (Cop3, Cop6 and Cop10 as described in (Greiner et al. 2017)) have been found in cluster H. More specifically, three phosphopeptides of Cop6, two of Cop3 and one of Cop10 are present in this cluster.

In Fig. 3.33 are the phosphopeptides (indicated with their corresponding gene IDs and their phosphorylated residues) which increase or decrease the most their abundance in the WT when the cultures are transferred from dark to blue light, while their abundances are at the same levels in Δ*phot* under both conditions. The phosphorylation of those peptides is considered to be strongly regulated by the presence and blue-light activation of PHOT. In this list, two particular peptides attracted my attention, based on their biological significance. The phosphopeptide with the third highest increase of its abundance in the WT is the recently characterised

MARS1 (product of the gene Cre16.g692228). MARS1 is a cytoplasmic protein which is the first known component of the chloroplast Unfolded Protein Response (cpUPR) (Perlaza et al. 2019). This proposes the involvement of PHOT on another response for maintenance of the chloroplast homeostasis other than photoprotection, the cpUPR. Another one of the phosphopeptides with the highest change in abundance between the dark acclimated WT cultures and the ones after the 5min exposure to blue light is Chlamyopsin 6, or Cop6. Cop6 is a putative photoreceptor, and more specifically a histidine- kinase rhodopsin (Greiner et al. 2017). Synergetic regulation between PHOT and another photoreceptor would have been a very interesting case for colour perception and cellular signalling in *C. reinhardtii*.

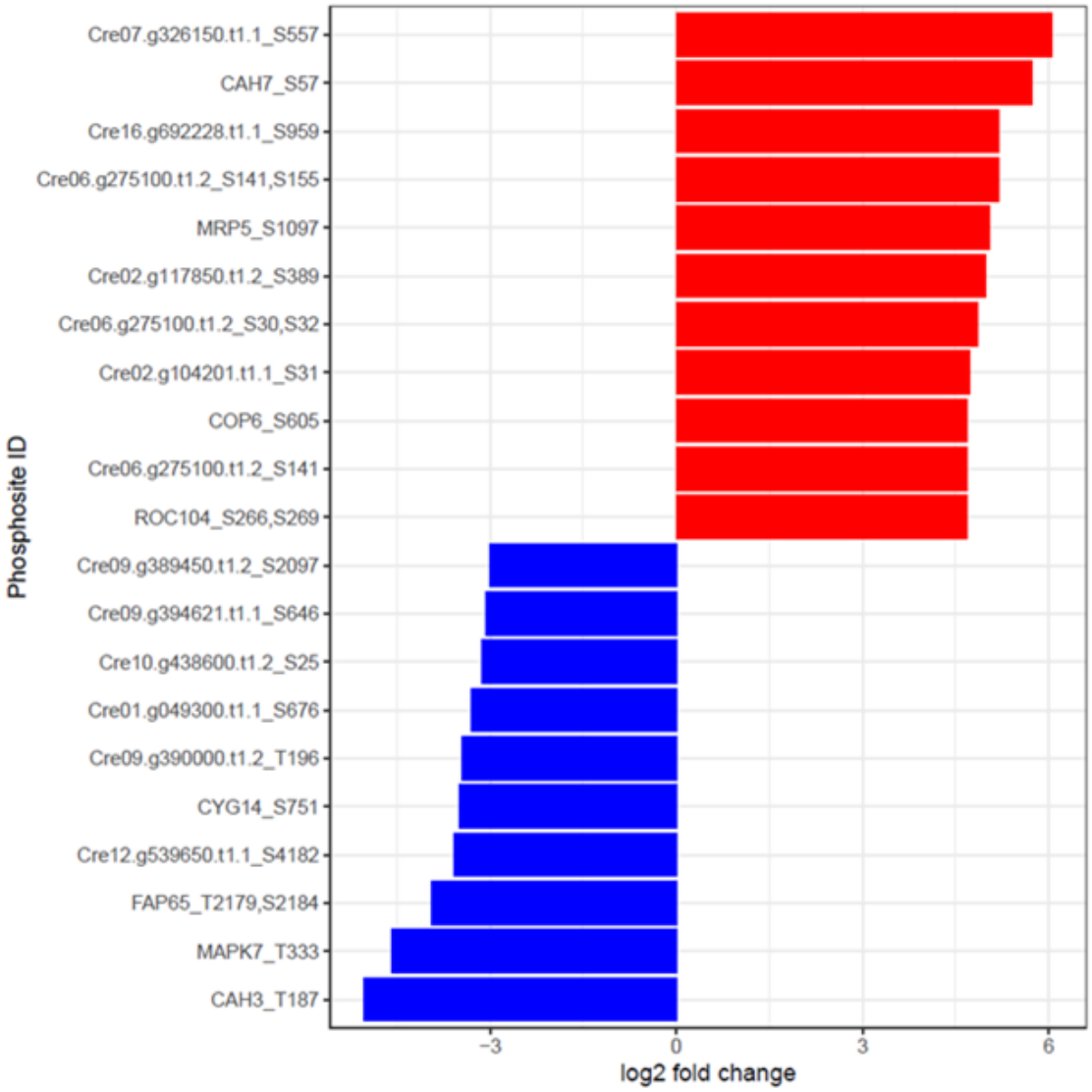

Figure 3.33: Phosphopeptides whose abundance increases or decreases the most in the WT when the cultures are transferred from dark to blue light, while it remains at the same levels at the Δphot (from the phosphoproteomic dataset). The differences in abundance are shown as log2 of the fold change of

the abundances from the dark acclimated cells to the blue-light exposure ones. The red bars represent the highest increases in abundance and the blue bars the highest decreases in abundance. Next to each bar, the gene ID of each phosphosite is being indicated with the corresponding phosphorylated residue.

3.2.3 Study of the Δ*Cop6* mutant

As it was mentioned earlier, the phosphorylated peptide of the putative photoreceptor Cop6 (phosphorylated at S605) increases significantly its abundance when transferred from dark to blue light within 5 min, while it remains at the same levels at the Δ*phot* mutant. Two other phosphorylated forms of Cop6 are found in cluster H. The first phosphorylated form has a phospho- group at Ser829 and the other at Ser701. All those three mentioned phosphorylated residues belong to the two-component sensor histidine kinase domain of the protein. Cop6 contains also a C-terminal cGMP or cAMP- effector domain. Note here that cGMP or cAMP are shown to act downstream of PHOT as signalling molecules at the *LHCSR3* induction pathway (Petroutsos et al. 2016). For these reasons and for reasons discussed earlier, Cop6 was an interesting candidate as a co-regulator of *LHCSR3* induction, alongside PHOT.

Thus, experiments in blue and white light had been conducted with Δ*Cop6*, a CRISPR-Cas9 mutant, which was kindly offered to us by Peter Hegemann's lab. More specifically, after an overnight dark acclimation of the mutant alongside its parent WT strain CC-125, both cultures were transferred for 4h under high white light (300 µmol photons m^{-2} s^{-1}) and blue light (100 µmol photons m^{-2} s^{-1}) (Fig. 3.34). The same protocol was followed for different light intensities of blue (50 and 100 µmol photons m^{-2} s^{-1}) (Fig. 3.35). As it was evidenced by those experiments the LHCSR3 levels on those strains were at the same levels between the two strains under all the light conditions

that were examined. Thus, despite the fact that Cop6 gets phosphorylated in a PHOT-dependent manner, this protein is not regulating the expression of LHCSR3.

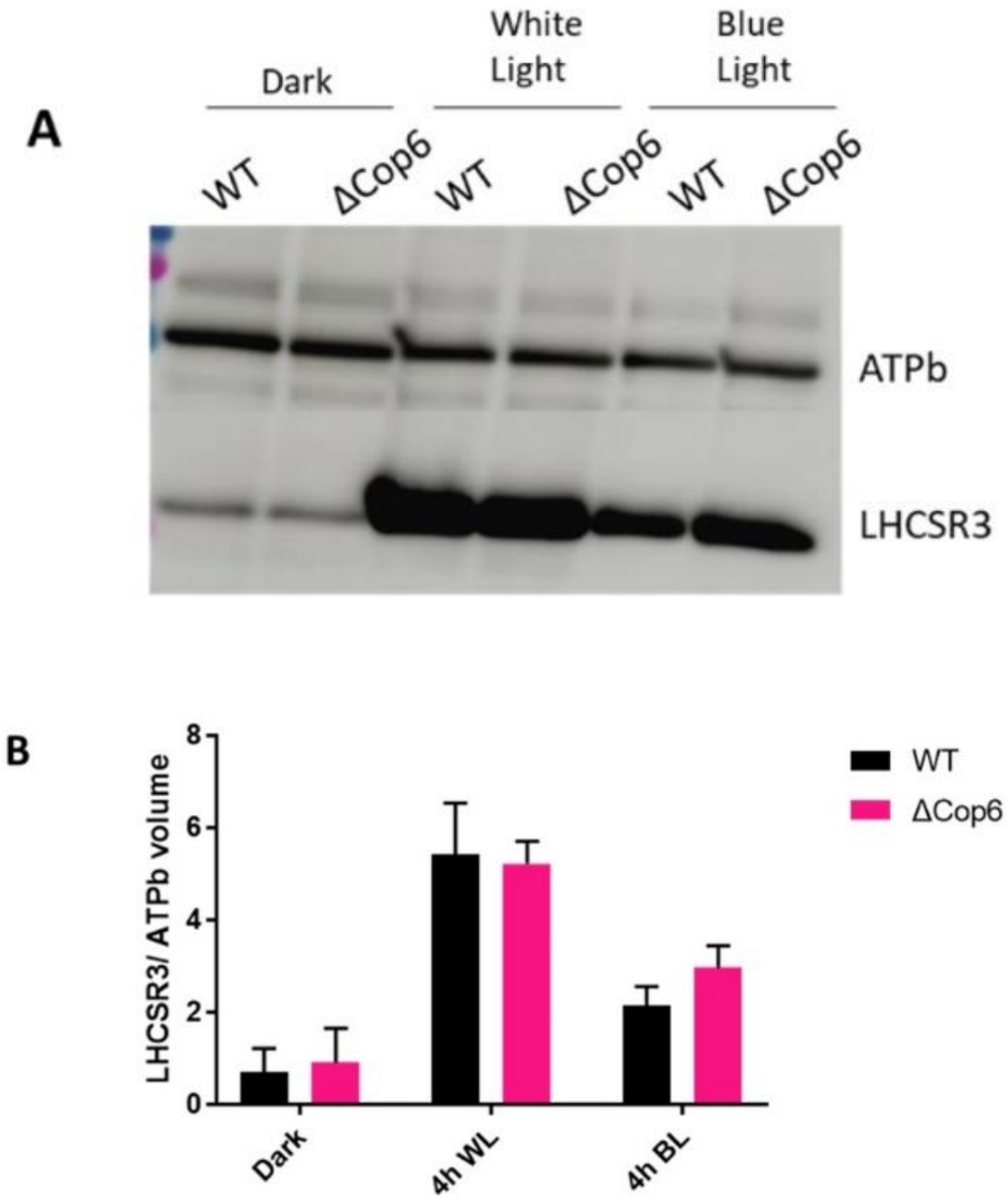

Figure 3.34: A) LHCSR3 levels at the WT and ΔCop6 after the overnight dark acclimation and after 4h incubation at 300 µmol photons m^{-2} s^{-1} of white and 100 µmol photons m^{-2} s^{-1} of blue light. Anti-ATPb was used as a loading control. B) Densitometric analysis of the bands from blots of three independent lines of samples (second and third blots not shown)

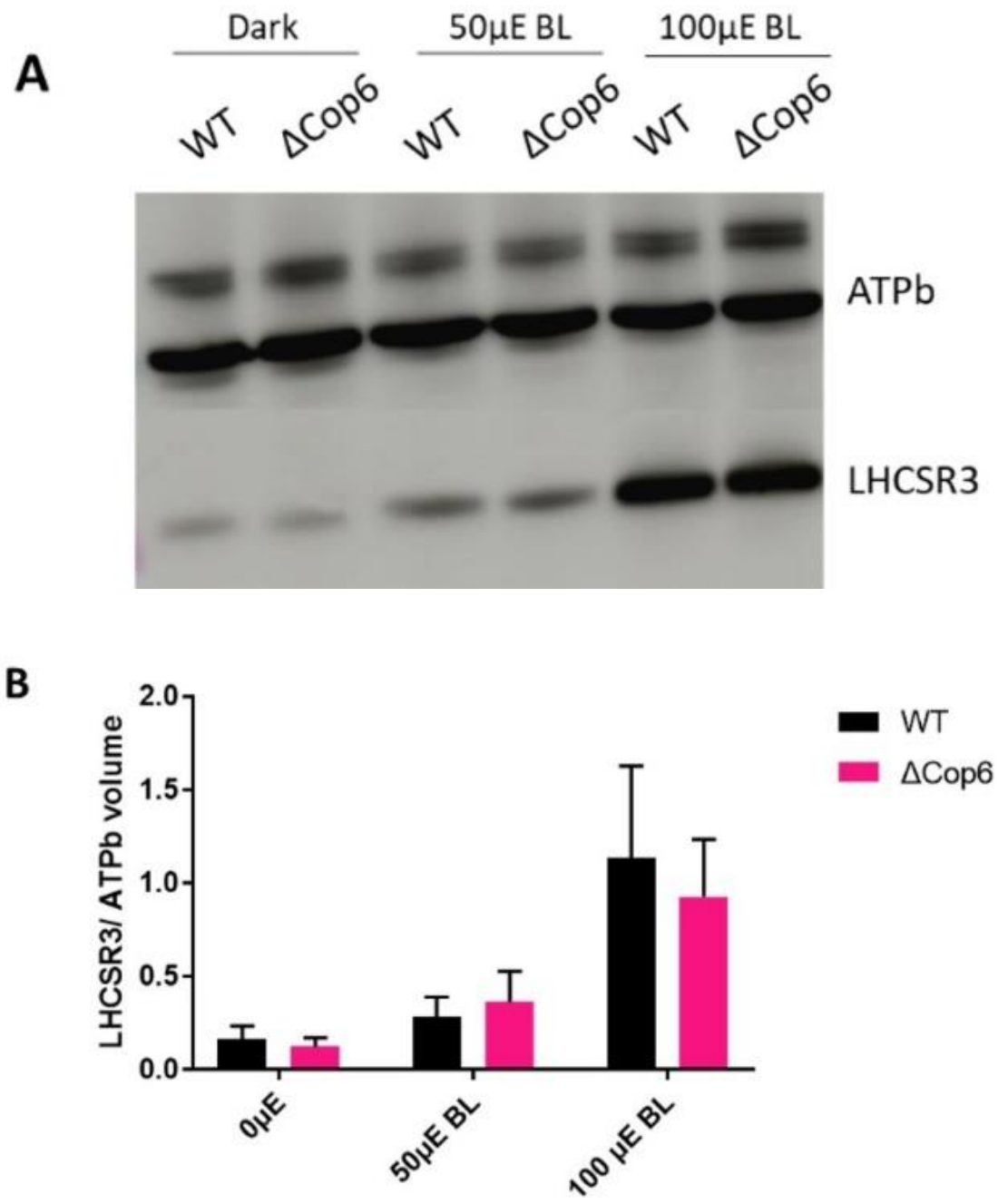

Figure 3.35: A) LHCSR3 levels at the WT and Δcop6 after the overnight dark acclimation and after 4h incubation at 50 µmol photons m^{-2} s^{-1} and 100 µmol photons m^{-2} s^{-1} of blue light. Anti-ATPb was used as a loading control. B) Densitometric analysis of the bands from blots of three independent lines of samples (second and third blots not shown)

3.2.4 PHOT is involved in the cpUPR response

As it is shown in Fig. 3.26, the phosphorylated MARS1 at S959 is among those phosphopeptides with the highest induction in abundance upon 5 min exposure to

blue light in the WT, while it remains at the same levels in the Δ*phot* strain. MARS1 is located in the cytoplasm and it transmits the cpUPR signal; its depletion from the cell leads to no expression of the highly responsive cpUPR genes *VIPP2* and *HSP22 E/F* (Perlaza et al. 2019). In (Perlaza et al. 2019) an alternative reading frame of *MARS1* has been proposed. Based on that reading frame the abovementioned phosphorylated residue actually corresponds to S1097. Hereafter, I will refer to that reading frame. Different phosphopeptides of MARS1, phosphorylated at S280 and at S1104 are also present in the phosphoproteomic data, but these have no significant difference in abundance between the two strains and do not belong in any cluster. All those Serine residues are upstream of the catalytic domain which is determinable for the transmission of the cpUPR signal. Additionally, when the kinase domain of MARS1 gets deactivated, three residues which were getting phosphorylated under oxidative stress were no longer getting phosphorylated: S69, S280 and S1888, the last one being part of the catalytic domain. Therefore, MARS1 is a protein which can get phosphorylated in multiple regions and there is a possible synergetic relation between these phosphorylations for the signal transaction.

Since MARS1 is getting phosphorylated in a PHOT-depended manner, the main question that arose was: is the cpUPR response also under the control of PHOT? In order to address that, WT, Δ*phot* and phot-c (a *PHOT* complemented line described in (Redekop et al. 2021) were grown both in TAP and in HSM under 50 µmol photons m^{-2} s^{-1}, with and without the addition of 2mM of hydrogen peroxide (H_2O_2) for 4h. The addition of 2mM of H_2O_2 is creating enough oxidative stress to induce the cpUPR response within 4h (Theis et al. 2020). In order to observe the response, the protein levels of VIPP2 and HSP22E/F, whose induction is drastic after the activation of the cpUPR, were observed via Western blot. As shown in Fig. 3.36, both VIPP2 and HSP22 E/F and being induced 4h after the addition of the H_2O_2. This induction is significantly higher at the WT and the complemented line, than the Δ*phot* mutant. It is also evident that the presence of acetate in the medium leads to higher expression of the cpUPR responsive genes. Evidentially, since the Δ*phot* mutant is able to express VIPP2 and HSP22 E/F but in lower levels than the WT, PHOT seems to be involved in the cpUPR signal transaction and to act as an ‘’amplifier’’ of the signal.

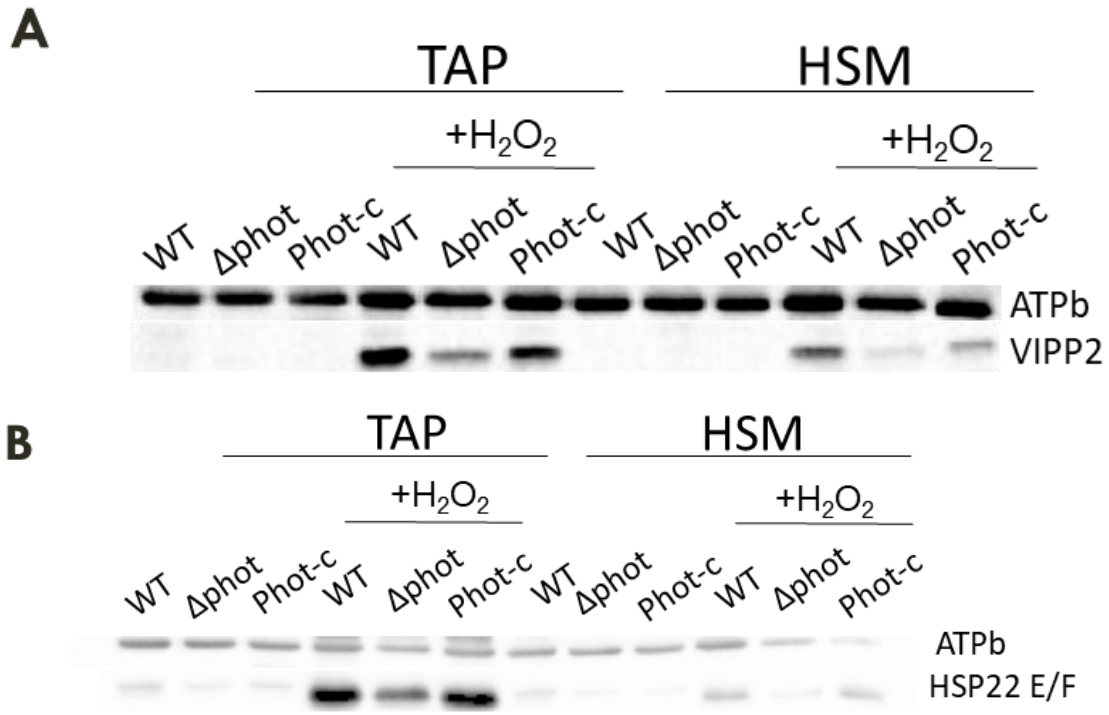

Figure 3.36: The levels of the cpUPR-responsive proteins at the WT, Δphot and the PHOT complemented line (phot-c) in response to oxidative stress (2mM H_2O_2). The cultures have been exposed to 50 µmol photons m^{-2} s^{-1} for 4h. The protein levels were observed in cultures grown either in TAP or in HSM. A) Protein levels of VIPP2. Anti-ATPb was used as a loading control. B) Protein levels of HSP22 E/F. Anti-ATPb was used as a loading control.

Under the same conditions, the LHCSR3 levels were also observed. It should be noted here that, based on previous observations, 50 µmol photons m^{-2} s^{-1} is not considered to be a high enough light intensity to induce strong accumulation of LHCSR3. However, some significant induction can be observed in the WT and -to a lesser extent- in the complemented line at the cultures grown in HSM without the addition of H_2O_2 (Fig. 3.37). Thus, both the presence of acetate and H_2O_2 in the medium seem to supress LHCSR3. Given the fact that the *LHCSR3* expression is MARS1-independent under cpUPR-inducing conditions (Perlaza et al. 2019), one could conclude to the hypothesis that qE and cpUPR, while both aiming to retain the homeostasis of the chloroplast under photooxidative stress, they are induced under contrasting conditions.

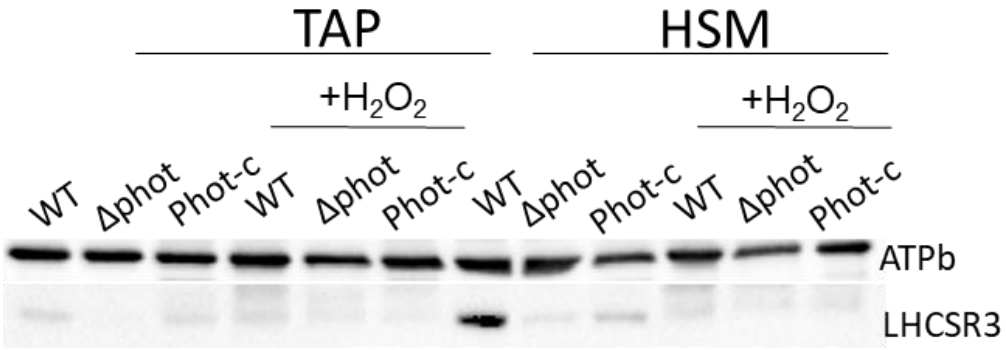

Figure 3.37: The levels of LHCSR3 at the WT, Δphot and the PHOT complemented line (phot-c) in response oxidative stress (2mM H_2O_2). The cultures have been exposed to 50 µmol photons m^{-2} s^{-1} for 4h. The protein levels were observed in cultures grown either in TAP or in HSM. Anti-ATPb was used as a loading control.

These experiments were repeated, this time with cultures growing just in TAP. Other than H_2O_2, 1.1 mM of Metronidazole (MZ) was also added in the cultures to trigger the cpUPR by creating oxidative stress. Metronidazole, is proposed to get reduced in the chloroplast in antagonism with proteins of the electron transport chain. The radical anion of metronidazole reacts with molecular oxygen and reduces it to radical superoxide, which leads to the formation of H_2O_2 (Schmidt, Matlin, and Chua 1977). In other words, with this experiment the cpUPR response was observed when H_2O_2 is being provided extracellularly or when it is being produced within the chloroplast. Incubation with 1.1 mM of MZ for 15h is shown to initiate the expression of the cpUPR genes (Perlaza et al. 2019) and, thus, that was the incubation time it was followed here as well. Surprisingly, in total contrast with what we observed in the cultures grown with H_2O_2, when MZ is added in the cultures, the Δ*phot* strain expresses multiple times higher levels of VIPP2 and HSP22E/F than the WT and the complemented line after 15h (Fig. 3.38). It is evident that the two treatments, while both inducing the cpUPR-responsive genes, seem to initiate different signalling pathways, and PHOT has a contradicting role at those separate responses. When H_2O_2 is being produced within the chloroplast, instead of being provided in the medium, PHOT seems to supress the expression of VIPP2 and HSP22 E/F.

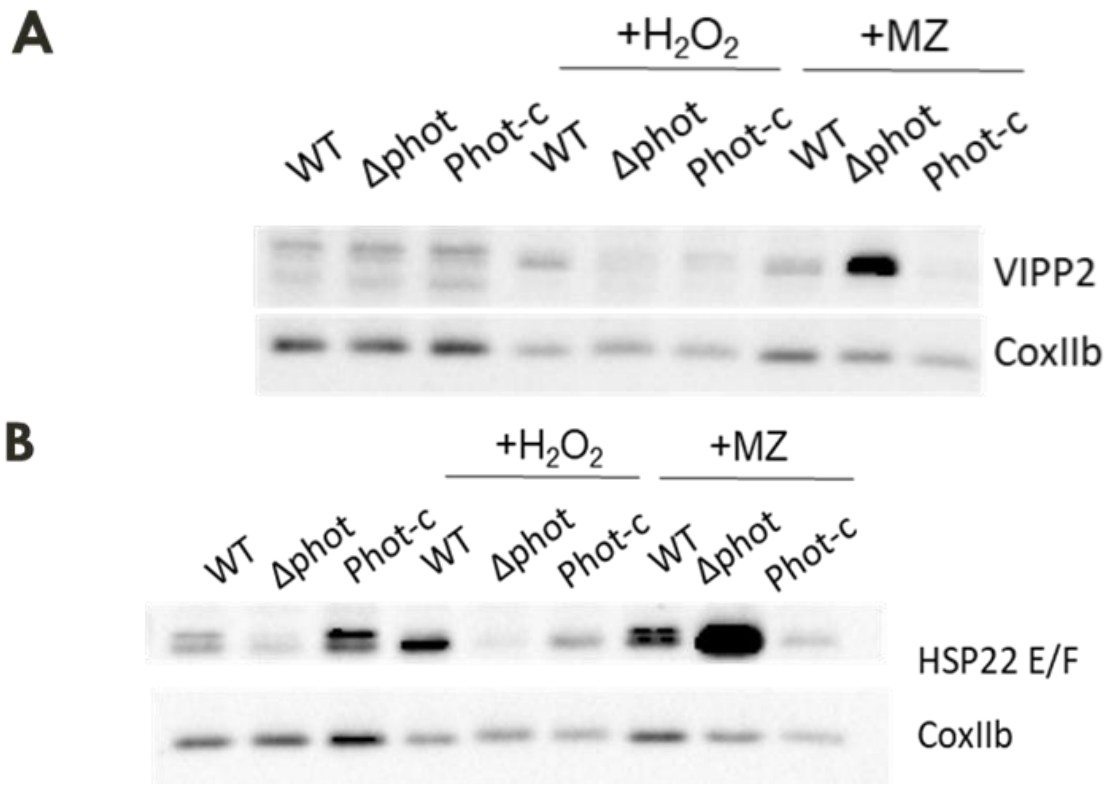

Figure 3.38: The levels of the cpUPR-responsive proteins at the WT, Δphot and the PHOT complemented line (phot-c) in response to oxidative stress (2mM H_2O_2, 1mM Metronidazole -MZ-). The cultures were grown is TAP and have been exposed to 50 µmol photons m^{-2} s^{-1} for 4h when H_2O_2 was added and for 15h when MZ was added. A) Protein levels of VIPP2. Anti-CoxIIb was used as a loading control. B) Protein levels of HSP22 E/F. Anti-CoxIIb was used as a loading control.

Focusing to the PHOT involvement at the cpUPR when H_2O_2 is added to the medium, it was unclear if this involvement was also blue-light regulated. For this, WT cultures either containing or not 2mM of H_2O_2 were exposed to 50 µmol photons m^{-2} s^{-1} for 4h. The protein expression of VIPP2 and HSP22 E/F, as well as the transcript levels of *VIPP2* at the first hour of the treatment were observed in every condition via Western blot and qPCR, respectively. As presented in Fig. 3.39, no significant differences at the levels of those proteins were observed under those three light qualities. The same trend was shown at the transcript levels of *VIPP2* (Fig. 3.40); while there is a clear induction of the transcript linked with the addition of H_2O_2, there does not seem to be a chromatic regulation of that response. Consequently, PHOT, while contributing to the cpUPR, it seems that it does not do so in a blue-light-depended manner.

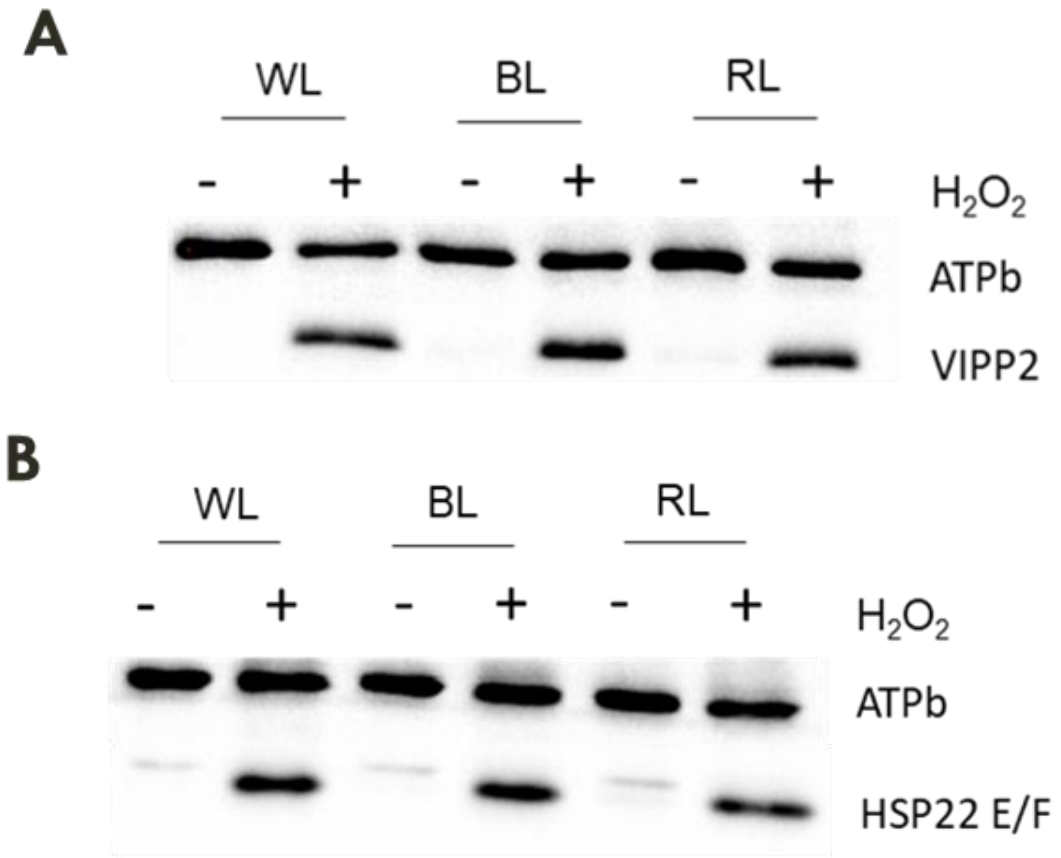

Figure 3.39: The levels of the cpUPR-responsive proteins at the WT in response to oxidative stress (2mM H_2O_2). The cultures were grown is TAP and have been exposed to 50 µmol photons m^{-2} s^{-1} of white light (WL), blue light (BL) and red light (RL) for 4h. A) Protein levels of VIPP2. Anti-ATPb was used as a loading control. B) Protein levels of HSP22 E/F. Anti-ATPb was used as a loading control.

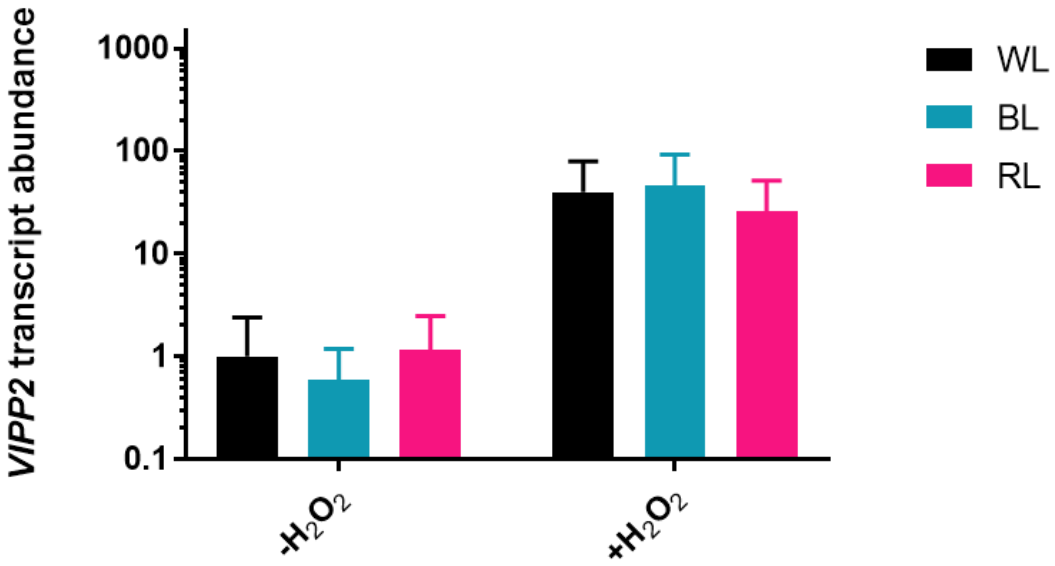

Figure 3.40: The transcript abundance of VIPP2 in the WT, when exposed to 50 µmol photons m^{-2} s^{-1} of white light (WL), blue light (BL) and red light (RL), with and without the addition of H_2O_2 for 1h. The results were obtained after cDNA synthesis and qPCR (see Materials and Methods).

4. CONCLUSION

On this Thesis, my aim was to elucidate the role of PHOT in *C. reinhardtii* and to identify putative PHOT interactors that mediate the blue-light induced signals.

At the first phosphoproteomic analysis, I compared the phosphoproteome of the WT and the Δ*phot* strain during the transition from low to high light. From this comparison, a number of phosphoproteins have emerged, whose abundance was changing based on two parameters: the light intensity and the presence of PHOT. Those proteins are possible to transmit the high-light responses of PHOT and more particularly the induction of LHCSR3 and the activation of qE. In between those proteins, there were numerous signal transduction proteins, transcriptional regulators, membrane transporters, metabolic enzymes and homoiotherm-related proteins. Also, from this analysis it was revealed that several CCM-related phosphoproteins, such as CAH7, LCI23 and LCIC are being regulated in a high-light/PHOT manner, showcasing a link between blue-light perception and the CCM.

One of the phosphoproteins which increased 5-fold their abundance in the WT while transitioning from low to high light, while remaining at the same levels at Δphot was an unspecific Ser/Thr kinase, which I named FLKIN. To elucidate the role of this protein I have studied and characterised the knockout mutant strain of *FLKIN* (Δ*flkin*). Δ*flkin* overaccumulates LHCSR3 and has higher qE levels than the WT, especially in non-saturating light intensities (the biggest difference has been observed in cultures exposed to 100 μmol photons m^{-1} s^{-1}). In the same light intensities, the mutant also overaccumulates, alongside the transcript of *LHCSR3*, also the transcripts of several CCM genes, namely *LCIA, LCIB*, *CAH3*, *CAH4* and the CCM transcriptional factor *LCR1*. This mutant strain, while activating qE in lower light intensities than the WT, it had higher Fv/Fm than the WT, as well. From growth studies, it was observed that Δ*flkin* showed a growth defect in autotrophic medium (HSM), since it was reaching a lower cell density that the WT in both low and high light intensities. Additionally, the cells of Δ*flkin* had bigger diameter than the ones of the WT and, also, contained higher chlorophyl content. From my studies I was driven to a hypothesis model on the FLKIN role: FLKIN gets dephosphorylated in a PHOT-dependent manner at low light and the dephosphorylated form mediates the suppression of LHCSR3 and the CCM.

In order to investigate the early responses to blue light by PHOT, a second phosphoproteomic analysis was setup. This time, the phosphoproteome of the WT and the Δ*phot* in dark and after 5min of exposure to blue light had been compared. I focused on the phosphoproteins changing their abundance after the transition from dark to blue light only in the WT. This dataset was including a diverse set of proteins both on their cellular localisation (membranes, cytoplasm, nucleus, flagella) and on their cellular function (signalling, transcriptional regulation, lipid biosynthesis and others). In particular, the phosphoproteins of 3 carbonic anhydrases (CAH3, CAH6 and CAH7), three histidine-kinase rhodopsins (Cop3, Cop6 and Cop10) and the circadian clock regulator ROC104 were found, between others, to be controlled by PHOT, widening the perspectives for the PHOT-regulated responses in *C. reinhardtii*.

MARS1, the first known component of the cpUPR response (Perlaza et al. 2019), is increasing the abundance of its phosphopeptide notably when transitioning from dark to blue light in the WT but not in Δ*phot*. That led to the study of the cpUPR response at the Δ*phot* strain. More specifically, I observed the expression of the two highest cpUPR responsive proteins (VIPP2 and HSP22 E/F) under oxidative stress. When H_2O_2 was supplemented in the medium, the expression of these genes was lower in Δ*phot* than the WT. However, the opposite result was observed when metronidazole was added in the medium and, thus, H_2O_2 was produced intracellularly in the chloroplast. This result shows that PHOT is an important player in the transmission of the cpUPR signal, with opposing role when the H_2O_2 is intracellularly produced than when it is extracellularly supplemented. It has been also showed that PHOT regulates the induction of VIPP2 and HSP22 E/F in a blue-light independent way.

5. REFERENCES

Abadie, C., E. R. Boex-Fontvieille, A. J. Carroll, and G. Tcherkez. 2016. 'In vivo stoichiometry of photorespiratory metabolism', Nat Plants, 2: 15220.

Ahmad, M., and A. R. Cashmore. 1993. 'HY4 gene of A. thaliana encodes a protein with characteristics of a blue-light photoreceptor', Nature, 366: 162-6.

Aihara, Y., K. Fujimura-Kamada, T. Yamasaki, and J. Minagawa. 2019. 'Algal photoprotection is regulated by the E3 ligase CUL4-DDB1(DET1)', Nat Plants, 5: 34-40.

Akella, S., X. Ma, R. Bacova, Z. P. Harmer, M. Kolackova, X. Wen, D. A. Wright, M. H. Spalding, D. P. Weeks, and H. Cerutti. 2021. 'Co-targeting strategy for precise, scarless gene editing with CRISPR/Cas9 and donor ssODNs in Chlamydomonas', Plant Physiol, 187: 2637-55.

Allen, J. F., W. B. de Paula, S. Puthiyaveetil, and J. Nield. 2011. 'A structural phylogenetic map for chloroplast photosynthesis', Trends Plant Sci, 16: 645-55.

Allorent, G., L. Lefebvre-Legendre, R. Chappuis, M. Kuntz, T. B. Truong, K. K. Niyogi, R. Ulm, and M. Goldschmidt-Clermont. 2016. 'UV-B photoreceptor-mediated protection of the photosynthetic machinery in Chlamydomonas reinhardtii', Proc Natl Acad Sci U S A, 113: 14864-69.

Allorent, G., R. Tokutsu, T. Roach, G. Peers, P. Cardol, J. Girard-Bascou, D. Seigneurin-Berny, D. Petroutsos, M. Kuntz, C. Breyton, F. Franck, F. A. Wollman, K. K. Niyogi, A. Krieger-Liszkay, J. Minagawa, and G. Finazzi. 2013. 'A dual strategy to cope with high light in Chlamydomonas reinhardtii', Plant Cell, 25: 545-57.

Arend, Marius, Yizhong Yuan, M. Águila Ruiz-Sola, Nooshin Omranian, Zoran Nikoloski, and Dimitris Petroutsos. 2022. 'Widening the landscape of transcriptional regulation of algal photoprotection', bioRxiv: 2022.02.25.482034.

Asadian, M., M. Saadati, F. B. Bajestani, J. Beardall, F. Abdolahadi, and N. Mahdinezhad. 2022. 'Knockout of Cia5 gene using CRISPR/Cas9 technique in Chlamydomonas reinhardtii and evaluating CO2 sequestration in control and mutant isolates', J Genet, 101.

Baek, K., D. H. Kim, J. Jeong, S. J. Sim, A. Melis, J. S. Kim, E. Jin, and S. Bae. 2016. 'DNA-free two-gene knockout in Chlamydomonas reinhardtii via CRISPR-Cas9 ribonucleoproteins', Sci Rep, 6: 30620.

Baek, K., J. Yu, J. Jeong, S. J. Sim, S. Bae, and E. Jin. 2018. 'Photoautotrophic production of macular pigment in a Chlamydomonas reinhardtii strain generated by using DNA-free CRISPR-Cas9 RNP-mediated mutagenesis', Biotechnol Bioeng, 115: 719-28.

Baier, T., J. Wichmann, O. Kruse, and K. J. Lauersen. 2018. 'Intron-containing algal transgenes mediate efficient recombinant gene expression in the green microalga Chlamydomonas reinhardtii', Nucleic Acids Res, 46: 6909-19.

Ballottari, M., T. B. Truong, E. De Re, E. Erickson, G. R. Stella, G. R. Fleming, R. Bassi, and K. K. Niyogi. 2016. 'Identification of pH-sensing Sites in the Light Harvesting Complex Stress-related 3 Protein Essential for Triggering Non-photochemical Quenching in Chlamydomonas reinhardtii', J Biol Chem, 291: 7334-46.

Barth, J., S. V. Bergner, D. Jaeger, A. Niehues, S. Schulze, M. Scholz, and C. Fufezan. 2014. 'The interplay of light and oxygen in the reactive oxygen stress response of Chlamydomonas reinhardtii dissected by quantitative mass spectrometry', Mol Cell Proteomics, 13: 969-89.

Beel, B., N. Muller, T. Kottke, and M. Mittag. 2013. 'News about cryptochrome photoreceptors in algae', Plant Signal Behav, 8: e22870.

Beel, B., K. Prager, M. Spexard, S. Sasso, D. Weiss, N. Muller, M. Heinnickel, D. Dewez, D. Ikoma, A. R. Grossman, T. Kottke, and M. Mittag. 2012. 'A flavin binding cryptochrome photoreceptor responds to both blue and red light in Chlamydomonas reinhardtii', Plant Cell, 24: 2992-3008.

Berthold, P., S. P. Tsunoda, O. P. Ernst, W. Mages, D. Gradmann, and P. Hegemann. 2008. 'Channelrhodopsin-1 initiates phototaxis and photophobic responses in chlamydomonas by immediate light-induced depolarization', Plant Cell, 20: 1665-77.

Blaby, I. K., C. E. Blaby-Haas, M. E. Perez-Perez, S. Schmollinger, S. Fitz-Gibbon, S. D. Lemaire, and S. S. Merchant. 2015. 'Genome-wide analysis on Chlamydomonas reinhardtii reveals the impact of hydrogen peroxide on protein stress responses and overlap with other stress transcriptomes', Plant J, 84: 974-88.

Boccalandro, H. E., M. L. Rugnone, J. E. Moreno, E. L. Ploschuk, L. Serna, M. J. Yanovsky, and J. J. Casal. 2009. 'Phytochrome B enhances photosynthesis at the expense of water-use efficiency in Arabidopsis', Plant Physiol, 150: 1083-92.

Bonente, G., M. Ballottari, T. B. Truong, T. Morosinotto, T. K. Ahn, G. R. Fleming, K. K. Niyogi, and R. Bassi. 2011. 'Analysis of LhcSR3, a protein essential for feedback de-excitation in the green alga Chlamydomonas reinhardtii', PLoS Biol, 9: e1000577.

Botto, J. F., R. A. Sanchez, G. C. Whitelam, and J. J. Casal. 1996. 'Phytochrome A Mediates the Promotion of Seed Germination by Very Low Fluences of Light and Canopy Shade Light in Arabidopsis', Plant Physiol, 110: 439-44.

Boyden, E. S., F. Zhang, E. Bamberg, G. Nagel, and K. Deisseroth. 2005. 'Millisecond-timescale, genetically targeted optical control of neural activity', Nat Neurosci, 8: 1263-8.

Briantais, J. M., C. Vernotte, M. Picaud, and G. H. Krause. 1979. 'A quantitative study of the slow decline of chlorophyll a fluorescence in isolated chloroplasts', Biochim Biophys Acta, 548: 128-38.

Buchanan, B. B. 1991. 'Regulation of CO2 assimilation in oxygenic photosynthesis: the ferredoxin/thioredoxin system. Perspective on its discovery, present status, and future development', Arch Biochem Biophys, 288: 1-9.

Buchanan, B. B., P. Schurmann, R. A. Wolosiuk, and J. P. Jacquot. 2002. 'The ferredoxin/thioredoxin system: from discovery to molecular structures and beyond', Photosynth Res, 73: 215-22.

Camargo, F. V. A., F. Perozeni, G. C. Valbuena, L. Zuliani, S. Sardar, G. Cerullo, C. D'Andrea, and M. Ballottari. 2021. 'The Role of Acidic Residues in the C Terminal Tail of the LHCSR3 Protein of Chlamydomonas reinhardtii in Non-Photochemical Quenching', J Phys Chem Lett, 12: 6895-900.

Casson, S. A., K. A. Franklin, J. E. Gray, C. S. Grierson, G. C. Whitelam, and A. M. Hetherington. 2009. 'phytochrome B and PIF4 regulate stomatal development in response to light quantity', Curr Biol, 19: 229-34.

Cazzaniga, S., M. Kim, F. Bellamoli, J. Jeong, S. Lee, F. Perozeni, A. Pompa, E. Jin, and M. Ballottari. 2020. 'Photosystem II antenna complexes CP26 and CP29 are essential for nonphotochemical quenching in Chlamydomonas reinhardtii', Plant Cell Environ, 43: 496-509.

Cecchin, M., J. Jeong, W. Son, M. Kim, S. Park, L. Zuliani, S. Cazzaniga, A. Pompa, C. Young Kang, S. Bae, M. Ballottari, and E. Jin. 2021. 'LPA2 protein is involved in photosystem II assembly in Chlamydomonas reinhardtii', Plant J, 107: 1648-62.

Ceriani, M. F., T. K. Darlington, D. Staknis, P. Mas, A. A. Petti, C. J. Weitz, and S. A. Kay. 1999. 'Light-dependent sequestration of TIMELESS by CRYPTOCHROME', Science, 285: 553-6.

Chaves, I., R. Pokorny, M. Byrdin, N. Hoang, T. Ritz, K. Brettel, L. O. Essen, G. T. van der Horst, A. Batschauer, and M. Ahmad. 2011. 'The cryptochromes: blue light photoreceptors in plants and animals', Annu Rev Plant Biol, 62: 335-64.

Cheng, X., G. Liu, W. Ke, L. Zhao, B. Lv, X. Ma, N. Xu, X. Xia, X. Deng, C. Zheng, and K. Huang. 2017. 'Building a multipurpose insertional mutant library for forward and reverse genetics in Chlamydomonas', Plant Methods, 13: 36.

Cho, H. Y., T. S. Tseng, E. Kaiserli, S. Sullivan, J. M. Christie, and W. R. Briggs. 2007. 'Physiological roles of the light, oxygen, or voltage domains of phototropin 1 and phototropin 2 in Arabidopsis', Plant Physiol, 143: 517-29.

Chou, M. F., and D. Schwartz. 2011. 'Biological sequence motif discovery using motif-x', Curr Protoc Bioinformatics, Chapter 13: Unit 13 15-24.

Christie, J. M. 2007. 'Phototropin blue-light receptors', Annu Rev Plant Biol, 58: 21-45.

Christie, J. M., A. S. Arvai, K. J. Baxter, M. Heilmann, A. J. Pratt, A. O'Hara, S. M. Kelly, M. Hothorn, B. O. Smith, K. Hitomi, G. I. Jenkins, and E. D. Getzoff. 2012. 'Plant UVR8 photoreceptor senses UV-B by tryptophan-mediated disruption of cross-dimer salt bridges', Science, 335: 1492-6.

Christie, J. M., M. Salomon, K. Nozue, M. Wada, and W. R. Briggs. 1999. 'LOV (light, oxygen, or voltage) domains of the blue-light photoreceptor phototropin (nph1): binding sites for the chromophore flavin mononucleotide', Proc Natl Acad Sci U S A, 96: 8779-83.

Christie, J. M., T. E. Swartz, R. A. Bogomolni, and W. R. Briggs. 2002. 'Phototropin LOV domains exhibit distinct roles in regulating photoreceptor function', Plant J, 32: 205-19.

Christie, J. M., H. Yang, G. L. Richter, S. Sullivan, C. E. Thomson, J. Lin, B. Titapiwatanakun, M. Ennis, E. Kaiserli, O. R. Lee, J. Adamec, W. A. Peer, and A. S. Murphy. 2011. 'phot1 inhibition of ABCB19 primes lateral auxin fluxes in the shoot apex required for phototropism', PLoS Biol, 9: e1001076.

Chua, N. H., and P. Bennoun. 1975. 'Thylakoid membrane polypeptides of Chlamydomonas reinhardtii: wild-type and mutant strains deficient in photosystem II reaction center', Proc Natl Acad Sci U S A, 72: 2175-9.

Chua, N. H., K. Matlin, and P. Bennoun. 1975. 'A chlorophyll-protein complex lacking in photosystem I mutants of Chlamydomonas reinhardtii', J Cell Biol, 67: 361-77.

Claros, M. G. 1995. 'MitoProt, a Macintosh application for studying mitochondrial proteins', Comput Appl Biosci, 11: 441-7.

Corellou, F., C. Schwartz, J. P. Motta, B. Djouani-Tahri el, F. Sanchez, and F. Y. Bouget. 2009. 'Clocks in the green lineage: comparative functional analysis of the circadian architecture of the picoeukaryote ostreococcus', Plant Cell, 21: 3436-49.

Crosson, S., and K. Moffat. 2001. 'Structure of a flavin-binding plant photoreceptor domain: insights into light-mediated signal transduction', Proc Natl Acad Sci U S A, 98: 2995-3000.

Crosson, S., S. Rajagopal, and K. Moffat. 2003. 'The LOV domain family: photoresponsive signaling modules coupled to diverse output domains', Biochemistry, 42: 2-10.

Davies, J. P., F. H. Yildiz, and A. R. Grossman. 1999. 'Sac3, an Snf1-like serine/threonine kinase that positively and negatively regulates the responses of Chlamydomonas to sulfur limitation', Plant Cell, 11: 1179-90.

de Carbonnel, M., P. Davis, M. R. Roelfsema, S. Inoue, I. Schepens, P. Lariguet, M. Geisler, K. Shimazaki, R. Hangarter, and C. Fankhauser. 2010. 'The Arabidopsis PHYTOCHROME KINASE SUBSTRATE2 protein is a phototropin signaling element that regulates leaf flattening and leaf positioning', Plant Physiol, 152: 1391-405.

Deininger, W., P. Kroger, U. Hegemann, F. Lottspeich, and P. Hegemann. 1995. 'Chlamyrhodopsin represents a new type of sensory photoreceptor', EMBO J, 14: 5849-58.

Demarsy, E., I. Schepens, K. Okajima, M. Hersch, S. Bergmann, J. Christie, K. Shimazaki, S. Tokutomi, and C. Fankhauser. 2012. 'Phytochrome Kinase Substrate 4 is phosphorylated by the phototropin 1 photoreceptor', EMBO J, 31: 3457-67.

Depauw, F. A., A. Rogato, M. Ribera d'Alcala, and A. Falciatore. 2012. 'Exploring the molecular basis of responses to light in marine diatoms', J Exp Bot, 63: 1575-91.

Devlin, P. F., P. R. Robson, S. R. Patel, L. Goosey, R. A. Sharrock, and G. C. Whitelam. 1999. 'Phytochrome D acts in the shade-avoidance syndrome in Arabidopsis by controlling elongation growth and flowering time', Plant Physiol, 119: 909-15.

Dhokane, D., B. Bhadra, and S. Dasgupta. 2020. 'CRISPR based targeted genome editing of Chlamydomonas reinhardtii using programmed Cas9-gRNA ribonucleoprotein', Mol Biol Rep, 47: 8747-55.

Dinc, E., L. Tian, L. M. Roy, R. Roth, U. Goodenough, and R. Croce. 2016. 'LHCSR1 induces a fast and reversible pH-dependent fluorescence quenching in LHCII in Chlamydomonas reinhardtii cells', Proc Natl Acad Sci U S A, 113: 7673-8.

Duanmu, D., D. Casero, R. M. Dent, S. Gallaher, W. Yang, N. C. Rockwell, S. S. Martin, M. Pellegrini, K. K. Niyogi, S. S. Merchant, A. R. Grossman, and J. C. Lagarias. 2013. 'Retrograde bilin signaling enables Chlamydomonas greening and phototrophic survival', Proc Natl Acad Sci U S A, 110: 3621-6.

Dutcher, S. K. 2014. 'The awesome power of dikaryons for studying flagella and basal bodies in Chlamydomonas reinhardtii', Cytoskeleton (Hoboken), 71: 79-94.

Eitzinger, N., V. Wagner, W. Weisheit, S. Geimer, D. Boness, G. Kreimer, and M. Mittag. 2015. 'Proteomic Analysis of a Fraction with Intact Eyespots of Chlamydomonas reinhardtii and Assignment of Protein Methylation', Front Plant Sci, 6: 1085.

Emanuelsson, O., H. Nielsen, and G. von Heijne. 1999. 'ChloroP, a neural network-based method for predicting chloroplast transit peptides and their cleavage sites', Protein Sci, 8: 978-84.

Engel, B. D., M. Schaffer, L. Kuhn Cuellar, E. Villa, J. M. Plitzko, and W. Baumeister. 2015. 'Native architecture of the Chlamydomonas chloroplast revealed by in situ cryo-electron tomography', Elife, 4.

Erickson, E., S. Wakao, and K. K. Niyogi. 2015. 'Light stress and photoprotection in Chlamydomonas reinhardtii', Plant J, 82: 449-65.

Ermilova, E. V., Z. M. Zalutskaya, K. Huang, and C. F. Beck. 2004. 'Phototropin plays a crucial role in controlling changes in chemotaxis during the initial phase of the sexual life cycle in Chlamydomonas', Planta, 219: 420-7.

Ernst, O. P., D. T. Lodowski, M. Elstner, P. Hegemann, L. S. Brown, and H. Kandori. 2014. 'Microbial and animal rhodopsins: structures, functions, and molecular mechanisms', Chem Rev, 114: 126-63.

Falciatore, A., and C. Bowler. 2005. 'The evolution and function of blue and red light photoreceptors', Curr Top Dev Biol, 68: 317-50.

Fang, W., Y. Si, S. Douglass, D. Casero, S. S. Merchant, M. Pellegrini, I. Ladunga, P. Liu, and M. H. Spalding. 2012. 'Transcriptome-wide changes in Chlamydomonas reinhardtii gene expression regulated by carbon dioxide and the CO2-concentrating mechanism regulator CIA5/CCM1', Plant Cell, 24: 1876-93.

Favory, J. J., A. Stec, H. Gruber, L. Rizzini, A. Oravecz, M. Funk, A. Albert, C. Cloix, G. I. Jenkins, E. J. Oakeley, H. K. Seidlitz, F. Nagy, and R. Ulm. 2009. 'Interaction of COP1 and UVR8 regulates UV-B-induced photomorphogenesis and stress acclimation in Arabidopsis', EMBO J, 28: 591-601.

Fedorov, R., I. Schlichting, E. Hartmann, T. Domratcheva, M. Fuhrmann, and P. Hegemann. 2003. 'Crystal structures and molecular mechanism of a light-induced signaling switch: The Phot-LOV1 domain from Chlamydomonas reinhardtii', Biophys J, 84: 2474-82.

Fernandez, M. B., V. Tossi, L. Lamattina, and R. Cassia. 2016. 'A Comprehensive Phylogeny Reveals Functional Conservation of the UV-B Photoreceptor UVR8 from Green Algae to Higher Plants', Front Plant Sci, 7: 1698.

Ferrante, P., M. Ballottari, G. Bonente, G. Giuliano, and R. Bassi. 2012. 'LHCBM1 and LHCBM2/7 polypeptides, components of major LHCII complex, have distinct functional

roles in photosynthetic antenna system of Chlamydomonas reinhardtii', J Biol Chem, 287: 16276-88.

Flowers, J. M., K. M. Hazzouri, G. M. Pham, U. Rosas, T. Bahmani, B. Khraiwesh, D. R. Nelson, K. Jijakli, R. Abdrabu, E. H. Harris, P. A. Lefebvre, E. F. Hom, K. Salehi-Ashtiani, and M. D. Purugganan. 2015. 'Whole-Genome Resequencing Reveals Extensive Natural Variation in the Model Green Alga Chlamydomonas reinhardtii', Plant Cell, 27: 2353-69.

Ford, M. M., S. R. Lawrence, 2nd, E. G. Werth, E. W. McConnell, and L. M. Hicks. 2020. 'Label-Free Quantitative Phosphoproteomics for Algae', Methods Mol Biol, 2139: 197-211.

Franklin, K. A., and P. H. Quail. 2010. 'Phytochrome functions in Arabidopsis development', J Exp Bot, 61: 11-24.

Franz-Badur, S., A. Penner, S. Strass, S. von Horsten, U. Linne, and L. O. Essen. 2019. 'Structural changes within the bifunctional cryptochrome/photolyase CraCRY upon blue light excitation', Sci Rep, 9: 9896.

Gabilly, S. T., C. R. Baker, S. Wakao, T. Crisanto, K. Guan, K. Bi, E. Guiet, C. R. Guadagno, and K. K. Niyogi. 2019. 'Regulation of photoprotection gene expression in Chlamydomonas by a putative E3 ubiquitin ligase complex and a homolog of CONSTANS', Proc Natl Acad Sci U S A, 116: 17556-62.

Gallaher, S. D., S. T. Fitz-Gibbon, A. G. Glaesener, M. Pellegrini, and S. S. Merchant. 2015. 'Chlamydomonas Genome Resource for Laboratory Strains Reveals a Mosaic of Sequence Variation, Identifies True Strain Histories, and Enables Strain-Specific Studies', Plant Cell, 27: 2335-52.

Gallaher, S. D., S. T. Fitz-Gibbon, D. Strenkert, S. O. Purvine, M. Pellegrini, and S. S. Merchant. 2018. 'High-throughput sequencing of the chloroplast and mitochondrion of Chlamydomonas reinhardtii to generate improved de novo assemblies, analyze expression patterns and transcript speciation, and evaluate diversity among laboratory strains and wild isolates', Plant J, 93: 545-65.

Galvan-Ampudia, C. S., and R. Offringa. 2007. 'Plant evolution: AGC kinases tell the auxin tale', Trends Plant Sci, 12: 541-7.

Gegear, R. J., L. E. Foley, A. Casselman, and S. M. Reppert. 2010. 'Animal cryptochromes mediate magnetoreception by an unconventional photochemical mechanism', Nature, 463: 804-7.

Gehl, K. A., and B. Colman. 1985. 'Effect of External pH on the Internal pH of Chlorella saccharophila', Plant Physiol, 77: 917-21.

Gelvin, S., P. Heizmann, and S. H. Howell. 1977. 'Identification and cloning of the chloroplast gene coding for the large subunit of ribulose-1,5-bisphosphate carboxylase from Chlamydomonas reinhardi', Proc Natl Acad Sci U S A, 74: 3193-7.

Genty, Bernard, Jean-Marie Briantais, and Neil R. Baker. 1989. 'The relationship between the quantum yield of photosynthetic electron transport and quenching of chlorophyll fluorescence', Biochimica et Biophysica Acta (BBA) - General Subjects, 990: 87-92.

Gibson, D. G., L. Young, R. Y. Chuang, J. C. Venter, C. A. Hutchison, 3rd, and H. O. Smith. 2009. 'Enzymatic assembly of DNA molecules up to several hundred kilobases', Nat Methods, 6: 343-5.

Girolomoni, L., S. Cazzaniga, A. Pinnola, F. Perozeni, M. Ballottari, and R. Bassi. 2019. 'LHCSR3 is a nonphotochemical quencher of both photosystems in Chlamydomonas reinhardtii', Proc Natl Acad Sci U S A, 116: 4212-17.

Gonzalez-Ballester, D., D. Casero, S. Cokus, M. Pellegrini, S. S. Merchant, and A. R. Grossman. 2010. 'RNA-seq analysis of sulfur-deprived Chlamydomonas cells reveals aspects of acclimation critical for cell survival', Plant Cell, 22: 2058-84.

Gorman, D. S., and R. P. Levine. 1965. 'Cytochrome f and plastocyanin: their sequence in the photosynthetic electron transport chain of Chlamydomonas reinhardi', Proc Natl Acad Sci U S A, 54: 1665-9.

Govorunova, E. G., K. H. Jung, O. A. Sineshchekov, and J. L. Spudich. 2004. 'Chlamydomonas sensory rhodopsins A and B: cellular content and role in photophobic responses', Biophys J, 86: 2342-9.

Govorunova, E. G., O. A. Sineshchekov, H. Li, and J. L. Spudich. 2017. 'Microbial Rhodopsins: Diversity, Mechanisms, and Optogenetic Applications', Annu Rev Biochem, 86: 845-72.

Greiner, A., S. Kelterborn, H. Evers, G. Kreimer, I. Sizova, and P. Hegemann. 2017. 'Targeting of Photoreceptor Genes in Chlamydomonas reinhardtii via Zinc-Finger Nucleases and CRISPR/Cas9', Plant Cell, 29: 2498-518.

Gushchin, I., and V. Gordeliy. 2018. 'Microbial Rhodopsins', Subcell Biochem, 87: 19-56.

Guzman-Zapata, D., J. M. Sandoval-Vargas, K. S. Macedo-Osorio, E. Salgado-Manjarrez, J. L. Castrejon-Flores, M. D. C. Oliver-Salvador, N. V. Duran-Figueroa, F. Nogue, and J. A. Badillo-Corona. 2019. 'Efficient Editing of the Nuclear APT Reporter Gene in Chlamydomonas reinhardtii via Expression of a CRISPR-Cas9 Module', Int J Mol Sci, 20.

Haga, K., T. Tsuchida-Mayama, M. Yamada, and T. Sakai. 2015. 'Arabidopsis ROOT PHOTOTROPISM2 Contributes to the Adaptation to High-Intensity Light in Phototropic Responses', Plant Cell, 27: 1098-112.

Harada, A., A. Takemiya, S. Inoue, T. Sakai, and K. Shimazaki. 2013. 'Role of RPT2 in leaf positioning and flattening and a possible inhibition of phot2 signaling by phot1', Plant Cell Physiol, 54: 36-47.

Harper, S. M., L. C. Neil, and K. H. Gardner. 2003. 'Structural basis of a phototropin light switch', Science, 301: 1541-4.

Hart, J. E., S. Sullivan, P. Hermanowicz, J. Petersen, L. A. Diaz-Ramos, D. J. Hoey, J. Labuz, and J. M. Christie. 2019. 'Engineering the phototropin photocycle improves photoreceptor performance and plant biomass production', Proc Natl Acad Sci U S A, 116: 12550-57.

Harz, Hartmann, Christina Nonnengasser, Peter Hegemann, C. Brownlee, and Dale Sanders. 1992. 'The photoreceptor current of the green alga Chlamydomonas', Philosophical Transactions of the Royal Society of London. Series B: Biological Sciences, 338: 39-52.

Hegemann, P. 1997. 'Vision in microalgae', Planta, 203: 265-74.

Heijde, M., and R. Ulm. 2012. 'UV-B photoreceptor-mediated signalling in plants', Trends Plant Sci, 17: 230-7.

Hiyama, A., A. Takemiya, S. Munemasa, E. Okuma, N. Sugiyama, Y. Tada, Y. Murata, and K. I. Shimazaki. 2017. 'Blue light and CO2 signals converge to regulate light-induced stomatal opening', Nat Commun, 8: 1284.

Huang, C., S. Wang, L. Chen, C. Lemieux, C. Otis, M. Turmel, and X. Q. Liu. 1994. 'The Chlamydomonas chloroplast clpP gene contains translated large insertion sequences and is essential for cell growth', Mol Gen Genet, 244: 151-9.

Huang, K., T. Merkle, and C. F. Beck. 2002. 'Isolation and characterization of a Chlamydomonas gene that encodes a putative blue-light photoreceptor of the phototropin family', Physiol Plant, 115: 613-22.

Huang, X., X. Ouyang, P. Yang, O. S. Lau, L. Chen, N. Wei, and X. W. Deng. 2013. 'Conversion from CUL4-based COP1-SPA E3 apparatus to UVR8-COP1-SPA complexes underlies a distinct biochemical function of COP1 under UV-B', Proc Natl Acad Sci U S A, 110: 16669-74.

Hubbard, R., and A. Kropf. 1958. 'The Action of Light on Rhodopsin', Proc Natl Acad Sci U S A, 44: 130-9.

Im, C. S., S. Eberhard, K. Huang, C. F. Beck, and A. R. Grossman. 2006. 'Phototropin involvement in the expression of genes encoding chlorophyll and carotenoid biosynthesis enzymes and LHC apoproteins in Chlamydomonas reinhardtii', Plant J, 48: 1-16.

Inada, S., M. Ohgishi, T. Mayama, K. Okada, and T. Sakai. 2004. 'RPT2 is a signal transducer involved in phototropic response and stomatal opening by association with phototropin 1 in Arabidopsis thaliana', Plant Cell, 16: 887-96.

Inoue, H., H. Nojima, and H. Okayama. 1990. 'High efficiency transformation of Escherichia coli with plasmids', Gene, 96: 23-8.

Inoue, K., R. Nishihama, and T. Kohchi. 2017. 'Evolutionary origin of phytochrome responses and signaling in land plants', Plant Cell Environ, 40: 2502-08.

Inoue, S., A. Takemiya, and K. Shimazaki. 2010. 'Phototropin signaling and stomatal opening as a model case', Curr Opin Plant Biol, 13: 587-93.

Ishizuka, T., M. Kakuda, R. Araki, and H. Yawo. 2006. 'Kinetic evaluation of photosensitivity in genetically engineered neurons expressing green algae light-gated channels', Neurosci Res, 54: 85-94.

Itakura, A. K., K. X. Chan, N. Atkinson, L. Pallesen, L. Wang, G. Reeves, W. Patena, O. Caspari, R. Roth, U. Goodenough, A. J. McCormick, H. Griffiths, and M. C. Jonikas. 2019. 'A Rubisco-binding protein is required for normal pyrenoid number and starch sheath morphology in Chlamydomonas reinhardtii', Proc Natl Acad Sci U S A, 116: 18445-54.

Jaeger, Daniel, Thomas Baier, and Kyle J. Lauersen. 2019. 'Intronserter, an advanced online tool for design of intron containing transgenes', Algal Research, 42: 101588.

Jinkerson, R. E., and M. C. Jonikas. 2015. 'Molecular techniques to interrogate and edit the Chlamydomonas nuclear genome', Plant J, 82: 393-412.

Johnson, E., M. Bradley, N. P. Harberd, and G. C. Whitelam. 1994. 'Photoresponses of Light-Grown phyA Mutants of Arabidopsis (Phytochrome A Is Required for the Perception of Daylength Extensions)', Plant Physiol, 105: 141-49.

Jumper, John, Richard Evans, Alexander Pritzel, Tim Green, Michael Figurnov, Olaf Ronneberger, Kathryn Tunyasuvunakool, Russ Bates, Augustin Žídek, Anna Potapenko, Alex Bridgland, Clemens Meyer, Simon A. A. Kohl, Andrew J. Ballard, Andrew Cowie, Bernardino Romera-Paredes, Stanislav Nikolov, Rishub Jain, Jonas Adler, Trevor Back, Stig Petersen, David Reiman, Ellen Clancy, Michal Zielinski, Martin Steinegger, Michalina Pacholska, Tamas Berghammer, Sebastian Bodenstein, David Silver, Oriol Vinyals, Andrew W. Senior, Koray Kavukcuoglu, Pushmeet Kohli, and Demis Hassabis. 2021. 'Highly accurate protein structure prediction with AlphaFold', Nature, 596: 583-89.

Kagawa, T., and M. Wada. 2002. 'Blue light-induced chloroplast relocation', Plant Cell Physiol, 43: 367-71.

Kaiserli, E., and G. I. Jenkins. 2007. 'UV-B promotes rapid nuclear translocation of the Arabidopsis UV-B specific signaling component UVR8 and activates its function in the nucleus', Plant Cell, 19: 2662-73.

Kaiserli, E., S. Sullivan, M. A. Jones, K. A. Feeney, and J. M. Christie. 2009. 'Domain swapping to assess the mechanistic basis of Arabidopsis phototropin 1 receptor kinase activation and endocytosis by blue light', Plant Cell, 21: 3226-44.

Kang, S., S. Jeon, S. Kim, Y. K. Chang, and Y. C. Kim. 2020. 'Development of a pVEC peptide-based ribonucleoprotein (RNP) delivery system for genome editing using CRISPR/Cas9 in Chlamydomonas reinhardtii', Sci Rep, 10: 22158.

Kasahara, M., T. E. Swartz, M. A. Olney, A. Onodera, N. Mochizuki, H. Fukuzawa, E. Asamizu, S. Tabata, H. Kanegae, M. Takano, J. M. Christie, A. Nagatani, and W. R. Briggs. 2002. 'Photochemical properties of the flavin mononucleotide-binding domains of the phototropins from Arabidopsis, rice, and Chlamydomonas reinhardtii', Plant Physiol, 129: 762-73.

Kateriya, S., G. Nagel, E. Bamberg, and P. Hegemann. 2004. '"Vision" in single-celled algae', News Physiol Sci, 19: 133-7.

Kim, E., S. Akimoto, R. Tokutsu, M. Yokono, and J. Minagawa. 2017. 'Fluorescence lifetime analyses reveal how the high light-responsive protein LHCSR3 transforms PSII light-harvesting complexes into an energy-dissipative state', J Biol Chem, 292: 18951-60.

Kim, J., S. Lee, K. Baek, and E. Jin. 2020. 'Site-Specific Gene Knock-Out and On-Site Heterologous Gene Overexpression in Chlamydomonas reinhardtii via a CRISPR-Cas9-Mediated Knock-in Method', Front Plant Sci, 11: 306.

Kinoshita, T., T. Emi, M. Tominaga, K. Sakamoto, A. Shigenaga, M. Doi, and K. Shimazaki. 2003. 'Blue-light- and phosphorylation-dependent binding of a 14-3-3 protein to phototropins in stomatal guard cells of broad bean', Plant Physiol, 133: 1453-63.

Krauss, U., B. Q. Minh, A. Losi, W. Gartner, T. Eggert, A. von Haeseler, and K. E. Jaeger. 2009. 'Distribution and phylogeny of light-oxygen-voltage-blue-light-signaling proteins in the three kingdoms of life', J Bacteriol, 191: 7234-42.

Krogh, A., B. Larsson, G. von Heijne, and E. L. Sonnhammer. 2001. 'Predicting transmembrane protein topology with a hidden Markov model: application to complete genomes', J Mol Biol, 305: 567-80.

Kroth, P. G., C. Wilhelm, and T. Kottke. 2017. 'An update on aureochromes: Phylogeny - mechanism - function', J Plant Physiol, 217: 20-26.

Kume, K., M. J. Zylka, S. Sriram, L. P. Shearman, D. R. Weaver, X. Jin, E. S. Maywood, M. H. Hastings, and S. M. Reppert. 1999. 'mCRY1 and mCRY2 are essential components of the negative limb of the circadian clock feedback loop', Cell, 98: 193-205.

Lariguet, P., I. Schepens, D. Hodgson, U. V. Pedmale, M. Trevisan, C. Kami, M. de Carbonnel, J. M. Alonso, J. R. Ecker, E. Liscum, and C. Fankhauser. 2006. 'PHYTOCHROME KINASE SUBSTRATE 1 is a phototropin 1 binding protein required for phototropism', Proc Natl Acad Sci U S A, 103: 10134-9.

Ledford, H. K., I. Baroli, J. W. Shin, B. B. Fischer, R. I. Eggen, and K. K. Niyogi. 2004. 'Comparative profiling of lipid-soluble antioxidants and transcripts reveals two phases of photo-oxidative stress in a xanthophyll-deficient mutant of Chlamydomonas reinhardtii', Mol Genet Genomics, 272: 470-9.

Lee, D. Y., and O. Fiehn. 2008. 'High quality metabolomic data for Chlamydomonas reinhardtii', Plant Methods, 4: 7.

Levine, R. P. 1960. 'Genetic Control of Photosynthesis in Chlamydomonas Reinhardi', Proc Natl Acad Sci U S A, 46: 972-8.

Li, F. W., C. J. Rothfels, M. Melkonian, J. C. Villarreal, D. W. Stevenson, S. W. Graham, G. K. Wong, S. Mathews, and K. M. Pryer. 2015. 'The origin and evolution of phototropins', Front Plant Sci, 6: 637.

Li, X., D. V. Gutierrez, M. G. Hanson, J. Han, M. D. Mark, H. Chiel, P. Hegemann, L. T. Landmesser, and S. Herlitze. 2005. 'Fast noninvasive activation and inhibition of neural and network activity by vertebrate rhodopsin and green algae channelrhodopsin', Proc Natl Acad Sci U S A, 102: 17816-21.

Li, X., W. Patena, F. Fauser, R. E. Jinkerson, S. Saroussi, M. T. Meyer, N. Ivanova, J. M. Robertson, R. Yue, R. Zhang, J. Vilarrasa-Blasi, T. M. Wittkopp, S. Ramundo, S. R. Blum, A. Goh, M. Laudon, T. Srikumar, P. A. Lefebvre, A. R. Grossman, and M. C. Jonikas. 2019. 'A genome-wide algal mutant library and functional screen identifies genes required for eukaryotic photosynthesis', Nat Genet, 51: 627-35.

Li, X., R. Zhang, W. Patena, S. S. Gang, S. R. Blum, N. Ivanova, R. Yue, J. M. Robertson, P. A. Lefebvre, S. T. Fitz-Gibbon, A. R. Grossman, and M. C. Jonikas. 2016. 'An Indexed, Mapped Mutant Library Enables Reverse Genetics Studies of Biological Processes in Chlamydomonas reinhardtii', Plant Cell, 28: 367-87.

Liguori, N., V. Novoderezhkin, L. M. Roy, R. van Grondelle, and R. Croce. 2016. 'Excitation dynamics and structural implication of the stress-related complex LHCSR3 from the green alga Chlamydomonas reinhardtii', Biochim Biophys Acta, 1857: 1514-23.

Liguori, N., L. M. Roy, M. Opacic, G. Durand, and R. Croce. 2013. 'Regulation of light harvesting in the green alga Chlamydomonas reinhardtii: the C-terminus of LHCSR is the knob of a dimmer switch', J Am Chem Soc, 135: 18339-42.

Lin, J. R., and J. Hu. 2013. 'SeqNLS: nuclear localization signal prediction based on frequent pattern mining and linear motif scoring', PLoS One, 8: e76864.

Liscum, E., and R. P. Hangarter. 1993. 'Genetic Evidence That the Red-Absorbing Form of Phytochrome B Modulates Gravitropism in Arabidopsis thaliana', Plant Physiol, 103: 15-19.

Mackinder, L. C., M. T. Meyer, T. Mettler-Altmann, V. K. Chen, M. C. Mitchell, O. Caspari, E. S. Freeman Rosenzweig, L. Pallesen, G. Reeves, A. Itakura, R. Roth, F. Sommer, S. Geimer, T. Muhlhaus, M. Schroda, U. Goodenough, M. Stitt, H. Griffiths, and M. C. Jonikas. 2016. 'A repeat protein links Rubisco to form the eukaryotic carbon-concentrating organelle', Proc Natl Acad Sci U S A, 113: 5958-63.

Maruyama, S., R. Tokutsu, and J. Minagawa. 2014. 'Transcriptional regulation of the stress-responsive light harvesting complex genes in Chlamydomonas reinhardtii', Plant Cell Physiol, 55: 1304-10.

Matsuo, T., T. Iida, A. Ohmura, M. Gururaj, D. Kato, R. Mutoh, K. Ihara, and M. Ishiura. 2020. 'The role of ROC75 as a daytime component of the circadian oscillator in Chlamydomonas reinhardtii', PLoS Genet, 16: e1008814.

Maxwell, K., and G. N. Johnson. 2000. 'Chlorophyll fluorescence--a practical guide', J Exp Bot, 51: 659-68.

Merchant, S. S., S. E. Prochnik, O. Vallon, E. H. Harris, S. J. Karpowicz, G. B. Witman, A. Terry, A. Salamov, L. K. Fritz-Laylin, L. Marechal-Drouard, W. F. Marshall, L. H. Qu, D. R. Nelson, A. A. Sanderfoot, M. H. Spalding, V. V. Kapitonov, Q. Ren, P. Ferris, E. Lindquist, H. Shapiro, S. M. Lucas, J. Grimwood, J. Schmutz, P. Cardol, H. Cerutti, G. Chanfreau, C. L. Chen, V. Cognat, M. T. Croft, R. Dent, S. Dutcher, E. Fernandez, H. Fukuzawa, D. Gonzalez-Ballester, D. Gonzalez-Halphen, A. Hallmann, M. Hanikenne, M. Hippler, W. Inwood, K. Jabbari, M. Kalanon, R. Kuras, P. A. Lefebvre, S. D. Lemaire, A. V. Lobanov, M. Lohr, A. Manuell, I. Meier, L. Mets, M. Mittag, T. Mittelmeier, J. V. Moroney, J. Moseley, C. Napoli, A. M. Nedelcu, K. Niyogi, S. V. Novoselov, I. T. Paulsen, G. Pazour, S. Purton, J. P. Ral, D. M. Riano-Pachon, W. Riekhof, L. Rymarquis, M. Schroda, D. Stern, J. Umen, R. Willows, N. Wilson, S. L. Zimmer, J. Allmer, J. Balk, K. Bisova, C. J. Chen, M. Elias, K. Gendler, C. Hauser, M. R. Lamb, H. Ledford, J. C. Long, J. Minagawa, M. D. Page, J. Pan, W. Pootakham, S. Roje, A. Rose, E. Stahlberg, A. M. Terauchi, P. Yang, S. Ball, C. Bowler, C. L. Dieckmann, V. N. Gladyshev, P. Green, R. Jorgensen, S. Mayfield, B. Mueller-Roeber, S. Rajamani, R. T. Sayre, P. Brokstein, I. Dubchak, D. Goodstein, L. Hornick, Y. W. Huang, J. Jhaveri, Y. Luo, D. Martinez, W. C. Ngau, B. Otillar, A. Poliakov, A. Porter, L. Szajkowski, G. Werner, K. Zhou, I. V. Grigoriev, D. S. Rokhsar, and A. R. Grossman. 2007. 'The Chlamydomonas genome reveals the evolution of key animal and plant functions', Science, 318: 245-50.

Michelet, L., M. Zaffagnini, S. Morisse, F. Sparla, M. E. Perez-Perez, F. Francia, A. Danon, C. H. Marchand, S. Fermani, P. Trost, and S. D. Lemaire. 2013. 'Redox regulation of the Calvin-Benson cycle: something old, something new', Front Plant Sci, 4: 470.

Miller, R., G. Wu, R. R. Deshpande, A. Vieler, K. Gartner, X. Li, E. R. Moellering, S. Zauner, A. J. Cornish, B. Liu, B. Bullard, B. B. Sears, M. H. Kuo, E. L. Hegg, Y. Shachar-Hill, S. H. Shiu, and C. Benning. 2010. 'Changes in transcript abundance in Chlamydomonas reinhardtii following nitrogen deprivation predict diversion of metabolism', Plant Physiol, 154: 1737-52.

Miura, K., T. Yamano, S. Yoshioka, T. Kohinata, Y. Inoue, F. Taniguchi, E. Asamizu, Y. Nakamura, S. Tabata, K. T. Yamato, K. Ohyama, and H. Fukuzawa. 2004. 'Expression profiling-based identification of CO2-responsive genes regulated by CCM1 controlling a carbon-concentrating mechanism in Chlamydomonas reinhardtii', Plant Physiol, 135: 1595-607.

Mockler, T., H. Yang, X. Yu, D. Parikh, Y. C. Cheng, S. Dolan, and C. Lin. 2003. 'Regulation of photoperiodic flowering by Arabidopsis photoreceptors', Proc Natl Acad Sci U S A, 100: 2140-5.

Morel, André. 1988. 'Optical modeling of the upper ocean in relation to its biogenous matter content (case I waters)', Journal of Geophysical Research, 93: 10749-68.

Moroney, J. V., and R. A. Ynalvez. 2007. 'Proposed carbon dioxide concentrating mechanism in Chlamydomonas reinhardtii', Eukaryot Cell, 6: 1251-9.

Moseley, J. L., C. W. Chang, and A. R. Grossman. 2006. 'Genome-based approaches to understanding phosphorus deprivation responses and PSR1 control in Chlamydomonas reinhardtii', Eukaryot Cell, 5: 26-44.

Motchoulski, A., and E. Liscum. 1999. 'Arabidopsis NPH3: A NPH1 photoreceptor-interacting protein essential for phototropism', Science, 286: 961-4.

Muhlhaus, T., J. Weiss, D. Hemme, F. Sommer, and M. Schroda. 2011. 'Quantitative shotgun proteomics using a uniform (1)(5)N-labeled standard to monitor proteome dynamics in time course experiments reveals new insights into the heat stress response of Chlamydomonas reinhardtii', Mol Cell Proteomics, 10: M110 004739.

Muller, P., X. P. Li, and K. K. Niyogi. 2001. 'Non-photochemical quenching. A response to excess light energy', Plant Physiol, 125: 1558-66.

Nagatani, A., J. W. Reed, and J. Chory. 1993. 'Isolation and Initial Characterization of Arabidopsis Mutants That Are Deficient in Phytochrome A', Plant Physiol, 102: 269-77.

Nagel, Georg, Doris Ollig, Markus Fuhrmann, Suneel Kateriya, Anna Maria Musti, Ernst Bamberg, and Peter Hegemann. 2002. 'Channelrhodopsin-1: A Light-Gated Proton Channel in Green Algae', Science, 296: 2395-98.

Nagel, Georg, Tanjef Szellas, Wolfram Huhn, Suneel Kateriya, Nona Adeishvili, Peter Berthold, Doris Ollig, Peter Hegemann, and Ernst Bamberg. 2003. 'Channelrhodopsin-2, a directly light-gated cation-selective membrane channel', Proceedings of the National Academy of Sciences, 100: 13940-45.

Nakasako, M., K. Zikihara, D. Matsuoka, H. Katsura, and S. Tokutomi. 2008. 'Structural basis of the LOV1 dimerization of Arabidopsis phototropins 1 and 2', J Mol Biol, 381: 718-33.

Naumann, B., A. Busch, J. Allmer, E. Ostendorf, M. Zeller, H. Kirchhoff, and M. Hippler. 2007. 'Comparative quantitative proteomics to investigate the remodeling of bioenergetic pathways under iron deficiency in Chlamydomonas reinhardtii', Proteomics, 7: 3964-79.

Nelson, D. C., J. Lasswell, L. E. Rogg, M. A. Cohen, and B. Bartel. 2000. 'FKF1, a clock-controlled gene that regulates the transition to flowering in Arabidopsis', Cell, 101: 331-40.

Neupert, J., S. D. Gallaher, Y. Lu, D. Strenkert, N. Segal, R. Barahimipour, S. T. Fitz-Gibbon, M. Schroda, S. S. Merchant, and R. Bock. 2020. 'An epigenetic gene silencing pathway selectively acting on transgenic DNA in the green alga Chlamydomonas', Nat Commun, 11: 6269.

Nguyen, A. V., J. Toepel, S. Burgess, A. Uhmeyer, O. Blifernez, A. Doebbe, B. Hankamer, P. Nixon, L. Wobbe, and O. Kruse. 2011. 'Time-course global expression profiles of Chlamydomonas reinhardtii during photo-biological H(2) production', PLoS One, 6: e29364.

Niyogi, K. K., A. R. Grossman, and O. Bjorkman. 1998. 'Arabidopsis mutants define a central role for the xanthophyll cycle in the regulation of photosynthetic energy conversion', Plant Cell, 10: 1121-34.

Nordhues, A., M. A. Schottler, A. K. Unger, S. Geimer, S. Schonfelder, S. Schmollinger, M. Rutgers, G. Finazzi, B. Soppa, F. Sommer, T. Muhlhaus, T. Roach, A. Krieger-Liszkay, H. Lokstein, J. L. Crespo, and M. Schroda. 2012. 'Evidence for a role of VIPP1 in the structural organization of the photosynthetic apparatus in Chlamydomonas', Plant Cell, 24: 637-59.

Okajima, K. 2016. 'Molecular mechanism of phototropin light signaling', J Plant Res, 129: 149-57.

Okajima, K., Y. Aihara, Y. Takayama, M. Nakajima, S. Kashojiya, T. Hikima, T. Oroguchi, A. Kobayashi, Y. Sekiguchi, M. Yamamoto, T. Suzuki, A. Nagatani, M. Nakasako, and S. Tokutomi. 2014. 'Light-induced conformational changes of LOV1 (light oxygen voltage-sensing domain 1) and LOV2 relative to the kinase domain and regulation of kinase activity in Chlamydomonas phototropin', J Biol Chem, 289: 413-22.

Okajima, K., S. Kashojiya, and S. Tokutomi. 2012. 'Photosensitivity of kinase activation by blue light involves the lifetime of a cysteinyl-flavin adduct intermediate, S390, in the photoreaction cycle of the LOV2 domain in phototropin, a plant blue light receptor', J Biol Chem, 287: 40972-81.

Onodera, A., S. G. Kong, M. Doi, K. Shimazaki, J. Christie, N. Mochizuki, and A. Nagatani. 2005. 'Phototropin from Chlamydomonas reinhardtii is functional in Arabidopsis thaliana', Plant Cell Physiol, 46: 367-74.

Oravecz, A., A. Baumann, Z. Mate, A. Brzezinska, J. Molinier, E. J. Oakeley, E. Adam, E. Schafer, F. Nagy, and R. Ulm. 2006. 'CONSTITUTIVELY PHOTOMORPHOGENIC1 is required for the UV-B response in Arabidopsis', Plant Cell, 18: 1975-90.

Palczewski, K. 2006. 'G protein-coupled receptor rhodopsin', Annu Rev Biochem, 75: 743-67.

Park, R. V., H. Asbury, and S. M. Miller. 2020. 'Modification of a Chlamydomonas reinhardtii CRISPR/Cas9 transformation protocol for use with widely available electroporation equipment', MethodsX, 7: 100855.

Pazour, G. J., N. Agrin, J. Leszyk, and G. B. Witman. 2005. 'Proteomic analysis of a eukaryotic cilium', J Cell Biol, 170: 103-13.

Pedmale, U. V., and E. Liscum. 2007. 'Regulation of phototropic signaling in Arabidopsis via phosphorylation state changes in the phototropin 1-interacting protein NPH3', J Biol Chem, 282: 19992-20001.

Peers, G., T. B. Truong, E. Ostendorf, A. Busch, D. Elrad, A. R. Grossman, M. Hippler, and K. K. Niyogi. 2009. 'An ancient light-harvesting protein is critical for the regulation of algal photosynthesis', Nature, 462: 518-21.

Perlaza, K., H. Toutkoushian, M. Boone, M. Lam, M. Iwai, M. C. Jonikas, P. Walter, and S. Ramundo. 2019. 'The Mars1 kinase confers photoprotection through signaling in the chloroplast unfolded protein response', Elife, 8.

Perozeni, F., S. Cazzaniga, and M. Ballottari. 2019. 'In vitro and in vivo investigation of chlorophyll binding sites involved in non-photochemical quenching in Chlamydomonas reinhardtii', Plant Cell Environ, 42: 2522-35.

Petroutsos, D., A. Busch, I. Janssen, K. Trompelt, S. V. Bergner, S. Weinl, M. Holtkamp, U. Karst, J. Kudla, and M. Hippler. 2011. 'The chloroplast calcium sensor CAS is required for photoacclimation in Chlamydomonas reinhardtii', Plant Cell, 23: 2950-63.

Petroutsos, D., R. Tokutsu, S. Maruyama, S. Flori, A. Greiner, L. Magneschi, L. Cusant, T. Kottke, M. Mittag, P. Hegemann, G. Finazzi, and J. Minagawa. 2016. 'A blue-light photoreceptor mediates the feedback regulation of photosynthesis', Nature, 537: 563-66.

Pfeifer, A., T. Mathes, Y. Lu, P. Hegemann, and T. Kottke. 2010. 'Blue light induces global and localized conformational changes in the kinase domain of full-length phototropin', Biochemistry, 49: 1024-32.

Picariello, T., Y. Hou, T. Kubo, N. A. McNeill, H. A. Yanagisawa, T. Oda, and G. B. Witman. 2020. 'TIM, a targeted insertional mutagenesis method utilizing CRISPR/Cas9 in Chlamydomonas reinhardtii', PLoS One, 15: e0232594.

Piccioni, R. G., P. Bennoun, and N. H. Chua. 1981. 'A nuclear mutant of Chlamydomonas reinhardtii defective in photosynthetic photophosphorylation. Characterization of the algal coupling factor ATPase', Eur J Biochem, 117: 93-102.

Polukhina, I., R. Fristedt, E. Dinc, P. Cardol, and R. Croce. 2016. 'Carbon Supply and Photoacclimation Cross Talk in the Green Alga Chlamydomonas reinhardtii', Plant Physiol, 172: 1494-505.

Porra, R. J., W. A. Thompson, and P. E. Kriedemann. 1989. 'Determination of accurate extinction coefficients and simultaneous equations for assaying chlorophylls a and b extracted with four different solvents: verification of the concentration of chlorophyll standards by atomic absorption spectroscopy', Biochimica et Biophysica Acta (BBA) - Bioenergetics, 975: 384-94.

Prochnik, S. E., J. Umen, A. M. Nedelcu, A. Hallmann, S. M. Miller, I. Nishii, P. Ferris, A. Kuo, T. Mitros, L. K. Fritz-Laylin, U. Hellsten, J. Chapman, O. Simakov, S. A. Rensing, A. Terry, J. Pangilinan, V. Kapitonov, J. Jurka, A. Salamov, H. Shapiro, J. Schmutz, J. Grimwood, E. Lindquist, S. Lucas, I. V. Grigoriev, R. Schmitt, D. Kirk, and D. S. Rokhsar. 2010. 'Genomic analysis of organismal complexity in the multicellular green alga Volvox carteri', Science, 329: 223-6.

Ramundo, S., D. Casero, T. Muhlhaus, D. Hemme, F. Sommer, M. Crevecoeur, M. Rahire, M. Schroda, J. Rusch, U. Goodenough, M. Pellegrini, M. E. Perez-Perez, J. L. Crespo, O. Schaad, N. Civic, and J. D. Rochaix. 2014. 'Conditional Depletion of the Chlamydomonas Chloroplast ClpP Protease Activates Nuclear Genes Involved in Autophagy and Plastid Protein Quality Control', Plant Cell, 26: 2201-22.

Redekop, P., N. Rothhausen, N. Rothhausen, M. Melzer, L. Mosebach, E. Dulger, A. Bovdilova, S. Caffarri, M. Hippler, and P. Jahns. 2020. 'PsbS contributes to photoprotection in Chlamydomonas reinhardtii independently of energy dissipation', Biochim Biophys Acta Bioenerg, 1861: 148183.

Redekop, Petra, Emanuel Sanz-Luque, Yizhong Yuan, Gaelle Villain, Dimitris Petroutsos, and Arthur R. Grossman. 2021. 'Transcriptional regulation of photoprotection in dark-to-light transition - more than just a matter of excess light energy', bioRxiv: 2021.10.23.463292.

Reed, J. W., P. Nagpal, D. S. Poole, M. Furuya, and J. Chory. 1993. 'Mutations in the gene for the red/far-red light receptor phytochrome B alter cell elongation and physiological responses throughout Arabidopsis development', Plant Cell, 5: 147-57.

Reisdorph, N. A., and G. D. Small. 2004. 'The CPH1 gene of Chlamydomonas reinhardtii encodes two forms of cryptochrome whose levels are controlled by light-induced proteolysis', Plant Physiol, 134: 1546-54.

Richard, C., H. Ouellet, and M. Guertin. 2000. 'Characterization of the LI818 polypeptide from the green unicellular alga Chlamydomonas reinhardtii', Plant Mol Biol, 42: 303-16.

Ritz, T., S. Adem, and K. Schulten. 2000. 'A model for photoreceptor-based magnetoreception in birds', Biophys J, 78: 707-18.

Rizzini, L., J. J. Favory, C. Cloix, D. Faggionato, A. O'Hara, E. Kaiserli, R. Baumeister, E. Schafer, F. Nagy, G. I. Jenkins, and R. Ulm. 2011. 'Perception of UV-B by the Arabidopsis UVR8 protein', Science, 332: 103-6.

Robson, P., G. C. Whitelam, and H. Smith. 1993. 'Selected Components of the Shade-Avoidance Syndrome Are Displayed in a Normal Manner in Mutants of Arabidopsis thaliana and Brassica rapa Deficient in Phytochrome B', Plant Physiol, 102: 1179-84.

Rockwell, N. C., and J. C. Lagarias. 2010. 'A brief history of phytochromes', Chemphyschem, 11: 1172-80.

Rockwell, N. C., Y. S. Su, and J. C. Lagarias. 2006. 'Phytochrome structure and signaling mechanisms', Annu Rev Plant Biol, 57: 837-58.

Rredhi, A., J. Petersen, M. Schubert, W. Li, S. Oldemeyer, W. Li, M. Westermann, V. Wagner, T. Kottke, and M. Mittag. 2021. 'DASH cryptochrome 1, a UV-A receptor, balances the photosynthetic machinery of Chlamydomonas reinhardtii', New Phytol, 232: 610-24.

Ruiz-Sola, M. Águila, Serena Flori, Yizhong Yuan, Gaelle Villain, Emanuel Sanz-Luque, Petra Redekop, Ryutaro Tokutsu, Anika Kueken, Angeliki Tsichla, Georgios Kepesidis, Guillaume Allorent, Marius Arend, Fabrizio Iacono, Giovanni Finazzi, Michael Hippler, Zoran Nikoloski, Jun Minagawa, Arthur R. Grossman, and Dimitris Petroutsos. 2021. 'Photoprotection is regulated by light-independent CO₂ availability', bioRxiv: 2021.10.23.465040.

Sager, R., and G. E. Palade. 1957. 'Structure and development of the chloroplast in Chlamydomonas. I. The normal green cell', J Biophys Biochem Cytol, 3: 463-88.

Sakamoto, K., and W. R. Briggs. 2002. 'Cellular and subcellular localization of phototropin 1', Plant Cell, 14: 1723-35.

Sali, A., and T. L. Blundell. 1993. 'Comparative protein modelling by satisfaction of spatial restraints', J Mol Biol, 234: 779-815.

Salome, P. A., and S. S. Merchant. 2019. 'A Series of Fortunate Events: Introducing Chlamydomonas as a Reference Organism', Plant Cell, 31: 1682-707.

Salomon, M., J. M. Christie, E. Knieb, U. Lempert, and W. R. Briggs. 2000. 'Photochemical and mutational analysis of the FMN-binding domains of the plant blue light receptor, phototropin', Biochemistry, 39: 9401-10.

Salomon, M., E. Knieb, T. von Zeppelin, and W. Rudiger. 2003. 'Mapping of low- and high-fluence autophosphorylation sites in phototropin 1', Biochemistry, 42: 4217-25.

Schloss, J. A. 1990. 'A Chlamydomonas gene encodes a G protein beta subunit-like polypeptide', Mol Gen Genet, 221: 443-52.

Schmidt, G. W., K. S. Matlin, and N. H. Chua. 1977. 'A rapid procedure for selective enrichment of photosynthetic electron transport mutants', Proc Natl Acad Sci U S A, 74: 610-4.

Schnabel, J., P. Hombach, T. Waksman, G. Giuriani, J. Petersen, and J. M. Christie. 2018. 'A chemical genetic approach to engineer phototropin kinases for substrate labeling', J Biol Chem, 293: 5613-23.

Schroda, M. 2019. 'Good News for Nuclear Transgene Expression in Chlamydomonas', Cells, 8.

Schultz, T. F., T. Kiyosue, M. Yanovsky, M. Wada, and S. A. Kay. 2001. 'A role for LKP2 in the circadian clock of Arabidopsis', Plant Cell, 13: 2659-70.

Schwartz, D., and S. P. Gygi. 2005. 'An iterative statistical approach to the identification of protein phosphorylation motifs from large-scale data sets', Nat Biotechnol, 23: 1391-8.

Semchonok, D. A., K. N. Sathish Yadav, P. Xu, B. Drop, R. Croce, and E. J. Boekema. 2017. 'Interaction between the photoprotective protein LHCSR3 and C2S2 Photosystem II supercomplex in Chlamydomonas reinhardtii', Biochim Biophys Acta Bioenerg, 1858: 379-85.

Shin, S. E., J. M. Lim, H. G. Koh, E. K. Kim, N. K. Kang, S. Jeon, S. Kwon, W. S. Shin, B. Lee, K. Hwangbo, J. Kim, S. H. Ye, J. Y. Yun, H. Seo, H. M. Oh, K. J. Kim, J. S. Kim, W. J. Jeong, Y. K. Chang, and B. R. Jeong. 2016. 'CRISPR/Cas9-induced knockout and knock-in mutations in Chlamydomonas reinhardtii', Sci Rep, 6: 27810.

Shin, Y. S., J. Jeong, T. H. T. Nguyen, J. Y. H. Kim, E. Jin, and S. J. Sim. 2019. 'Targeted knockout of phospholipase A2 to increase lipid productivity in Chlamydomonas reinhardtii for biodiesel production', Bioresour Technol, 271: 368-74.

Shinomura, T., A. Nagatani, H. Hanzawa, M. Kubota, M. Watanabe, and M. Furuya. 1996. 'Action spectra for phytochrome A- and B-specific photoinduction of seed germination in Arabidopsis thaliana', Proc Natl Acad Sci U S A, 93: 8129-33.

Sineshchekov, O. A., K. H. Jung, and J. L. Spudich. 2002. 'Two rhodopsins mediate phototaxis to low- and high-intensity light in Chlamydomonas reinhardtii', Proc Natl Acad Sci U S A, 99: 8689-94.

Sinetova, M. A., E. V. Kupriyanova, A. G. Markelova, S. I. Allakhverdiev, and N. A. Pronina. 2012. 'Identification and functional role of the carbonic anhydrase Cah3 in thylakoid membranes of pyrenoid of Chlamydomonas reinhardtii', Biochim Biophys Acta, 1817: 1248-55.

Sizova, I., S. Kelterborn, V. Verbenko, S. Kateriya, and P. Hegemann. 2021. 'Chlamydomonas POLQ is necessary for CRISPR/Cas9-mediated gene targeting', G3 (Bethesda).

Somers, D. E., T. F. Schultz, M. Milnamow, and S. A. Kay. 2000. 'ZEITLUPE encodes a novel clock-associated PAS protein from Arabidopsis', Cell, 101: 319-29.

Somers, D. E., R. A. Sharrock, J. M. Tepperman, and P. H. Quail. 1991. 'The hy3 Long Hypocotyl Mutant of Arabidopsis Is Deficient in Phytochrome B', Plant Cell, 3: 1263-74.

Song, I., J. Kim, K. Baek, Y. Choi, B. Shin, and E. Jin. 2020. 'The generation of metabolic changes for the production of high-purity zeaxanthin mediated by CRISPR-Cas9 in Chlamydomonas reinhardtii', Microb Cell Fact, 19: 220.

Spexard, M., C. Thoing, B. Beel, M. Mittag, and T. Kottke. 2014. 'Response of the Sensory animal-like cryptochrome aCRY to blue and red light as revealed by infrared difference spectroscopy', Biochemistry, 53: 1041-50.

Spreitzer, R. J., and L. Mets. 1981. 'Photosynthesis-deficient Mutants of Chlamydomonas reinhardii with Associated Light-sensitive Phenotypes', Plant Physiol, 67: 565-9.

Strenkert, D., S. Schmollinger, S. D. Gallaher, P. A. Salome, S. O. Purvine, C. D. Nicora, T. Mettler-Altmann, E. Soubeyrand, A. P. M. Weber, M. S. Lipton, G. J. Basset, and S. S. Merchant. 2019. 'Multiomics resolution of molecular events during a day in the life of Chlamydomonas', Proc Natl Acad Sci U S A, 116: 2374-83.

Sueoka, N. 1960. 'Mitotic Replication of Deoxyribonucleic Acid in Chlamydomonas Reinhardi', Proc Natl Acad Sci U S A, 46: 83-91.

Sullivan, S., E. Kharshiing, J. Laird, T. Sakai, and J. M. Christie. 2019. 'Deetiolation Enhances Phototropism by Modulating NON-PHOTOTROPIC HYPOCOTYL3 Phosphorylation Status', Plant Physiol, 180: 1119-31.

Sullivan, S., C. E. Thomson, E. Kaiserli, and J. M. Christie. 2009. 'Interaction specificity of Arabidopsis 14-3-3 proteins with phototropin receptor kinases', FEBS Lett, 583: 2187-93.

Sullivan, S., C. E. Thomson, D. J. Lamont, M. A. Jones, and J. M. Christie. 2008. 'In vivo phosphorylation site mapping and functional characterization of Arabidopsis phototropin 1', Mol Plant, 1: 178-94.

Sullivan, S., T. Waksman, D. Paliogianni, L. Henderson, M. Lutkemeyer, N. Suetsugu, and J. M. Christie. 2021. 'Regulation of plant phototropic growth by NPH3/RPT2-like substrate phosphorylation and 14-3-3 binding', Nat Commun, 12: 6129.

Swartz, T. E., S. B. Corchnoy, J. M. Christie, J. W. Lewis, I. Szundi, W. R. Briggs, and R. A. Bogomolni. 2001. 'The photocycle of a flavin-binding domain of the blue light photoreceptor phototropin', J Biol Chem, 276: 36493-500.

Takakado, A., Y. Nakasone, K. Okajima, S. Tokutomi, and M. Terazima. 2017. 'Light-Induced Conformational Changes of LOV2-Kinase and the Linker Region in Arabidopsis Phototropin2', J Phys Chem B, 121: 4414-21.

Takemiya, A., N. Sugiyama, H. Fujimoto, T. Tsutsumi, S. Yamauchi, A. Hiyama, Y. Tada, J. M. Christie, and K. Shimazaki. 2013. 'Phosphorylation of BLUS1 kinase by phototropins is a primary step in stomatal opening', Nat Commun, 4: 2094.

Tardif, M., A. Atteia, M. Specht, G. Cogne, N. Rolland, S. Brugiere, M. Hippler, M. Ferro, C. Bruley, G. Peltier, O. Vallon, and L. Cournac. 2012. 'PredAlgo: a new subcellular localization prediction tool dedicated to green algae', Mol Biol Evol, 29: 3625-39.

Theis, J., J. Niemeyer, S. Schmollinger, F. Ries, M. Rutgers, T. K. Gupta, F. Sommer, L. S. Muranaka, B. Venn, M. Schulz-Raffelt, F. Willmund, B. D. Engel, and M. Schroda. 2020. 'VIPP2 interacts with VIPP1 and HSP22E/F at chloroplast membranes and modulates a retrograde signal for HSP22E/F gene expression', Plant Cell Environ, 43: 1212-29.

Tilbrook, K., M. Dubois, C. D. Crocco, R. Yin, R. Chappuis, G. Allorent, E. Schmid-Siegert, M. Goldschmidt-Clermont, and R. Ulm. 2016. 'UV-B Perception and Acclimation in Chlamydomonas reinhardtii', Plant Cell, 28: 966-83.

Toepel, J., S. P. Albaum, S. Arvidsson, A. Goesmann, M. la Russa, K. Rogge, and O. Kruse. 2011. 'Construction and evaluation of a whole genome microarray of Chlamydomonas reinhardtii', BMC Genomics, 12: 579.

Tokutsu, R., K. Fujimura-Kamada, T. Matsuo, T. Yamasaki, and J. Minagawa. 2019. 'The CONSTANS flowering complex controls the protective response of photosynthesis in the green alga Chlamydomonas', Nat Commun, 10: 4099.

Tokutsu, R., K. Fujimura-Kamada, T. Yamasaki, T. Matsuo, and J. Minagawa. 2019. 'Isolation of photoprotective signal transduction mutants by systematic bioluminescence screening in Chlamydomonas reinhardtii', Sci Rep, 9: 2820.

Trebst, A. 2007. 'Inhibitors in the functional dissection of the photosynthetic electron transport system', Photosynth Res, 92: 217-24.

Trippens, J., A. Greiner, J. Schellwat, M. Neukam, T. Rottmann, Y. Lu, S. Kateriya, P. Hegemann, and G. Kreimer. 2012. 'Phototropin influence on eyespot development and regulation of phototactic behavior in Chlamydomonas reinhardtii', Plant Cell, 24: 4687-702.

Wakao, S., P. M. Shih, K. Guan, W. Schackwitz, J. Ye, D. Patel, R. M. Shih, R. M. Dent, M. Chovatia, A. Sharma, J. Martin, C. L. Wei, and K. K. Niyogi. 2021. 'Discovery of photosynthesis genes through whole-genome sequencing of acetate-requiring mutants of Chlamydomonas reinhardtii', PLoS Genet, 17: e1009725.

Wang, H., B. Gau, W. O. Slade, M. Juergens, P. Li, and L. M. Hicks. 2014. 'The global phosphoproteome of Chlamydomonas reinhardtii reveals complex organellar phosphorylation in the flagella and thylakoid membrane', Mol Cell Proteomics, 13: 2337-53.

Wang, L., T. Yamano, S. Takane, Y. Niikawa, C. Toyokawa, S. I. Ozawa, R. Tokutsu, Y. Takahashi, J. Minagawa, Y. Kanesaki, H. Yoshikawa, and H. Fukuzawa. 2016. 'Chloroplast-mediated regulation of CO2-concentrating mechanism by Ca2+-binding protein CAS in the green alga Chlamydomonas reinhardtii', Proc Natl Acad Sci U S A, 113: 12586-91.

Wang, Y., D. J. Stessman, and M. H. Spalding. 2015. 'The CO2 concentrating mechanism and photosynthetic carbon assimilation in limiting CO2 : how Chlamydomonas works against the gradient', Plant J, 82: 429-48.

Wichmann, Julian, Thomas Baier, Eduard Wentnagel, Kyle J. Lauersen, and Olaf Kruse. 2018. 'Tailored carbon partitioning for phototrophic production of (E)-α-bisabolene from the green microalga Chlamydomonas reinhardtii', Metabolic Engineering, 45: 211-22.

Wingfield, J. L., and K. F. Lechtreck. 2018. 'Chlamydomonas Basal Bodies as Flagella Organizing Centers', Cells, 7.

Wittkopp, T. M., S. Schmollinger, S. Saroussi, W. Hu, W. Zhang, Q. Fan, S. D. Gallaher, M. T. Leonard, E. Soubeyrand, G. J. Basset, S. S. Merchant, A. R. Grossman, D. Duanmu, and J. C. Lagarias. 2017. 'Bilin-Dependent Photoacclimation in Chlamydomonas reinhardtii', Plant Cell, 29: 2711-26.

Yamano, T., K. Miura, and H. Fukuzawa. 2008. 'Expression analysis of genes associated with the induction of the carbon-concentrating mechanism in Chlamydomonas reinhardtii', Plant Physiol, 147: 340-54.

Yamano, T., T. Tsujikawa, K. Hatano, S. Ozawa, Y. Takahashi, and H. Fukuzawa. 2010. 'Light and low-CO2-dependent LCIB-LCIC complex localization in the chloroplast supports the carbon-concentrating mechanism in Chlamydomonas reinhardtii', Plant Cell Physiol, 51: 1453-68.

Yoon, H. S., J. D. Hackett, C. Ciniglia, G. Pinto, and D. Bhattacharya. 2004. 'A molecular timeline for the origin of photosynthetic eukaryotes', Mol Biol Evol, 21: 809-18.

Zhang, Z., J. Shrager, M. Jain, C. W. Chang, O. Vallon, and A. R. Grossman. 2004. 'Insights into the survival of Chlamydomonas reinhardtii during sulfur starvation based on microarray analysis of gene expression', Eukaryot Cell, 3: 1331-48.

Zhao, X., Y. L. Wang, X. R. Qiao, J. Wang, L. D. Wang, C. S. Xu, and X. Zhang. 2013. 'Phototropins function in high-intensity blue light-induced hypocotyl phototropism in Arabidopsis by altering cytosolic calcium', Plant Physiol, 162: 1539-51.

Zhao, X., Q. Zhao, C. Xu, J. Wang, J. Zhu, B. Shang, and X. Zhang. 2018. 'Phot2-regulated relocation of NPH3 mediates phototropic response to high-intensity blue light in Arabidopsis thaliana', J Integr Plant Biol, 60: 562-77.

Zones, J. M., I. K. Blaby, S. S. Merchant, and J. G. Umen. 2015. 'High-Resolution Profiling of a Synchronized Diurnal Transcriptome from Chlamydomonas reinhardtii Reveals Continuous Cell and Metabolic Differentiation', Plant Cell, 27: 2743-69.

Zorin, B., Y. Lu, I. Sizova, and P. Hegemann. 2009. 'Nuclear gene targeting in Chlamydomonas as exemplified by disruption of the PHOT gene', Gene, 432: 91-6.

Scientific communication

Meetings and conferences

- Sfphi2019 : Meeting of the French Photosynthesis Society, Paris (*Participation*)
- I-BE-C 2020: International Bioenergy and Environment Congress (*Virtual participation*)
- ISPP's 2020 Annual Meeting (*Virtual participation*)
- 19th International Conference on the Cell and Molecular Biology of Chlamydomonas, Ile des Embiez, France, 2021 (*Participation with a poster*)
- Annual Plant-INT 2021 (Planta INTERNATIONAL master program) Symposium, Jardin du Lautaret (*Participation with two posters, delegating Signal team of LPCV*)

Formations

- Introduction to Algae (Coursera)
- Engineering Life: Synbio, Bioethics & Public Policy (Coursera)
- Intégrité scientifique dans les métiers de la recherche (Fun MOOC)
- Langue Francais (CEA Grenoble)
- Prevention of chemical risk (CEA Grenoble)
- Job-hunting strategies (UGA)

Teaching

- Teaching the practical courses of MEP 202-232 (Plants' anatomy) for the first-year students (International group) of the department of Biology, UGA (Academic year: 2020-2021)

- Mentoring for master students of the Planta INTERNATIONAL master program (UGA- University of Milan) for the course ''Evolutionary biology of plants''. Title of project: ''Evolutionary aspects of plant photoreceptors''.

Publications

Ruiz-Sola, M. Águila, Serena Flori, Yizhong Yuan, Gaelle Villain, Emanuel Sanz-Luque, Petra Redekop, Ryutaro Tokutsu, Anika Kueken, Angeliki Tsichla, **Georgios Kepesidis**, Guillaume Allorent, Marius Arend, Fabrizio Iacono, Giovanni Finazzi, Michael Hippler, Zoran Nikoloski, Jun Minagawa, Arthur R. Grossman, and Dimitris Petroutsos. 2021. 'Photoprotection is regulated by light-independent CO_2 availability', bioRxiv: 2021.10.23.465040

Acknowledgements

The last three and a half years have been the most intense and eventful of my life. Doing my PhD helped me develop and progress not only scientifically and professionally, but also personally. I would have been enormously ungrateful if I didn't thank a number of people that helped me and supported me throughout this amazing journey.

At first, I would like to thank my supervisor Dr. Dimitris Petroutsos for trusting me and giving me the opportunity to do my PhD is his team. During these years he helped me develop my scientific skills and achieve personal progress in levels way beyond I was initially anticipating to. I am also thankful to CEA and CNRS for the funding of my research and for allowing me to carry out and communicate my scientific project. Also, to the UGA, for all the technical and bureaucratic support and for offering me the platform to communicate my study with a broad number of colleagues. Especially during the quarantine period, UGA's support was enormously comforting.

I would like also to express my enormous gratitude for my Defence Jury members, Elena Monte, Matteo Ballottari, Christel Carles, Pierre Crozet and Norbert Rolland. I have a great admiration for these scientists and it is a real honour to be examined by them. I am also thankful for the members of my CSI committee Renaud Dumas and Pierre Crozet. Their scientific feedback at all three of our meetings was significant to my study and revitalised my perception for my project, when this was very much needed.

I am especially thankful for the members of my team (Team Signal) in the Cell & Plant Physiology Laboratory (LPCV), CEA, Grenoble. More specifically, I want to thank Gaelle, for all her help and tutoring during my early days in the lab. She helped me acclimate to a new scientific field and introduced me to the biochemical techniques that I used for the entirety of my PhD. Also, I thank Marcello, the post-doc of the team, for all his scientific and moral support. He introduced me to the ''Chlamy world'' and his advice on the scientific writing and presenting was very valuable. I am also thankful to my good PhD colleague, Yizhong Yuan for all his help and for carrying on to me all his

precious experience. His technical help for the Δ*flkin* genotyping and complementation is of fundamental importance for my project and I have great gratitude for that. All my gratefulness, as well, to Anne-Flore, Xiaoye, Laura, Nicolas, Celeste and Batoul for their everyday help and support. I am really glad that I got to share the bench and the office with these people. Finally, big credits should be acknowledged to the former members of the team, Aguila Ruiz Sola (post-doc) and Angeliki Tsichla (Research Engineer). Aguila has constructed the setup and done the sampling for the first phosphoproteomic analysis. Angeliki's groundwork on the blue light regulation of the cpUPR inspired my study on this subject.

The realisation of my thesis would have been impossible without the scientific contribution of a number of valuable collaborators. Namely, Anthony Iannetta, Emily Werth and Leslie Hicks from the Department of Chemistry, University of North Carolina at Chapel Hill, Chapel Hill, NC, USA conducted the mass spectrometry analysis of our samples for the phosphoproteomic analyses and also contributed at the data evaluation. Also, Marius Arend and Zoran Nikoloski from the Max Planck Institute of Molecular Plant Physiology, Potsdam, Germany provided their valuable assistance to the statistical and computational analysis of the phosphoproteomic analyses. Finally, Silvia Ramundo, from GMI - Gregor Mendel institute of molecular plant biology, Vienna, Austria shared with me a number of cpUPR-defective mutants from her lab's collection.

I would like also to thank the lab which hosted me for the entirety of my thesis, the Cell & Plant Physiology Laboratory (LPCV), CEA, Grenoble and its directors Eric Maréchal and François Parcy. LPCV was not only the ''incubator'' for my experiments and studies, but also, in an era of almost two years of sanitary restrictions from public and social life, my second house. A number of people from the lab provided me with moral help and support and, without this being an attempt of exaggeration, without their presence the completion of my PhD would have been an enormously challenging task. I will namely thank them here in alphabetical order. Thanks to Antonin (PhD student), with whom I shared the same trajectory of setbacks and overcomes throughout this 3-year effort and with mutual aid we managed to see ourselves progress and mature scientifically in parallel. His support and solidarity helped me

going on, even at moments when this was seeming impossible. Of course, I am also thankful for all the breaks and the end-of-the-day discussions we had while coming back home. I am considering him a great friend of mine. To Camille (master and PhD student) for all the laughs and the great times we had, both in the lab and at the bars. I am really glad I did not finally demotivate her from doing a PhD! To Damien (PhD student), who taught me how to ski, after being in Grenoble for 3 years, and for all his support in the lab. To Elise, who, despite getting to meeting her late, her kind words really helped me through difficult times. To Etienne, for his company, the great times we had and for his amazing cooking. He had showed me great support when I was needing it. To Laura (master and PhD student), my -almost- roommate for all her advice, the endless hours that she had to hear me complaining and for pretending to enjoy my jokes to not hurt my feelings. To Loic (engineer), for all the joy and fun in the lab and on breaks and for helping me reach my drinking limits in the after-works. To Louise (PhD student), the unpredictable wild card of the lab, for all the times that she helped me, both as a friend and as a student representative. Her insistence towards my colleagues on speaking a commonly spoken language, improved significantly my integration in the lab. I also thank her for considering me a ''high soul'', though I consider the term poorly defined and unscientific. To Manon (PhD student), my office companion, with Antonin, during the writing of our theses. I truly regret not getting to know her earlier, since her support was really valuable for me. It is an honest bless to have colleagues who are also comrades. To Mattia (post-doc), the 14-years-old 30-years old, for his insightful scientific feedback and his never-ending will to help me technically. Also, for all the fun and the games we played together. To Nolween (PhD student) and Mauro, who, since the quarantine, were my board gaming companions. Nolween was particularly helpful with my PhD problems and I have nothing but gratitude for her support during times that I needed that the most. Finally, to Vangeli (master and PhD student), my roommate since the summer of 2020. He helped me, like no other, to revitalise my interest on my project during the quarantine of March 2020 and since then he helped me tremendously to increase my scientific insight. I am really glad I have been his roommate; both for his moral support and for indicating the only known instance of cohabitation of a Greek and a Macedonian. The later

represents a milestone on international diplomatic relations and I am awaiting the Peace Nobel Prize any time now.

I would like, also, to give special thanks to Gabrielle Tichtinsky, from the Flo_Re team of LPCV, Associate Professor in the UGA and Vice-director of the master program PLANTA-International, who helped me gain teaching experience. More specifically, she assisted me into taking the responsibility to mentor master students of the master program PLANTA-International for a bibliographic project in the terms of the course ''Evolutionary Biology of Plants''. She also convinced me to teach the practicals of Plants Anatomy for 1st year international biology students in the UGA. The latter was an amazing and refreshing experience, probably one of the most vividly memorable from these 3 years of my PhD.

I should also express my gratitude to my Grenoble friends outside of LPCV for their solidarity. Thanks to Dorina and Andrea, the original members of the, now historical, group '' Poor PhD students, unite!'', for all their enormous help and support. I owe nothing but great gratitude for all the times that Dorina listened to my work-related problems and for all her inexhaustible will for support and solidarity. To Kyprianos and Sofia for all the nights of the Greek-referential jokes and discussions. To Nefeli, the only person during the years of my PhD with whom I could have such deep discussions about theatre.

I would also like to thank my Greek friends (Christina, Nikos, Despoina, Yiorgos) for being a much-needed company during the lockdowns, for helping me rehearse presentations throughout all the period of my PhD and for trying to be present for my defence despite that being significantly difficult to them.

Finally, I must express my gratitude to my family. To my parents, Voula and Dimitris, for being enormously supportive and helpful since the beginning of that step of mine, while, in parallel, being respectful of my time schedule and my working hours. The elaboration of my PhD in Grenoble would have been impossible without their support, which goes way beyond the last few years. To my brothers Panagiotis and Aggelos, for their respect and support, which I deeply appreciate. Especially to Panagiotis who did

his practice in Grenoble during the winter/spring of 2021 and whose mutual solidarity during the period of the strict public restrictions was vital and much needed.